University of Novi Sad
FACULTY OF TECHNICAL SCIENCES
DEPARTMENT FOR PRODUCTION ENGINEERING
21000 NOVI SAD, Trg Dositeja Obradovica 6, SERBIA

UDK 621 ISSN 1821-4932

JOURNAL OF

PRODUCTION ENGINEERING

Volume 12 Number 1

Novi Sad, December 2009

Journal of Production Engineering, Vol.12 (2009), Number 1

Publisher: FACULTY OF TECHNICAL SCIENCES
DEPARTMENT FOR PRODUCTION ENGINEERING
21000 NOVI SAD, Trg Dositeja Obradovica 6
SERBIA

Manuscript submitted for publication: December 23, 2009.
Printing: 1st
Circulation: 300 copies

CIP classification:

CIP – Катаголизација у публикацији
Библиотека Матице српске, Нови Сад

621

JOURNAL of Production Engineering / editor in chief Pavel Kovač. – Vol. 12, No. 1 (2009)- . – Novi Sad : Faculty of Technical Sciences, Department for Production Engineering, 2009-. – 30 cm

Godišnje. Je nastavak: Časopis proizvodno mašinstvo = ISSN 0354-6446
ISSN 1821-4932
COBISS.SR-ID 250243079

Printing by: FTN, Graphic Center ***GRID,*** *Novi Sad*

ISSN: 1821-4932

INTERNATIONAL EDITORIAL BOARD

Editorial

The Journal for Production Engineering starts with publishing again after a 16 year break. It is our intention to continue publishing original scientific papers from the area of production engineering.

Published in this issue are reviewed papers from International Scientific Conference MMA 2009 with a few other contributions.

This jubilee 10th International Scientific Conference MMA 2009 – FLEXIBLE TECHNOLOGIES successfully maintains the high level set by the previous conferences. Participation of a large number of domestic and international authors, as well as the diversity of topics, justifies efforts to organize this conference and contributes to exchange of knowledge, research results and experience of industry experts, research institutions and faculties which all share common interest in the broad area of production engineering

Editor in Chief

Professor Pavel Kovač, PhD,

Journal of Production Engineering
Vol.12 No.1

Contents

Section: METAL CUTTING

Section: MACHINE TOOLS

Section: TOOLS, TRIBOLOGY, FIXTURES, METROLOGY AND QUALITY

Section: FLEXIBLE MANUFACTURING SYSTEMS, *CAD*, *CAPP*, *CAM*, *CAQ*, ..., *CIM*

Section: OTHER AREAS

Journal of Production Engineering
Vol.12 No.1

Antic, A., Zeljkovic, M., Hodolic, J., Zivkovic, A.

MODEL OF CLASSIFICATION SYSTEM OF TOOL WEAR CONDITION WHILE MACHINING BY TURNING

Abstract: *This work deals with a model of a developed fuzzy system for tool wear classification. The system consists of three modules: module for acquisition and data processing, for tool wear classifying and for decision making. In addition, some of the methods of signal processing used for defining the entering fuzzy classifier vector have been given.*

Key words: *Tool monitoring, Signal processing, Vibration signal, Fuzzy system*

1. INTRODUCTION

The basic requirements for the automation of the process of scraping in modern production conditions are the reliability of the tool monitoring system and the machining process. The shortcoming of the classical systems for tool wear monitoring is the fact that they work within the given boundaries, which often do not meet the requirements in an adequate way. The development of the modern monitoring systems, which work at real time, make the basis for monitoring the tool state and the machining process in an automatic production. Thus, modern diagnostic and managing systems are required to have a level of automation which can make conditions for managing the quality of a product and the production process, which is often called "intelligent" production system.

The machining process contains several different parameters difficult to measure which, combined with the dynamics of the very process, represent a stochastic and non-stationary process. A great number of parameters influence the very course of the machining process, some of them being: the characteristics of the materials processed, the state of the machining system, vibrations occurring during the machining process and a number of unknown but very influential parameters which together make the creation of an adequate processing model harder. This work deals with defining the model of the classification systems for the state of tool wear with special emphasis on the module for gathering and processing vibration acceleration signals by means of applying discrete wavelet transformation (DWT) on signal decomposing. Distinguishing the adequate characteristics of the fuzzy classifier entering vector for the tool wear classifying is one of the most important functions of the system.

2. TOOL WEAR MONITORING PRESENTATION

By developing new technologies and by mutual integration of measuring equipment and other mechatronic elements of a machine, as well as new more flexible managing approaches (open architecture managing system, applying of artificial intelligence algorithms for monitoring and process managing), conditions are met for intelligent processing systems development. [1]

Tool wear is a primary generator of accidental stochastic disturbances with a direct influence on stability, quality and economizing of the machining process. Some estimates show that 20% of the cutting process stoppages belong to the group of those caused by the consequence of the opportune reactions and tool wear discovering.

Getting reliable information about the tool state at real time represents and obligatory condition for identifying the degree of tool wear, which reasonably rises the stability of the machining process quality.

By the mid-80s of the last century several models of wear based on classical mathematical models have been suggested (Bayes` classificatory, the closest neighbors method, linear discriminators, and so on). However, that process was hard to describe by means of classical mathematical models due to its outstanding non - linear and stochastic qualities. Some more intense research on development of tool monitoring systems during the cutting process began in the 90s of the last century by applying a multi sensor approach, i.e. tool wear classifier based on artificial intelligence algorithm, which are in use today as well. The beginning of research in this area assumed that applying of these methods should result in industrially applicable solutions for cutting tools wear monitoring.

Among the most frequently used algorithms are the artificial neural networks (ANN) and fuzzy logics, which are widely applied nowadays and give possibilities for additional research [2].

The reasons for these models being widely applied should be looked for in: the possibility of complex non-linear processes described without sufficient information and burdened with different kinds of disturbance and unwanted noise in
signals, usually appearing because of the very stochastic nature of the wearing process and the possibility of brief processing of a larger amount of information at real time. The above mentioned advantages become distinct in problems of the degree of tool wear estimate, where an adequate mathematical

wearing model does not exist. In order to increase the quality of the tool wear monitoring system, a number of experimental surveys have been carried out, by using classifying models based on fuzzy logics and recently some hybrid combinations such as Neuro-fuzzy (NF) models and Fuzzy Neural Networks (FNN) appear more often. For this reason distinguishing of a number of different statistical parameters from signals and achieving a group of mutually independent and relevant wearing parameters of satisfactory quality, which are able to fully identify a complex dynamics of cutting tools wear comes as an imperative. The first step is collecting monitoring signals such as forces, vibrations, acoustic emission (AE), temperature and/or engine current etc. The second step is signal processing in order to separate its useful content. The last step is classification, where useful information from the signal are used for current tool state classifying [1].

The vibrating of the cutting tools while machining occurs as a consequence of: chip lamina creating, tools` vibrations, friction on the front and back surface of a tool, wearing of the cutting edge of the tool, the wavy structure of the surface processed and they are also connected to the vibrations caused by conjugated gear action in a kinetic machine chain. Different surveys have shown that tool vibrating occurring during continuous machining is the main reason for the friction between the back surface of a tool and the object being machined. The basic tool vibrating frequency is the resonant system frequency caused by friction on the cutting edge. Vibrations accelerating represent their best measure when appearing at high frequencies. Since the vibrations of cutting tools are the ones of high frequency (over 1 kHz), tool accelerating has been chosen to be a parameter of tool wear monitoring [3].

Applying the value analysis for selecting the identified parameters of the machining process is an important part of parameter adequacy determination. Analyses like this one appear as an adequate response and compensation for following several different and stochastic parameters of the classical systems.

3. BASIC DATA ABOUT THE MODEL

Tool wear monitoring system model can basically be regarded through four segments bound together making a whole, represented in the picture 1.

System modules are the following:

- acquisition and data processing module,
- decision-making data classifying module,
- fuzzy decision-making module.

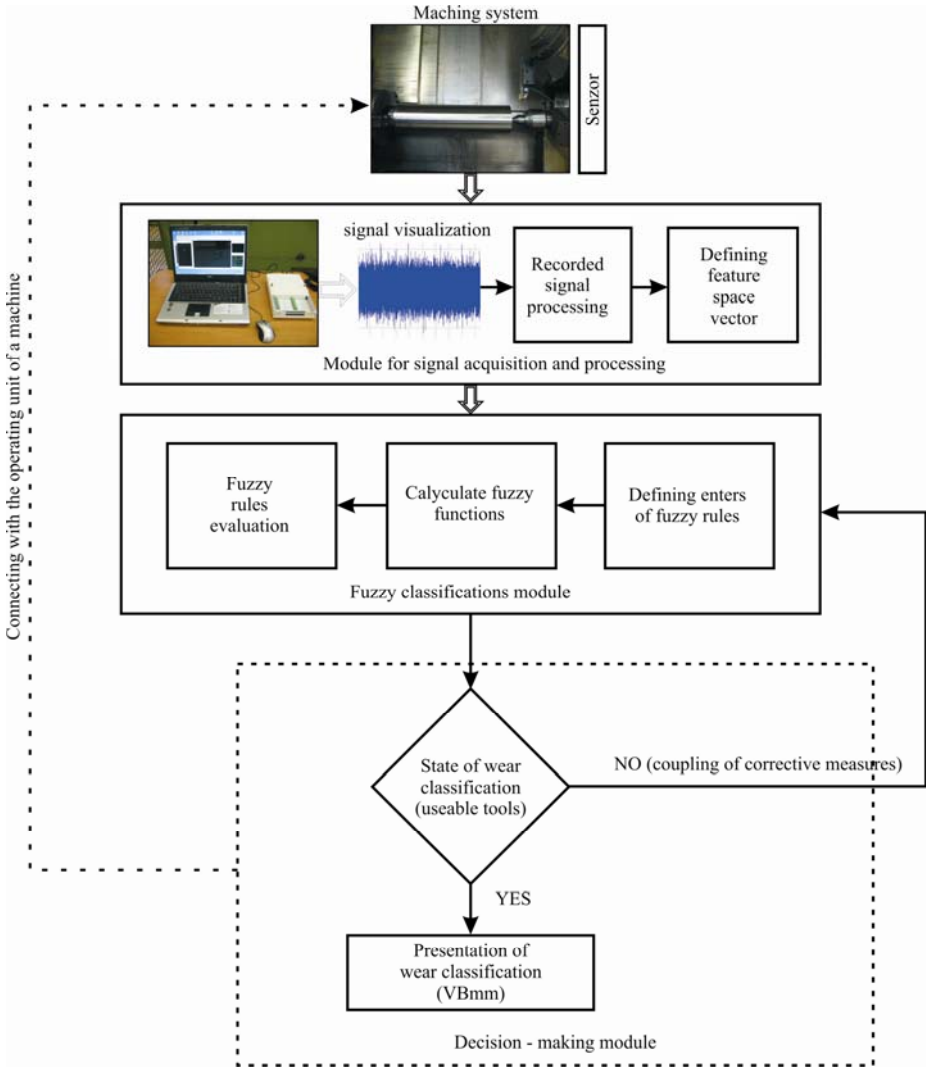

Fig. 1. Presentation of developed system structure for tool wear classification

3.1 Subsystem for data acquisition and processing

Accelerometer measuring vibration accelerations and mounted on the tool handle makes the sensory part of the data collecting module. The part of the module used for data acquisition, processing and analyzing consists of A/D card NI USB 6281 18bit, 625 kS/s, which receives analogous data from the existing sensor, converts them into digital information and sends them to the entering data base. A software system of the Matlab version R2008b has been used for card managing. The system enables the vital working functions to be defined.

By means of the suggested approach the entering data "vectors" are being additionally filtrated in the training data classifying system module, thus acquiring better results at more complex evaluation concerning more complex processing. The structure of the suggested system can be regarded through two phases. In the first phase, the initial model structure establishing phase, the initial structure of the "classifier" is being established, the parameters of structure for a number of combinations of machining parameters (velocity, depth and motion, characteristics of materials and tools etc) and for each wearing parameter respectively, are being determined. In this part of the classifying system, initializing all parameters is equally non-limited. If the testing shows that system responses could be improved at a higher or lower extent, the initial structure can additionally be improved during the phase of secondary learning i.e. structure stabilizing. Data standardization is being done here, as well. It is essential to go through data standardization in order to get more precise data without disturbances that can occur during sampling. Moreover, different mathematical functions for signal processing at real time can be additionally used and then the measuring data can be transformed into other measuring quantities if necessary. The aim of data selecting and standardization is choosing the most influential and accurate data relevant for the process, on the basis of which fuzzy system will be drilled.

The software system has been projected for information collecting and processing as well as managing hardware components, and thus supervising and classifying tool ware on the basis of given restrictions. The remaining tool validity is determined on the basis of wear trend acquired by simultaneous analysis with the calculated wear and the real state.

Selecting the right kind of filter will depend, in the first place, on the kind of the signal followed, tool characteristics, machines, work piece, machining parameter and other machining conditions. As it follows, the filtering procedure is not uniquely defined and it should be carefully determined for each particular case, regarding the individual characteristics of the process. Thus, the suppression of the parts of the signal which carry vital information about the state of cutting tools will be avoided. According to the literature available, it can be concluded that the lowpass and bandpass filters implemented in the measuring equipment and realized by means of computing processing, i.e. program support in the phase of additional signal filtering, are most frequently applied. Filter selecting will depend on its velocity and the quality of the outgoing signal. It should be mentioned that in literature the right kind of used filter is rarely specified, and that in a large number of works it can be noticed that additional filtering is not mentioned at all, although it has been carried out. Within the research the lowpass FIR (Finite Impulse Response) filter has been used for vibration signals.

The above mentioned forms of filtering can be applied in situations when the frequency range of a signal is of interest a priori and completely defined. There are also situations in which it is not always possible to distinguish properly the range with information about the tools state from the ones representing noise [4]. Concrete examples are the high frequencies of vibration signals and the acoustic emission signal, where elastic waves occur due to the effort in the zones of deforming. The waves occur as a consequence of freeing energy produced by separating molecules in a crystal grid of a material. One of the main advantages of using these kinds of signals follow from the fact that their frequencies are considerably higher (ultrasound area) from the vibration frequency of a machine and the surrounding area. In that way unwanted influences can be directly avoided, as well as the occurring of lower frequency spectrum which is not related to the tool wear. However, a problem occurs in cases when it is necessary to isolate more harmonics which appear because of the plastic deformation and breaking of degraded particles, particles-tools collision and all other disturbances for which it is difficult to determine the area of frequency. It turned out that this kind of disturbance is possible to isolate considerably by applying wavelet transformation method. It is a kind of method based on the signal decomposing procedure after which the partial filtering of its segments follows

3.2 Signal processing by means of discreet wavelet transformation

Wavelet transformation is the most frequently used and the most important signal analyzing method in a time-frequent area. Its basic advantage related to methods of frequency area analysis (e.g. Fourier`s transformations) represents a high-quality and simultaneous signal presentation both in a frequency and time areas. In that way, a possibility of signal analysis on the local level is acquired, which is especially important for non-stationary signal processing. This function, while being analyzed, gets a number of different forms related to its width modification. The transformation procedure is based on comparison of wavelet function of a certain width (frequency) defined by a scaling parameter (s) and by parts of signals of the same width in a certain time interval (t – kτ), the scale being inversely defined, considering signal frequency. The record of the continuous wavelet transformation (CWT) in a general form is given in the scheme:

$$\gamma(\tau, s) \frac{1}{\sqrt{|s|}} \int_{-\infty}^{\infty} x(t) \varphi^* \left(\frac{t-\tau}{s} \right) dt \qquad (1)$$

Where τ is a translation parameter, s scale parameter,

x(t) signal being transformed, γ frequency structure of the signal x(t) at a given time interval k$ and with the s scale, and $ the scaled and translated projection of the original wavelet kτ. When analysis of the whole signal is being carried out with the original function of a given scale, the procedure is being repeated for another scale value, i.e. time interval. If the signal contains a spectral component corresponding to the current scale value, multiplying of the wavelet function and the signal located where the component is existing is relatively high. Wavelet moving in time leads to signal localizing in time, while the scale changing produces information of the signal frequencies in each of the analyzed time intervals. In the low-frequency area signal basis (signal approximation) is determined, while the high-frequency area gives more detailed information.

4. WEAR PARAMETERS

4.1 Selecting the tool wear defining parameters

A good selection of the best group of wear parameters, which can classify the degree of tool wear with required accuracy during the process of classification, is the last step of the signal processing procedure. Analysis show that in most cases the aim of the process of parameter selection is selection of the optimal number of parameters and only after that the most suitable parameter group, considering the influence of each parameter separately on the degree of tool wear recognizing.

Although it is better to use a larger number of independent parameters as a rule, too many parameters can cause overnoising, for example when neural frameworks are used (overfitting), which are still used by most of the authors at wear process modeling. Overnoising leads to decrease of the general features of the frameworks and consequently worse quality of the system responding.

It can be noticed that the problem of wear parameter analysis and selection has been treated in literature in several ways. Generally, explanation for their particular selection does not exist. They are followed by works in which the analysis of the influence of recorded signals on the wear dynamics was primarily done. On the basis of these observations wear parameters which describe accurately some segments or appearing of wear process were suggested [5]. A group of methods use the so called parameter sequential selection, which imply their mutual independence when tool wear evaluating, while another group is independent when choosing parameter combinations. Generally speaking, as opposed to the combined approach, when the individual parameter selection is concerned, their growth influences less the increase of the model complexity then the increase of additional data analysis. On the other hand, certain situations show that mutual influences of parameters can result in higher degree of correlation with the wear dynamics than in the case of individual approach. Finally, the last group contains the parameters where the wear parameter selection is done depending on their influence on the classifying results. This approach, as well as the individual analysis of wear parameter influence, has been used in this paper, as well.

5. CONCLUSION

The presented model of tool wear fuzzy classifier uses the processed signal of vibration acceleration from a sensor allocated on the tool in order to evaluate tool wear. This technique provides an acceptable method for the process of fuzzy modeling on the basis of which are calculated the parameters of membership functions which represent the incoming/outgoing data in the best possible way. Once the model is formed, it can evaluate the degree of tool wear for certain cutting parameters (the ones it has been taught). The model is formed rather rapidly and it can evaluate tool wear on-line. The time needed for the model formation depends on the quantity of entering data, while the model accuracy depends on the data selection

6. ACKNOWLEDGMENTS

This paper is a part of research in the framework of the projects: "Research and Development of Roller and Bearing Assemblies Their Components," TR 14048, and the project "Enhancing the quality of processes and products utilizing modern engineering techniques with goal to increase of competitiveness on global market", project TR 14003 part of the technological development program for period from 2008. to 2010., financed by Ministry of science of Republic of Serbia.

7. REFERENCES

[1] Sick, B., 2002, On-line and Indirect Tool Wear Monitoring in Turning with Artificial Neural Networks, Mechanical Systems and Signal Processing, No 16(4), 487 – 546., ISSN 0888-3270

[2] Antić A., Hodolič, J., Soković, M., 2006, Development of a Neural-Networks Tool-Wear Monitoring System for a Turning Process, Strojniški vjesnik Journal of Mechanical Engineering, 52(11), 763-776, ISSN 0039-2480

[3] Sharma V.S., Sharma S. K., Sharma A. K., 2007, Cutting tool wear estimation for Turning, Journal Intell Manuf, No 19, 99–108.

[4] Antić A., Petrović, B., Zeljković, M., Dinamika obradnog sistema i njene implikacije na indirektno prepoznavanje stanja reznog alata, 32. Savetovanje proizvodnog mašinstva Srbije, Novi Sad: Fakultet tehničkih nauka, 18-20 septembar, 2008, 341- 346, ISBN 978-86-7892-131-5.

[5] Al-Habaibeh, A., & Gindy, N., , 2001, Self-Learning Algorithm for Automated Design of Condition Monitoring Systems for Milling Operations, The International Journal of Advanced Manufacturing Technology, No 18, pp. 448-459., ISSN 0268-3768

Authors: **Prof. dr Janko Hodolič, Prof. dr Milan Zeljković, M.Sc. Aco Antić**, **M.Sc. Živković Aleksandar,** University of Novi Sad, Faculty of Technical Sciences, Departman for Production Engineering, Trg Dositeja Obradovica 6, 21000 Novi Sad, Serbia, Phone.: +381 21 4852320, Fax: +381 21 454-495. E-mail: hodolic@uns.ac.rs, milanz@uns.ac.rs, antica@uns.ac.rs, acoz@uns.ac.rs,

Journal of Production Engineering
Vol.12 No.1

Gostimirovic, M., Kovac, P., Sekulic, M., Savkovic B.

AN INVERSE HEAT TRANSFER METHOD FOR DETERMINATION OF THE WORKPIECE TEMPERATURE IN GRINDING

Abstract: *This paper present investigation of the thermal state in grinding process, using inverse heat transfer problems. Based on a temperature measured at any point within a workpiece, this experimental and analytical method allows determination of the maximal temperature on wheel/workpiece interface as well as the complete temperature field in the workpiece surface layer. To solve the inverse heat transfer problems, a numerical method of finite differences in implicit form was chosen.*
Key words: *Grinding process, Temperature field, Inverse problems.*

1. INTRODUCTION

Unlike other machining technologies, due to lack of a continuous cutting edge, simultaneous cutting of a large number of grinding particles, inconsistent cutting geometry and the transient nature of cutting of a single grinding particle, substantial quantity of thermal energy develops during grinding process. The thermal energy and the problems of its evacuation from the cutting zone account for high contact temperatures which [1]. These increased temperatures instantaneously burst to a maximum, have short duration and exert a pronounced negative effect on wheel surface, workpiece quality and accuracy.

Systematic research in cutting technologies has yielded a number of various analytical and experimental methods for determination of temperatures not only in the narrow and wider cutting zone, but also in the machining system [2]. Due to the rudimentary measuring equipment, first research on temperatures in grinding was mostly theoretical. Later advancements in measuring equipment allowed development of various experimental methods for temperature measurement in grinding, which have been undergoing modification and advancement until today.

Since the main task of grinding is to achieve satisfactory part quality with as large productivity as possible, special attention is focused on the effect that grinding temperatures have on the change of material properties in the workpiece surface layer. If the temperatures thus generated are high enough to cause structural and phase transformations of the workpiece material, the machined surface shall suffer from a number of disadvantages [3]. Should, in addition, dimensional errors appear as well, the overall effect can substantially diminish exploitation features of the finished part.

Efficient machining of parts, free of thermal defects in the surface layer, requires methods for control of thermal phenomena by regulation of grinding temperatures. For a particular grinding wheel and coolant, temperatures in the cutting zone can be controlled by proper selection of cutting condition parameters [4 and 5].

Although the cutting temperature is an essential parameter in grinding, its utilization for the purpose of control and optimization of grinding is fairly complex. The main obstacle on the road to its utilization for control and optimization purposes lies in the difficult monitoring of cutting temperatures during grinding. Therefore, in order to describe thermal state in grinding, efforts are aimed at improving the existing and development of novel measurement methods, while at the same time focusing on analytical optimization models which can successfully relate to experimental research [6].

As the research so far has shown, non-stationary and non-linear technical processes involving intensive heat transfer, such as grinding, can be successfully solved using novel approach based on inverse heat transfer problems [7, 8 and 9]. Inverse problems allow the closest possible experimental-model approximation of thermal regimes for grinding.

2. INVERSE HEAT TRANSFER PROBLEMS

2.1 Thermal process modeling

The process of heat transfer between solid bodies or between a system and its environment, of which heat transfer in grinding is also a part, is mostly considered from the standpoint of mutual relations between input and output process parameters. It is widely accepted that such process can be schematized as in Fig. 1.

The first step in the research of any thermal phenomenon is to model the real process. This means development of a model which is valid over a narrow domain limited by boundary conditions. The model, which describes a segment of the real process, correlates input $\boldsymbol{u}(t)$ and output $\boldsymbol{z}(t)$

parameters which define the state of the process at every moment in time ***t***.

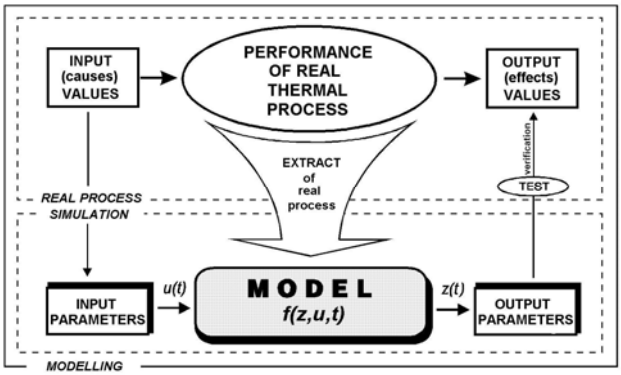

Fig. 1. Diagram of a thermal process

If the input parameters $\boldsymbol{u}(t)$ are known and output parameters $\boldsymbol{z}(t)$ define process state in time, then the output parameters are a function of input parameters, i.e.:

$$z = f(u,t) \qquad (1)$$

The real thermal process is most often described analytically. The goal is to set up a most adequate analytical model, while, on the other side, keeping its form as simple as possible in order to facilitate solution. Given the right mathematical method, the model thus defined, solves problems quickly and efficiently.

Analytical model of thermal process most often takes form of a system of differential and algebraic equations. Considering the fact that thus modeled task is easily transformed into algorithm and efficiently processed on computer, the differential models are widespread today in the investigation of thermal processes.

2.2 General case of inverse method

If for the adopted thermal model there exist unique conditions, then any particular input parameters of the thermal process shall result in that same or any other thermal state defined by the temperature field of the analyzed object. Determination of the input-output relationship is the direct task of heat transfer. Conversely, the inverse method of heat transfer solves the problem of finding input characteristics of the process for the known temperature field.

If for every unknown parameter $\boldsymbol{u}$ there is a linear, smooth operator $\boldsymbol{A}$ which allows determination of output parameter $\boldsymbol{z}$, the general case of inverse task is formulated by the following equation:

$$Au = z \qquad (2)$$

If we represent the unknown input parameter of the thermal state with $\boldsymbol{u}(t)$, where $0<\boldsymbol{t}<t_K$, and if $\boldsymbol{z}(t_K)$ denotes the known output parameter of the process, where $0<\boldsymbol{t}_K<t_m$, then the inverse method becomes:

$$Au \equiv \int_0^{t_K} u(t)\theta(t_K,t)dt = z(t_K) \qquad (3)$$

where $\boldsymbol{\theta}(t_K,t)$ is the initial characteristic of the process.

In equation (3), $\boldsymbol{u}(t)$ is the solution, i.e. heat flux or surface temperature of body, while function $\boldsymbol{z}(t_K)$ represents the temperatures measured outside the body at a point ***K***.

3. INVERSE METHOD OF THE GRINDING PROCESS

The role of mathematical theory behind thermal phenomena in grinding is to adopt the most adequate model of workpiece, grinding wheel and their inter-relationships. It is well known that, due to lack of continuous cutting edge, irregular geometry of grinding particles and their inconsistent distribution on the grinding wheel, it is very difficult to model the grinding process. If the numerous variable parameters were taken into consideration, analytical modeling of the grinding process would become an impossible task. Therefore, some simplifications are necessary where the final solution is verified by experiments. Despite simplification, such analytical and experimental model yields reliable results.

One can assume that the elementary heat source on the grinding particle is the result of friction between the grinding particle, workpiece and chip in the workpiece material shear plane. Summing up all the heat sources, i.e. grinding particles in contact with the workpiece, gives the total heat source for the entire cutting zone, $\boldsymbol{q}$. This total heat source, whose strength varies within a narrow range, acts continuously, shifting across the workpiece surface with constant velocity $\boldsymbol{v}_w$.

In surface grinding, considering that the cutting depth is many times smaller than the length and width of wheel/workpiece interface, the heat source can be treated as a strip of infinite length and constant heat distribution, Fig. 2. The assumption of constant heat distribution across the interface is valid approximation in case of the heating of thin surface layers of workpiece material.

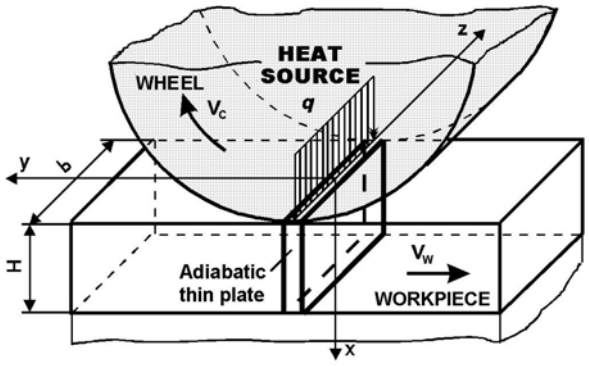

Fig. 2. Model of heat transfer in an elementary workpiece part in surface grinding

If we disregard the dissipation of heat flow in the direction of heat source movement, then the workpiece can be approximated with a semi-infinite plate, or, in other words, be divided up in a series of adiabatic thin plates, Fig. 2. Substitution of the real workpiece with the semi-infinite plate is completely justified, bearing in mind that the heat source in grinding is generated within a small volume of workpiece material while the heat loading of the surface workpiece layer is considered depth-wise.

For such defined thermal model of grinding, the following differential equation general case of a one-dimensional heat transfer:

$$\rho c(\theta)\frac{\partial\theta}{\partial t}=\frac{\partial}{\partial x}\left(\lambda(\theta)\frac{\partial\theta}{\partial x}\right)\qquad \begin{matrix} x\in(0,H) \\ t\in(0,t_m] \end{matrix} \qquad (4)$$

where: $\theta=\theta(x,t)$ - workpiece temperature at point coordinate x at moment t; $\lambda=\lambda(\theta)$ - heat transfer coefficient; $\rho c=C(\theta)$ - specific heat capacity (ρ - material density, c - specific heat); H - thickness of the surface layer of workpiece material; t_m - largest time increment.

Differential equation (4) should be considered in conjunction with the initial temperature distribution and boundary conditions [9].

The initial temperature distribution in the workpiece for the initial moment t=0:

$$\theta(x,t)\big|_{t=0}=\varphi(x)\qquad x\in[0,H] \qquad (5)$$

An additional condition is the fact that at the point $x=K$ ($0<K\le H$), there is a known temperature, measured during a time interval:

$$\theta(x,t)\big|_{x=K}=\xi(t)\qquad t\in[0,t_m] \qquad (6)$$

Boundarys of the considered workpiece surface layer are defined by the known temperature at the lower bound of the machined surface:

$$\theta(x,t)\big|_{x=H}=\overline{\psi}(t)\qquad t\in[0,t_m] \qquad (7)$$

and unknown temperature at the upper bound of the machined surface:

$$\theta(x,t)\big|_{x=0}=\psi(t)\qquad t\in[0,t_m] \qquad (8)$$

The final solution of the inverse problems is the maximal temperature on wheel/workpiece interface $\psi(t)$, and the temperature field $\theta=\theta(x,t)$ throughout entire elementary part of workpiece, $D=\{(x,t)$: $x\in(0,H]$, $t\in[0,t_m]\}$.

Due to high complexity, differential equations of the second order which describe the process of heat transfer in grinding are mostly solved using numerical methods. These methods transform exact differential equation into approximate algebraic equations.

To solve the partial differential equation (4) an implicit form of the finite differences method was chosen [7]. The concept of this method very much resembles the physical process, where the temperature at each observed point is calculated after a time increment as the result of heat exchange which the neighboring points.

Implicit form of finite differences extracted from the mesh area is shown in Fig. 3. Based on the five known temperatures at the neighboring points, the temperature at the next moment in time is calculated.

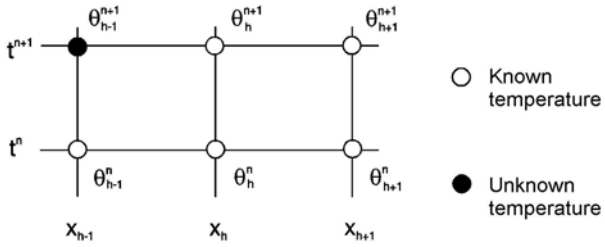

Fig. 3. Numerical method of finite differences in implicit form

System of linear algebraic equations is used to calculate the maximal temperature $\psi(t)$ on workpiece surface and the temperature field of the workpiece surface layer as follows:

$$[\mathbf{R}]\cdot\{\Theta\}=\{\mathbf{B}\} \qquad (9)$$

Solving the matrix system (9) requires the initial task to be divided into two parts.

Direct method of heat transfer within the area $D_2=\{(x,t)$: $x\in[K,H]$, $t\in[0,t_m]\}$. The solution yields the unknown temperatures θ_h^{n+1} (K+1,...,H).

Now, one can tackle the problems of inverse heat transfer in the area of $D_1=\{(x,t)$: $x\in[0,K]$, $t\in[0,t_m]\}$. Starting from the first unknown temperature θ_{K-1}^{n+1}, calculated the unknown temperature θ_h^{n+1} (h=0, ... ,K-1).

4. THE RESULTS USING INVERSE METHOD

As the proposed system uses experiment and analytical model to control the heat loading of wokrpiece surface layer in grinding, it requires distribution of temperatures to be determined experimentally at a point within the workpiece.

The experiment work was carried out on a surface creep-feed grinding machine »Majevica« type CF 412 CNC. The workpiece material was high-speed steel (DIN S 2-10-1-8) at 66 HRc hardness. The test was used an aluminum oxide wheel »Winterthur« type 53 A80 F15V PMF. The depth of cut was a=0,5 mm, the workpiece speed was v_w=5 mm/s and the wheel speed was v_s=30 m/s. A water-based coolant (emulsion 6%) was used during the grinding test.

For measurement, processing and control of grinding temperatures used modern information system. The temperature was measured in the workpiece surface layer using a thermocouple built into the workpiece at a specified clearance from the wheel/workpiece interface area. Application of

thermocouple is simple, reliable and cost-efficient, and does not interfere with the real cutting conditions.

In this case of verification, to calculate the workpiece heat loading by inverse heat transfer, the known temperature distribution at depth z = 1 mm was taken for additional boundary condition, Fig. 4.

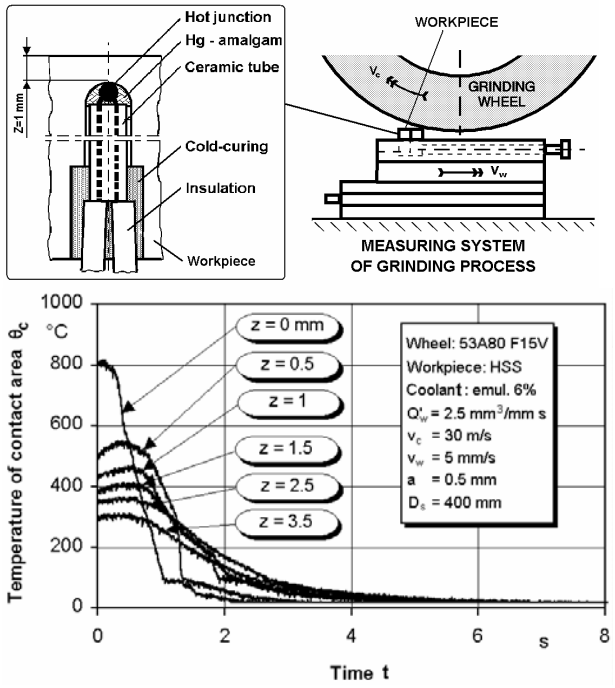

Fig. 4. Experimentally temperature distribution in time within the workpiece surface layer

Based on the previous experimental results, and considering the process boundary conditions and thermal/physical characteristics of grinding, the temperature field in workpiece surface layer was obtained by computation, as well as the maximal temperature on wheel/workpiece interface, Fig 5.

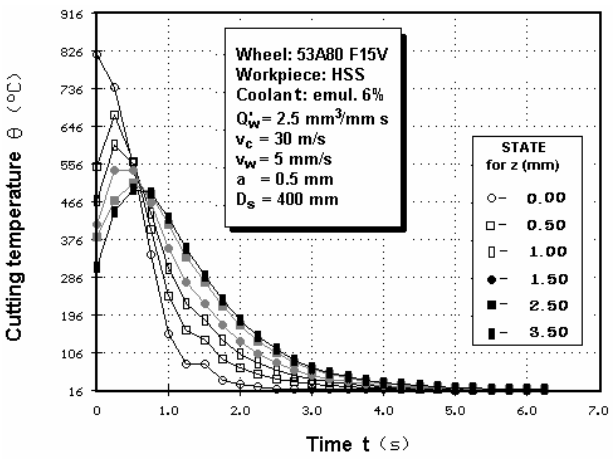

Fig. 5. Computation of temperature change over time in the workpiece surface layer

The computed time and depth-related change of temperature in the interface zone of the workpiece surface layer, shows high degree of conformity with the experimentally obtained results.

5. CONCLUSIONS

- Analytical inverse heat transfer method allows approximation of the temperature field in the surface layer of workpiece material with maximal temperature on wheel/workpiece interface;
- The inverse heat transfer method was solved using method of finite differences in implicit form;
- Analytically obtained temperature field in the workpiece surface layer largely agrees with experimental results.

6. REFERENCES

[1] Shaw M.C.: *A production engineering approach to grinding temperatures.* Journal of Materials Processing Technology, Vol. 44, 1994, pp. 159-169.

[2] Gostimirovic M., Milikic D.: *Control of the thermal effects in the grinding process (in Serbia)*, Monograph, Faculty of Engineering, Novi Sad, 2002.

[3] Guo S., Malkin S.: *Analytical and Experimental Investigation of Burnout in Creep-Feed Grinding*. Annals of the CIRP, Vol. 43/1/1994, pp. 283-286.

[4] Rowe W.B.: *Thermal analysis of high efficiency deep grinding*. Journal of Machine Tools and Manufacture, No 41, 2001, pp. 1-19.

[5] Lin B., Morgan M.N., Chen X.W., Wang Y.K.: *Study on the convection heat transfer coefficient of coolant and the maximum temperature in the grinding process*, Journal Adv Manufacture Technology, Vol. 42, 2009, pp.1175-1186

[6] Kim H.J., Kim N.K., Kwak J.S.: *Heat flux distribution model by sequential algorithm of inverse heat transfer determining workpiece temperature in creep feed grinding*. Journal of Machine Tools and Manufacture, No 46, 2006, pp. 2086-2093.

[7] Alifanov O.M.: *Inverse problems of heat transfer: theory and practice*, V Minsk international heat and mass transfer forum, Minsk, 2004.

[8] Beck J.V., Blackwell B., C.R. St. Clair: *Inverse Heat Conduction: Ill-posed Problems*. Wiley-Intercience Publication, New York, 1985.

[9] Ozisik M.N, Orlande R.B.: *Inverse Heat Transfer: Fundamentals and Applications*. Taylor & Francis, 2000.

Authors: **Assoc. Prof. Dr. Marin Gostimirovic, Prof. Dr. Pavel Kovac, Assis. Prof. Dr. Milenko Sekulic, Borislav Savkovic, dipl. ing.**, University of Novi Sad, Faculty of Technical Sciences, Institute for Production Engineering, Trg Dositeja Obradovica 6, 21000 Novi Sad, Serbia, Phone.: +381 21 450-366, Fax: +381 21 454-495.

E-mail: maring@uns.ac.rs
kovacp@uns.ac.rs
milenkos@uns.ac.rs
savkovic@uns.ac.rs

Note: This paper present a part of researching at the project *" Research and application of high-processing procedure"* Project number TR 14206, financed by Ministry of Science and Technological Development of Serbia.

Journal of Production Engineering
Vol.12 No.1

Kovač, P., Gostimirović, M., Sekulić, M., Savković B.

A REVIEW OF RESEARCH RELATED TO ADVANCING MANUFACTURING TECHNOLOGY

***Abstract*:** *Reviewed in this paper are some of the main developments in cutting technology and the most modern methods which are used in research of metal cutting technologies, as well as the methods which are already established in everyday application. Discussed are the methods of modeling and simulation of metal cutting processes and application of artificial intelligence, micromachining, monitoring of cutting processes, high-speed cutting (HSC), high-productivity cutting (HPC), machining of hard materials and dry cutting or minimum-lubricant micro-spraying (MMS*

Key words: *modeling, simulation, monitoring, HSC-machining, HPC machining, MMS-systems, Dry machining*

1. INTRODUCTION

Studies [1] came to the conclusion that there should be a strong integration of technologies and management using information technologies (IT), for example, integration of the process planning and production planning, simulation of manufacturing systems, agile manufacturing, fast redesign of new products, modeling of manufacturing equipment performance, including the human operator, functional product analysis, virtual machining and inspection algorithms etc.

Material removal processes can take place at considerably higher performance levels in the range up to Q_w = 150 - 1500 cm^3/min for most workpiece materials at cutting speeds up to some 8.000 m/min. Super hard cutting tool materials embody hardness levels in the range 3000 -9000 HV with toughness exceeding 1000 MPa.

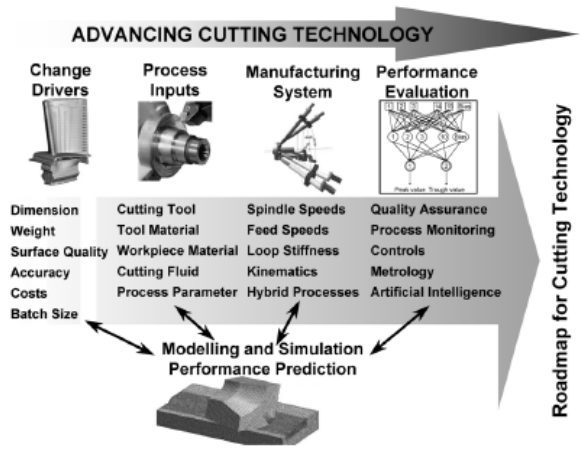

Fig. 1. Primary aspects associated with advancing cutting technology

The key change drivers in the case of cutting technology include: diminishing component size, enhanced surface quality, and tighter tolerances and manufacturing accuracies, reduced costs, diminished component weight and reduced batch sizes (Figure 1). These change drivers have a direct influence on the primary inputs to the cutting process namely the cutting tool and tool material, the workpiece material and the cutting fluid.

In parallel with the achievement of increased manufacturing accuracy there has been significant development in the reduction of the size of engineering components. One of the important issues associated with miniature components is that the surface area to volume ratio increases.

One of the key inputs to the cutting process is the cutting tool. The development of cutting tool materials has permitted a significant increase not just of cutting speed but also of feed rates.

In the last years emphasis has been placed on High Performance Cutting (HPC). Identified were the following aspects of cutting as being of particular significance in the quest for high performance cutting at high levels of productivity:

- Non Productive Times (NPT) in cutting processes,
- Dry and Near Dry Cutting (usage of minimal quantities of cutting fluids),
- Chip formation and chip handling processes and
- Strategies for burr minimization.

The economic efficiency of production facilities is a central issue for cutting technology. Conventional processes such as grinding and turning have come under close scrutiny from a productivity perspective and process chains have been analyzed and redesigned to minimize throughput times. The trend in recent years has been towards integrated processes. The requirement for integrated processes place new and demanding challenges on the design and technology of the cutting processes

2. MODELING AND SIMULATION

Generally the terms modeling and simulation were

use interchangeably in manufacturing research literature. In the case of cutting, there are many phenomenon that are not easily observed or not subject to direct experimentation so the models are developed so that the influence of a number of process parameters can be simulated using this model. Common models used are based on Eulerian or Lagrangian finite element techniques. Four primary categories of methodologies for modeling of cutting are evident:

- analytical modeling (determining the relationship between the forces in cutting based on cutting geometry and including experimentally determined values of shear angle, friction conditions and chip flow angle;
- slip-line modeling (predicts mechanical response and temperature distributions based on assumptions about slip line field geometry in the shear zone and around the tool;
- mechanistic modeling (predicts cutting forces for a wide range of complex machining processes based on the assumption that cutting forces are the product of the uncut chip area and specific cutting energy where specific cutting energy is empirically derived from workpiece material, cutting parameters, and cutting geometry;
- finite element modeling (FEM techniques use small mesh representations of the material and tooling as the basis for determining material stress and strain conditions and, ultimately, flow of material based on assumptions of continuity between adjacent elements)

The application of these modeling techniques covers the range of cutting processes and interests including cutting forces (static and dynamic), power, tool wear and life, chip flow angle/curl/form, built up edge, temperatures, workpiece surface conditions and integrity, tool geometry, coating and design influences, burr formation, part distortion and accuracy, tool deflection, dynamic stability limits and thermal damage. Processes modeled range from orthogonal cutting to multi-tooth milling, hard-turning and drilling.

Understanding the mechanisms of chip formation combined with the thermo-mechanical influence of the work-tool zone is critical to controlling the generation of a machined surface by pure plastic deformation required in this application. The cutting simulation includes realistic tool materials and a developed friction model to account for both sticking and sliding conditions. Chip flow, chip morphology, cutting forces, residual stresses, and cutting temperatures are predicted.

Burr formation – Understanding the mechanics of burr formation has been greatly enhanced by modeling of the burr formation process analytically, mechanistically and with finite element techniques.

Chip formation – Much attention has been paid to understanding the mechanisms of chip formation and the role of influential parameters. However, much progress is being made and models, especially finite element, are having an impact on the ability to understand this complex aspect of cutting. The increasing use of high speed machining has encouraged modeling of chip formation as well since the optimization of cutting at high speeds with exotic materials is not straightforward. Temperature and tool wear in cutting – Beside burr formation, cutting forces and chip formation quality of the cutting process is determined by the tool wear behavior and thermal load on the tool and workpiece [5]

A newer class of modeling of cutting, at the nanometer level, is referred to as molecular dynamics modeling. With the increase in micromachining to create molds and other features for a variety of components, it is interesting to see the "scale-ability" of larger scale phenomena to the nanoscale and, thus, the ability to control the quality of these components.

3. HIGH SPEED MACHINING

The inventor of HSM, C. Salomon, found that above a certain cutting speed machining temperatures start dropping again. His fundamental research showed that there is a certain range of cutting speeds where machining cannot be made due to excessively high temperatures. For this reason, HSM can also be termed as cutting speeds beyond that range. In compliance with modem knowledge, some researchers modern high-speed machining as machining whereby conventional cutting speeds are exceeded by a factor of 5 to 10.

With the wide use of CNC machines together with high-performance C AD/C AM systems, high-speed machining (HSM) has demonstrated its superior advantages to other rapid manufacturing techniques. In addition to increased productivity, HSM is capable of generating high-quality surfaces, burr-free edges, and virtually stress-free components after machining, and can be used to machine thin-wall workpieces, because the cutting forces involved in HSM conditions are lower. Another significant advantage of high-speed machining is minimization of effects of heat on machined parts. Most of the cutting heat is removed, reducing thermal warping and increasing the life of the cutting tool. In many cases, the need for a cooling fluid is eliminated. Furthermore, the elimination of cutting fluids reduces subsequent contribution to pollution and aids in the recovery and recycling of such expensive materials as aluminum-lithium alloys. Since HSM has so many advantages, it is widely used in the aerospace industry, automotive industry, precision engineering industry for machine tools, equipment, and tooling used in the manufacture of domestic appliances, optics, etc.

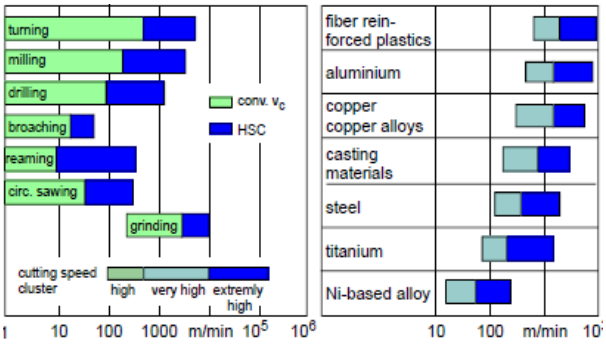

Fig. 2. Achievable cutting speeds [8]

Although high-speed milling of aluminum has been applied in industries successfully for more than a decade, high-speed applications on difficult-to-cut materials, such as titanium alloys, are still relatively new. Boeing's military aircraft group has begun to apply its expertise with aluminum toward faster milling of titanium. And they concluded that compared to aluminum, titanium imposes certain constraints. Speed is constrained as heat builds up more quickly. But within those constraints, there is still considerable room for faster cutting.

Titanium alloys have been widely used in the aerospace, biomedical, automotive and petroleum industries because of their good strength-to-weight ratio and superior corrosion resistance. However, it is very difficult to machine them due to their poor machinability. During the machining of titanium alloys with conventional tools, tool wear progresses rapidly because of their low thermal conductivity and high chemical reactivity, resulting in higher cutting temperature and strong adhesion between the tool and the work material. Titanium alloys are generally difficult to machine at cutting speeds of over 30 m/min with high-speed steel (HSS) tools, and over 60 m/min with cemented tungsten carbide (WC) tools, resulting in very low productivity.

4. ADVANCES IN MECHANICAL MICROMACHINING

4.1 Process physics

Micromachining incorporates many characteristics of conventional machining. At the same time, micromachining raises a great number of issues mainly due to size or scale. Downsizing the scale of machining does not change the general characteristics of the process to some reasonable limit. However, when either the ratio of part size to be produced or size of the microstructure of the work material to the tool dimension used (say diameter) becomes small (approaching a single digit), size effects can change the whole aspect of machining. There are two different aspects of size effects of concern, e.g. when the depth of cut is on the same order as the tool edge radius, and where the microstructure of workpiece material has significant influence on the cutting mechanism

4.2 Micro-tools

Commercially-available micro-drills are typically on the order of 50 μm in diameter, and have similar twist geometry to that of conventional drills. Flat drills with simplified geometries are more common for diameters smaller than 50 μm.

Fabrication of micro-tools is another challenge in micromachining. Imprecise geometry and the irregularity of tools often negate the advantages of ultra precision process control, state of the art machine tools, and ultra fine tuning of process parameters.

Due to its hardness, single crystal diamond is the preferred tool material for microcutting. Diamond cutting tools were used in most of the early micromachining research due to their outstanding hardness (for wear resistance) and ease by which a sharp cutting edge could be generated through grinding. However, as diamond has a very high affinity to iron, microcutting is mostly limited to the machining of nonferrous materials such as brass, aluminum, copper, and nickel. Hence, micromachining tests have been limited to non-ferrous materials. In [10] developed a machine tool fabrication process utilizing ELID grinding technology to fabricate various cross sectional shapes of the tool with high surface quality, Figure 3.

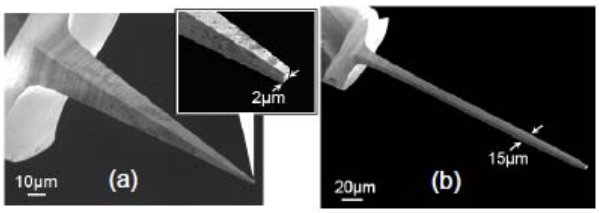

Fig. 3. Overviews of produced micro-tools under optimum machining conditions: (a) Ultra precise tool (b) Extremely large aspect ratio micro-tool [10].

4.3 Microfactories

In general, micromachining is performed on precision machine tools with conventional dimensions. However, the work size and the required power for processing are relatively much smaller for micromachining. Downsizing the machine tool itself has been pursued by several machine tool builders and researchers in order to achieve economic benefits such as structural cost savings, shop floor space savings, energy reduction and performance benefits including reduction of thermal deformation, enhancement of static rigidity and dynamic stability as well.

One unique effort is to build a microfactory system where one or several machine tools are small enough to be placed on the desktop. In late 1980s, Japanese researchers started fabricating microfactory prototypes, and the first realization of the concept was a microlathe smaller than a human palm with 1.5W spindle motor [11], followed by more powerful and precise desktop and portable machines.

5. TURNING OF HARDENED STEEL

In our days the machining of steel parts in hard state has great significance. The primary goal is to substitute the grinding technology with turning, milling or drilling. Turning operations are called hard turning, which are performed

- in order to required shape and surface roughness,
- to substitute grinding operation, on at least 45 HRc hard steel part, with hard metal, ceramic or polycrystalline cubic boron nitride (PCBN) tools,
- in CNC lathe machines or a rigid conventional lathes.

The occasional occurrence of white layers in machining hardened steel proves that short-time metallurgical processes can be induced by the respective chip formation mechanisms. The occasional occurrence of white layers in machining hardened steel proves that short-time metallurgical processes can be induced by the respective chip formation mechanisms.

The Table 1 shows the advantages and disadvantages of hard turning [7].

Hard turning	
Advantages	Disadvantages
Short operation	Heavy tool wear
Less investment	Cutting edge is reactive to break
Free grinding capacities	Rigid machine tool with high spindle speed
High accuracy in case of accurate blank	Up-to-date CNC control is needed (tool break control)
The heat of cutting is removed by chips	Tool holders for high speed machining is required
2-4 times higher material removal speed	Application of up-to-date tool materials and coats
Good surface roughness	Inhomogeneous part material is unfavorable
More operation elements are performed in one setup	In case of grinding the sparking process can increase accuracy and decrease surface roughness
Appropriate for dry machining	In certain cases, better surface roughness is produced by grinding

Table 1. Advantages and disadvantages of hard turning

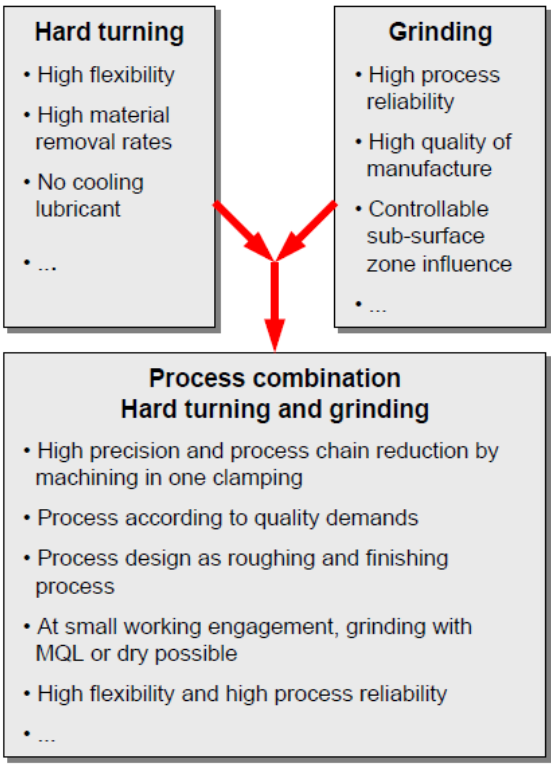

Fig. 4. Utilization of process specific advantages by process combination [7]

The chip formation mechanisms in hard machining were first investigated by Ackerschott [7], who postulated high compressive stresses in the surface layer causing cracks in front of the cutting tool under an angle of 45° to the surface. At the same time the material is plastically deformed by the rounded cutting edge. The sliding of a chip segment along the crack reduces the compressive stresses until a further crack is induced due to the continuous movement of the tool.
Due to their characteristics, the processes hard turning and grinding are not arbitrarily interchangeable. They rather complement each other. This motivated the development of machine tool concepts, which permit the hard turning and grinding operations in one chucking. As a result, the advantages of each process can be combined, Figure 4. [7].

6. MONITORING OF CUTTING OPERATIONS

The complex interactions between machines, tools, workpieces, fluids, measurement systems, material handling systems, humans and the environment in cutting operations requires that sensors be employed to insure efficient production, protect investment, indicate needs for maintenance, and protect workers and the environment. Early developments have proven that process monitoring is essential for economic production. Most significant for availability and quality are tool wear and tool breakage. An excellent overview of monitoring of machining for tool condition monitoring can be found in [3]. Standard approaches on process monitoring are the measurement or identification of the interaction between process and machine structure. Particularly the vibration behavior plays an important role, since it significantly affects the workpiece accuracy as shown by simulation and experiment e.g. in [3].

An indication of the evolution of monitoring systems in manufacturing was presented by Tönshoff. Frankly, there has not been much advancement from the state outlined by Tönshoff. But now there are additional requirements for increased flexibility. Specifically, sensor systems must be able to be interfaced with open system architecture controllers for machines and systems must be designed to accommodate needs of so called “reconfigurable” systems. Activity in both of these areas is still predominately in the research stage with few industrial applications.

To achieve the “intelligent machine tool,” which has as its objective to be able to maintain an optimized cutting performance, requires sensor along with control systems with the knowledge accumulation capability to store the acquired “experience” for use in future production.

Further, given the development of reconfigurable systems, monitoring strategies must be flexible enough to accommodate different machine configurations and processes. This would be logically tied in with machine control hardware and software in an “open” environment. In that sense, this would be an example of the “intelligent sensor”. Recent developments aim at different directions. Some are based on new fields of production, other use new sensor concepts. Most process monitoring systems are designed for processes of limited complexity like drilling, thread cutting or straight pass milling. Whereas solutions for sculptured

surface milling, especially ball end finishing operations, are still not available on the market. These have a great significance in die and mould finishing with only small process forces. New approaches use special sensors to measure force or accelerations for process monitoring in milling of sculptured surfaces.

The standard fixed threshold method has been adapted to be more universal. Dynamic boundaries combined with neural networks. Neural networks have proven to be effective for small size productions. Especially flank wear of tools in milling can be monitored with neural networks.

It seems to be an obvious solution to use dynamic systems for the supervision of a dynamic process like a cutting process. Probably due to stability problems, the output of pure dynamic networks is limited. A promising approach is a model in which a static and a dynamic networks are combined hierarchically as a "state space representation" of the cutting process. The field of high speed cutting (HSC) introduces new dynamic effects to the process monitoring. The standard analysis methods dominated by the Fast Fourier Transformation (FFT) are extended by Wavelet Transforms and Cepstrum Analysis, the later proven to be especially sufficient for machine and process monitoring.

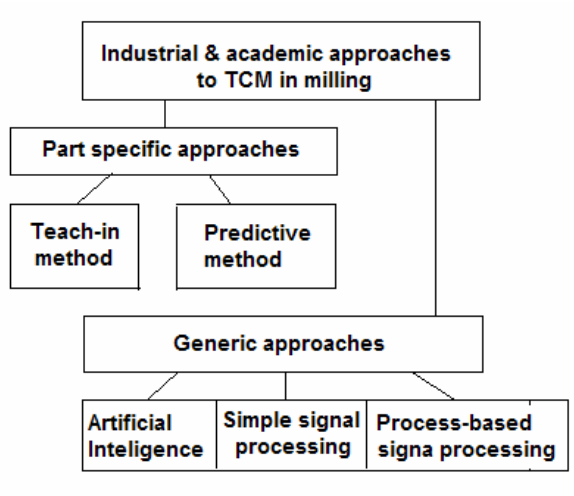

Fig. 5. TCM Classification

Considering the range of sensors and applications in the cutting process, the machine tool requires a large number of sensors. Integrated sensor systems can today accomplish several tasks and cooperate to insure process optimization. Cutting performance overall requires reduction in process and non-productive times, verification and maintenance of process capability, while reducing direct production costs and ensuring environmentally-friendly production.

7. SUSTANABILITY CONCEPTS IN MACHINING

The paradigm of product manufacturing towards low cost and high profits is unlikely to change significantly in the near future. The integration of environmental requirements into every single stage of product development from very beginning is very likely approach, it will not purely add-on some constrains, but it will identified new environmental features of a product that have potential to improve the overall quality of the product in the eyes of the customer and eventually decrease the overall cost. In the area of technologies, processes and products efficiency has the dimension of economy, ecology and socials. Cost of energy and materials have an impact on economic effectiveness. The reduction of resources is contribution to the economic and ecology effectiveness. The way to help to companies to improve their economical, environmental and social performance is by [12]:

- minimizing waste and increase reusing or recycle
- using materials, water and energy more efficiently,
- avoiding or improving managements of cooling and lubricating fluids and hydraulic oils
- adopting lean manufacturing and other sustainable techniques
- improve working conditions and use best practice machining
- train employees about sustainable practices, etc

7. 1. Dry machining and minimum quantity lubrication

A change in environmental awareness and increasing cost pressures on industrial enterprises have led to a critical consideration of conventional cooling lubricants used in most machining processes. Depending on the workpiece, the production structure, and the production location the costs related to the use of cooling lubricants range from 7 - 17% of the total costs of the manufactured workpiece [2]. By abandoning conventional cooling lubricants and using the technologies of dry machining or minimum quantity lubrication (MQL), this cost component can be reduced significantly. Besides an improvement in the efficiency of the production process, such a technology change makes a contribution to the protection of labor and the environment. The reduction of substantial exposure to cooling lubricants at the work place raises job satisfaction and improves the work result at the same time. Furthermore, an enterprise can use economically-friendly production processes for advertising purposes, which leads to a better image in the market.

The implementation of dry machining cannot be accomplished by simply turning off the cooling lubricant supply. In fact, the cooling lubricant performs several important functions, which, in its absence, must be taken over by other components in the machining process. Cooling lubricants reduce the friction, and thus the generation of heat, and dissipate the generated heat. In addition, cooling lubricants are responsible for a variety of secondary functions, like the transport of chips as well as the cleaning of tools, work pieces and fixtures. They provide for a failure-free, automated operation of the production system. In addition, cooling lubricants help to provide a uniform temperature field inside the workpiece and machine tool and help to meet specified tolerances.

7.2 MQCL

In many machining operations, minimum quantity cooling lubrication (MQCL) is the key to successful dry machining. Any move to manufacture functional components under dry machining conditions depends on an understanding of MQCL as a system, whose individual components – feed technology, MQCL media, parameter settings, tools, and machine tools mutually affect the operation of all of the others (Figure 6.). All of the components in the MQLC system must be very carefully coordinated in order to achieve the desired outcome, which is optimal, both technologically and economically.

In MQCL operations, the media used is generally straight oil, but some applications have also utilized an emulsion or water. These fluid media are fed to the tool and/or machining point in tiny quantities. This is done with or without the assistance of a transport medium, e.g., air. In the case of the former, the so-called airless systems, a pump supplies the tool with the medium, usually oil, in the form of a rapid succession of precision-metered droplets.

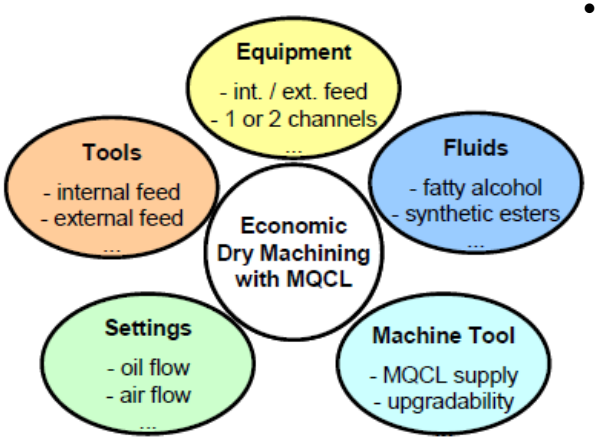

Fig. 6. Minimum quantity cooling lubrication system

In the case of the latter, the medium is atomized in a nozzle to form extremely fine droplets, which are then fed to the machining point in form of an aerosol spray.

Within the context of dry machining, the term MQCL is generally used to refer to the supply of the cooling lubricant in the form of an aerosol. Depending on the type and on the main function of the fluid medium supplied, a distinction can be drawn between minimum quantity lubrication (MQL) and minimum quantity cooling (MQC).

7.3 Supply Systems

A distinction is drawn in the minimum quantity lubrication technique between external supply via nozzles fitted separately in the machine area and internal supply of the medium via channels built into the tool (Figure 7.). Each of these systems has specialized individual areas of application.

Fatty alcohols and synthetic esters (chemically modified vegetable oil) are the media most commonly used in MQL applications. The medium selected depends on the type of supply, the material involved, the machining operation, and subsequent finishing operations required by the part (e.g., annealing, coating, and painting).

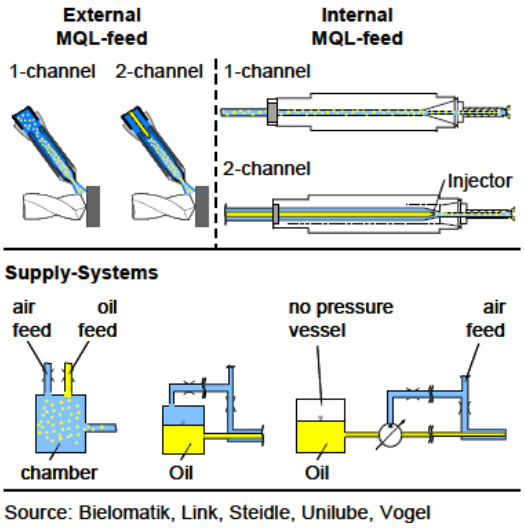

Fig. 7. MQL-feed systems [2]

7.4 Cryogenic machining

- Cryogenics express study and use of materials at very low temperatures, below -150 ºC. However, normal boiling points of permanent gases such as helium, hydrogen, neon, nitrogen, oxygen, normal air as cryogens lie below -180 ºC. Cryogenic gases have a wide variety of applications in industry such as health, electronics, manufacturing, automotive and aerospace industry particularly for cooling purposes. Liquid nitrogen is the most commonly used element in cryogenics. It is produced industrially by fractional distillation of liquid air and is often referred to by the abbreviation, LN2. Nitrogen melts at -210.01 ºC and boils at -198.79 'C, it is the most abundant gas, composes about four-fifths (78.03%) by volume of the atmosphere. It is a colorless, odorless, tasteless and non-toxic gas. Some potential benefits of cryogenic machining are [14]:
  - Sustainable machining (cleaner, safer and environmentally friendly)
  - Increased material removal rate without increasing in tool wear
  - Increasing tool life due to lower abrasion and chemical wear,
  - Improve machining part surface integrity
  - Chip breaking improvement
  - Decrease of BUE and burr formation probability

  Cryogenic cooling approaches in material machining could be classified into four groups according to applications of the researchers: cryogenic pre-cooling the workpiece by repulsing or an enclosed bath and cryogenic chip cooling, indirect cryogenic cooling or cryogenic tool back cooling or conductive remote cooling, cryogenic jet cooling by injection of cryogen to the cutting zone by general flooding or to the cutting tool edges or faces, tool–chip and tool–work interfaces by micro-nozzles, Figure 8. [13].

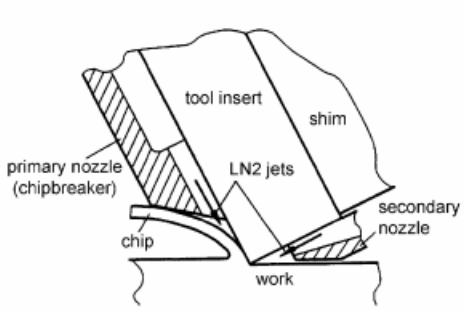

Fig. 8. Schematic diagram of LN2 nozzle system

7.5 High pressure jet assisted machining

High pressure jet assisted machining is an innovative method of cooling and lubrication of the cutting zone. It relates to delivering the oil base or water based in relatively small flow rates under extremely high pressure up to 300 Mpa. CLF under such pressure penetrate closer to the share zone and cools it Figure 9. [14]. This offers control of chip breakability through forming a physical hydraulic effect between rake face and chip. HPJAM involves high pressure pump, high pressure tubing, and outlet nozzle. Some potential benefits are:

- Sustainable machining through lower rates of fluid and providing better cooling and lubricant mechanisms,
- Decrease cutting tool contact length
- Lower cutting forces and extend tool life
- Improve chip breakability and decrease BUE formation

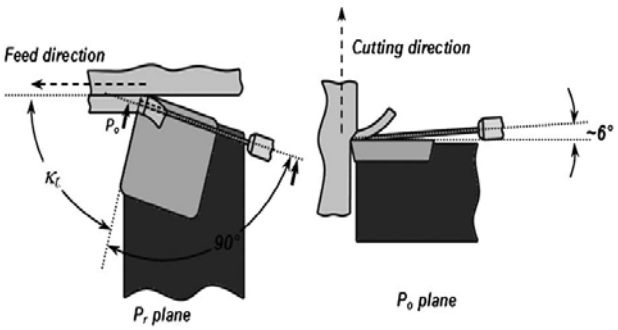

Fig. 9. Cutting fluid jet injection position

7.3 Cutting Materials

Especially in dry machining processes cutting edges and guiding pads are subject to high mechanical, thermal, and chemical loads. To ensure a good performance and a high wear resistance, the cutting materials have to fulfill certain requirements regarding their physical properties. Figure 10 illustrates an ideal cutting material, combining properties like high hardness, good toughness, and chemical stability. However, these requirements represent opposing properties so that an optimal and universal cutting material is not realizable from a technological point of view.

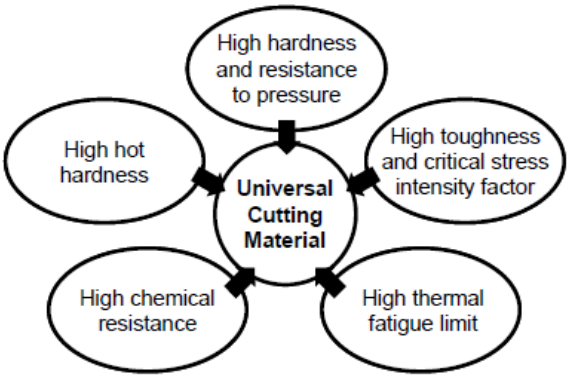

Fig. 10. Optimal cutting materials for dry machining

8. CONCLUSION

It is obvious that cutting technology has made remarkable progress in the last years. The thrust towards the application of higher performance workpiece and cutting tool materials, towards usage of minimal quantities of cutting fluid, to higher precision and to the application of micro-systems will continue. The technological capabilities of cutting systems will continue to develop and higher performance with enhanced safety standards and environmental cleanliness and lower manufacturing costs will result.

Disparate sensor systems as part of open architecture control will contribute to the development of "intelligent" machining systems with learning ability. Specific cutting process and process effects will benefit from continued modeling research including cutting hard materials, burr formation, and chip formation. Molecular dynamics modeling offers potential for coupling micro and nano scale process features with macro scale processes. The improvement in modeling capability from macro to nano scale processes drives improved process simulation and process understanding.

9. REFERENCES

[1] G. Byrne, D. Dornfeld, B. Denkena: Advancing Cutting Technology, CIRP Annals, 52/2, 2003, pp 483-507

[2] K. Weinert1, I. Inasaki, J. W. Sutherlan, T. Wakabayashi: Dry Machining and Minimum Quantity Lubrication, Anals of the CIRP Vol 55/2, 2004, pp

[3] Byrne, G., Dornfeld, D., Inasaki, I., König, W., Teti, R., 1995, Tool Condition Monitoring (TCM) – The Status of Research and Industrial Application, Anals of the CIRP 44/2:541-567

[4] Dorfeld D., Min S., Takeuchi Y.: Recent Advances in Mechanical Micromachining, Anals of the CIRP Vol 55/2, 2006, pp 745-768

[5] F. Klocke, H. W. Raedt, S. Hoppe: 2D –FEM Simulation of orthogonal High Speed Cutting Process. Mach. Sci. And Tech, 5/3, 2002, 323-340

[6] Komanduri, R., Chandrasekaran, N., Raff, L.M.: MD Simulation of Exit Failure in Nanometric

Cutting, Materials Science and Engineering A, 311/1-2, 2001, pp 1-12F.
[7] Klocke1, E. Brinksmeier, K. Weinert: Capability Profile of Hard Cutting and Grinding Processes, CIRP Annals, 55/2, 2005, pp 557-580
[8] Schulz H., at all.: 20 Jahre HSC, Sonderfeld, Werkstadt und Betrieb, 1981
[9] P. Sriyotha, K. Nakamoto, M. Sugai, K. Yamazaki:, A Design Studyon, and the Development of, a 5-Axis Linear Motor Driven Super-Precision Machine, CIRP Annals, 55/1, 2006
[10] Ohmori, H., Katahira, K., Uehara, Y., Watanabe, Y., Lin, W, Improvement of Mechanical Strength of Micro Tools by Controlling Surface Characteristics, CIRP Annals, 52/1, 2003467-470.
[11] Tanaka, M.: Development of Desktop Machining Microfactory, Riken Review, 34, 2001, 46-49.
[12] Pusavac F., Kopac J.: Achiving and Implementation of Sustanability Principles in Machining Proceses, Advances in production Engineering Management, 4, 2009,3, 151-160
[13] Yildiz, Y., Nalb, M.: A review of cryogenic cooling in machining processes International Journal of Machine Tools & Manufacture 48 (2008) 947–964
[14] Courbon C., Kramar, D., Krajnik, P., Pusavec F., Rech, J., Kopac J.: Investigation of machining performance in high-pressure jet assisted turning of Inconel 718: An experimental study International Journal of Machine Tools & Manufacture 49 (2009) 1114–1125
[15] Rahman M., Wang, Z. G., Wong, Y. S.: A Review on High-Speed Machining of Titanium Alloys, JSME I J, Series C, Vol. 49, No.1, 2006
[16] Fang, F.Z., Wu, H., Liu, X.D., Liu, Y.C., Ng, S.T., 2003, Tool Geometry Study in Micromachining, Journal of Micromechanics and Microengineering, 3/5:726-731.

Authors: **Prof. Dr. Pavel Kovac, Assoc. Prof. Dr. Marin Gostimirovic, doc. Dr. Milenko Sekulic, dipl.ing**. **Borislav Savkovic,** University of Novi Sad, Faculty of Tehnical Sciences, Production Engineering Institute, Trg Dositeja Obradovica 6, 21000 Novi Sad, Serbia, Phone.: +381 21 485-2324,
E-mail: pkovac@uns.ac.rs
maring@uns.ac.rs
milenkos@uns.ac.rs
savkovic@uns.ac.rs

Note: This paper present a part of researching at the project *" Research and application of high-processing procedure"* Project number TR 14206, financed by Ministry of Science and Technological Development of Serbia.

Journal of Production Engineering
Vol.12 No.1

Kovač, P., Gostimirović, M., Sekulić, M., Savković B.

A REWIEV TO ADVANCED MODELING AND SIMULATION OF MACHINING PROCESS

Abstract: *In the case of machining process, there are many phenomenon that are not easily observed or not subject to direct experimentation so the models are developed so that the influence of a number of process parameters can be simulated using this model. Common models used are based on Eulerian or Lagrangian finite element techniques. Four primary categories of methodologies for modeling and simulation of machining process are evident. Analytical modeling (determining the relationship between the forces in cutting based on cutting geometry and including experimentally determined values of shear angle, friction conditions and chip flow angle. To obtain as much information as possible the design of experiments (DOE) is applied to the modeling and simulation process.*
Key words: *modeling, simulation, FEM, virtual machining process*

1. INTRODUCTION

The manufacturing process research should lead to improved design of tools, machine tool structures, spindle and feed drives and the optimal planning of individual machining operations based on physical constraints. The research activities and industrial applications of metal cutting process simulation are presented in the following sections. The amplitude and frequency of cutting forces, torque and power are used in sizing machine tool structures, spindle and feed drive mechanisms, bearings, motors and drives as well as the shank size of the tools and the fixture rigidity.

The stress and temperature field in the cutting tool edge, chip and finished work piece surface are used in designing the cutting edge shape as well as in optimizing feed, speed and depth of cut to avoid residual stresses on the finished surface. Modeling the interaction between the cutting process and structural vibrations of machine tool, cutting tool and fixture leads to the identification of weak links in the machine structure and to the determination of chatter vibration free spindle speeds and depths of cut [5]. The complete model of the machining process is therefore used in both design of cutting tools and machine tools, as well as in planning of machining operations for maximum productivity and accuracy.

1.1 Analytical modeling of cutting processes

The first step is to model the cutting process as a function of work material, tool geometry and material, chip load and cutting speed. The macro-mechanics of cutting lead to the identification of cutting coefficients, which are used in predicting the cutting forces, torque, power and chatter stability limits for a specified tool geometry and work material. The cutting coefficients can be modeled using either orthogonal cutting mechanics or mechanistic models. The micro-mechanics of metal cutting on the other hand, are used to predict the stress, strain and temperature distribution in the chip and tool. This simulation results are primarily used for tool design, the analysis of material behavior under high strain and temperature, and optimal selection of chip load and speed to avoid tool chipping, tool wear, and residual stresses left on the finished surface.

1.3 Numerical simulation of cutting processes

For cutting processes involving geometrically defined cutting edges, high speed cutting (HSC) is widely used in aerospace, and the die and mold machining industry. High speed machining allows the operation of machine tool spindles in large stability pockets where deeper cuts are possible. While keeping small chip loads to avoid thermal overload of the tool edge and mechanical overload of the spindle power limits, high material removal rates can be achieved with high spindle speeds and table feeds while maintaining a good surface finish on the part. However, the practical application of HSC methods depends on empirical cutting data which has to be obtained through cost- and time-consuming cutting experiments.

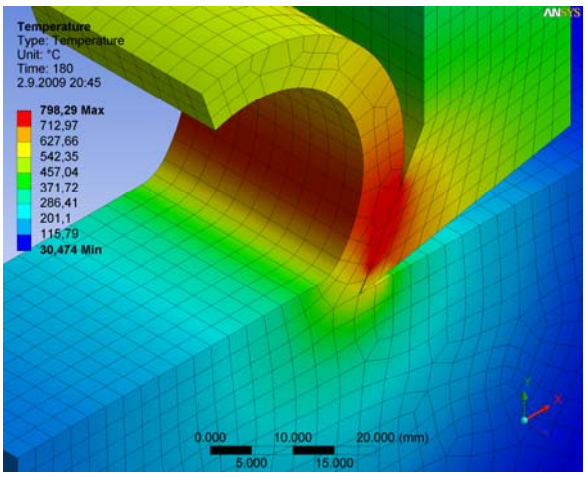

Fig. 1. FEM simulation of cutting temperature during turning and mesh

Authors FEM simulation of cutting temperature distribution during turning is shown in Fig 1.

The Finite-Element-Method (FEA) is a tool that is suited for optimization of the cutting edge geometry and material. Hence the cutting edge can withstand high thermal and impact loads during machining. Finite-Element- Analysis belongs to the class of micro-mechanics of metal cutting and is widely used by the cutting tool industry. However, the key bottle neck is to model the flow stress of the work material reflecting high strain, strain rate and temperature experienced in metal cutting processes. The thermo-plastic properties of the material are usually evaluated under high strain rate conditions using either Orthogonal Cutting Tests or Hopkinson Bar tests [1]. Three main methods of mechanical formulation are commonly used in Finite-Element-Modeling of metal cutting [1], [2]:

- Eulerian formulation, where the grid is not attached to the material, is computationally efficient but needs the updating of the free chip geometry,
- Lagrangian formulation, where the grid is attached to the material, requires updating of the mesh (remeshing algorithm) or the use of a chip separation criterion to form a chip from the workpiece,
- Arbitrary Lagrangian Eulerian (ALE) formulation, where the grid is not attached to the material and it can move to avoid distortion and update the free chip geometry.

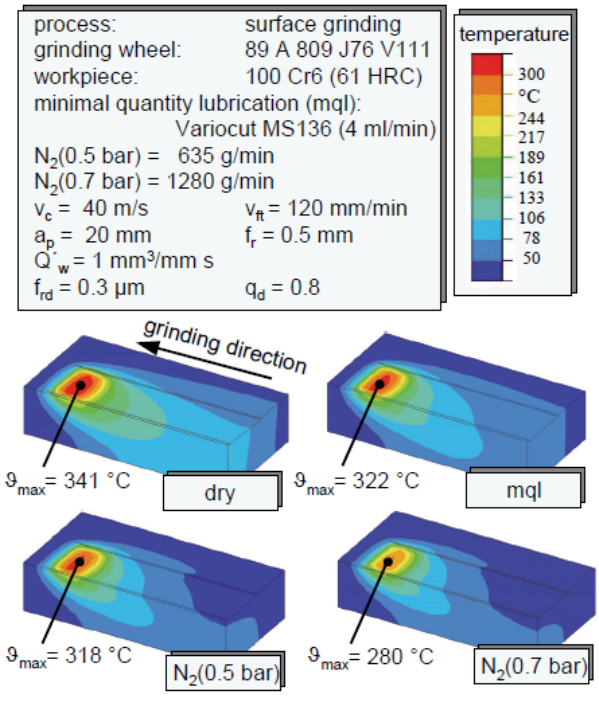

Fig. 2 Temperature field distribution for cooling and lubrication conditions [8]

A successful simulation is dependent on the accurate knowledge of the boundary conditions and the material behavior which is different from simple metal models obtained from tensile tests due to the influence of large strain, strain rate, and temperature. In order to achieve an accurate prediction of chip flow, stress and temperature distribution within the chip and tool, an accurate model of flow stress of the material and friction between the rake face of the tool and chip is absolutely necessary. The validity of all numerical models is proven experimentally by comparing predicted forces, average shear angles and shear stresses in metal cutting tests.

For surface grinding, several FEA models have been developed. A three dimensional FEA workpiece model was applied by Hoffmeister to simulate the temperature distribution during grinding. Figure 2. illustrates the effects of different coolant supply conditions on the temperature distribution in the workpiece [8]. It is also possible to calculate the longitudinal shape deviation of the workpiece after grinding. During grinding with continuous dressing a longitudinal shape deviation was smaller by a factor of 10 than during grinding without continuous dressing

Afore mentioned FE modeling is primarily for isotropic micromachining where no crystallographic effects were considered. Chuzhoy et al. [1] developed a FE model for micromachining of heterogeneous material, Figure 3. Their model was capable of describing the microstructure of multi phase materials and thus captured the microcutting mechanism in cast iron. Microcutting of multi phase materials exerts larger variations in the resulting chip shape and the cutting force than seen in cutting of a single phase material.

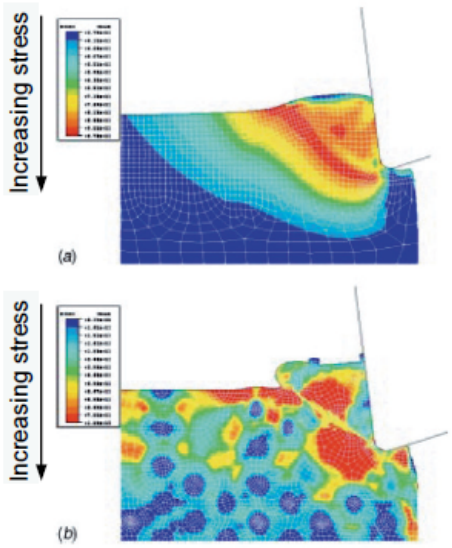

Fig. 3. Computed equivalent stress for 125 µm depth of cut and 25 µm edge radius at t=0.00012 s with (a) ferritic workpiece, (b) ductile iron workpiece [1]

Park et al. [2] tried to calibrate the mechanistic cutting force through FEM simulation for ferrous materials including increasing stress Increasing stress - 751- ductile and gray irons and carbon steels. Their model is primarily based on analysis of the microstructure of the work materials in their various phases, such as the graphite, ferrite, and pearlite grains seen in ductile iron, gray iron, and carbon steel microstructures. Their model was mainly used to calibrate a cutting force model, Figure 4.

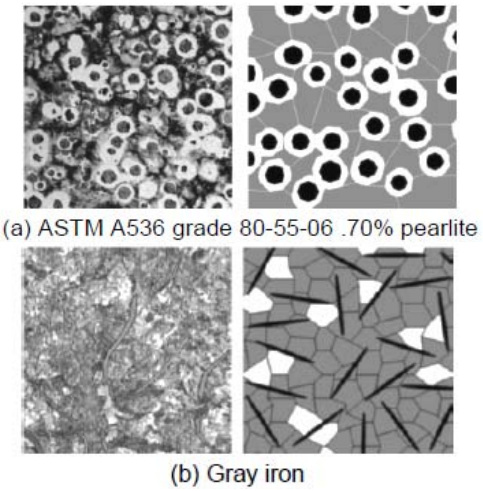

Fig. 4. Actual (left column) and simulated (right column) microstructures of different materials [2]

2. APPLICATION OF DESIGN OF EXPERIMENTS TO THE CUTTING SIMULATION

The simulation of metal cutting processes should be suitable to enlarge the understanding of the chip formation mechanism. To achieve this aim the simulation results have to be verified by experimental values such as resultant forces and temperatures. As these values strongly depend on the input values of the two dimensional simulation the current chapter examines the influence of different input parameters on the simulation results. To obtain as much information as possible the design of experiments (DOE) is applied to the simulation process.

Design of Experiments (DOE) or Experimental Design was defined as follows: Experimental Design consists of purposeful changes of the inputs (factors) to a process in order to observe the corresponding changes of the outputs (responses). The process is defined as some combination of machines, materials, methods, people, environment and measurement which - when used together - perform a service, produce a product or complete a task.

A further advantage of applying experimental design is that more information can be gathered by conducting fewer experiments. This advantage was first used in agriculture where experiments would last several months. Thanks to the improvement of computing systems, the duration of a cutting simulation is reduced from weeks to several hours. Nevertheless, because of the high amount of input variables and assumption that have to be made, many simulations have to be conducted to identify the influences of the variables. The process is considered as “black box”, only the inputs and outputs are known (Figure 5). In the current work the simulation is this “black box” which means that all numerical iterations and calculations are assumed to be unknown. Therefore, the design of experiments (DOE) is applied to identify the influence of input variables on the simulation result (figure 7.8 right). These inputs can be of numerical nature as well as physical properties of the examined materials. In the current investigation, the numerical inputs were kept constant and only the influence of the physical properties on the simulation result was considered. It may seem astonishing that physical values are set on two levels and were not implemented as temperature dependent variables. Of course better simulation results can be expected when the input parameter is given as a function of the temperature. On the other hand the assumption of constant values on two levels has three advantages:

- The DOE can be applied to identify the significant inputs. The number of inputs has to be reduced because of the high efforts that are necessary to obtain them.
- The direction of the output change (e.g. increase in temperature) can be assigned to the high or low level of the input.
- Some inputs are not defined or cannot be measured over the whole range of temperature.

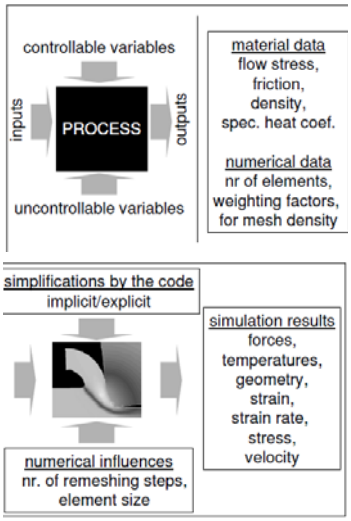

Fig. 5. Design of experiments and its application to cutting simulation

3. MOLECULAR DYNAMIC SIMULATION

Research work on molecular dynamic simulation (MD) of cutting can be traced back to early 1990s. Most of the early researchers used copper as a work material because of its well established structure and potential function. A diamond was used as a cutting tool since it can be reasonably assumed to have a very sharp edge, needed at the MD level.

The work of Inamura et al. focused on a trial of molecular dynamics at an atomic level cutting simulation with a couple of potential functions. This computational study showed that MD is a possible modeling tool for the micro cutting process. The simulation was able to correlate the intermittent drop of potential energy accumulated in the workpiece during cutting with the heat generation associated with plastic deformation of the workpiece and impulsive temperature rise on the tool rake face. They also reported that the rate of energy dissipation in plastic deformation at this scale is larger than in conventional cutting and that a concentrated shear zone did not appear, contrary to what is normally observed in conventional cutting. In general, MD simulation requires impressive computational power in order to

model a cutting process. Hence, many MD models have been applied to two dimensional orthogonal cutting with a very small model size, or unrealistically high cutting speed. Komanduri et al. [3] proposed a new method called a length-restricted molecular dynamics (LRMD) simulation by fixing the length of the work material and shifting atoms along the cutting direction and applied it to nanometric cutting with realistic cutting speeds. They also studied the effect of tool geometry using several ratios of tool edge radius to the depth of cut with various parameters such as cutting force, specific energy, and subsurface damage [7] and further investigated the effect of crystal orientation and direction of cutting on single crystal aluminum and silicon. They also applied MD simulation to exit failure and burr formation in ductile and brittle materials with a face centered cubic (FCC) structure. They successfully simulated burr formation on a ductile material and crack propagation in brittle material, Figure 6 [3].

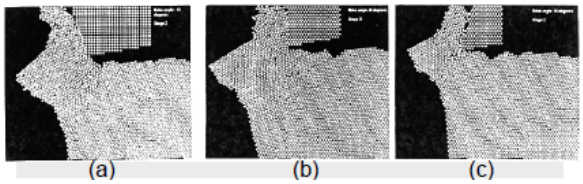

Fig. 6. MD plots of the nanometric cutting process performed on a ductile work material with no elastic constraint at the exit for various tool rake angles (a) −15° (b) 0° (c) 15° (d) 30° (e) 45° and (f) 60° [3]

4. CHIP FORMATION

Because of the segmented chip formation the shearing in the primary shear zone is interrupted by the compression of the workpiece material. Therefore, this zone has to be called “compression and shearing zone”. Nevertheless, to allow the comparison with the continuous chip formation the description “primary shear zone” is used for this area. The mechanism and the periodical character of this area can be described properly by the resultant force and the chip thickness. An increase in resultant forces and chip thickness can be found experimentally and in the simulation result. At the moment when the adiabatic shearing occurs the cutting forces drop and the chip thickness decreases, Figure 7.

By considering the evolution of plastic dissipation energy during cutting and its relation to stress and strain, an explanation linking material microstructure, chip formation, and the formation of dimples on a machined steel surface could be drawn up. The plastic dissipation energy during the QSE chip formation process from the microscale FE model in Figure 8 was closely examined. Initially, the cutting process is concentrated in the first A grain (harder material). As cutting progresses the shear plane moves forward in front of the cutting edge. As the shear plane encounters the first B grain (soft material), the softer B grain begins to absorb the cutting energy as shown in Figure 7a. Energy absorption in the softer B grain well before the cutting edge nears the actual B grain results from the fact that less work is required to plastically deform the soft material. The absorption of cutting energy in the softer B grain results in the immediate bulging of

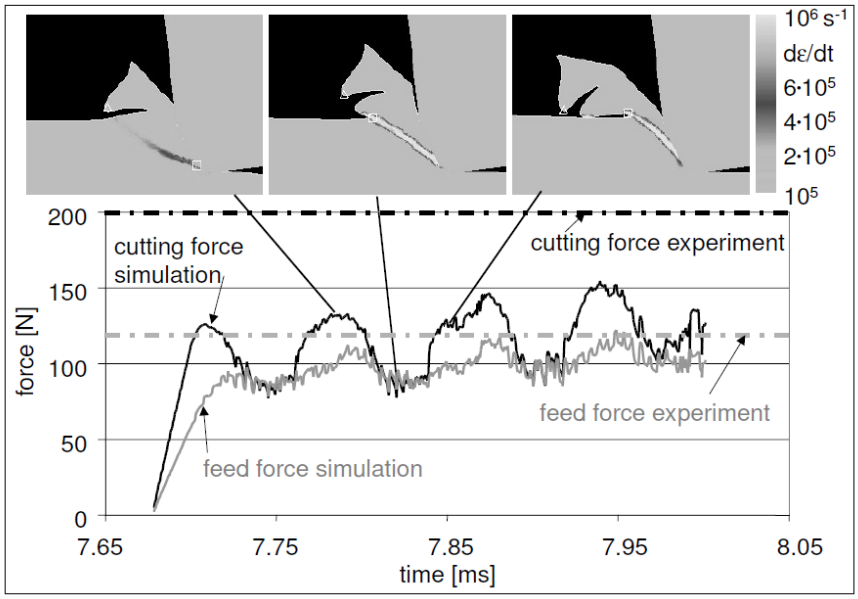

Fig. 7. Cutting and feed forces in segmented chip formation (AISI 1045, v = 1000 m/min, f=0.1 mm) [7]

the B grain at the chip free surface. This softer grain eventually forms a large plume at the chip free surface as the softer material is extruded out the chip free surface. As cutting approaches the A-B grain boundary, the plastic dissipation energy continues to increase inside the soft B grain with little change in the hard A grain. This indicates that once the soft B grain began to absorb the cutting energy, very little work was being done in the first A grain except at the tool-chip interface. Early absorption of cutting energy in the soft B grain can be explained by considering that cutting energy can be translated into stress and plastic strain. While cutting a hard grain, a stress field will exist and a corresponding plastic strain will occur. As cutting

approaches the softer grain, the stress field will decrease in magnitude. In order for an energy balance to exist at the grain boundary, the corresponding strain must increase in this lower stress field. As a result, there is a strain mismatch at the A-B grain boundary and a dimple forms. When the cutting edge is inside of the B grain exclusively as in Figure 8b and 8c, all of the plastic dissipation energy is absorbed by the soft B grain with little change in the hard A grain.

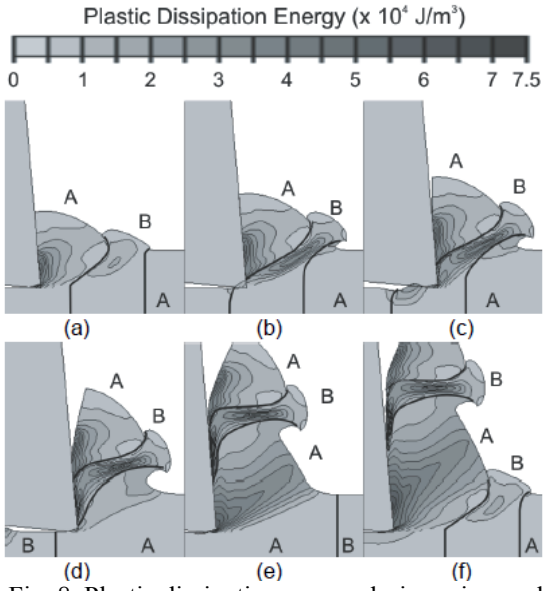

Fig. 8. Plastic dissipation energy during microscale cutting from the microscale FE cutting model [4]

This indicates that once the soft B grain began absorbing this energy, very little work was being done in the first A grain. In the B grain, the relatively soft material is 'pulled' as the cutting edge moves across the B grain. This 'pull' at the newly machined surface contributes to an already existing strain mismatch and aids the dimple formation at the A-B grain boundary. As cutting approaches and crosses the B-A grain boundary in Figure 8d the strain mismatch is very small compared to the mismatch that was observed at the A-B grain boundary as shown in Figure 8a and 8c. If an energy balance exists at the B-A grain boundary then there should be a large strain mismatch given the change from a relatively low to a relatively high stress field as cutting moves from material B to material A.

The typical FEA models in ''isothermal'' mode producing continuous chips as shown in Fig. 9 (a) are incapable of describing the cutting mechanism of nickel alloys where saw tooth chips with clear shear banding were produced even under very low cutting speeds [9]. In this paper, a Lagrangian FEA model in ABAQUS_ was developed under the adiabatic shear mode. The simulated chip morphology represents the actual chips more closely as in Fig. 9 (b) with shear bandings caused by thermal softening and strain hardening.

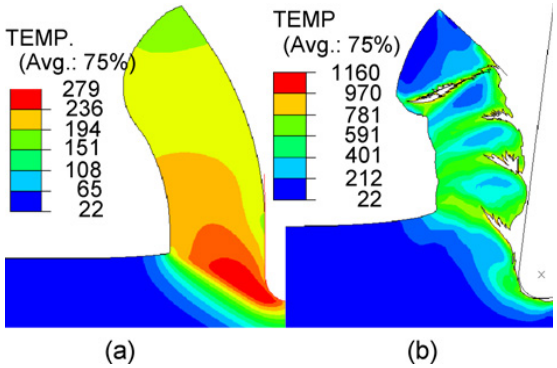

Fig. 9. Simulated chips: (a) isothermal and (b) adiabatic.

5. MODELING OF BURR FORMATION

Increasing demands on function and performance call for burr-free workpiece edges after machining. Since deburring is a costly and non-value-added operation, the understanding and control of burr formation is a research topic with high relevance to industrial applications.

Several investigations have been carried out in order to simulate burrs. A three-dimensional finite element model is developed by [10] to investigate the mechanisms of drilling burr formation with a backup material (Fig. 10). This model also predicts cutting forces in drilling, and explains the correlation of thrust force and burr size. Simulation results show that negative shear situation near the edge of the hole and gap formation are the primary mechanisms in drilling burr formation with backup material. The use of a bushing having zero clearance will result in significantly shorter and thinner exit burrs than typical for conventional drilling. The use of a solid backup material was less effective in minimizing burr size above an unsupported exit surface.

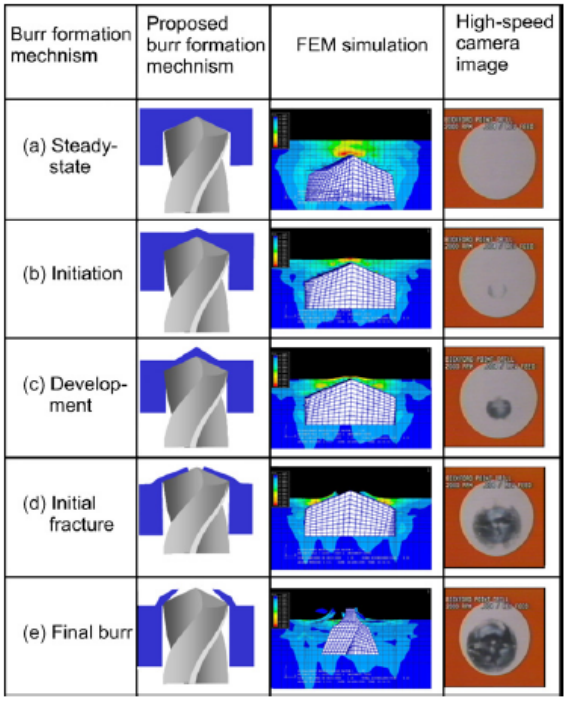

Fig 10. FEM simulation of burr formation in drilling

6. 3D NUMERICAL MODELING

The 3D ALE simulation was carried out using SFTC Deform 3D1 V. 6.1. The utilized numerical procedure can be summarized as follows: the first step is a coupled thermo-mechanical analysis using an updated Lagrangian formulation, to reach mechanical steady state conditions. Then, the Eulerian step is carried out to determine temperature distribution. Finally, the wear subroutine is called, tool wear is calculated and the geometry of the worn tool is updated. For each tool node the wear rate is calculated, afterwards the direction of the node movement is identified and, in the last step of the subroutine, the tool mesh and the tool geometry are updated. The procedure is carried out subdividing the total cutting time in several steps and repeating the procedure until the total cutting time is reached. It is important to underline that the geometry updating is carried out starting from the tool worn geometry of the previous step and changing the node positions on the basis of the new wear rate values. Indeed, the first step of the wear loop starts from the new flat tool geometry. Fig. 11 shows the updated tool geometry after 1, 2, 4 and 6 min cutting time [6].

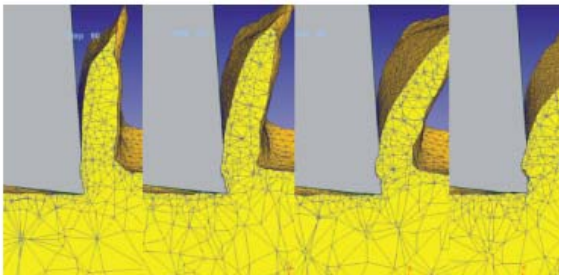

Fig. 11. Development of tool wear after 1, 2, 4 and 6 min cutting time (V_c=160m/min, f=0,25mm/rev)

7. ARTIFICIAL NEURAL NET MODELS

Artificial neural network (ANN) models are distinguished by several properties which make them suitable for modeling of complex, non stationary processes that depend on many input variables. First, to construct an ANN model of a process no analytical expressions for the underlying physical phenomena are required. The ANN model is constructed automatically through a training procedure based on process data. Second, ANN models are able to simultaneously process information from different sensors and physical quantities, which need not to be related. Such processing of information from various sources is called sensor fusion. Third, ANN models can be effectively combined with physical models to further improve the modeling performance. Due to these properties, the ANN models continue to be considered as a tool suitable for modeling of different machining processes [8].

8. CONCLUSION

Specific cutting process and process effects will benefit from continued modeling research including cutting hard materials, burr formation, and chip formation. Molecular dynamics modeling offers potential for coupling micro and nano scale process features with macro scale processes. The improvement in modeling capability from macro to nano scale processes drives improved process simulation and process understanding..

9. REFERENCES

[1] L. Chuzhoy, R. E. DeVor, S. G. Kapoor: Machining Simulation of Ductile Iron and Its Constituents, Part 2: Numerical Simulation and Experimental Validation of Machining, Journal of Manufacturing Science and Engineering, Transactions of the ASME, 125/2, 2003, pp 192-201.

[2] S. Park, S. G. Kapoor, R. E. DeVor: Mechanistic Cutting Process Calibration via Microstructure-Level Finite Element Simulation Model, Journal of Manufacturing Science and Engineering, Trans, of the ASME, 126/4, 2004, pp 706-709.

[3] R. Komanduri, N. Chandrasekaran, L. M. Raff, MD Simulation of Exit Failure in Nanometric Cutting, Materials Science and Engineering A, 2001, 311/1-2, pp 1-12.

[4] A. Simoneau, E. Ng, M.A. Elbestawi: The Effect of Microstructure on Chip Formation and Surface Defects in Microscale, Mesoscale, and Macroscale Cutting of Steel , Annals of CIRP Vol.55/1/2006, pp 97-102

[5] Y. Altinas, C. Brecher, M. Weck, S. Witt: Virtual Machine Tool, Annals of CIRP Vol.54/2/2005, pp 651-674

[6] Chen L., El-Wardany T.I., Harris W.C.: Modeling the Effects of Flank Wear Land and Chip Formation on Residual Stresses, CIRP Annals, 53/1, 2004:75-78

[7] S. Hoppe Experimental and numerical analysis of chip formation in metal cutting, Dissertation, RWTH Aachen, 2004, pp200

[8] E. Brinksmeier, J. C. Aurich, E. Govekar, C. Heinzel, H.-W. Hoffmeister, F. Klocke, J. Peters, R. Rentsch, D. J. Stephenson, E. Uhlmann, K. Weinert, M. Wittmann: Advances in Modeling and Simulation of Grinding Processes, Annals of the CIRP Vol. 55/2/2006

[9] S. Ranganath, C. Guo, P. Hegde: A finite element modeling approach to predicting white layer formation in nickel super alloys CIRP Annals - 58 (2009) 77–80

[10] .C. Aurich (1)a,*, D. Dornfeld (1)b, P.J. Arrazola (3)c, V. Franke a, L. Leitz a, S. Min (2) Burrs—Analysis, control and removal, CIRP Annals - 58 (2009) 519–542

Authors: **Prof. Dr. Pavel Kovac, Assoc. Prof. Dr. Marin Gostimirovic, doc. Dr. Milenko Sekulic, dipl.ing**. **Borislav Savkovic,** University of Novi Sad, Faculty of Tehnical Sciences, Production Engineering Institute, Trg Dositeja Obradovica 6, 21000 Novi Sad, Serbia, Phone.: +381 21 485-2324,

E-mail: pkovac@uns.ac.rs
maring@uns.ac.rs
milenkos@uns.ac.rs
savkovic@uns.ac.rs

Note: This paper present a part of researching at the project *" Research and application of high-processing procedure"* Project number TR 14206, financed by Ministry of Science and Technological Development of Serbia.

Journal of Production Engineering
Vol.12 No.1

Kuzinovski, M., Tomov, M., Cichosz, P.

EFFECT OF SAMPLING SPACING UPON CHANGE OF HYBRID PARAMETERS VALUES OF THE ROUGHNESS PROFILE

Abstract: *The study presents results gained from analysis of roughness measurements on deterministic and stochastic etalon surfaces, representatives of machining processes: turning and grinding. The effect of the sampling spacing change upon hybrid parameter values of roughness profiles is determined. Measurements were made by application of profilometer Surtronic 3+ with sampling spacing of 0,5 μm, while as hybrid parameter values of roughness were calculated by means of software TalyProfile. Sampling spacing change was provided by the program Microsoft Office Excel. Researches were made with sampling spacing of 0,5; 1,0; 1,5; 2,0; 2,5 and 3,0 μm. Analysis refers to change of hybrid parameter values RDa(RΔa), RDq(RΔq), RLa, RLq, RLo, Rfd and RVo for deterministic and stochastic etalon surface.*

Key words: *Hybrid parameters, surface roughness, contact (stylus) profilometer.*

1. INTRODUCTION WITH SHORT OVERVIEW OF APPLIED LITERATURE

Knowing geometric characteristics of surface on micro plan, expressed through roughness profile, are more often connected to functional characteristics of mechanical parts [1]. Roughness profile is described through parameters grouped per the profile characteristic they describe: peak, average, horizontal, hybrid, functional parameters and Rk parameters [2,3].

Against [2] hybrid parameter group consists of: Rda (or RΔa)- arithmetical mean slope, RDq(or RΔq)- root mean square slope, RLa- arithmetical mean wavelength, RLq – root mean square wavelength, RLo –developed profile length, Rfd – fractal dimension and RVo – volumetric parameter. Graphical presentation of some hybrid parameters is presented on Figure 1.

Hybrid parameters are not standardized yet however are of particular interest in the scientific-research activities of exploitation characteristics of the surface layer that are performed by method engineers and tribologists [1,2,5,6,7].

Friction, wear, reflectivity, surface elasticity, noise, adhesion, etc. are functional characteristics directly dependent upon hybrid parameter values for one surface [1,2].

Therefore against [2], by increase of values of RΔa and RΔq also increase values of friction, wear, surface elasticity, noise and vibrations, while as reflectivity value decreases.

Against [5], by increase of values of RΔa, RΔq, Rfd and RLq, the coefficient of friction increases. Largest influence upon friction coefficient change for various materials has RΔa, where the correlation coefficient amounts 0,92. By RLa increase, friction coefficient decreases.

Against stated, it is certain that inclinations of roughness surface unleveled areas, expressed by hybrid parameters, have significant effect on behaviour of parts in exploitation process.

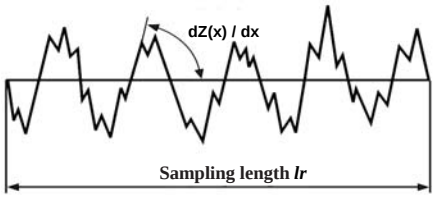

(a) RΔa and RΔq, [4].

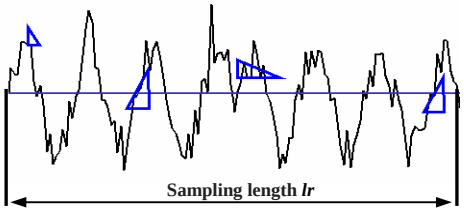

(b) RLa, [2].

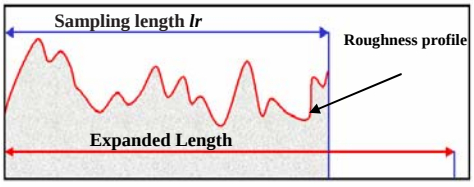

(c) Lo, [2].

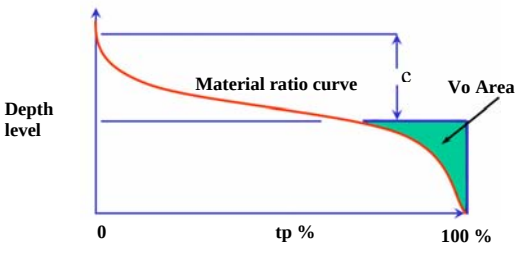

(d) Vo, [2].

Figure1. Graphical interpretation of hybrid parameters

The determination of hybrid parameter values has direct effect upon forecasts for part behaviour in exploitation. In this sense researches were performed for determining the measurement condition effect upon the defining of hybrid parameter, by application of contact (stylus) profilometers [6,7].

Namely, the effect of sampling spacing change upon hybrid parameter value change is determined.

In ISO 3274-1996 the selection of max. sampling spacing is defined in dependence on stylus peak radius and size of λ_c and λ_s profile filters. In ISO 4288-1996 sampling length l_r (that is λ_c) is selected in dependence on expected values for Ra and Rz for random surface i.e. in dependence on value of RSm for periodical surface. Recommendation or dependence does not exist, at least not in international standards (ISO), between hybrid parameters and any segment of measurement conditions. This is the second reason for justification of researches performed in [6,7].

The effect of sampling spacing change upon roughness profile parameter values, as one of the measurement conditions for surface roughness measurement, is reviewed in references [6,7,8,9,10,11,12,13,14]. In [8] is determined the effect of sampling spacing change upon change of values of average Ra, Rq and peak Rp, Rv, Rz (ISO), Rt parameters of roughness profile. In [9] is determined the effect of sampling spacing change upon average slope of modeleded random profile. It is noticed that by sampling spacing increase the slope of modeleded random profile decreases.

Theoretically, by sampling spacing increase possibilities also increase for omission of some information for one roughness profile, thereof also "ironing" and reducing the slope of roughness. This would mean direct effect upon hybrid parameter values. This study presents the results of the research of the effect of sampling spacing upon hybrid parameter value change.

2. DEFINING MEASUREMENT CONDITIONS AND MEASURING EQUIPMENT

Original roughness profile is analyzed in the research, gained by measurements performed on realistic etalon surfaces with deterministic character (machined by turning with nominal Ra=0,2 μm) and stochastic character (machined by grinding with nominal Ra=0,2 μm).

Measurements of etalon surfaces were made in Laboratory for metrology of geometrical characteristics and quality research at the Faculty of Mechanical Engineering in Skopje by utilization of contact profilometer Surtronic 3+ connected to a Personal computer. Coordinates of original profile were taken by the professional software TalyProfile. Measuring unit was calibrated by means of etalon type C with value for Ra = 6 μm, in accordance with [15,16].

Profilometer Surtronic 3+ characterizes with vertical and horizontal resolution. Vertical resolution amounts 10 μm, while as horizontal resolution amounts 0.5 μm for cases where evaluation length (ln) is smaller or equal to 8 mm, and 1.0 μm for cases where evaluation length is larger than 8 mm.

Measurement conditions are in conformance with recommendations prescribed in ISO 3274-1996 and ISO 4288-1996. Pick-up TYPE 112-2672 (DCN 001) with stylus radius of 2 μm and skid radius of 8.7 mm is used, as well as pick-up TYPE 112-1502 (DCN 001) with stylus radius of 5 μm and skid radius of 8.7 mm.

A stylus of 5μm is also used in the research for measured etalons with Ra=0,2 μm, which is not in compliance with recommendations in ISO 3274-1996 and ISO 4288-1996. A deliberate omission is in question in order to determine the effect of mechanical filtration of profile caused by stylus radius and how such filtration is reflected upon further research procedure at sampling spacing change.

Reader speed used in researches is 1 mm/s. Sampling length (lr) is 0.8 mm, while as evaluation length (ln) contains five sampling lengths.

3. EXPERIMENTAL RESEARCHES

Independent variable in researches is the sampling spacing size, which is defined as distance between two adjacent points of roughness profile against x-axis. This is constant for all points of a profile. Applied measuring equipment does not have ability to provide sampling spacing change.

For the purpose of removing effects by measuring equipment mistakes at multiple measurements of researched dependence, it is necessary to generate various sampling spacing for one same recorded roughness profile. This condition, various lengths of sampling spacing for one same recorded profile was gained by using the program Microsoft Office Excel.

Sampling spacing change is simulated by change of x-distance between sampling points of original roughness profile through omission of one, two, three, four or five points, always starting from one same starting point. In this way roughness profiles are gained with sampling spacing of 1,0; 1,5; 2,0; 2,5 and 3,0 μm. An algorithm is presented on Figure 2 with which profiles with sampling spacing of 1,0; 1,5; 2,0; 2,5 and 3,0 μm are gained, from one same original profile with sampling spacing of 0,5 μm .

At sampling spacing change, evaluation length remains unchanged. Hybrid parameters are calculated by applying software TalyProfile. When calculating, the software uses Gaussian filter with size of 0,8 mm, and micro-filtration with filter λs with size 2,5 μm, while as values of hybrid parameters RΔa (^{0}), RΔq (^{0}), RLa (mm), RLq (mm), RLo (%), Rfd (not have unit of measurement) and RVo (mm^3/mm^2) are calculated as mean values of all sampling lengths (total five). These conditions are applied on all profiles.

4. ANALYSIS OF GAINED RESULTS

Results gained for reviewed hybrid parameters for various sampling spacing are presented in Table 1, 2, 3 and 4. The percentage differences among values of hybrid parameters for various sampling spacing and values of hybrid parameters of original profile are also shown in tables. The minus prior percentage difference

indicates that gained values are smaller than values of original profile with sampling spacing 0,5 µm. Percentage differences gained for sampling spacing 1,0; 1,5; 2,0; 2,5 and 3,0 µm in terms of original roughness profile, are shown as a diagram on Figure 3, 4, 5 and 6.

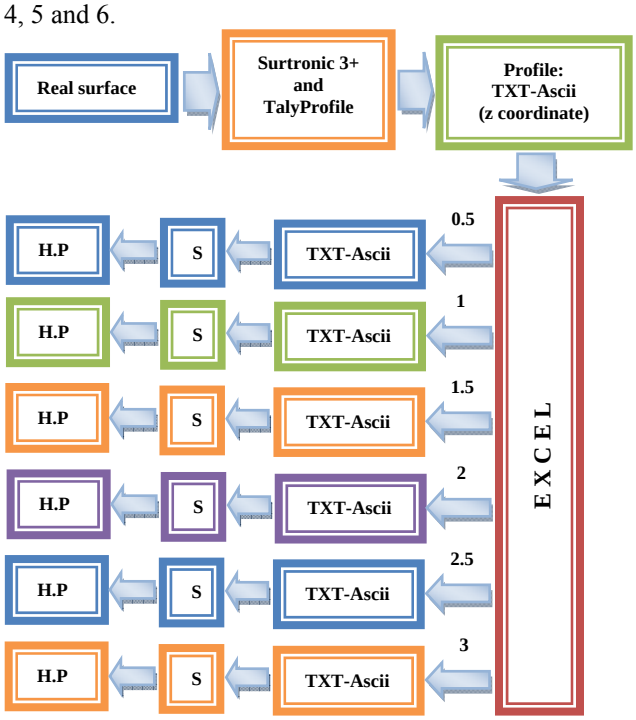

Figure 2. Algorithm for gaining roughness profile with various sampling spacing from one same original profile

Results gained for various sampling spacing and percentage difference among them provide conclusion that significant effect by sampling spacing size upon hybrid parameter values exists, regardless whether a deterministic or stochastic surface is in question.
Change of values of RDa(RΔa) and RDq(RΔq) parameters confirmed the theoretical assumptions that by sampling spacing increase, the slope of roughness decrease

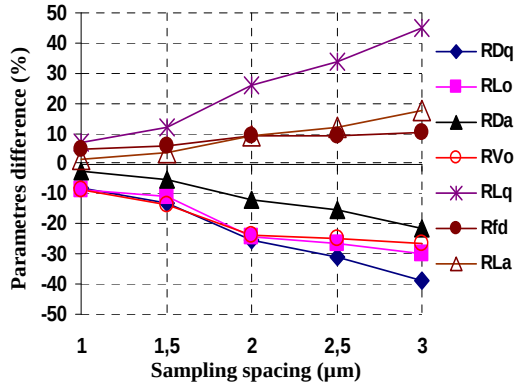

Figure 3. Percentage differences between hybrid parameters for various sampling spacing in terms of original profile with sampling spacing of 0.5 µm. Original profile is deterministic (turned etalon surface), measured with stylus of 2 µm.

Parameters	Sampling spacing (µm)					
	0.5	1	1.5	2	2.5	3
RDq	4,24	3,89	3,69	3,17	2,92	2,59
RLq	0,0221	0,0237	0,0248	0,0278	0,0296	0,0321
RLo	0,283	0,258	0,252	0,214	0,208	0,198
Rfd	1,65	1,73	1,75	1,8	1,8	1,82
RDa	2,89	2,82	2,74	2,54	2,44	2,27
RLa	0,0258	0,0262	0,0267	0,0282	0,0289	0,0303
RVo (x 10^{-4})	4,52	4,12	3,91	3,44	3,39	3,32
Difference (%)						
RDq		-8,25	-12,97	-25,24	-31,13	-38,92
RLq		7,24	12,22	25,79	33,94	45,25
Rlo		-8,83	-10,95	-24,38	-26,50	-30,04
Rfd		4,85	6,06	9,09	9,09	10,30
Rda		-2,42	-5,19	-12,11	-15,57	-21,45
Rla		1,55	3,49	9,30	12,02	17,44
Rvo		-8,85	-13,50	-23,89	-25,00	-26,55

Table1. Hybrid parameter values for various sampling spacing. Original profile is deterministic (turned etalon surface), measured with stylus of 2 µm.

Parameters	Sampling spacing (µm)					
	0.5	1	1.5	2	2.5	3
RDq	4,28	3,74	3,44	2,69	2,45	2,1
RLq	0,0213	0,024	0,0258	0,0318	0,0343	0,039
RLo	0,287	0,24	0,225	0,172	0,168	0,16
Rfd	1,57	1,61	1,6	1,65	1,64	1,63
RDa	2,85	2,6	2,43	1,97	1,8	1,56
RLa	0,0245	0,0264	0,0279	0,0332	0,0357	0,0403
RVo (x 10^{-4})	2,07	2,01	1,77	1,61	1,37	1,34
Difference (%)						
RDq		-12,62	-19,63	-37,15	-42,76	-50,93
RLq		12,68	21,13	49,30	61,03	83,10
Rlo		-16,38	-21,60	-40,07	-41,46	-44,25
Rfd		2,55	1,91	5,10	4,46	3,82
Rda		-8,77	-14,74	-30,88	-36,84	-45,26
Rla		7,76	13,88	35,51	45,71	64,49
Rvo		-2,90	-14,49	-22,22	-33,82	-35,27

Table 2. Hybrid parameter values for various sampling spacing. Original profile is stochastic (grinded etalon surface), measured with stylus of 2 µm.

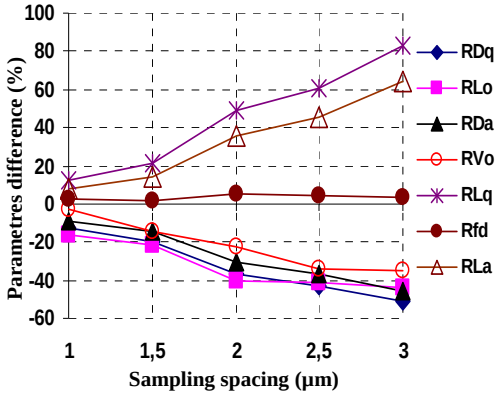

Figure 4. Percentage differences between hybrid parameters for various sampling spacing in terms of original profile with sampling spacing of 0.5 µm. Original profile is stochastic (grinded etalon surface), measured with stylus of 2 µm.

Param-eters	Sampling spacing (μm)					
	0.5	1	1.5	2	2.5	3
RDq	3,93	3,71	3,52	3,08	2,86	2,57
RLq	0,0231	0,0242	0,0251	0,0277	0,0291	0,0312
RLo	0,257	0,247	0,244	0,213	0,208	0,198
Rfd	1,68	1,76	1,78	1,84	1,83	1,84
RDa	2,89	2,82	2,77	2,59	2,47	2,28
RLa	0,0245	0,0249	0,0252	0,0266	0,0275	0,0293
RVo (x 10^{-4})	4,28	4,31	4,09	4,01	3,43	3,22
Difference (%)						
RDq		-5,60	-10,43	-21,63	-27,23	-34,61
RLq		4,76	8,66	19,91	25,97	35,06
Rlo		-3,89	-5,06	-17,12	-19,07	-22,96
Rfd		4,76	5,95	9,52	8,93	9,52
Rda		-2,42	-4,15	-10,38	-14,53	-21,11
Rla		1,63	2,86	8,57	12,24	19,59
Rvo		0,70	-4,44	-6,31	-19,86	-24,77

Table1. Hybrid parameter values for various sampling spacing. Original profile is deterministic (turned etalon surface), measured with stylus of 5 μm.

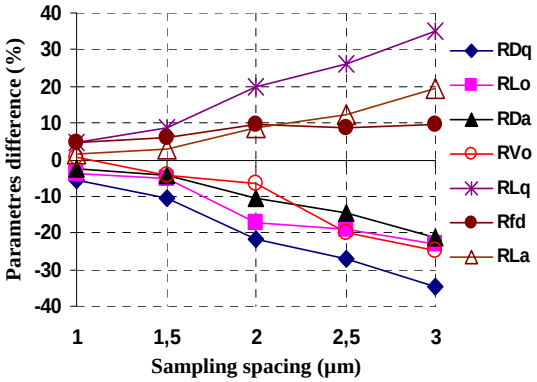

Figure 5. Percentage differences between hybrid parameters for various sampling spacing in terms of original profile with sampling spacing of 0.5 μm. Original profile is deterministic (turned etalon surface), measured with stylus of 5 μm.

Param-eters	Sampling spacing (μm)					
	0.5	1	1.5	2	2.5	3
RDq	3,95	3,57	3,32	2,66	2,4	2,04
RLq	0,0205	0,0222	0,0237	0,0284	0,0306	0,035
RLo	0,253	0,227	0,216	0,173	0,169	0,161
Rfd	1,59	1,63	1,36	1,66	1,65	1,65
RDa	2,89	2,65	2,47	2,03	1,83	1,57
RLa	0,0219	0,0235	0,025	0,0292	0,0316	0,0358
RVo (x 10^{-4})	1,5	1,46	1,44	1,3	1,46	1,15
Difference (%)						
RDq		-9,62	-15,95	-32,66	-39,24	-48,35
RLq		8,29	15,61	38,54	49,27	70,73
Rlo		-10,28	-14,62	-31,62	-33,20	-36,36
Rfd		2,52	-14,47	4,40	3,77	3,77
Rda		-8,30	-14,53	-29,76	-36,68	-45,67
Rla		7,31	14,16	33,33	44,29	63,47
Rvo		-2,67	-4,00	-13,33	-2,67	-23,33

Table 4. Hybrid parameter values for various sampling spacing. Original profile is stochastic (grinded etalon surface), measured with stylus of 5 μm.

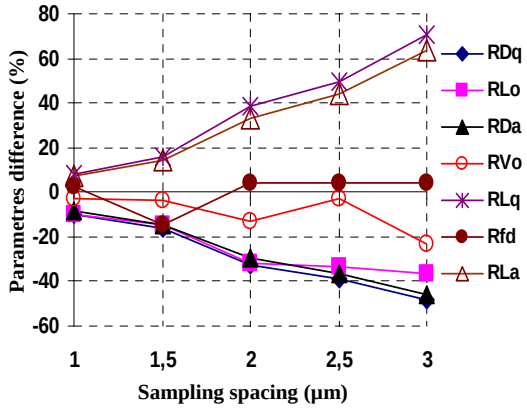

Figure 6. Percentage differences between hybrid parameters for various sampling spacing in terms of original profile with sampling spacing of 0.5 μm. Original profile is stochastic (grinded etalon surface), measured with stylus of 5 μm.

A change of slope till 50% from original profile slope is noticed in performed researches.

From tables 1, 2, 3 and 4, paritcularly from percentage differences, hybrid parameter grouping can be made in terms of the effect of sampling spacing change. RDa(RΔa), RDq(RΔq), RLo and RVo are in the group where by sampling spacing increase, there values decrease. RLa and RLq are parameters where by sampling spacing increase, there values also increase. Only parameter Rfd shows smallest, insignificant change. Highest percentage change, which can reach even 80%, is noticed on parameter RLq for all profiles. So, RDq(RΔq) is more sensitive to slope change of roughness than RDa(RΔa). Comparison of gained results between stochastic and deterministic surface indicated possible larger influences of change of sampling spacing on stochastic surfaces.

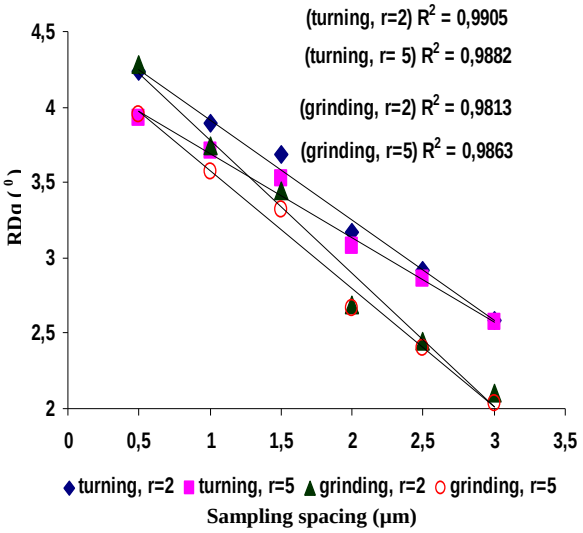

Figure 7. Correlation dependence and value of correlation coefficient between RDq and sampling spacing, for turned and grinded etalon surface with stylus radius of 2 and 5 μm.

The dependence and value of correlation coefficient RDq is shown on Figure 7 as most suitable indicator of roughness slope size change, by sampling spacing change.

Interesting are the considerations of the caused mechanical filtration when measuring profile with bigger stylus radius than recommendations in standards. This mechanical filtration, which has its effect even when gaining the original profile, has effect also in the further research process and is manifested by hybrid parameter difference occurrence. Results gained are somewhat smaller than those gained when measurements were performed with smaller radius.

5. CONCLUSION

Results gained, literature analyzed and own experiences indicate following conclusions:

- It has been determined that parameters that describe slope of roughness profile are significant in two aspects. Hybrid parameters directly effect functional characteristics, while as measurement conditions expressed through sampling spacing, with which same are determined, have direct effect upon hybrid parameter values.

- A significant change of hybrid values occurs by sampling spacing increase. Values of RDa, RDq, RLo and RVo decrease by sampling spacing increase, RLa and RLq increase, while as Rfd has smallest dependence on sampling spacing.

- Maybe in future further researches are necessary that shall provide dependence between Ra, Rq, and RSm and hybrid parameters for same sampling spacing change, all with the purpose of precise determination or at least expansion of recommendations prescribed in ISO 3274-1996 and ISO 4288-1996.

6. REFERENCES

[1]. D. J. Whitehouse. *Handbook of Surface Metrology*. Inst. of Physics, Bristol, 1994.

[2]. Taylor Hobson. *The Parameter Tree of Surface Roughness*. Centre of Excellence. 2000.

[3]. ISO 4287:1997; Geometrical product specifications (GPS) - Surface texture: Profile method – *Terms, defenitions and surface texture parameters*

[4]. JIS B0601 Standard. Explanation of Surface Characteristic, Japan

[5]. Pradeep L. Menezes, Kishore and Satish V. Kailas. *Influence of roughness parameters on coefficient of friction under lubricated conditions*, Sadhana Vol. 33, Part 3, June 2008, pp 181-190.

[6]. Tomov Mite. *Contribution to methods and measurement techniques development for research of influential factors of surface topography identification*. Application for Ph.D. dissertation, Mechanical Engineering Faculty, Skopje, 2008.

[7]. Mikolaj Kuzinovski, Mite Tomov, Piotr Cichosz, Trajčevski Neven, ...: : *Study on possibilities and accuracy of surface layer geometrical structure determination by using contact profilometers.* Scientific-research project, finance by Ministry of Education and Science on Republic of Macedonia. Number: 13-977/3-05, 1.7.2006-30.6.2009.

[8].Tomov M., Kuzinovski M., Cichosz P.: *Effect of sampling spacing on surface roughness parameter values.* XXXII Conference on Production Engineering with foreign participants, Novi Sad, Serbia, 18-20.09. 2008.

[9]. Pawel Pawlus. *An Analysis of slope of surface topography*. Metrology and Measurement System 2005, 12 (3/2005); 299-314.

[10]. Pawel P. Pawlus. *Mechanical filtration of surface profiles.* Measurement 35 (2004); pp 325-341.

[11]. Pawel Swornowski. *The influence of the mechanical filtration of the measuring-pin on the waviness and surface roughness*.Arhives of Mechanical Technology and Automation. Poznan 2006. ISSN 1233-9709, Vol. 26 nr 2. pp 129-137.

[12]. K. J. Stout. *Thre-Dimensional Surface Topography; Measurements, Interpretation and Applications*. Center for Metrology the University of Birmingham, 1994.

[13]. K. J. Stout and L. Blunt. *Tree-Dimensional Surface Topography. Secont edition.* School of Engineering. University of Huddersfield, Penton Pres, London, 1994.

[14].Tomov M., Kuzinovski M., Cichosz P.: Effect *of evaluation length on results of surface roughness measurements*. XXXII Conference on Production Engineering with forign participants, Novi Sad, Serbia, 18-20.09. 2008.

[15]. EAL-G20. *Calibration of Surface Instruments for Measuring Surface Roughness,* 1996.

[16]. ISO 12179: 2000; Geometrical product specifications (GPS) - Surface texture: Profile method - *Calibration of contact (stylus) instruments.*

[17]. ISO 3274:1996; Geometrical Product Specifications (GPS) - Surface texture: Profile method - *Nominal characteristics of contact stylus instruments.*

[18]. ISO 4288:1996; Geometrical product specifications (GPS) - Surface texture: Profile method - *Rules and procedures for the assessment of surface texture.*

Authors: **Prof. Kuzinovski Mikolaj, PhD, Ass. Tomov Mite, MSc,** University "Ss. Cyril and Methodius", Faculty of Mechanical Engineering, Skopje, , Karposh II bb, P. Fax 464, 1000 Skopje R.Macedonia., **Prof. Cichosz Piotr, DSc,** Institute of Production Engineering and Automation of the Wroclaw University of Technology, str. Lukasiewicza 3/5, 50-371 Wroclaw, Polska

E-mail:

mikolaj@mf.edu.mk
mitetomov@mf.edu.mk
piotrc@itma.pwr.wroc.pl

Journal of Production Engineering
Vol.12 No.1

Kuzinovski, M., Trajčevski, N., Cichosz, P.

INVESTIGATION OF CUTTING FORCES DURING MACHINING PROCESS BY HIGH SPEED TURNING

Abstract: *This paper presents the obtained mathematical models of cutting forces during machining process by high speed turning as a function of processing parameters* v, f, a *and* r_e. *The machining process by turning is performed on NC lathe using ceramic cutting tool inserts and the workpiece material is* ***C*** *1630 (DIN C 55). Processing parameters are varied in range between* v *=300 and 700 m/min ,* f *=0,16-0,32 mm/rev, a=0,5-1,6 mm and* r_e*=1,2-2,0 mm. Cutting forces measurement is done at the Institute of Production Engineering and Automation of the Wroclaw University of Technology, Poland using computerized experimental setup with three component piezoelektric dynamometer type Kistler. Experiments are realized acording first order four factorial experimental plan. Mathematical processing is performed at the Faculty of Mechanical Engineering in Skopje using the program CADEX combined with MATLAB.*

Key words: *Machining by turning, cutting forces, mathematical models, factorial experiments*

1. INTRODUCTION

Knowing the magnitude of the cutting forces in the turning process as function of the parameters and conditions of treatment is necessary for determining of cutting tool strength, cutting edge wearing, limit of the maximum load of the cutting machine and forecasting the expected results of the processing. In particular, during machining with high cutting speed, using modern materials and modern cutting machines imposes the necessity of studying physical phenomena in the cutting process and their mathematical modeling. Moreover, analysis of physical phenomena has shown that conditions are created for processing by material removal, in substantially different conditions, primarily due to the use of larger cutting speeds [1]. In such circumstances the creation of possibilities for identification of physical phenomena in the cutting process allows: the creation of the basis for selection of optimal processing parameters, forecasting the process of wear of the cutting edge, determination of time to change the cutting tools, quality management of workpiece surface layer, optimization of cutting tool stereometry, chip shape and removal conducting, upgrading the technology of production of cutting tool inserts and their properties. During intensive machining conditions, monitoring of the cutting forces is possible only with the use of computer aided research systems [2]. Experiences show that the determination of cutting forces in an analytical way not fully reflect the real situation [3]. Basis of mathematical models for cutting forces obtained in an analytical way are spreadsheet data obtained in surveys, conducted in certain treatment conditions that can be changed. From here emerges the justification for carrying out research activities for the determination of mathematical models to describe the change of cutting forces as a function of processing parameters.

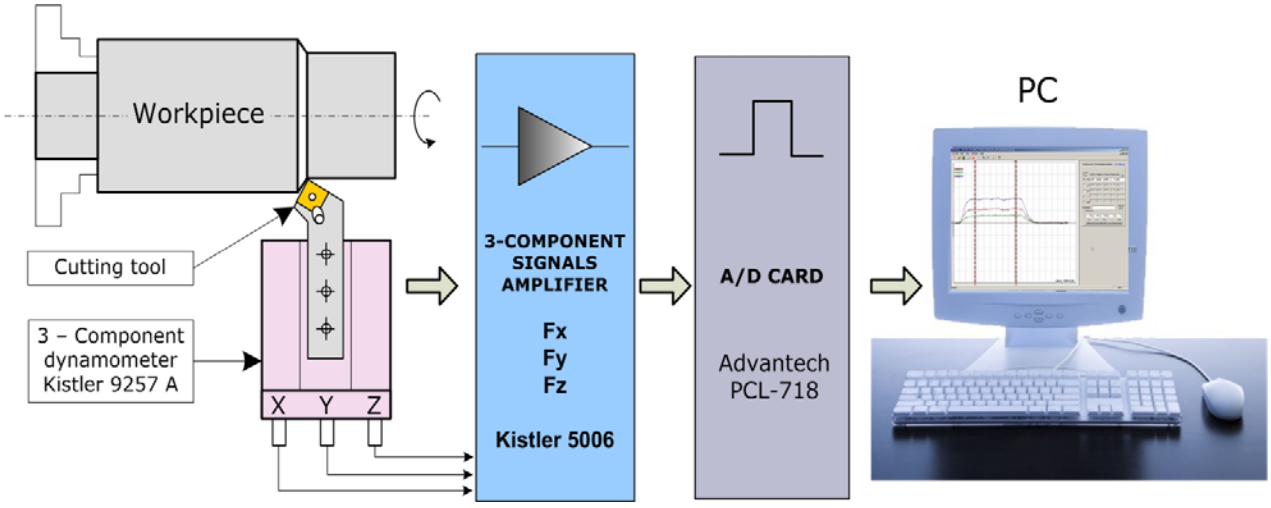

Fig. 1. Schematic view of the research experimental setup

2. EXPERIMENTAL CONDITIONS

2.1 Cutting tool

The processing is performed by use of ceramic cutting tool inserts type SNGN 120712- 120716-120720 made of zircon-oxide ceramics AC 5 (Al_2O_3 +10% ZrO_2) and cutting tool holder type CSRNR 25x25 M12H3, manufactured by HERTEL. Cutting tool stereometry is:

$\chi = 75°,\ \chi_1 = 15°,\ \gamma = -6°,\ \alpha = 6°,\ \lambda = -6°,$

$\gamma_f = -20°,\ b_f = 0{,}2\,\text{mm}$

2.2 Workpiece

Material C 1630 (DIN C 55), normalized to the hardness of 200 HB.

2.3 Metal cutting machine

NC lathe TUR 50 SN-DC, with power P = 18,5 kW with the area of continuous change in the numbers of revolutions n=50-2250 rev/min.

2.4 Cutting parameters

Cutting speed v = 300-700 m/min, feed f=0,16-0,32 mm/rev, depth a=0,5-1,6 mm, cutting tool insert top radius r_ε =1,2-1,6-2,0 mm.

2.5 Experimental plan

It is used first-order full four factorial plan of experiments (2^4 + 4), presented in Table 1. Power function is accepted for the mathematical model to describe the changes of cutting forces [1, 6]. Mathematical processing is performed at the Faculty of Mechanical Engineering in Skopje with the application of program CADEX in connection with *Model-Based Calibration (MBC) Toolbox Version 1.1,* contained in the *Matlab* software package, which is intended for design of experiments and statistical modeling. Using the advanced features of *Matlab* and *MBC* provides significant advantages in the realization of experimental studies, with an option for graphic interpretation of results.

2.6 Research equipment

Monitoring of cutting forces *Fa*, *Fr* and *Ft* in the cutting process is done with computer aided research experimental setup, presented in Fig. 1. Part of the research setup is three-component piezoelectric dynamometer type Kistler 9257 A. Measurements are done at the Institute of Production Engineering and Automation of the Wroclaw University of Technology, Poland. The software FORTMON does graphical presentation of the measurement data, shown on Fig. 2, [4].

3. RESEARCH RESULTS ANALYSIS

The changes on cutting forces *Fa*, *Fr* and *Ft* were monitored in the research. The power function has been adopted for describing these changes:

$$F_a, F_r, F_t = \mathrm{C}\, v^x f^y a^z r_\varepsilon^{\,q} \quad \cdots\cdots\cdots\cdots \quad (1)$$

Experiment plan and results are presented in Table 1. Some graphical interpretation of the influence of cutting speed - v, feed - f, cutting depth - a, and

Obs No	Independent variables - Real matrix				Result		
	v [m/min]	f [mm/rev]	a [mm]	r_ε [mm]	F_{aav} [N]	F_{rav} [N]	F_{tav} [N]
1	300,00	0,16	0,50	1,20	140,55	224,37	272,21
2	700,00	0,16	0,50	1,20	105,55	165,75	235,24
3	300,00	0,32	0,50	1,20	156,95	296,94	431,46
4	700,00	0,32	0,50	1,20	110,02	221,01	327,86
5	300,00	0,16	1,60	1,20	468,82	347,80	744,78
6	700,00	0,16	1,60	1,20	395,21	295,06	675,11
7	300,00	0,32	1,60	1,20	638,83	500,41	1241,52
8	700,00	0,32	1,60	1,20	520,05	419,39	1063,80
9	300,00	0,16	0,50	2,00	121,86	248,47	285,39
10	700,00	0,16	0,50	2,00	103,01	206,30	262,47
11	300,00	0,32	0,50	2,00	179,85	382,75	525,69
12	700,00	0,32	0,50	2,00	138,78	304,31	427,61
13	300,00	0,16	1,60	2,00	461,87	442,69	789,79
14	700,00	0,16	1,60	2,00	403,47	392,22	739,88
15	300,00	0,32	1,60	2,00	596,41	642,49	1302,48
16	700,00	0,32	1,60	2,00	489,69	530,27	1146,87
17	458,26	0,23	0,89	1,55	267,85	349,18	563,28
18	458,26	0,23	0,89	1,55	250,31	338,25	546,02
19	458,26	0,23	0,89	1,55	264,66	351,44	571,50
20	458,26	0,23	0,89	1,55	256,86	341,94	556,54

Table 1. First order four factorial experimental plan

cutting tool insert tip radius - r_ε on the changes of axial *Fa*, radial *Fr* and tangential force component *Ft* are shown on Fig. 3.

Processing of obtained results includes analysis of mathematical models with and without mutual effect, determination of 95% confidence interval for analyzed models, evaluation of significance of coded polynomial coefficients, determination of experiment error, check of mathematical model adequacy and determination of multiple regression coefficient. Analysis performed, after the complete computer processing, showed adequacy of obtained mathematical models (2), (3) and (4).

$$F_a = 2355{,}2 \cdot v^{-0{,}26} \cdot f^{0{,}34} \cdot a^{1{,}14} \cdot r_\varepsilon^{-0{,}019} \quad (2)$$

$$F_r = 2714{,}55 \cdot v^{-0{,}25} \cdot f^{0{,}5} \cdot a^{0{,}48} \cdot r_\varepsilon^{0{,}47} \quad (3)$$

$$F_t = 4403{,}58 \cdot v^{-0{,}17} \cdot f^{0{,}68} \cdot a^{0{,}89} \cdot r_\varepsilon^{0{,}22} \quad (4)$$

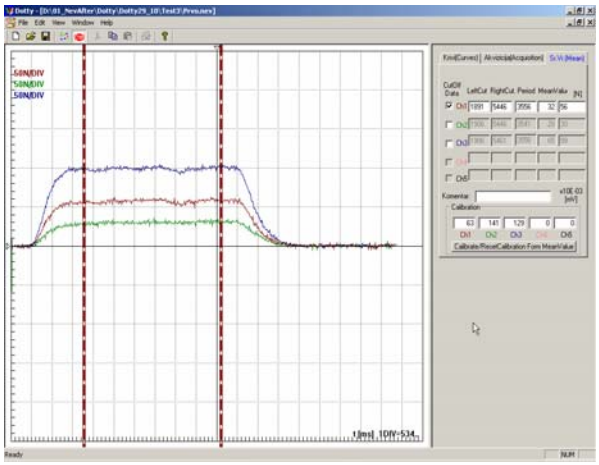

Fig. 2. Graphical presentation of measurements results by using FORTMON software

Researches show dominant influence of feed and cutting depth on cutting force change. This is explained by the fact that by feed increase, contact increase is caused between chip and face surface of cutting wedge as result of increased removed material thickness. Therefore friction between chip and face surface of cutting tool is increased, which alternatively causes higher chip ramming. Actually, a higher plastic deformation is present.

Cutting depth has direct influence on contact length between chip and face surface of cutting wedge. Therefore higher influence of cutting depth outcomes onto axial *Fa*, then on tangential *Ft*, and smallest on radial component *Fr*. It can be concluded that cutting depth has higher influence on force *Fa* and *Ft* than cutting feed. It is vice-versa for the radial component *Fr*, where feed shows higher influence than cutting depth.

The cutting speed influence onto cutting forces change is interesting. At its increase the contact between face surface of cutting wedge and chip decreases, which causes reduction of chip ramming. The last is connected also to reduction of friction coefficient between chip and face surface of cutting tool as a result of increased temperature caused by cutting speed increase. This indicates cutting forces decrease by cutting speed increase.

It can be noticed from equations 2-4 that cutting speed has higher influence onto axial *Fa* and radial *Fr*, while as smaller onto tangential component *Ft*. Such influence order of cutting speed upon cutting components is explained by the occurrence of various temperature conditions.

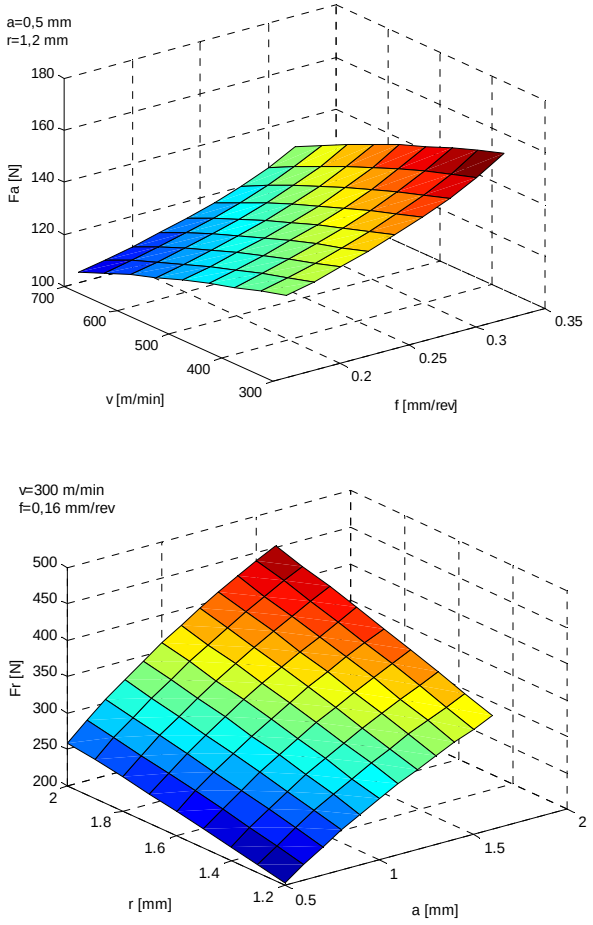

Fig. 3. Graphical interpretation of the influence of cutting speed - *v*, feed - *f*, cutting depth - *a*, and cutting tool insert tip radius - r_ε on the changes of axial *Fa*, radial *Fr* and tangential force component *Ft*

Namely, by cutting speed increase the contact surface in radial direction decreases, where due to higher temperature gradients there is reduction of mechanical characteristics of machined material and significant reduction of friction coefficient between cutting tool insert tip and machined surface. In addition to this is also the fact that cutting speed increase causes temperature and mechanical load change onto cutting blade. Similar is the condition also in direction of force *Fa*, where contact between cutting blade in initial stage is theoretically linear, which causes smaller heat

discharge i.e. high temperature occurrence near cutting blade [5].

From this outcomes friction coefficient reduction between rear surface of cutting tool and machined surface. Here, mechanical properties of machined materials are reduced due to high temperature. The condition on face surface of cutting wedge is different, where reduction of tangential component *Ft* is smaller due to larger contact surface between chip and cutting tool. Areas with plastic deformation and abrasive wearing of surface layer of cutting tool insert are noticed here [5]. This indicates existence of various friction coefficients i.e. various terms when chip wears against face surface.

Tip radius of the cutting tool insert r_ε has a different but proportional influence upon change of cutting forces components. Its increase causes contact length increase between cutting blade and machined surface, which indicates a possibility for larger decrease of axial force *Fa*. However, axial resistance *Fa* insignificantly decreases by increase of r_ε. This is caused by reduction of setting angle of cutting tool χ positioning, by increase of r_ε, which, actually, is different on the circular part against cutting blade length. Radial *Fr* and tangential *Ft* cutting force component increase by increase of r_ε. Then, higher is the influence of r_ε onto the radial component mostly due to larger contact with machined surface.

4. CONCLUSIONS

From the exhaustive experimental researches performed, obtained mathematical models, as well the analysis of results, following remarks and conclusions can be reached:

- The statistical analysis indicated that the describing of changes in cutting forces *Fa, Fr* and *Ft* as function of machining parameters *v, f, a*, and cutting tool insert tip radius r_ε, by means of power function, correctly describes the physics of change of forces as function of machining parameters;

- All factors adopted in models are significant, apart in model (2), and their influence is as follows:

- cutting speed affects cutting forces counter-proportionally, meaning that cutting forces decrease by cutting speed increase;
- feed, as well as cutting depth, have proportional influence on cutting forces change;
- cutting tool insert tip radius r_ε influences cutting forces in a mode where by its increase causes significant increase of forces *Fr* and *Ft*, and insignificant increase of *Fa*;
- cutting depth - *a* and feed - *f* have higher influence, smaller r_ε, and smallest and counter-proportional cutting speed *v* on the change of main cutting force.

- Since small differences of influences are gained and when in a research an influence sign change occurs, justified is to perform more intensified research activities in sense of reducing uncertainty of results that are gained from measurements and determination of the confidential interval onto the influence of separate factors, all with the purpose of reducing or eliminating the negative influence that outcomes from research hardware equipment, the validity of the application of adopted machining parameters, the experiment planning methodology, the mathematical processing of results and applied software solutions.

5. REFERENCES

[1] Pavlovski, V., Kuzinovski, M., Zebrovski, H., Cichosz, P.: *Experimental research of the physical phenomena in turning with ceramic cutting inserts*, Third International Conference on advanced manufacturing systems and technology, AMST '93, Udine, Italy, 1993.

[2] Kuzinovski, M., Trajčevski, N., Cichosz, P., Tomov, M.: *Monitoring system for investigation of the cutting forces in the machining with turning*, 9th International Scientific Conference, MMA 2006, p.p. 19-20, Novi Sad, Srbija i Crna Gora, 15-16, June, 2006.

[3] Stanić, J.: *Metod inžinjeriskih merenja*, Mašinski fakultet, Beograd, 1990.

[4] Trajčevski, N.: *Monitoring system in experimental investigation in machining with turning*, Master thesis, Skopje, February 2008.

[5] Cichosc, P., Zebrowski, H.: Meßung der schnittemperatur beim drehen mit keramischen schneiden, VII Internationale konferenz für werkzeuge und ausstellung. Miskolc (H), 29-31.8.1989.

[6] Jurković, Z., Jurković, M.: *Modeling and simulation of the cutting force using experimental data*, 7-th International Research/Expert Conference "Trends in the Development of Machinery an Associated Technology", TMT 2003, p.p. 81-84, Lloret de Mar, Barcelona, Spain, 15-16 September, 2003.

Authors: **Prof. Kuzinovski Mikolaj, PhD,** University "Ss. Cyril and Methodius", Faculty of Mechanical Engineering, Skopje, Macedonia. **Trajčevski Neven, MSc,** Military Academy - Skopje, Macedonia. **Prof. Cichosz Piotr, DSc**, Institute of Production Engineering and Automation of the Wroclaw University of Technology, Wroclaw, Poland.
E-mail: mikolaj@mf.edu.mk
neven.trajchevski@gmail.com
piotrc@itma.pwr.wroc.p

Journal of Production Engineering
Vol.12 No.1

Pechacek, F., Hruskova, E.

POWER ULTRASOUND IN MACHINING

Abstract: *Ultrasound energy consisted of oscillating mechanical and acoustic energy is often called ultrasound. There are a few fields with usage of ultrasound oscillation in mechanical material machining. One of this ways is physical principle of ultrasound machining by abrasive suspension and the second is intension grinding technique by ultrasound. Paper deals with general information about ultrasound and with his application in machining process.*
Keywords: *technology, ultrasound, intension technique.*

1. INTRODUCTION

One way of the economical development is considered the increasing of the industry production through the slower development of production usage. The way of technological process rationalization is intensification of technological processes by ultrasound.

2. CHARACTERISTIC OF ULTRASOUND

Special properties and influences of ultrasound energy in the conditions of broadening ultrasound oscillation are showed in the research results. Ultrasound energy consisted of oscillation mechanical and acoustic energy is often called ultrasound. Ultrasound falls under to acoustic field with acoustic zone up to audibility of hearing and ultrasound technique delimits this zone above limit 20 kHz with respect to safety aspect. Effect of ultrasonic energy for its dissemination in the environment depends on the size of amplitude. In this regard, ultrasound can distinguish between small amplitude - ultrasonic energy in this case is passive (it does not effect any physical or chemical change) by a large amplitude - active ultrasonic energy is often called macrosound or ultrasound power (the effect of affecting the properties respectively structure subjected to environmental its effects).

3. ULTRASOUND MACHINING AND MACHINING AIDED BY ULTRASOUND

In technical practice, the generally used two terms to express the working material through ultrasound. It is Ultrasonic machining (USM - Ultrasonic Machining / and working with the support of ultrasound. The principle of ultrasonic machining is based on the abrasive effect of the suspension and fine abrasives, circulating between the workpiece and tool. It is a broad-based technology that is used for cutting materials, dredging grooves, deep hole drilling, milling and thread cutting, polishing, lapping and grinding of glass and so forth.
Machining with the support of ultrasound technology is a combination of processes, for example. turning, drilling, grinding with a combination of vibrant tool ultrasonic energy. Grinding with the support of ultrasound is also referred to as rotary ultrasonic machining. / Rotary Ultrasonic Machining - RUM /.

Fundamental differences between the ultrasonic treatment and ultrasonic rotary cultivation are:

- Movement of the tool during operation with the support of ultrasound-RUM is higher axial and axial rotation in the ultrasonic machining-USM only vibrating movement of the tool,
- For grinding with the support of ultrasound - RUM – are used classic diamond tools in the form of conventional grinding wheels,
- For the removal of material used abrasive particles of diamond tool - grinding grains.

In ultrasonic machining USM - tool is used for the transmission of vibration, pressure and flow guide of suspension and the suspension is not in direct contact with the workpiece, on the contrary, in the RUM is in direct contact with the workpiece.

4. ULTRASOUND USAGE IN MACHINING

There are several areas where the use ultrasonic oscillations in the mechanical machining of materials. One of these areas is the physical principle of the ultrasonic machining abrasive suspension. (Fig. 1) This method of ultrasonic machining abdominal suspension and vibrant tool allows producing hard and brittle materials, different aspect holes (blind and transient) of very complex shapes. Allows to carry out such operations, when other methods of machining have been very difficult, would be unreasonable or not performed at all. Vibrant tool to the workpiece is pressed with frequency of approximately 20 000 oscillations per second at a time and retract abrasive grains dispersed in water in the working materials.
These grains with their sharp edges rip small particles from the surface of the material. Together with the abrasive suspension are then removed to the surface, taking the place flows in the new grinding suspension.

The whole cycle is repeated continuously.

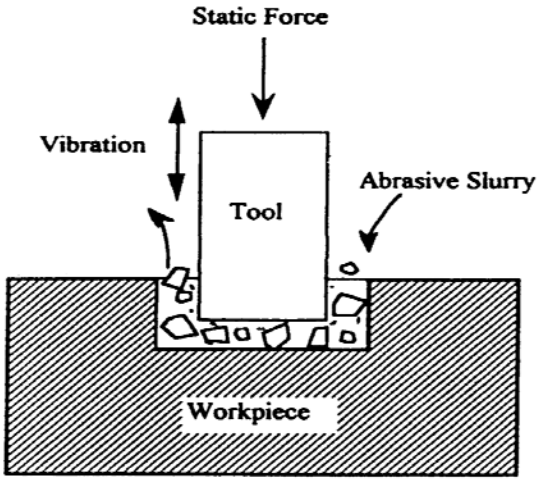

Fig. 1 Ultrasound machining by abrasive slurry

The second is the intensification of grinding methods by ultrasound. Getting to the point of ultrasonic oscillations sharpened substantially affects the entire process to create the conditions for the intensification and increased productivity grinding process.

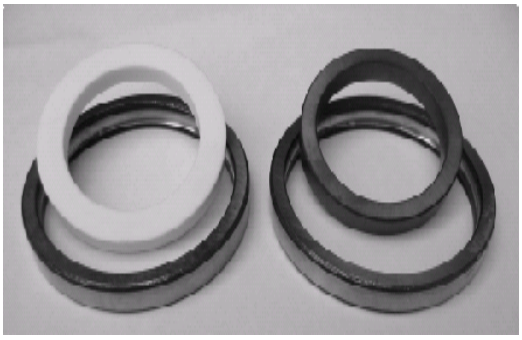

Fig.2 SiSiC and Al_20_3 rings

Fig.3 Diamond grinding tool1A1 D30 T15x2, 5H10 D76 C

In terms of utilization of ultrasound to influence the process grinding to pay attention to these methods and technologies:

- Ultrasonic drilling diamond abrasive tools
- Ultrasonic grinding,
- Ultrasonic honing and superfinishing,
- Ultrasonic cleaning grinding wheels,
- Ultrasonic grinding compensating coil.

Ultrasonic drilling using diamond abrasive tools (Fig. 3) represents a special method of grinding the material in which the diamond tool rotates while axial oscillation.

Abrasive tools have full rotational shape or tubular cross-section. In the space below the abrasive face of diamond bearing material is machined by grinding and coolant floatation on the surface.

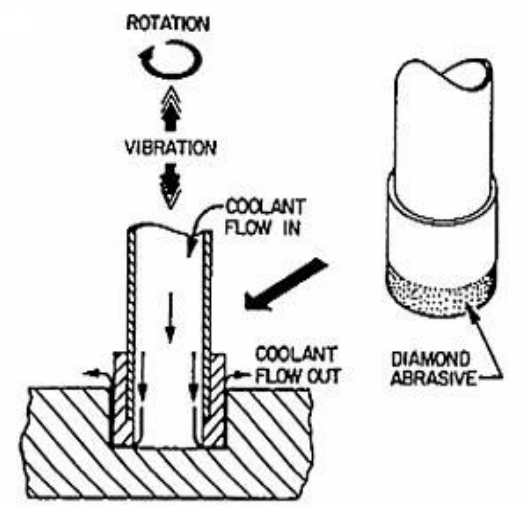

Fig.4 Schematic illustration of rotary ultrasonic machining (RUM) process

Technology (Fig. 4) ultrasonic grinding materials by rotated and ultrasound oscillated abrasive tool allows you to increase productivity and the intensification of the technological process of grinding. The influence of ultrasound arises in the process of continuous renewal sharpened cutting properties of grinding the tool (Fig. 5) which can be described as the "cleaning and self – sharpening" of grinding tools.

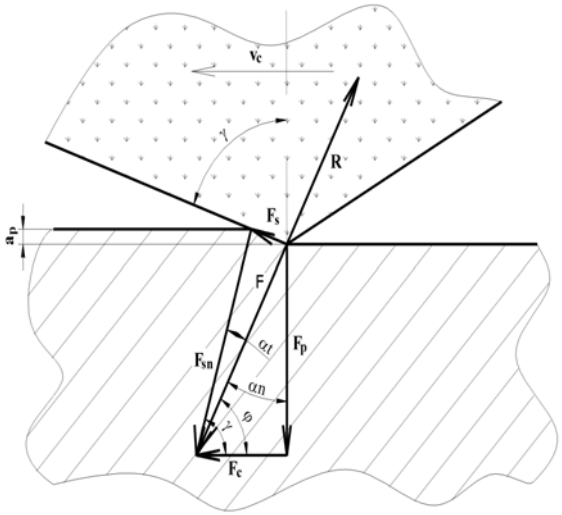

Fig. 5 Resolution of ultrasound grinding forces,
F – final cutting force, F_p – pressed force, F_c – cutting force of grinding wheel, F_s – friction force, F_{sn} – normal force, R – final force charged to a grinding grain, a_p – depth of grinding, γ - rake, φ – angle of feed moving, α_n – friction angle on the workpiece, α_t – angle of friction., v_c – cutting speed

Ultrasonic honing and superfinishing are one of the successful application of ultrasonic methods applied to grinding processes in the finishing operations of precision rotary surfaces. It was found that the process under the influence of ultrasonic grinding, honing and superfinishing permanently continued, without a gradual slowdown and decline in the effect of cutting abrasive grain.

Another area is the intensification of some classical methods of metal machining by vibrant tools such as. turning, milling, drilling, cutting threads.

The effectiveness of the impact of ultrasound on the process of cutting chips depend on several factors: the frequency and amplitude of oscillations, the ratio of the speed of oscillation of circuit speed of machined parts, sectional chips, physic-chemical properties of working material and tool.

Ultrasonic oscillations tool in turning in the direction of cutting speeds directly affect the deformation process of cutting. Separation of chip is made in full cutting speeds. Pressing the chip is smaller, which significantly reduces the cutting force (40 to 50%).

Diminishes the fortifying of the cutting area and improves the quality of machined surface area, which takes the mirror shine. To the ultrasound usable field consists the surface strengthening of metal workpieces by suitable finished and oscillated ultrasound tool.

Ultrasound oscillations as intensification factor are effective in surface balling of workpieces of cloudy and

Fig. 6 Ultrasound grinding by Al_2O_3

no cloudy steel and cast iron.

This method of strengthening surfaces, improving the fatigue properties, reduce roughness, increase wear resistance as well as ultrasonic microhardness can achieve in considerably by smaller static forces balling.

The principle of that method is based on the use of erosion activity of cavitations acting in a suitable fluid containing abrasives.

5. CONCLUSION

The favorable impact of power ultrasound on the process of grinding of hard brittle materials by grinding diamond tools for the use of appropriate types of tools and technology with proper choice of conditions seen in general:

- several cutting increasing rate of speed and feed speed of tool to cut,
- a substantial decrease in the value of specific wear diamond grinding tools,
- the machining of hard and brittle materials with tool of greater depth of cut,
- significantly higher productivity and deepening the process of machining in comparison with ultrasonic free abrasives machining, improving the quality of machined surfaces of hard brittle materials by reducing the surface roughness.

The article describes about field only of power in the ultrasonic machining. Despite the positive laboratory research has failed to implement on a broader scale, these applications of active sonar to practice.

It can be expected that further research in this area could increase the current knowledge and the issue adopts a greater number of qualified specialists, who gradually extended their use in practice.

This paper was created thanks to national project VEGA 1/009/08 **Optimalization systems and processes of power ultrasound.**

6. REFERENCES

[1] Mankova, I.: *Progresívne technológie, Progressive technologies.* Vienala Košice, 2000, 275s, ISBN 80-7099-430-4

[2] Mihalcak, P., Liptak, O., Pis, P.: *Skúmanie vplyvu ultrazvuku na vŕtanie tvrdých krehkých materiálov brúsnymi diamantovými nástrojmi.* Searching of ultrasound influence to drilling to hard brittle materials by grinding diamante tools. Volume of Research Works, Slovakia, SjF STU Bratislava, Vol. 15, 1977, pp 105-122

[3] Svehla, S., Figura, Z.: *Ultrazvuk v technológií, Ultrasound in technology,* Alfa Bratislava, 1984.

[4] Matusova, M., Javorova, A: *Modular clamping fixtures design for unrotary workpieces.* In: Annals of Faculty of Engineering Hunedoara - Journal of Engineering. - ISSN 1584-2673. - Tom VI, Fasc. 3 (2008), pp. 128-130

[5] Danisova, N.: *Application of intelligent manufacturing system in the flexible assembly cell***,** In: Annals of Faculty of Engineering Hunedoara - Journal of Engineering. - ISSN 1584-2673. - Tom V, Fasc. 3 (2007), pp 41-45,

[6] Lipa, Z., Charbulova, M.: *Quality of machined surface at grinding*, In: Proceeding of 9th. International conference TECHNOLÓGIA 2005. Bratislava: STU, 2005, pp. 445 – 450, ISBN 80-227-2264-2

[7] Matusova, M., Oravcova, J., Kostal, P.: *Gripping in robotized workplaces.* - Vega 1/0206/09. In: Machine Design. - ISSN 1821-1259. - 2009: 49th anniversary of the Faculty of technical sciences, Novi Sad. May 18th 2009. - Novi Sad : University of Novi Sad, 2009, pp. 355-358

[8] Ciutrila, G.: *Stand and results of the researches on the processing technology of internal grinding using ultrasonic vibrations.* In: International Symposium MTeM Cluj –Napoca, Romania, 2001

Authors: **Dipl. Ing. Frantisek Pechacek, PhD.; Dipl. Ing. Erika Hruskova**, University of Technology in Bratislava, Faculty of Materials Sciences and Technology, Razusova 2, 91724 Trnava, Slovakia, Phone.: +421 33 55 11 601, kl. 26, 21.
E-mail: frantisek.pechacek@stuba.sk
erika.hruskova@stuba.sk

Journal of Production Engineering
Vol.12 No.1

Radonjić, S., Baralić, J., Sovilj-Nikić, I.

CENTERLESS GRINDING AND POLISHING OF CIRCULAR STAINLESS STEEL TUBES

Abstract: *This paper describes the process of grinding and polishing of circular stainless steel tubes carried out by special centerless machines. It is a machine used for grinding and polishing of stainless steel tubes made by Surface Engineering, Italian company from Milan. The machine consists of four grinding and three polishing modules.*
Key words: *centerless, grinding, tube*

1. INTRODUCTION

Centerless grinding process differs from other cylindrical grinding processes in that the workpiece is not mechanically constrained. On traditional, old design machines, a workpiece is either held between centers or chucked and rotated against the faster spinning grinding wheel by an external motor usually located in a workhead. Parts made using a centreless process do not require center holes, drivers or workhead fixtures. Instead, the workpiece is supported on its own outer diameter by a work rest blade located between a high speed grinding wheel and a slower speed regulating wheel with a smaller diameter. Centerless grinding is proper for grinding cylindrical tubes and bullion.

2.CENTERLESS GRINDING

Grinding is one of the most significant production operations within final processing, for it provides:
- highly accurate proportions
- high quality of the processed surface.

Most commonly, grinding is subsequent to thermal treatment whereby it eliminates any defects caused by thermal deformations during the thermal treatment.

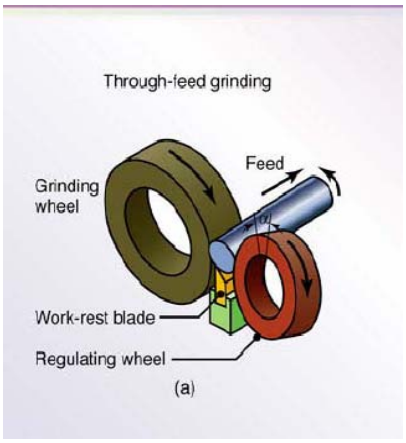

Fig. 1. Schematic view of the mode of operation [1]

The type of abrasive, machine performance and selection of the working parameters are of major importance for the final precision and surface quality of the machined components.

Centerless grinding makes it possible to quickly replace the processed parts with those to be processed. There are three main modes of centerless grinding:

1. Through-feed grinding
2. In-feed grinding
3. End-feed grinding.

Figure 1 shows the schematic view of through-feed grinding. [1]

As the figure shows, grinding and regulating wheel rotate in the same direction, a work-rest blade being in between. When centerless grinding is concerned, regulating wheel is usually rotated for α angle that ranges from 0° to 8°. This provides the occurrence of workpiece horizontal velocity component, therefore the external mechanism for axial motion of the workpiece is needless. Owing to this axial motion, objects processed in such manner can have only circular cross-section which is constant along the whole workpiece.

During the grinding process, number of revolutions of regulating wheel is much smaller than the one of grinding wheel, and this difference regulates the number of revolutions of a workpiece and its axial motion. In order for this mode of operation to be feasible, the machine must be regulated by PLC controller whose role is to adjust both the number of revolutions and the workpiece force on grinding wheel.

During the process of centerless grinding, grinding wheel performs the main rotary motion. Secondary motion is performed by the regulating wheel, it is rotary and it provides longitudinal tube feed. The axis of grinding and regulating wheels can shift from 1 to 10 mm, as related to the axis of the workpiece. The feed of the workpiece can vary according to change in the dip angle α and periferal velocity of the regulating wheel.

$$S_{workpiece} = V_r \cdot \sin\alpha = D_r \cdot \pi \cdot n_r \cdot \sin\alpha \quad [mm/min],$$

wherein:

$S_{workpiece}$– presents feed of the workpiece
V_r – periferal velocity of regulating wheel
α – dip angle of the regulating wheel in relation to grinding abrasive wheel

D_r – external diametar of the regulating wheel
n_r – number of revolutions of the regulating wheel

According to the diametar of the workpiece, two parameters of the operation mode are accepted: space between the grinding and regulating wheels, and change in the height of longitudinal work-rest blade. During the tube grinding process on the special centerless machine, grinding wheel is wrapped with changeable abrasive belt which is replaced after being worn out.

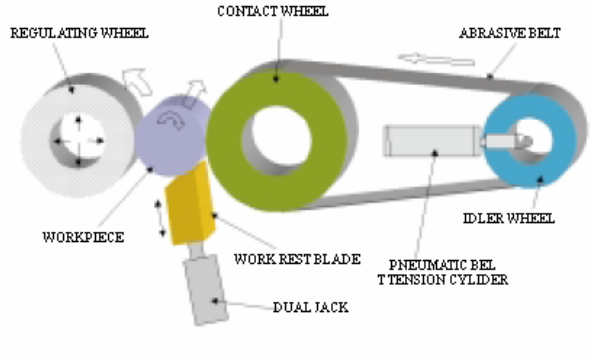

Fig. 2. Centerless grinding process setup [2]

The process of centerless belt grinding is utilized for the outher grinding of cylindrical surfaces. It works after the principle of through-feed of the workpiece. Centerless grinding process setup is shown in figure 2.

Centerless grinding is on the increase because it eliminates the operation of centering both ends of the workpiece. The workpiece is completely supported in the grinding zone. That fact permits a higher efficiency of the grinding process.

2.1. Abrasive belt centerless grinding

During the abrasive belt centerless grinding, removal of material is achived by the grinding head, which consists of the following main components:

- The regulating wheel,
- The contact wheel,
- The idler roll
- The work rest blade and
- Abrasive belt.

The workpiece is supported by an angular rest blade (through-feed support). Work rest blade can be adjusted for different heights, depending on the diameter of the workpiece. The abrasive belt is supported by a serrated rubber or plain-faced contact wheel and an idler wheel. The tension of the abrasive belt is achieved through a pneumatic device. The regulating wheel is placed opposite to the contact wheel. Its role is to ensure the contact between the workpiece and the grinding head. Its position is set under a certain angle to generate an axial feed and workpiece's rotation. The surface speed of the regulating wheel is usually about 1/20 of the contact wheel speed. [2]

The cutting forces hold the workpiece against the rest blade. The workpiece rotates at the same surface speed as the regulating wheel. The rest blade supports the workpiece and can be adjusted at a proper height relative to the contact wheel.

Outlet of the abrasive belt grinding process is workpiece surface roughness. For the best results of the grinding process, working parameters of the process must be properly determined. The most important working parameters on abrasive belt grinding process are cutting speed, feed rate, contact pressure, contact wheel hardness etc.

Abrasive belt centerless grinding technology offers many adventages. The most important are:

- High feed rates can be utilized, commonly up to 20m/min
- Workpiece is supported both by the regulating wheel and the work rest blade. In this way, cutting process is intense, with no distortion of the workpiece
- Because there is no wear of the abrasive belt, the surface speed is constant
- The process is cooler
- Setup time is short [2].

3. MACHINE FOR GRINDING AND POLISHING OF CIRCULAR STAINLESS STEEL TUBES

The main purpose of advanced machine systems is to achieve high productivity in conditions of high accuracy and surface quality for the workpiece. One of the ways to attain this goal is to group more operations, commonly carried out on different machines, on the same machining system. Some recently made tests show a significant improvement in roughness and accuracy of tubes machined on this machine systems.

Fig. 3. The entire machine for grinding and polishing of circular stainless steel tubes

The machine for grinding and polishing of circular stainless steel tubes is a product of the Italian company *Surface Engineering* from Milan, and it is the result of long time experience and cooperation with *Siemens* company. Figure 3 shows the entire machine. The machine for grinding and polishing of stainless steel tubes comprises a set of several minor machines – modules. The total nominal output of the machine is 80kW and it requires constant water supply of 2 bars water pressure for its functioning.

The total machine length is 21m and it functions with the assistance of a crane whose lifting capacity amounts to 10t. It is mounted in a machine hall, and its role is to transfer raw material (unmachined tubes) and ready made products.

The total machine length is 21m and it functions with the assistance of a crane whose lifting capacity amounts to 10t. It is mounted in a machine hall, and its role is to transfer raw material (unmachined tubes) and ready made products.

The machine consists of an infeed, four grinding modules, three polishing modules and a part for authomatic packaging of machined tubes into polyethylene foil. The assembled machine is controled by PLC *Siemens* company. It is the machine construction that enables shutting down some of its parts (according to circumstances or due to a failure/maintenance), which provides maximum working efficiency of the machine. [5]

The infeed is on the tube entrance into the machine, and it provides the entrance of the tubes 100mm – 6000mm long. Most commonly, 6000mm long tubes are utilized. The infeed is completely automatized and its maximum load is 2t, wherein the number of tubes it can receive depends on the diameters and thickness. The diameter of tubes varies between 10mm and 220mm.

The grinding modules ST 220 (Figures 4 and 5) are the first in the technological procedure of pipe grinding and polishing.

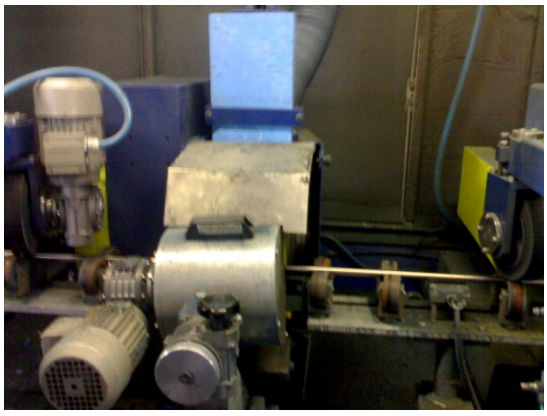

Fig. 4. Interior of the ST220 module

All the grinding modules are identical, however the power within particular modules varies, i.e. 17kW, 13kW, 10kW and 7kW. The first grinding module exerts the greatest power. Each of the modules may vary in the number of revolutions of the grinding wheel, within the range of 1500o/min to 3000o/min, which is governed by the PLC.

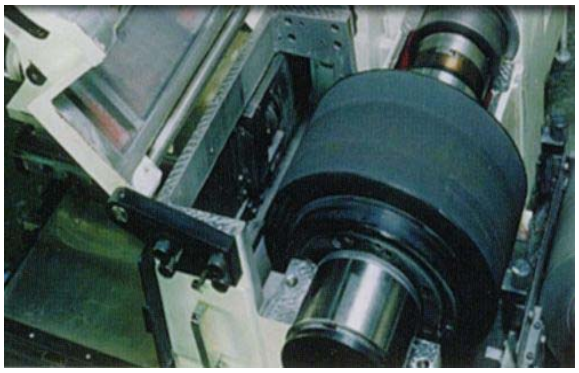

Fig.5. Grinding wheel inside the grinding module

The fineness of the abrasive bands of the grinding wheels also varies among modules. The fineness of the abrasive band of the first module is the lowest (400), and it grows with bands that follow, i.e. 600, 800 and 1000. [3]

Artificial materials, such as aluminium oxide, silicon carbide, cubic boron nitride and diamond are most commonly used for the production of grinding (abrasive) bands. For the different purposes, the ST 220 uses CBN (cubic boron nitride) and PCD (artificial diamond)-based bands produced by *Klingspor*.

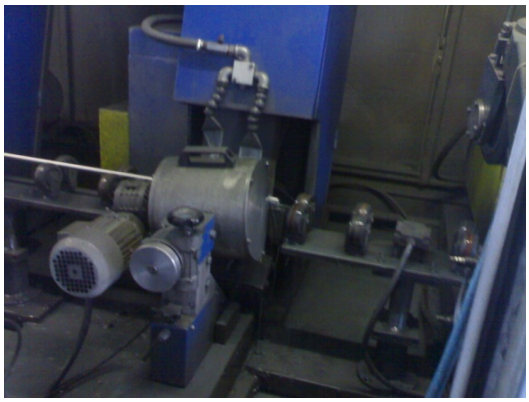

Fig.6. Interior of the PT 150 module

Having being worked in grinding modules, tubes enter the polishing modules, the PT 150 type (Fig. 6). All the modules are identical, nonetheless they exhibit different power, i.e. 7kW, 5kW and 3kW.

Fig.7.Polishing brushes

Within each module, polishing brushes (Fig. 7) can have different number of revolutions (100 o/min – 300 o/min), which is regulated by the PLC. [4]

The fineness of the polish paste in each of the modules is 1200, 1400 and 1600. Brushes and pastes are combined, depending on quality requirements (high, moderate or low tube finish).

Subsequent to the above phase, tubes are automatically placed into a special carrier. They are then transferred by an automatic packaging machine into the 70μm thick polyethylene foil, whereupon these are considered as final products. The entire process of tube engineering can include finishing of maxiumum 25 tubes per hour, whereby the actual speed is approximately 10 tubes per hour, since the speed of the process depends on quality requirements. The materials used in the process (grinding bands, polishing brushes and polish pastes) are produced by the *Klingspor* and *3M*.

4.CONSLUSION

The paper presents the process of abrasive belt centerless grinding and polishing of 6000 mm long stainless steel tubes worked on a special machine produced by the company *Surface Engineering* from Milan.

.

This process is carried out on a complex machine comprising four grinding and three polishing modules. Each of the modules ensures higher quality of the processed surface. Depending on quality requirements, some of the modules can be excluded.

This is the latest method of tube processing. It is highly productive, and it ensures high quality and accuracy of the processed surface. Multiple modules systems prove ability to obtain required specifications in a single pass.

5. BIBLIOGRAPHY

[1] Koepfer C.:*Centerless Grinding :Not Magic*, MODERN MACHINE SHOP Magazine, 2007.

[2] Carlson G., Dr Marinescu I.,: *New Improvements in Abrasive Belt Centerless Grinding*, ABRASIVES MAGAZINE, february/march 2002

[3] Surface Engineering ST220, Milan, Italy, 2007

[4] Surface Engineering ST150, Milan, Italy, 2007

[5] Siemens Programabile Logic Controlers, Vienna, Austria, 2005

Journal of Production Engineering
Vol.12 No.1

Tomov, M., Kuzinovski, M., Cichosz, P.

GENERAL EFFECT OF TOTAL DATA POINTS NUMBER ON MATERIAL RATIO CHANGE OF THE ROUGHNESS PROFILE

Abstract: *The study presents results gained from analysis of the effect of total data points change upon material ratio change of the roughness profile for constant evaluation length. Etalons were analyzed, representatives of the deterministic (turned) and stochastic (grinded) surface. Measurements were made by means of a stylus instrument Surtronic 3+, while as the analysis was performed by means of a professional software TalyProfile. The change of the amount of sampling spacing was provided by the program Microsoft Office Excel. Research was performed with sampling spacing in amount of 0,5; 1,0; 1,5; 2.0; 2.5 and 3.0 μm. The change of material ratio curve shape and material ratio for both deterministic and stochastic surface on depth 0,25Rt, 0,5Rt and 0,75Rt are analyzed.*
Key words: *Roughness profile, material ratio of the roughness profile, sampling spacing, contact (stylus) profilometer*

1. INTRODUCTION

Desired characteristics of mechanical parts' surface topography are more often stated as criteria for production quality evaluation. Large amount of functional characteristics that parts have to meet in exploitation depend precisely upon surface topography condition. Table 1 presents the dependence between functional characteristics and parameters that describe surface topography [1,2]. It is pointed out then that values of amplitude and functional parameters are decisive for correct part function.

Material ratio of the roughness profile [3,4,5], Figure 1, falls within functional parameters i.e. curve parameters [3]. Against ASME B46.1-2002 the material ratio is denote as t_p (denote also used in ISO 4287-1984 to 1997) and as Rmr(c) according to ISO 4287-1997. The value change of Rmr(c) is reviewed initiating from highest point of roughness profile peak above mean line till lowest point of roughness profile valley below mean line within sampling length, Figure 1, and is basis for surface bearing analysis.

Surface bearing is introduced as a term by Abbott and represents the size of overlapping of subject surface with nominal surface upon which certain force acts, when also the surface unleveled deviations are taken into account [6]. Change of Rmr(c) value against roughness profile depth within frames of Rt value is defined the material ratio curve of the roughness profile or Abbott-Firestone curve, Figure 1. Material ratio curve shape of the roughness profile can be proportional, digressive, progressive and combined as digressive-progressive and progressive-digressive.

Prompted by the high significance of roughness parameter values in parts function, as well as large differences gained in roughness parameter measurement processes [7], often researchers try to analyze and determine the effects of measurement conditions upon precision of roughness profile measured values. Results of such researches are presented in [8,9,10,11,12,13,14,15] and refer to analysis on sampling spacing change, stylus geometry, filtering, evaluation length, mean line determination mode, etc. Most expanded is the interest in research of the effect of sampling spacing change upon roughness parameters. Therefore, in [8] is determined the effect of sampling spacing change upon peak, direct measurable and average parameter values. In [9] is determined how sampling spacing change effect of value of average slope of modeleded random profile.

Function	PARAMETERS				
	Ampli-tude	*Distrib-ution*	*Spacing*	*Hybrid*	*Functi-onal(Rk)*
Bearings	↑	↑	↖	↖	↑
Seals	↑	↑	↖	↑	↑
Friction	↑	↑	↑	↑	↑
Slideways	↑	↑	↑	↖	↑
Wear	↑	↑	↑	↑	↑
Fitigue	↑	↖		←	↑
Stress and fracture	↑	←	↖		↑

Key: ↑-much evidence ↖-some evidence
← little or circumstantial evidence

Table 1.

It is clear that for unchanged evaluation length or surface, sampling spacing against x- or z-axis and total number of data points, which profile is described with, surface roughness in 2 and 3D are in direct mutual dependence. Namely, larger sampling spacing means smaller number of data points and vice-versa.

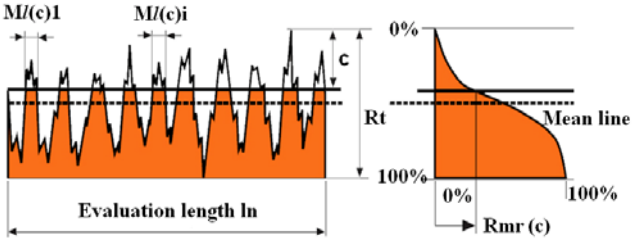

Figure 1. Material ratio curve of the roughness profile [4].

Measurement of machine parts surface topography, especially in 3D, includes several thousands of points [1, 2]. All these points pass through sampling process, transfer, A/D conversion, statistical processing and graphical presentation. Even though a very powerful digital technique is used nowadays for measurements, still particular time [16] is needed. If this is supplemented by the need of repeating measurements several times all with the purpose of gaining satisfactory statistical comparison of results, then the factor time is certainly worth paying more attention to.

Prompted by such fact, authors of this study decided to analyze the general influence of data points change upon material ratio change of the roughness profile for constant evaluation length and on several levels of vertical profile sections. Additional motive for such research was the large dependence of functional characteristics from material ratio curve (which determines the Rk parameters), which can be evidenced in Table 1, and the absence of dependence in international standards (ISO) between the measuring conditions and the Rk parameters.

Particularly vital is to review the intensity of coefficient change and material ratio curve for various profiles with various number of data points for deterministic and stochastic surface. Presented results were gained as a result of researches performed within frames of the international project [15], while as are also basis for defining scientific thesis in applied doctor's dissertation [14]. Based on the analysis of till today published studies in this field, as well as based on experiences gained, it can be concluded that sampling spacing change directly affects values of peak parameters and shape of roughness profile, which directly determines the coefficient and shape of material ratio curve. Precisely this conclusion for existence of a double dependence does not allow free theoretical interpretations of the behaviour of material ratio size and material ratio curve shape for various sampling spacing.

2. MEASUREMENT CONDITIONS AND MEASURING EQUIPMENT

Researches of such type require utilization of computer equipment for roughness measurements that provides access to measured profile coordinates. For the purpose, coordinates of original roughness profiles were gained by means of software TapyProfile connected to contact profilometer Surtronic 3+, with which measurements were taken, Figure 2. Various etalon surfaces were used in the research, representatives of deterministic surface (machined by turning, Figure 3, with nominal Ra = 0,2 μm) and stochastic surface (machined by grinding, Figure 4, with nominal R=0,2 μm). Measurements are in compliance with recommendations prescribed in ISO 3274-1996 and ISO 4288-1996. Measuring equipment verification was performed by means of calibration, applying etalon of type C with value for Ra of 6 μm in compliance with [17,18]. Vertical resolution of unit roughness measurement is 10 μm, while as horizontal resolution amounts 0,5 or 1 μm for evaluation lengths smaller or equal to or larger than 8 μm, appropriately. Pick-up: TYPE 112-2672 (DCN 001) with stylus radius of 2 μm and skid radius of 8.7 mm move with speed of 1 mm/s against measured surface. In the research also a stylus with radius of 5 μm is used for measured etalons with Ra = 0,2 μm, which is not in conformance with ISO 3274-1996 and 4288-1996.

Figure 2. Computer equipment for roughness measurements

A deliberate omission is in question for the purpose of defining also the affect of the mechanical filtering of roughness profile caused by stylus radius in terms of defining this affect upon further research process with sampling spacing change.

Evaluation length (ln) contains five sampling lengths (lr) with size of 0.8 mm.

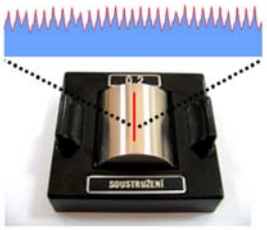

Figure 3. Deterministic etalon surface (machined by turning)

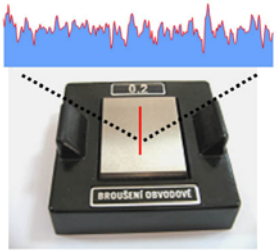

Figure 4. Stochastic etalon surface (machined by grinding)

3. EXPERIMENTAL RESEARCH

Applied professional software TalyProfile has ability to record measured (original) profiles in TXT-Ascii Profiless format, thereby providing opportunity for undertaking coordinates against x- and z-axis and there further processing.

Data points number change is provided by change of sampling spacing for constant evaluation length. So, original profiles with deterministic and incidental character were gained with sampling spacing of 0,5 µm and contain 8000 points with evaluation length of 3,9995 mm. Profiles with sampling spacing of 1 µm contain 4000 with evaluation length of 3,9995 mm.2667 points are contained in profiles with sampling spacing 1,5 µm at length of 3,999. At length of 3,998 mm match 2000 data points for sampling spacing of 2 µm. Profiles with sampling spacing of 2,5 µm contains 1600 points at length of 3,9975 mm an on length of 3,999 mm for sampling spacing of 3 µm match 1334 data points. Various size of sampling spacing for one same recorded profile was gained by using program Microsoft Office Excel since applied measuring equipment did not allow sampling spacing change thereby also data points number change.

By omission of one, two, three, four or five points on original profile the change of total number of data points is simulated, however always initiating from one same starting point. In that way, roughness profiles with sampling spacing of 1,0; 1,5; 2,0; 2,5 and 3,0 µm are gained. However, profile evaluation length suffers insignificant change due to the omission of points from original profile, which always initiates from same starting point. Largest deviation on evaluation length of 2 µm is noticed on profiles with sampling spacing of 2,5 µm.

The purpose of data points number change is to provide analysis of the influence of number of data points that define roughness profile upon the change of material ratio. Investigation include diferent section level of roughness profile, namely 0,25Rt; 0,5Rt and 0,75Rt. Also analysis was performed on the change of shape of material ratio curve by calculation of Rk parameters. Rk parameters are standardized in ISO 13565-2:1996 and presented on Figure 5. Each change of material ratio curve shape directly influences values of parameters: Rk, Rpk, Rvk, MR1, MR2, A1 and A2.

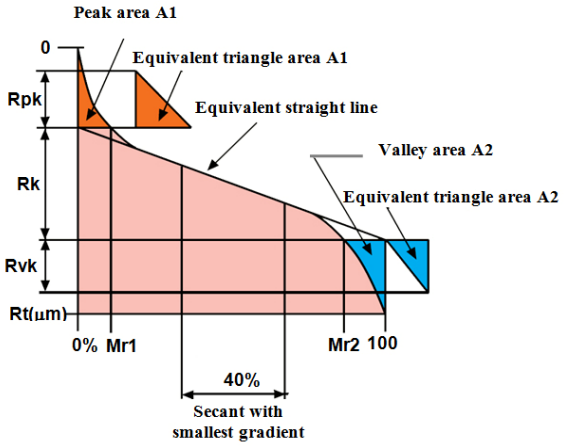

Figure 5. Rk parameters [4]

4. PRESENTATION AND ANALYSIS OF RESULTS GAINED

Values of material ratio of the roughness profile on section (depth) level of 0,25Rt, 0,5 Rt and 0,75Rt, as well as the percentage differences gained for profiles with various data points, for deterministic and stochastic surface and for original profiles measured with stylus radius of 2 and 5 µm, are presented in table 2, 3, 4 and 5. The minus prior ratio difference determines that gained values are smaller than values of original profile.

Rk parameter values for different profiles with mutual ratio differences are systematized in tables 6, 7, 8 and 9, with following units of measurement Rk (µm), Rpk (µm), Rvk (µm), MR1 (%), MR2 (%), A1 (µm^2 /mm) and A2 (µm^2 /mm).

Values gained for material ratio of profiles with various number of data points for section level of 0,25Rt, 0,5Rt and 0,75Rt confirmed the assumptions that coefficient change, even theoretically, is hard to be foreseen in sense of determining the change trend. Results in table 2 show material ratio coefficient change by change of number of data points and this change is reduced by depth increase of analyzed cross-section. It can be maybe herein concluded that some dependence exists between material ratio and number of data points for all levels of analyzed depth, which theoretical explanations exist for, which indicate that by omission of profile data points possible reduction of most protruded peak occurs, thereof moving of depth level towards the mean line, but also that by omission of data points from roughness irregularity slopes are reduced and cross-section surface increases i.e. surface material ratio.

Section level	Namber of profile data points					
	8000	4000	2667	2000	1600	1334
0.25 Rt (%)	6,2	6,26	6,96	6,96	9,1	9,82
0.5 Rt (%)	29,1	29,3	31,2	32,4	37,1	38,6
0.75 Rt (%)	79,3	79,2	81,2	81,9	84,9	85,3
Difference (%)						
0.25 Rt		0,97	12,26	12,26	46,77	58,39
0.5 Rt		0,69	7,22	11,34	27,49	32,65
0.75 Rt		-0,13	2,40	3,28	7,06	7,57

Table 2. Material ratio of turned etalon surface for various number of data points, measured with stylus of 2 µm.

Section level	Namber of profile data points					
	8000	4000	2667	2000	1600	1334
0.25 Rt (%)	12,7	12,9	12,8	12,8	12,2	12,3
0.5 Rt (%)	31,1	31,6	31,6	32,3	32	33,4
0.75 Rt (%)	80	79,8	79,5	79	76,9	76,4
Difference (%)						
0.25 Rt		1,57	0,79	0,79	-3,94	-3,15
0.5 Rt		1,61	1,61	3,86	2,89	7,40
0.75 Rt		-0,25	-0,63	-1,25	-3,87	-4,50

Table 3. Material ratio of turned etalon surface for various numbers of data points, measured with stylus of 5 µm.

Section level	Nanber of profile data points					
	8000	4000	2667	2000	1600	1334
0.25 Rt (%)	57,2	56,7	54,3	51	50,4	52,6
0.5 Rt (%)	98,8	98,8	98,7	98,3	98,2	98,7
0.75 Rt (%)	99,7	99,7	99,7	99,7	99,7	99,6
Difference (%)						
0.25 Rt		-0,87	-5,07	-10,84	-11,89	-8,04
0.5 Rt		0,00	-0,10	-0,51	-0,61	-0,10
0.75 Rt		0,00	0,00	0,00	0,00	-0,10

Table 4. Material ratio of grinded etalon surface for various numbers of data points, measured with stylus of 2 μm.

Use of inappropriate stylus significantly increased the material ratio at section level of 0,25 Rt, which indicates possibility of mechanical filtration and peak shortening, table 3. Possible mechanical filtration of stylus provided gaining results contrary to previously stated ones in Table 2.

Section level	Nanber of profile data points					
	8000	4000	2667	2000	1600	1334
0.25 Rt (%)	6,49	6,99	6,94	9,22	9,9	11,5
0.5 Rt (%)	60,4	62	61,5	65,4	66,7	68,2
0.75 Rt (%)	97,1	97,4	97,1	97,8	97,8	97,7
Difference (%)						
0.25 Rt		7,70	6,93	42,06	52,54	77,20
0.5 Rt		2,65	1,82	8,28	10,43	12,91
0.75 Rt		0,31	0,00	0,72	0,72	0,62

Table 5. Material ratio of grinded etalon surface for various numbers of data points, measured with stylus of 5 μm.

Param-eters	Nanber of profile data points					
	8000	4000	2667	2000	1600	1334
Rk	0,673	0,675	0,669	0,665	0,674	0,666
Rpk	0,319	0,306	0,308	0,295	0,274	0,257
Rvk	0,138	0,129	0,131	0,121	0,131	0,121
MR1	14,8	14,9	14,8	15,4	14,1	14,4
MR2	92,3	91,9	92	92,9	93,8	93,8
A1	23,6	22,8	22,8	22,7	19,3	18,5
A2	5,32	5,22	5,25	4,28	4,09	3,78
Difference (%)						
Rk		0,30	-0,59	-1,19	0,15	-1,04
Rpk		-4,08	-3,45	-7,52	-14,11	-19,44
Rvk		-6,52	-5,07	-12,32	-5,07	-12,32
MR1		0,68	0,00	4,05	-4,73	-2,70
MR2		-0,43	-0,33	0,65	1,63	1,63
A1		-3,39	-3,39	-3,81	-18,22	-21,61
A2		-1,88	-1,32	-19,55	-23,12	-28,95

Table 6. Rk parameters of turned etalon surface with various number of data points, measures with stylus of 2 μm.

Stochastic roughness profile has larger number of unit peaks and valley on unit length in comparison with deterministic one.

This fact leads us to an assumption that change of material ratio shall not vary much by change of number of data points, which theoretically would be explainable by matching the nature of change of material ratio coefficient with the change of data point number by accidental distribution of roughness profile ordinates. This assumption was confirmed in Table 4. At section level of 0,5 Rt and 0,75 Rt there isn't even any difference in the material ratio for various profiles. Stylus of 5 μm has fully changed the shape of stochastic roughness profile, thereof also of the material ratio gained, which can be evidenced in Table 5.

Material ratio curve shape for all reviewed profiles does not suffer any significant change by the change of data point number. Confirmation of this conclusion are the values of Rk parameters, particularly the Rk parameter. Its maximum change does not overcome more than 8% of all reviewed profiles, which gives us the right to conclude that central part of material ratio curve, which is defined with Rk (Figure 4) does not suffer changes in shape.

Param-eters	Nanber of profile data points					
	8000	4000	2667	2000	1600	1334
Rk	0,545	0,549	0,553	0,559	0,572	0,585
Rpk	0,378	0,369	0,354	0,335	0,296	0,271
Rvk	0,108	0,107	0,113	0,101	0,0992	0,0855
MR1	18,6	18,6	17,9	18,6	18	18,4
MR2	87,5	87,9	87,8	90,5	91,3	93,8
A1	35,1	34,3	31,7	31,2	26,6	25
A2	6,75	6,46	6,93	4,8	4,32	2,66
Difference (%)						
Rk		0,73	1,47	2,57	4,95	7,34
Rpk		-2,38	-6,35	-11,38	-21,69	-28,31
Rvk		-0,93	4,63	-6,48	-8,15	-20,83
MR1		0,00	-3,76	0,00	-3,23	-1,08
MR2		0,46	0,34	3,43	4,34	7,20
A1		-2,28	-9,69	-11,11	-24,22	-28,77
A2		-4,30	2,67	-28,89	-36,00	-60,59

Table 7. Rk parameters of turned etalon surface with various number of data points, measures with stylus of 5 μm.

Param-eters	Nanber of profile data points					
	8000	4000	2667	2000	1600	1334
Rk	0,649	0,645	0,647	0,638	0,625	0,608
Rpk	0,167	0,167	0,167	0,163	0,158	0,162
Rvk	0,39	0,386	0,386	0,37	0,352	0,36
MR1	7,16	7,07	7	7,53	7,54	7,19
MR2	89,7	89,6	89,8	90,2	89,4	89,3
A1	5,97	5,9	5,85	6,13	5,94	5,82
A2	20,1	20,1	19,6	18,1	18,6	19,3
Difference (%)						
Rk		-0,62	-0,31	-1,69	-3,70	-6,32
Rpk		0,00	0,00	-2,40	-5,39	-2,99
Rvk		-1,03	-1,03	-5,13	-9,74	-7,69
MR1		-1,26	-2,23	5,17	5,31	0,42
MR2		-0,11	0,11	0,56	-0,33	-0,45
A1		-1,17	-2,01	2,68	-0,50	-2,51
A2		0,00	-2,49	-9,95	-7,46	-3,98

Table 8. Rk parameters of grinded etalon surface with various number of data points, measures with stylus of 2 μm.

Param-eters	Namber of profile data points					
	8000	4000	2667	2000	1600	1334
Rk	0,681	0,674	0,669	0,661	0,647	0,642
Rpk	0,211	0,213	0,203	0,21	0,208	0,201
Rvk	0,308	0,306	0,299	0,291	0,278	0,278
MR1	9,35	9,69	9,59	9,59	9,78	9,91
MR2	89,9	89,9	89,4	89,7	89,2	89,7
A1	9,85	10,3	9,75	10,1	10,2	9,95
A2	15,7	15,56	15,9	14,9	15	14,3
Difference (%)						
Rk		-1,03	-1,76	-2,94	-4,99	-5,73
Rpk		0,95	-3,79	-0,47	-1,42	-4,74
Rvk		-0,65	-2,92	-5,52	-9,74	-9,74
MR1		3,64	2,57	2,57	4,60	5,99
MR2		0,00	-0,56	-0,22	-0,78	-0,22
A1		4,57	-1,02	2,54	3,55	1,02
A2		-0,89	1,27	-5,10	-4,46	-8,92

Table 9. Rk parameters of grinded etalon surface with various number of data points, measures with stylus of 5 μm.

Larger percentage changes were noticed on Rpk and A1 parameters, which refer to material ratio curve start, and Rvk and A2 parameters, which refer to material ratio curve end, where the change by omission of data points is most expressed.

5. CONCLUSION

Assumptions of authors that difficulties exist, even theoretically, for determining the material ratio change trend for known level of reviewing, which is in direct dependence by another parameter, were practically confirmed. Thereof, following can be concluded:

- Data point number change has some influence upon material ratio value when its is reviewed for level of cross-sections of 0,25Rt, 0,5Rt and 0,75Rt. Unfortunately a general conclusion can not be reached from this research concerning change trend for deterministic or incidental surface. Change trend determination is made impossible by dependence of material ratio on parameter Rt, which would mean that each change of Rt influences the material ratio, and the profile shape change with the data point number change.

- Maybe researches are necessary where material ratio change for known level for reviewing shall be analyzed along with the change of the parameters it dependents upon.

- Rk parameters indicate that significant change of material ratio curve shape by data point number change does not exist.

- From functional aspect, although material ratio indicated a change especially at a small level of cross-section, it can be concluded that data point number change does not have significant affect upon the ratio and the material ratio curve shape, since spring deviations and first friction processes occur in service on protruded surface peaks. In such circumstances significant is the change of the middle part of material ratio curve, which was here determined that is not under significant influence by the data point number

6. REFERENCES

[1]. K. J. Stout. *Thre-Dimensional Surface Topography; Measurements, Interpretation and Applications*. Center for Metrology the University of Birmingham, 1994.

[2]. K. J. Stout and L. Blunt. *Tree-Dimensional Surface Topography. Secont edition.* School of Engineering. University of Huddersfield, Penton Pres, London, 1994.

[3]. Taylor Hobson. *The Parameter Tree of Surface Roughness.* Centre of Excellence. 2000.

[4]. JIS B0601 Standard. *Explanation of Surface Characteristic*. Japan.

[5]. ISO4287:1997; Geometrical product specifications (GPS) - Surface texture: Profile method – *Terms, defenitions and surface texture parameters*

[6]. Mikolaj Kuzinovski, Dejan Pavlov, Piotr Cichosz, Henryk Zebrowski. *The influence of the wear of the cutting edge on the changes of the shape of the bearing curve of the machined surface by turning with ceramic cutting inserts.* Proceedings, Faculty of Mechanical Engineering, Skopje, Vol 13, No 1 (15) 1994, ISSN 0351 6067, pp 49-58.

[7]. Protocol of the discussion hold on the 8th June 1999 by the round table during the International Symposium "*Surface Engineering in Machining"*. Wroclaw – Szklarska Poreba, 7-9.06.1999. Poland.

[8].Tomov M., Kuzinovski M., Cichosz P.: *Effect of sampling spacing on surface roughness parameter values.* XXXII Conference on Production Engineering with foreign participants, Novi Sad, Serbia, 18-20.09. 2008.

[9]. Pawel Pawlus. *An Analysis of slope of surface topography.* Metrology and Measurement System 2005, 12 (3/2005); 299-314.

[10]. Pawel P. Pawlus. *Mechanical filtration of surface profiles.* Measurement 35 (2004); pp 325-341.

[11].Tomov M., Kuzinovski M., Cichosz P.: Effect *of evaluation length on results of surface roughness measurements*. XXXII Conference on Production Engineering with forign participants, Novi Sad, Serbia, 18-20.09. 2008.

[12]. Pawel Swornowski. *The influence of the mechanical filtration of the measuring-pin on the waviness and surface roughness.*Arhives of Mechanical Technology and Automation. Poznan 2006. ISSN 1233-9709, Vol. 26 nr 2. pp 129-137.

[13]. Pawel Pawlus. *TOPOGRAFIA POWIERZCHNI*. Pomiar, analiza, oddzialywanie. Oficyna Wydawnicza Poilitechniki Rzeszowskiej, Rzeszow 2005

[14]. Tomov Mite. *Contribution to methods and measurement techniques development for research of influential factors of surface topography identification.* Application for Ph.D. dissertation, Mechanical Engineering Faculty, Skopje, 2008.

[15]. Mikolaj Kuzinovski, Mite Tomov, Piotr Cichosz, Trajčevski Neven, ...: : *Study on possibilities and accuracy of surface layer geometrical structure determination by using contact profilometers.* Scientific-research project, finance by Ministry of Education and Science on Republic of Macedonia. Number: 13-977/3-05, 1.7.2006-30.6.2009.

[16]. D. J. Whitehouse. *Handbook of Surface Metrology*. Inst. of Physics, Bristol, 1994.

[17]. EAL-G20. *Calibration of Surface Instruments for Measuring Surface Roughness,* 1996.

[18]. ISO 12179: 2000; Geometrical product specifications (GPS) - Surface texture: Profile method - *Calibration of contact (stylus) instruments.*

[19]. ISO 3274:1996; Geometrical Product Specifications (GPS) - Surface texture: Profile method - *Nominal characteristics of contact stylus instruments.*

[20]. ISO 4288:1996; Geometrical product specifications (GPS) - Surface texture: Profile method - *Rules and procedures for the assessment of surface texture.*

Authors: **Ass. Tomov Mite, MSc, Prof. Kuzinovski Mikolaj, PhD,** University "Ss. Cyril and Methodius", Faculty of Mechanical Engineering, Skopje, , Karposh II bb, P. Fax 464, 1000 Skopje R.Macedonia., **Prof. Cichosz Piotr, DSc,** Institute of Production Engineering and Automation of the Wroclaw University of Technology, str. Lukasiewicza 3/5, 50-371 Wroclaw, Polska

E-mail: mitetomov@mf.edu.mk
mikolaj@mf.edu.mk
piotrc@itma.pwr.wroc.pl

Journal of Production Engineering
Vol.12 No.1

Trajcevski, N., Kuzinovski, M., Cichosz, P.

INVESTIGATION OF TEMPERATURE DURING MACHINING PROCESS BY HIGH SPEED TURNING

Abstract: *This paper presents the results and obtained mathematical models of temperature during machining process by high speed turning as a function of processing parameters* v, f, a *and* r_e. *The machining process by turning is performed on lathe type "Prvomajska TVP 250" with power P=11,2 kW and step change of number of revolutions between n=16 and 2240 rev/min, by using ceramic cutting tool inserts type SNGN 120712- 120716-120720 made from mixed ceramics type MC 2 (Al_2O_3 + TiC) and manufactured by HERTEL and tool holder type IK.KSZNR -064 25x25 manufactured by KENNAMETAL. Workpiece material is* ***C*** *1630 (DIN C 55). Cutting tool holder is reconstructed to provide transimission of the voltage signal from the cutting tool insert. Processing parameters are varied in range interval between* v *=300 and 500 m/min,* f *=0,16-0,30 mm/rev,* a*=0,5-1,0 mm and* r_e*=1,2-2,0 mm. Average temperature is determined by using of natural thermocouple method and computer aided research equipment. Experiments and the mathematical processing of the results are performed at the Faculty of Mechanical Engineering in Skopje using the program CADEX combined with MATLAB. Four factorial first order experimental plan was used.*

Key words: *Machining by turning, average cutting temperature, natural thermocouple, factorial experiments*

1. INTRODUCTION

It is known that during the transformation of workpiece machined layer into chips, because of energy transformations in the cutting zone it is released significant quantities of heat. Created heat in the cutting process is directly dependent on the applied processing parameters *(v, f, a,* .....), workpiece material condition and cutting tool stereometry $(\chi, \lambda, \gamma, r_\varepsilon, ...)$. The heat reflected through the maximum temperature is an important factor which has a dominant influence to: the mechanism of transformation of the workpiece machined layer into chip; on the phenomenon that occur in the process of cutting tool wear (abrasive, adhesive, diffusive, heat, oxidative); the magnitude of the cutting force components, which is in close correlation with thermal model of creation residual stresses; and thus to the creation of the resultant characteristics of the new constituted technological surface layer /TSL/ [1]. Therefore, in the machining process it is important accurately to know the magnitude of the temperature that occurs in the cutting zone as function of machining parameters. The temperature in the cutting process can be determined in an analytical and experimental way, which are developed many methods [2]. From the experimental methods, the most widespread is the method of natural thermocouple, where the natural thermocouple consists of the cutting tool and the workpiece. Methods of natural thermocouple are simple to implement, but require knowledge of the thermoelectric characteristics of the natural thermocouple, and its determination is only by experimental way [3]. The emergence of modern cutting materials, especially cutting ceramics, creates conditions for the application of significantly higher cutting speeds.

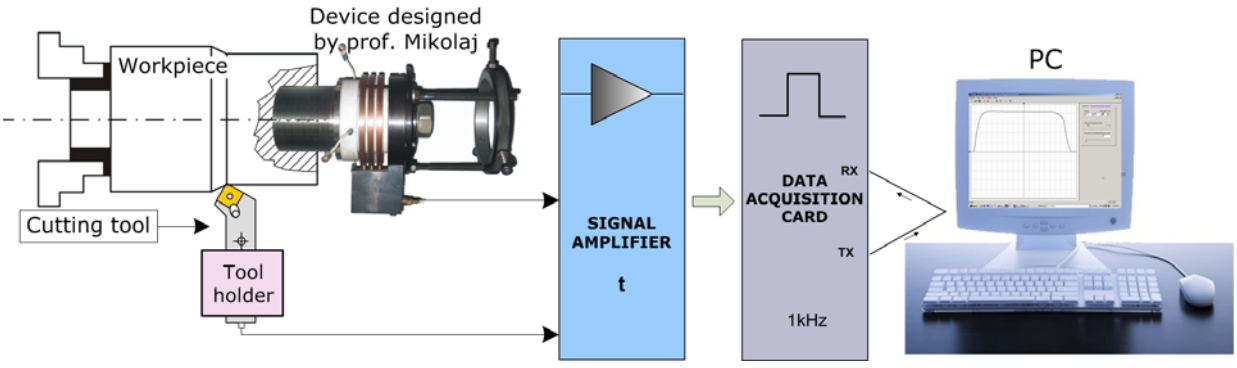

Fig. 1. Schematic view of the research experimental setup

The high temperatures and material removal dynamics in such conditions more intense influence on the mechanisms of chip creation and on the cutting tool wear, as well to technological effects in /TSL/. Increased stiffness is required from the system Machine - Device - Workpiece - cutting Tool (MDWT). The system for measuring the temperature is required: to reduce errors that occur in the transmission of the signal from the workpiece-cutting tool thermocouple; be able to record increased quantity of information in relatively short interval; application of computer technology for reliable determining of the temperature in the cutting process. The goal is to reduce the interval of measuring uncertainty of the results obtained from measurements performed. The creation of computer aided research equipment for measuring temperature in the cutting process is the result of joint research realized on the Faculty of Mechanical Engineering and the Faculty of Electrical Engineering in Skopje, in cooperation with the Institute of Production Engineering and Automation of the Wroclaw University of Technology, Poland. Using the research equipment, investigations of dependence of the temperature from the machining parameters *v, f, a* and r_ε are carried out.

2. EXPERIMENTAL CONDITIONS

2.1 Cutting tool

The processing is performed by use of ceramic cutting tool inserts type SNGN 120712- 120716-120720 made from mixed ceramics MC 2 (Al_2O_3 + TiC) manufactured by HERTEL and cutting tool holder type IK.KSZNR -064 25x25 manufactured by KENNAMETAL. Cutting tool stereometry is:

.

$$\chi = 85°,\ \chi_1 = 5°,\ \gamma = -6°,\ \alpha = 6°,\ \lambda = -6°,$$

$$\gamma_f = -20°,\ b_f = 0{,}2\,\text{mm},\ r_\varepsilon = 1{,}2 - 1{,}6 - 2{,}0\,mm$$

Cutting tool holder was previously reconstructed to provide transmission of the voltage signal from the cutting tool insert, which is presented on Fig. 2.

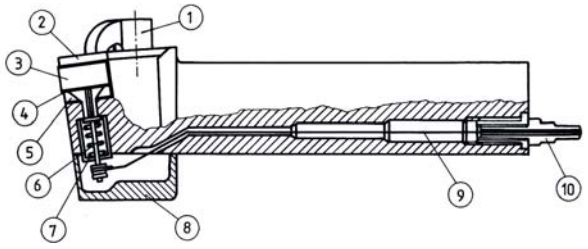

Fig. 2. Cutting tool holder cross-section, 1 - thumb, 2 - chip breaker made from Al_2O_3, 3 - cutting tool insert made from mixed ceramics MC 2, 4 - mica, 5 - washer, 6 - mechanism, 7 - isolation bushing, 8 - protective cap, 9 - signal conductor, 10 - connector.

To reduce the impact of disruption factors during transmission of the generated signal and thus to increase the accuracy of measurements, cutting tool insert is completely isolated in the nest of cutting tool holder, by using of mica. To obtain the required chip shape, a chip breaker made from zircon-oxide ceramics is used.

2.2 Workpiece

Material C 1630 (DIN C 55), normalized to the hardness of 200 HB.

2.3 Metal cutting machine

Lathe type "Prvomajska" TVP 250, with power P = 11,2 kW with step change in the numbers of revolutions between n=16 and 2240 rev/min.

2.4 Cutting parameters

Cutting speed v = 300-500 m/min, feed f=0,16-0,30 mm/rev, depth a=0,5-1,0 mm, cutting tool insert tip radius r_ε =1,2-1,6-2,0 mm.

2.5 Device for transmission of the signal from workpiece

For measuring the average temperature in the cutting process by using method of "natural thermocouple", for transmission of generated signal from the workpiece a specially designed device is constructed, Fig. 3. This device after screwing into workpiece, allows transmission of generated signal through three rotating rings and fixed brushes. Particular attention is paid to the choice of material for rings and brushes, which in this case is black-lead bronze. The thermocouple ring - brush when heated to 373,16 K (100 ° C) generate thermovoltage of 0,3 mV.

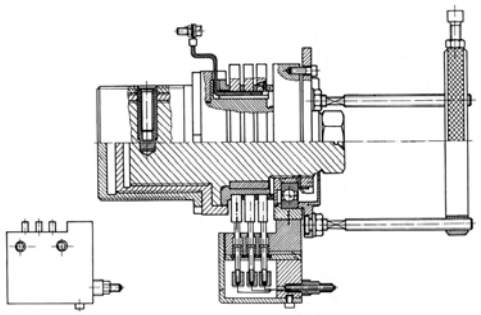

Fig. 3. Device for transmission of the signal from workpiece, cross-section [4]

2.6 Experimental plan

It is used first-order full four factorial plan of experiments (2^4 + 4), presented in Table 1. Power function is accepted for the mathematical model to describe the changes of the temperature. Mathematical processing is performed at the Faculty of Mechanical Engineering in Skopje with the application of program *CADEX* in connection with *Model-Based Calibration (MBC) Toolbox Version 1.1,* contained in the *Matlab* software package, which is intended for design of experiments and statistical modeling. Using the advanced features of *Matlab* and *MBC* provides significant advantages in the realization of experimental studies, with an option for graphic interpretation of results.

2.7 Research equipment

Monitoring of the thermovoltage (temperature) in the cutting process is done with computer aided research experimental setup, presented on Fig. 1 [5, 6]. Part of the research setup is specially designed PC interface that consist of signal amplifier and data acquisition card [7]. Measurements are done at the Faculty of Mechanical Engineering in Skopje. Graphical interpretation of monitored quantities by the software FORTMON is shown on Fig. 4.

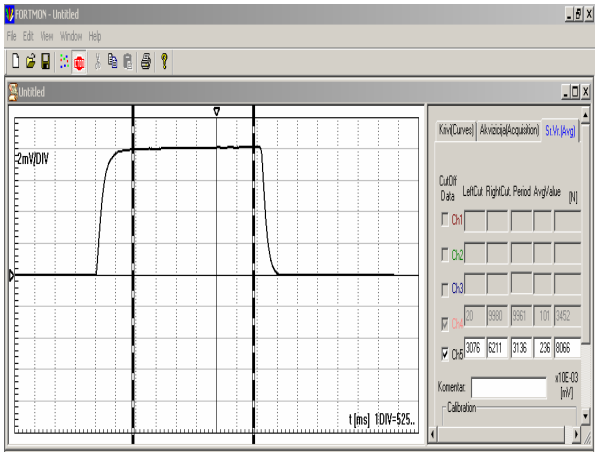

Fig. 4. Graphical interpretation of monitored quantities by the software FORTMON

Determining the average temperature by the method of natural thermocouple request to define of correlation between the thermovoltage measured by mV and the temperature expressed in °C. In this case, thermocouple is C 1630 - MC 2. For this purpose, a calibration installation is created. After regression analysis on the results obtained from the calibration measurements, the dependence between temperature T and thermovoltage u is obtained and represented as a polynomial of fourth degree [6]:

$$T = 104{,}426 - 42{,}646 \cdot u + 44{,}734 \cdot u^2 - 4{,}937 \cdot u^3 + 0{,}17 \cdot u^4 \cdots \quad (1)$$

By using of the equation (1) in the software of the research experimental installation, showed on Fig.1, it is enabled direct transformation of the measured thermovoltage into temperature.

3. RESEARCH RESULTS ANALYSIS

Changes of average cutting temperature T_C as function of machining parameters are investigated during researches. Power function was adopted for describing of these changes:

$$T_c = \mathrm{C}\, v^x f^y a^z r_\varepsilon^{\,q} \cdots\cdots\cdots\cdots \quad (2)$$

Experimental plan and results are presented in Table 1. Obtained results processing includes analysis of mathematical models with and without mutual effect, determination of 95% confidential interval for analyzed models, evaluation of significance of coded polynomial coefficients, determination of experimental error and determination of multiple regression coefficient. Performed analysis, after complete computer processing, showed adequacy of obtained mathematical model (3).

$$T_C = 444{,}662 \cdot v^{0{,}164} \cdot f^{0{,}138} \cdot a^{0{,}054} \cdot r_\varepsilon^{-0{,}088} \quad (3)$$

Obs No	Independent variables - Real matrix				Result
	v [m/min]	f [mm/rev]	a [mm]	r_ε [mm]	T_{Cav} [°C]
1	300,00	0,16	0,50	1,20	821,69
2	500,00	0,16	0,50	1,20	895,41
3	300,00	0,30	0,50	1,20	915,16
4	500,00	0,30	0,50	1,20	970,23
5	300,00	0,16	1,00	1,20	891,37
6	500,00	0,16	1,00	1,20	951,23
7	300,00	0,30	1,00	1,20	919,21
8	500,00	0,30	1,00	1,20	1043,63
9	300,00	0,16	0,50	2,00	819,56
10	500,00	0,16	0,50	2,00	845,19
11	300,00	0,30	0,50	2,00	879,32
12	500,00	0,30	0,50	2,00	961,36
13	300,00	0,16	1,00	2,00	819,57
14	500,00	0,16	1,00	2,00	887,23
15	300,00	0,30	1,00	2,00	873,42
16	500,00	0,30	1,00	2,00	998,38
17	387,30	0,22	0,71	1,55	909,53
18	387,30	0,22	0,71	1,55	917,18
19	387,30	0,22	0,71	1,55	903,37
20	387,30	0,22	0,71	1,55	901,28

Table 1. First order four factorial experimental plan

Some graphical interpretation of the influence of cutting speed - v, feed - f, cutting depth - a, and cutting tool insert tip radius - r_ε on the changes of average temperature T_C are shown on Fig. 5. It can be noticed that most significant effect on average temperature increase has cutting speed increase, then cutting feed, and, the least, cutting depth. Cutting tool insert tip radius increase results in temperature decrease. Average temperature increase as result of cutting speed increase is explained, mainly, by decreasing contact between chip and face surface of cutting tool insert, resulting with chip ramming decreases, chip sliding speed against face surface increases, heat discharge is worse and friction is increased. Heat created in cutting area is, mainly, a sum of heat of machined layer deformation, which decreases, due to cutting speed increase, till certain limit as well as of heat generated by chip friction against face surface of cutting tool, which increases by cutting speed increase, which is basic reason for average temperature increase. Average temperature increase due to feed increase is results of higher deformation, which alternatively causes higher heat quantity. However, feed increase also means increase of contact surface between chip and cutting tool, which results by conditions for improved heat discharge.

Therefore, de facto, there is smaller effect of feed onto average temperature. Similar is cutting depth effect. Namely, this means that deformation work increases by cutting depth increase, thereby generating higher heat quantity, however also increasing contact surface between chip and cutting tool and improving heat discharge. In addition, cutting blade active length directly increases. This provides much better conditions for heat discharge thereby smaller temperature gradients. The cutting tool insert tip radius r_ε effect is much interesting. Average temperature decreases by r_ε increase. This is due, mostly, to increased active length of cutting blade, which provides much better heat discharge. Besides this, reduction of angle χ, as result of increase of r_ε, is, also, a reason for smaller cutting forces, smaller deformation work and thereby smaller heat quantity. It should also be stated that increase of measured average cutting temperature is result of temperature increase on rear side of cutting wedge due to increased friction of rear main surface and auxiliary rear surface with machined surface.

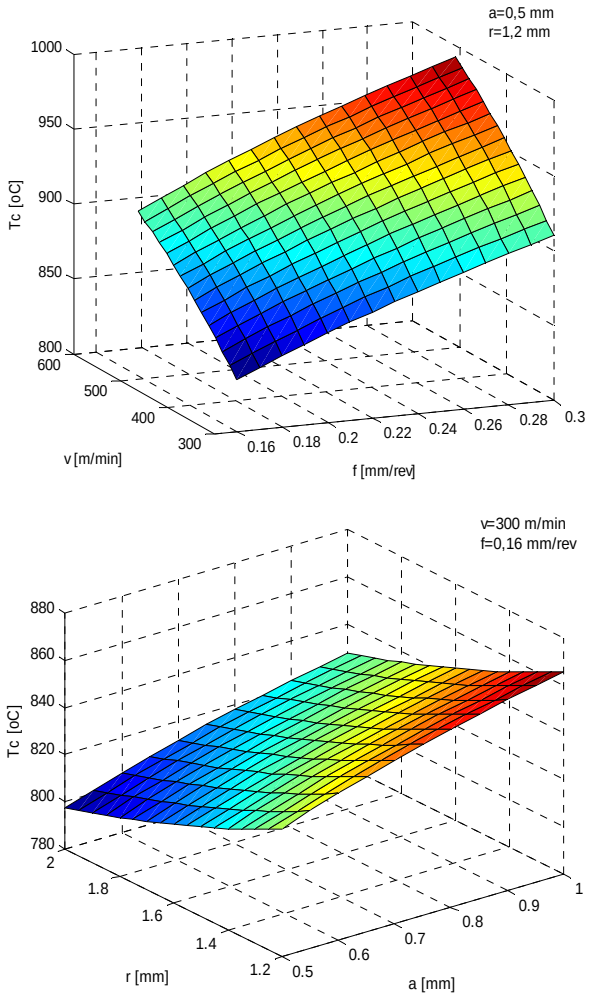

Fig. 5. Graphical interpretation of the influence of cutting speed - *v*, feed - *f*, cutting depth - *a*, and cutting tool insert tip radius - r_ε on the changes of average temperature T_C

4. CONCLUSIONS

Following remarks and conclusions can be reached from performed experimental researches, obtained mathematical models, as well as results analysis:

- Statistical analysis indicated that describing changes of average cutting temperature T_C as function of machining parameters *v, f, a* and cutting tool insert tip radius r_ε, by means of power function, is correct;

- All factors adopted in models are significant, and their effect is as follows:

- Average cutting temperature mostly depends upon cutting speed and feed, while from cutting depth, the least. The increase of these parameters causes average temperature increase, which reached highest value of 1043°C in the investigated domain.

5. REFERENCES

[1] Pavlovski, V., Kuzinovski, M., Zebrovski, H., Cichosz, P.: *Experimental research of the physical phenomena in turning with ceramic cutting inserts*, Third International Conference on advanced manufacturing systems and technology, AMST '93, Udine, Italy, 1993.

[2] Milikić D.: *Temperature pri obradi rezanjem i mogućnosti njihovog tačnog određivanja*, XIV Savetovanje proizvodnog mašinstva Jugoslavije, p.p. 292-305, Čačak, 1980.

[3] Stanić, J.: *Metod inžinjeriskih merenja*, Mašinski fakultet, Beograd, 1990.

[4]. Kuzinovski M.: PATENT MKP B23Q 11/14, G01K 13/08, 900600, 30.09.2000.

[5] Trajčevski, N., Kuzinovski, M., Filiposki, V., Cichosz, P.: *Computer aided measurement of the temperature in the cutting process by machining with turning*, Proceedings of the Scientific Conference with International Participation "Manufacturing and menagement in 21-st century", p.p.129-134, Ohrid, Republic of Macedonia, September 16-17, 2004.

[6] Trajčevski, N.: *Monitoring system in experimental investigation in machining with turning*, Master thesis, Skopje, February 2008.

[7] Trajčevski, N., Filiposki, V., Kuzinovski, M.: *Personal computer interface for temperature measuring in the cutting process with turning*, Proceedings, Faculty of Mechanical Engineering - Skopje, Vol.23, No.2, p.p. 65-74, 2004.

Authors: **Trajčevski Neven, MSc,** Military Academy - Skopje, Macedonia. **Prof. Kuzinovski Mikolaj, PhD,** University "Ss. Cyril and Methodius", Faculty of Mechanical Engineering, Skopje, Macedonia. **Prof. Cichosz Piotr, DSc**, Institute of Production Engineering and Automation of the Wroclaw University of Technology, Wroclaw, Poland.
E-mail: neven.trajchevski@gmail.com
mikolaj@mf.edu.mk
piotrc@itma.pwr.wroc.p

Journal of Production Engineering
Vol.12 No.1

Todic, V., Lukic, D., Milosevic, M.

FUNDAMENTALS FOR PLANNING AND CALCULATION OF MACHINING SYSTEMS' CAPACITY

Abstract *Standard process plans for rolling bearings manufacturing are fundamentals for the organization and effective implementation of the process serial and mass production of these products.*
The paper presents basic information for planning and calculation of machining systems' capacity for rolling bearings manufacturing in terms of products from this production system.
Key words**:** *Rolling bearings, Planning, Calculation, Capacity, Machining system*

1. INTRODACTION

In modern conditions of business activities, production systems are forced to redesign their production processes, or made their reengineering, in accordance with the diverse of needs and demands of the market. One of the main directions is process plans reengineering, which involves development and improvement of manufacturing process plans, development of the technological database, the application of modern and more efficient usage of existing production and technological resources, determining the real technological norms, more effective job preparation, etc.

Standard process plans for rolling bearings manufacturing are fundament of organization of manufacturing of these products. Development of standard technological process is based on the concept of typical and group technology.

With development of standard technological processes of rolling bearings production it will be provided the following, the most important goals:

- More efficient organization and implementation of technology and production processes,
- Better planning and management of production,
- Reduce the number of technology flows,
- Better planning and control of usage of technological capacity,
- Increased flexibility to market demands,
- Efficiency of technological preparation of production, etc.

In the development of standard process plans, except assortment of rolling bearings production and volume of production, it is also necessary to take into account the technological and installed equipment for the production of bearings.

The paper introduces basic information for planning and calculation of machining systems' capacity for rolling bearings manufacturing in terms of products from production system FKL.

2. SHORT REVIEW ON PRODUCTION PROGRAM OF ROLLING BEARINGS

Based on the analysis of rolling bearing production for 2008. year, it was determined a quantity, i.e. realized production volume, as for individual bearings, as for the total volume of production for the formed group, that make up the cylindrical roller bearings, spherical roller bearings, double row rolling bearings, single row deep groove rolling bearings and single row angular contact rolling bearings, single row angular contact rolling bearings with grub set screws and needle roller bearings (total more than one million).

Within this analysis it was determined a realized amounts for the production of above mentioned types of bearings, and with the application of ABC analysis it was determined the representative products for the individual groups of bearings, which are shown in detail in the project [1]. In this paper it will be shown necessary information for the selection of representative product for spherical roller bearings.

The observed production system spherical roller bearings are produced in five different variants, with a range of different sizes (Figure 1).

In Table 1 it is shown a production program of spherical roller bearings for 2008. year, on the basis of which was made quantitative, mass and value ABC analysis, Figs. 2a, 2b, and 2c.

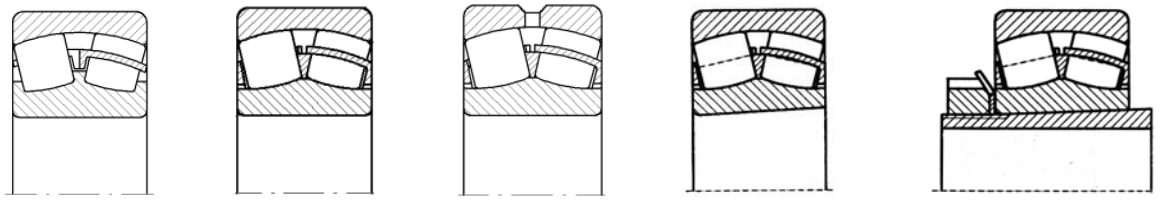

a) classical variants *b) C and E variants* *c) C and E variants W33* *d) C i E variants with tapered bored* *e) C i E variants with tapered bored and saddle*

Figure 1. Variants of spherical roller bearings [5]

Product	Identification number	Mark	Quantity piece/year	Mass kg/piece	Price €/piece
P1	519233	22205 ES.TVPB	12	0,18	20,5
P2	510092	22210 C.W33	98	0,60	15,1
P3	510091	22211 C.W33	29	0,82	16,7
P4	510132	22211 CK.W33	28	0,82	16,7
P5	510068	22214 C.W33	8	1,65	25,5
P6	510001	22215 C.W33	2	1,72	28
P7	510055	22215 CK.W33	9	1,72	33,6
P8	513246	22219 M	12	4,13	50,6
P9	519582	22220 JB	2	4,96	57
P10	510120	22220 JB *YU	12	4,96	58
P11	501188	22308 C.C3	3	1,0	18,9
P12	510097	22310 C.W33	17	1,85	25,4
P13	501985	22311 C.W33	3	2.35	29,8
P14	501965	22311 CK.W33 *YU	14	2,35	35,8
P15	501975	22312 C.C3.W33	6	2,95	24,8
P16	510098	22312 C.W33	25	2,95	35,3
P17	519636	22315 CC C3	2	5,40	39,2
P18	519583	22317 JB	3	7,40	70,6
P19	501699	22215 CK.W33	9	1,72	28

Tabela 1. Production program of spherical roller bearings

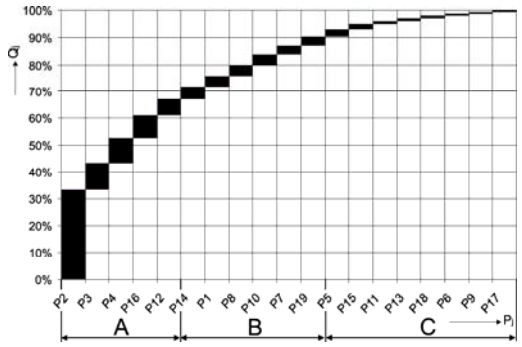

Figure 2a. Diagram for volume ABC analysis of spherical roller bearings

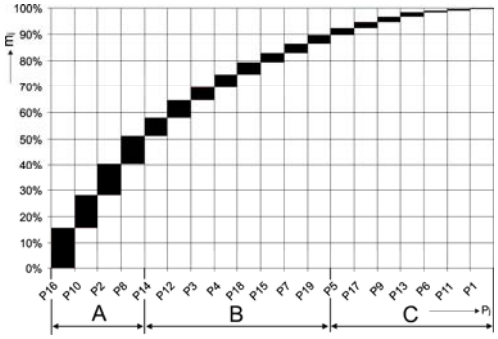

Figure 2b. Diagram for mass ABC analysis of spherical roller bearings

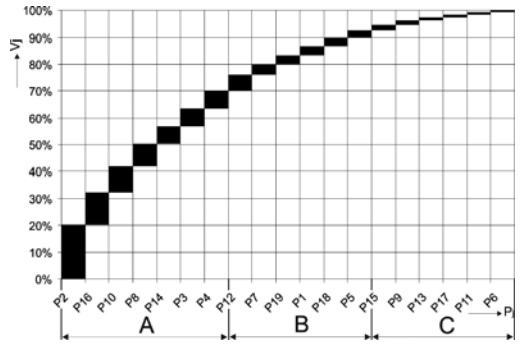

Figure 2c. Diagram for value ABC analysis of spherical roller bearings

As can be seen from the diagram for volume ABC analysis (Fig. 2a), diagram for mass ABC analysis (Fig. 2b) and diagram for value ABC analysis (Fig. 2c), a product 22210 C.W33 (P2) in all three cases is located in the A area of presented ABC analysis, on the basis of which it is chosen for the representative product for group of spherical roller bearings. Fig. 3 shown representative products for six formed groups of rolling bearings which are selected by applying ABC analysis [1, 2].

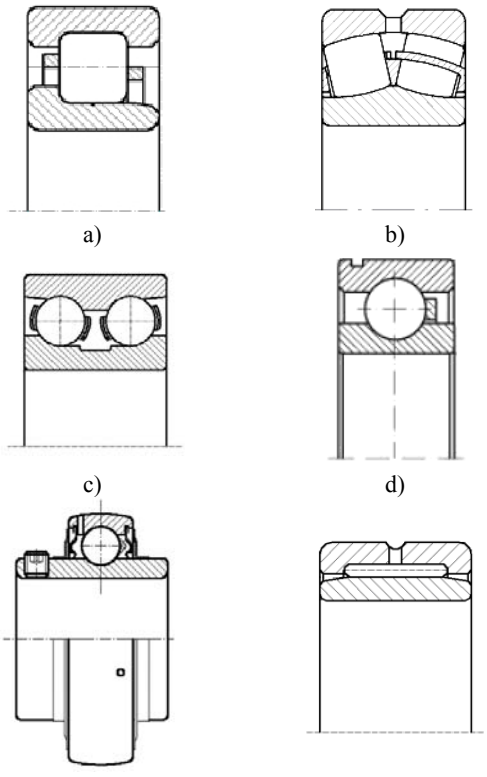

Figure 3. Representative products for formed groups of rolling bearings: a) Cylindrical roller, b) Spherical roller, c) Double row ball, d) Single row deep groove ball and Single row angular contact ball, e) Single row angular contact ball with grub set screws, f) Needle roller bearings

3. FOUNDATION FOR THE DEVELOPMENT OF STANDARD PROCESS PLANS

The terms of the observed production systems are designed standard manufacturing process plans of outer and inner rings of these six groups roller bearings on the principles of typical and group technology [1]. Content of manufacturing process plans of the rings bearings includes the following operations: Parting off, Turning, Drilling, Threading cutting, Heat treatment, Grinding facet, Grinding outside, Roll track grinding, Grinding openings, Super-finishing, Demagnetization, Final control.

Production volume and dimensions of the rings, require different types of raw material and different machining systems for operation turning, grinding and super-finishing. At Fig. 4 it is shown rules for machining system selection for turning of ring from rolling bearing, while in the works [2, 3] presented rules for the operations of grinding and super-finishing.

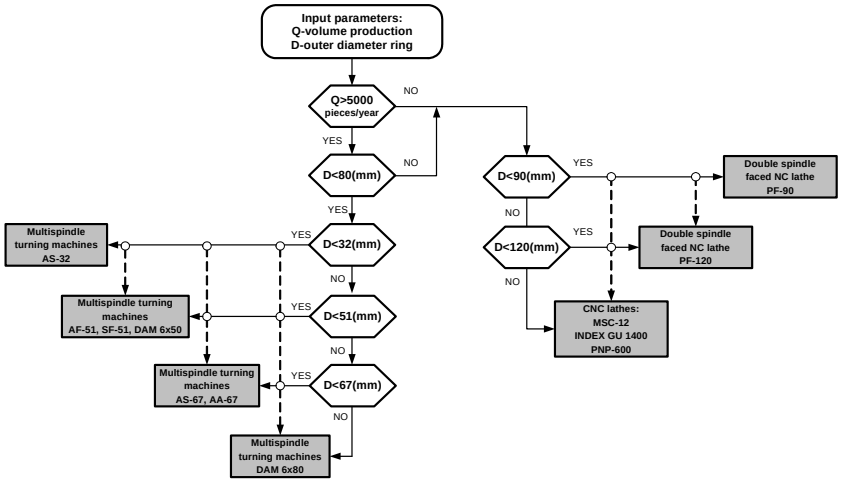

Figure 4. Rules for machining system selection for turning of ring from rolling bearing

Thus defined rules for the selection of machining systems for operation of turning, grinding and super-finish, enable for the group of rolling bearings, which are covered with this analysis, effectively defining of suitable standard manufacturing process plans, which enables fast refinement of process plans for each bearing.

In the scope of project [1] it was developed a standard process plans for the six groups of early mentioned rolling bearings and it was carried out the refinement of process plans for the appropriate representative products of these groups.

At Fig. 5 it is shown the group operation sheet for the standard process plan of outer ring production from group of double row spherical roller bearing, which are related to the operation of turning on the appropriate double-spindle faced NC lathe.

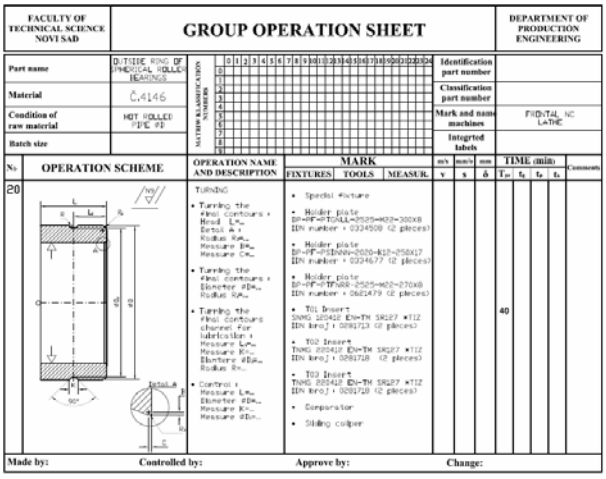

Figure 5. Group operation sheet for turning of outer ring from group of spherical roller bearing

Based standard ie group or typical operations processing specifies appropriate operations processing for outer and inner rings mentioned groups roller bearings, which detailed shown in project [1].

In Figure 6, shown is specified operations processing turning the outer ring of the product representative of group spherical roller bearings.

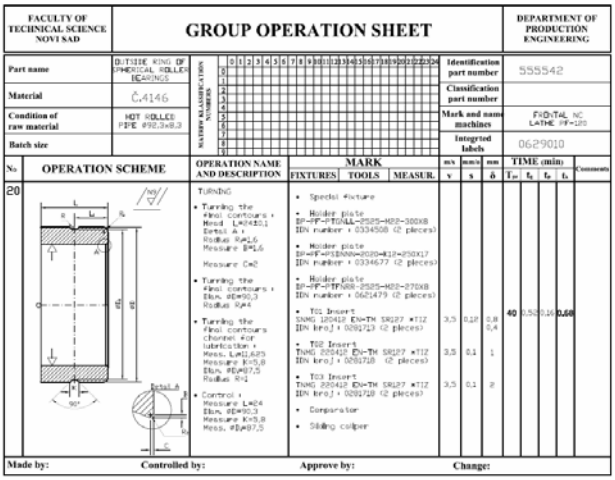

Figure 6. Refinement turning operations for the representatives of the group spherical roller bearings

4. CALCULATION OF CAPACITY MACHINING SYSTEM

For the effective use of technological resources installed can be applied methodology is based on data on the times in some processing operations, product representatives and the appropriate of reduced quantity [4].

4.1 Reduced quantities

It is generally known that the reduced quantity of one group of products is reduced to an appropriate quantity of product representatives. Thus the expression for the reduced quantity of ith products from these groups:

$$Q_{ri} = Q_i \cdot r_i \quad (1)$$

where the factor of reduction (r_i) of the ith product given expression:

$$r_i = r_{mi} \cdot r_{qi} \cdot r_{ci} \quad (2)$$

where the mass, quantity and value reduction factors given expressions, respectively:

$$r_{mi} = \frac{m_i}{m_p} \quad r_{qi} = \frac{q_i}{q_p} \quad r_{ci} = \frac{c_i}{c_p} \quad (3)$$

m_p, q_p, c_p, referring to mass, quantity and price of product representatives.

Reduced quantity of a group of roller bearings can be determined from the expression:

$$Q_r = \sum_{1}^{m} Q_i \cdot r_i \quad (4)$$

where m-number of bearings in a given group, m=19 for a group of spherical roller bearings.

According to the presented methodology and data in the project [1], is determined by the reduced quantity of group spherical bearings which is Q_r = 285 pieces/year.

Based on the reduced quantity and time of processing operations bearings representatives, it is possible to determine the time of engagement machining systems in the individual operations. So for the outer ring of representatives spherical bearing, according to Figure 6, processing time on a single processing operation turning is t_k= 0.68 min.

The time of this engagement machining system for processing outer rings spherical bearings during the year, will be:

$$T_2 = Q_r \cdot t_k + T_{pz} \cdot n_s \quad (5)$$

T_{pz} = 40 min/series
n_s = 4 series/year
ie:

$$T_2 = 285 \cdot 0{,}68 + 40 \cdot 4 = 353{,}8 \text{ min/year}$$

If you are using the same methodology determine the time of engagement of this machining system for processing rings other groups roller bearings, can be determined the total time T_{total}.

Efficiency of this machining system for processing only the outer rings spherical bearings will be:

$$\eta_2 = \frac{T_2}{K_e} \quad (6)$$

where the effective capacity of a time machine:

$$K_e = m_e \cdot s_e \cdot n_e \cdot \eta_e = 162000 \text{ min/year} \quad (7)$$

m_e=240 day/year.
s_e=2 shifts/day
n_e=7,5 h/shift
η_e=0,75

$$\eta_2 = \frac{353{,}8}{162000} = 0{,}22\ \%$$

5. CONCLUSION

On the basis of standard process plans for the six groups of rolling bearings, it is possible to accelerate the process of refinement process plans for all the bearings in certain groups, and of course, for the representative products of these groups.

Refinement (precisely) process plans for the representative products enable, that on the basis of reducing quantities, easy way to planning of limits of organization and realization of production process, as well as effective monitoring and planning of utilization installed technological capacity and human resources.

Standard manufacturing process plans of bearings, which are developed by applying the concept of typical and group technology, as well as layers for the selection of machining systems on the mentioned key operations, make solid base for the development of systems for automated design of manufacturing process plans of these products, and the corresponding CAPP system.

6. REFERENCES

[1] Todić, V., Borojev, LJ., Milošević, M., Lukić, D., Živković, A.: *Development of the Typical Process Plans for Rolling Bearings Manufacturing*, Projekat tehnološkog razvoja koji finansira Ministarstvo za nauku i tehnološki razvoj Republike Srbije.

[2] Todić, V., Milošević M., Lukić, D.*: Foundation for Development of The Standard Process Plans for Rolling Bearings Manufacturing*, 33 Conference on Production Engineering of Serbia 2009 with foreign participants, pp. 127-130, Faculty of Mechanical Engineering, Belgrade, 2009., ISBN 978-86-7083-662-4.

[3] Todić, V., Lukić, D., Milošević M.*: Analysis of the Process Plans for Rolling Bearings Production*, 9.th–Intenational Conference on Accomplishments in Electrical and Mechanical Engineering and Information Technology - DEMI 2009, pp 227-234, Faculty of Mechanical Engineering, Banja Luka, 2009., ISBN 978-99938-39-23-1.

[4] Zelenović, D.: *The Design of Production Systems*, Academic books, Belgrade, 1987.

[5] *FKL Rolling Bearings*, cataloge, Temerin, 2004, ISBN 86-906415-0-5.

Authors: **Prof. Dr. Velimir Todic, M.Sc. Dejan Lukic, M.Sc. Miodrag Milosevic**, University of Novi Sad, Faculty of Technical Sciences, Department of Production Engineering, Trg Dositeja Obradovica 6, 21000 Novi Sad, Republica Serbia, Phone: +381 21 485-2346, Fax: +381 21 454-495.
E-mail: todvel@uns.ac.rs, lukicd@uns.ac.rs mido@uns.ac.rs

Note: This paper present a part of researching at the project *"Development of the Typical Process Plans for Rolling Bearings Manufacturing"* Project number TR 14053, financed by Ministry of Science and Technological Development of Serbia.

Journal of Production Engineering
Vol.12 No.1

Brezocnik, M., Brezovnik, S., Balic, J., Sovilj, B.

SWARM INTELLIGENCE BASED ROBOT SYSTEM

Abstract: *The paper proposes the design of the intelligent robot system for resistance welding. The robot system incorporates the optimization module based on the swarm intelligence approach. The module is intended for optimization of robot path during welding.*
Key words: *Robotics, Robot cell, Optimization algorithm, Swarm intelligence, Ant colony optimization.*

1. INTRODUCTION

Robotics is gaining increasing importance in the modern world, since the demand for robots is growing due to opening of new, quickly growing areas of their use. At the beginning, as much as three thirds of robots were used, particularly for welding in the automobile industry, while now they are used also in other industrial branches, such as electronics, production and processing of food and drinks, pharmaceutics, production of household appliances etc. They are used wherever high quality of products is required, where the working operations are monotonous and harmful to health.

The basic reasons for automation and robotization are cost reduction, relief of people and assurance of adequate capacity and quality of production. The automation and robotization have a considerable influence on shortening of the manufacturing time, increasing of the capacity and reducing of production costs, which, however, is often hard to calculate accurately in advance and sometimes hard to justify.

The companies view the automation and robotization mainly from the stand point of savings and costs, but increasingly also as a chance to remain competitive in a certain industrial branch.

The paper proposes the design of the intelligent robot system by the swarm optimization of resistance welding application of the older ACMA XR701 robot made by Renault.

Swarm optimization is a swarm intelligence based algorithm for finding a solution to an optimization problem in a search space or model, and predict social behavior in the presence of objectives.

Swarm optimization is a stochastic, population-based evolutionary computer algorithm for problem solving. It is a kind of swarm intelligence that is based on social-psychological principles and provides insights into social behavior, as well as contributes to engineering applications. The swarm optimization algorithm was first described in 1995 by James Kennedy and Russell C. Eberhart. The techniques have evolved greatly since then, and the original version of the algorithm is barely recognizable in the current ones.

Intelligent optimization methods are finding their way into more and more diverse areas of human activity. The reason lies in the increase of the capabilities of computer systems and, consequently, in the increase of opportunities for the development and use of artificial intelligence systems (see, e.g., [1-2]).

Taking into account the problem encountered in designing of the welding application, the paper proposes the optimization algorithm with which the optimum time of transition of the electrode holder between welding spots will be reached.

When comparing the optimization algorithms, the analysis of optimization algorithms and methods was made and on the basis of the findings it was decided to use the optimization algorithm based on swarm intelligence with particle colony algorithm.

2. OPTIMIZATION WITH SWARM INTELLIGENCE (Particle Swarm Optimization)

This section is aimed at presenting the optimization with swarm intelligence and at describing the functioning of the optimization process.

The particle swarm optimization algorithm (PSOA) is the optimization algorithm based on the population stochastic optimization technique. The PSOA was developed by J. Kennedy and R.C. Eberhart in 1995, when they studied the social behaviour of swarms of birds and fish.

The PSOA is very similar to the genetic algorithm. In case of both methods (PSOA and GA) the optimization starts with randomly selected members of population searching for optimums with constant improvement of the subjects of the population in the course of improvements from generation to generation. Unlike the GA, the PSOA does not have evolutionary operators, such as crossover and mutation, which considerably simplifies the PSOA in comparison with the GA. In case of the PSOA the population members are called particles (to which the method owes its name) moving in the space of solutions in such a way that they follow the best particle. Like the GA also the PSOA is used for similar cases: optimization of functions, learning of neural networks, for setting of parameters of controllers by fuzzy logic etc., i.e., wherever the GA has already been well established.

2.1 How PSOA acts

The PSOA simulates the behaviour of swarms of birds or also insects. For example, let us imagine a swarm of birds randomly examining the space when looking for food. In the examined space there is only one source of food. None of the birds know where the food is, but each bird knows how far away from food it is. So, what is the best strategy of each individual bird in the swarm? The most effective strategy is to follow the bird nearest to the food.

The PSOA assumed the searching technique for solving optimization problems. In the PSOA each possible solution (bird, ant, bee) is called particle. All particles have the fitness value (distance of each particle from the food source) calculated by the fitness function for the purpose of optimization. Each particle also has its speed controlling "flying" of particles towards the optimum. The particles fly through the space of solutions so that they follow the currently most optimal particle [3-6].

The PSOA is initialized with the swarm of randomly placed particles into the space of solutions, afterwards searching for optimum from iteration to iteration (generation). In each iteration, each position of the particle is calculated again on the basis of three *"best"* positions of particles stored from iteration to iteration. The first best position of the particle is the position reached out of all hitherto iterations for the individual particle - it is called the local best (l_{best}). The next best position of the particle is the position reached out of all hitherto iterations among all particles - it is called the global best (g_{best}). The last best position of the particle is the position reached out of all hitherto iterations among the neighbouring particles - it is called the neighborhood best (n_{best}).

After searching for the said three best values (l_{best}, g_{best} and n_{best}), the particle speed is calculated for the particle $v_{ij}(k) = (v_1, v_2,...v_j)i$, where the index i is the number of particles in the population and the index j is the dimension of the space of solutions, followed by the calculation of the new position of the particle:

$x_{ij}(k) = [x_1, x_2, \dots x_j]i$:

$$v_{ij}(k) = c_0 * v_{ij}(k-1) + c_1 * rand(0,1) * (g_{bestj}(k-1) - x_{ij}(k-1)) + c_2 * rand(0,1) * (l_{bestij}(k-1) - x_{ij}(k-1)) + c_3 * rand(0,1) * (n_{bestj}(k-1) - x_{ij}(k-1)) \quad (1)$$

and

$$x_{ij}(k) = x_{ij}(k-1) + v_{ij}(k). \quad (2)$$

The function *rand(0,1)* calculates the random value between 0 and 1 including 0 and 1. The constant c_0 represents the value of speed of particle from previous iteration and represents the particle movement inertia. The usual value of c_0 is between 0 and 1 (best values are slightly below 1). The constants c_1, c_2 and c_3 are the learning constants and, usually, have the value of approximately 2. The calculation of the fitness function represents the conversion of the j-dimensional information about the particle position in the space of solutions into a one-dimensional scalar value representing the quality of the particle position and/or its distance from the optimum.

The simple pseudo code for building of the computer programme of PSOA is as follows:

FOR each particle
  Initialize particle
END
DO
 FOR each particle
  Calculate fitness value
  IF fitness value is better than l_{best}
    set current value of particle as new l_{best}
  END
 END
Select particle with best fitness value of all particles in hitherto iterations as g_{best}.
 FOR each particle
Calculate particle speed by equation (1).
Calculate new particle position by equation (2).
 END
WHILE maximum of iterations or minimum criterion has not been reached.

3. TRAVELLING SALESMAN PROBLEM

Optimum movement between welding spots represents the travelling salesman problem. Therefore, this section of the paper presents the theoretical and applicative approach to solving the optimization travelling salesman problem with the algorithm of ant colony optimization for the case of resistance spot welding application.

3.1 Solving minimum path in graph

The theoretical approach requires the specification of the facts important in searching for minimum paths in the graph.

Similarly as in case of natural ants, the task of the artificial ants is to find the minimum path between points in the graph. For example, the set *G=(N,A)* represents the linked up graph, where the number *N* is the number of all points of the graph and the number *A* is the number of all paths.

The number of points is $|N|$ = n. Solution of the task (Fig.1) is the path in the graph connecting the starting point *f* with the desired point *d(target)*, the length being determined with the number of transitions on the path [7-9].

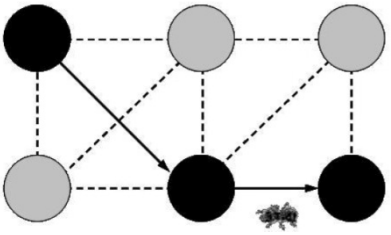

Fig. 1. Searching for minimum path in graph

Variable τ_{ij}, representing the artificial trace of the

feromone, is connected with each transition *(i,j)* in graph *G*. Thus, the ants leave the trace of feromone. In each point of the graph the stochastic (random) decision as to which point is the next occurs. The *k-th* ant placed in point *i* uses the feromone trace τ_{ij} for the calculation of probability to which point $j \in N_i$ it is necessary to go. N_i is the group of neighboring points *i*. The probability of selection of point j is given with the term (3):

$$p_{ij}^{k} = \begin{cases} \dfrac{\tau_{ij}}{\sum_{j \in N_i} \tau_{ij}}, & j \in N_i \\ 0, & j \notin N_i \end{cases} \qquad (3)$$

As long as there is a solution, the ant leaves the feromone trace on the existing path $\tau_{ij}(t) \leftarrow \tau_{ij}(t-1) + \Delta\tau$. However, the solution so defined can lead to convergence towards optimum solution, if the mechanism of feromone evaporation is introduced. In each interaction the quantity of feromone is exponentially reduced according to the following term (4):

$$\tau \leftarrow (1-\rho)\tau \quad , \rho \in [0,1] \qquad (4)$$

The behaviour of the algorithm depends on the number of neighbors of each point. If the points have more than two neighbors, the algorithm loses its stability.

Consequently, also the choice of parameters becomes difficult. The algorithm can be improved by changing the properties of the colony and by changing the individual ants in the colony.

For testing of the ant colony algorithm the algorithm, by which the above theoretical findings were verified also in the simulation, has been created in the programme environment MS Visual Studio.Net. The graphic environment has been created, with which solving of the travelling salesman problem between randomly placed spots was simulated. By changing the ant colony algorithm parameters various mutual dependences of the ant colony parameters were simulated [10].

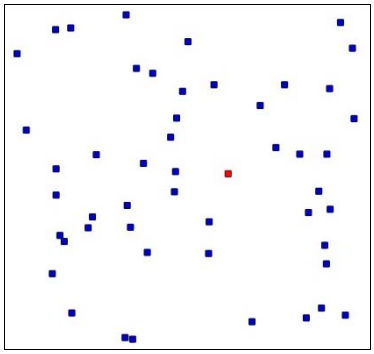

Fig. 2. Randomly placed spots

Fig. 2. shows the programme environment with randomly placed spots. The solution to be found by the ant colony algorithm represents the shortest path between all spots (in our case these are welding spots). Throughout the simulation process the solutions of the current iteration can be accompanied.

4. SIMULATION EXAMPLES OF THE WELDING APPLICATION OPTIMIZATION

The following are different examples of use of the optimum programme with ant colony. Particularly interesting is the incorrectly arranged configuration of placing of spots (random placing). It can be noticed on the final result that it is not deterministically determined and that the case can arise, when two output solution do not give identical solutions with the same number of spots and with the same parameters.

4.1 Incorrectly/randomly placed spots

In case of incorrect placing, the target function has a great number of local optimums and it may happen that the algorithm gets "caught" into the local optimum. As even the optimization with the ant colony algorithm does not represent an exact solution of optimization, it may happen that the final result is not the optimum solution. This can be seen in the examples in Fig. 3 and 4.

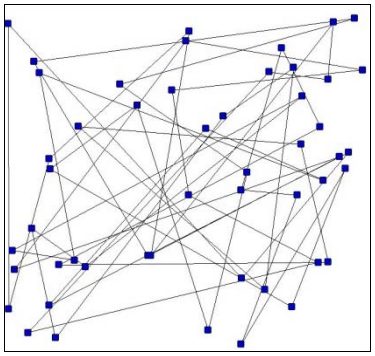

Fig. 3. First solution of travelling salesman problem

The first solution of the travelling salesman problem is the solution with random placing of spots in iteration 12 and with adjusted parameters (α = 1, β = 0, Rho = 1), the final solution being the length of 303333 units.

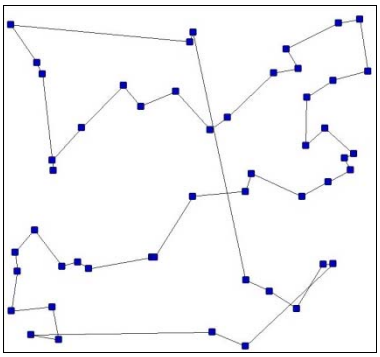

Fig. 4. Second solution of travelling salesman problem

The second solution of the travelling salesman problem is the solution with random placing of spots in

iteration 11 and with adjusted parameters (α =1, β =0.5, Rho=1), the final solution being the length of 69213 units, which is a better solution than in the first case.

The layout of spots has a very important influence on the behaviour of the optimization algorithm of the ant colony. If the spots are correctly (circularly) arranged, the algorithm converges very quickly, irrespective of the spot number. In this case it is not necessary and/or not reasonable to use large colonies of ants (great number of ants).

Also the analysis of mutual influences of the parameters alpha, beta and Rho is interesting, since each of them has an important influence on the problem solution. The analysis of said parameters, mutual influences and the influence of the ant number on the final solution will be extensively included in further research work [11].

5. CONSLUSION

The paper has presented an example of building of the intelligent robot system by the swarm intelligence.

The central part of the research has been devoted to the area of use of swarm intelligence for optimization of the robot welding system. The primary design concepts of the swarm intelligence are adopted from the world of animals, whose life cycle associates them into colonies, by copying the laws from the natural life of swarms into the computer artificial life of the swarm, called particle swarm theory, and thus a computer algorithm for solving optimization problems in robot systems is obtained.

Through building of the applicative programme environment, the findings of some well-known authors (Dorigo, M., Gambardella, L.M.,), stating that the spot arrangement importantly influences the behaviour of the optimization algorithm of ant colony have been confirmed. If the spots are correctly (circularly) arranged, the algorithm converges very quickly, irrespective of the spot number. In this case it is unnecessary and/or inappropriate to use large ant colonies (great number of ants). When the spot arrangement is incorrect/random, it is already more contestable whether the algorithm is optimum. Also the final solution is not unambiguously determined.

The findings reached by simulations have been successfully incorporated into the robot welding application and the minimum time of transition of robot electrode holder between the individual welding spots has been assured

6. REFERENCES

[1] Pandza, K., Polajnar, A. and Buchmeister, B., (2005) *Strategic management of advanced manufacturing technology*, Int. j. adv. manuf. technol., vol. 25, 3/4, (pp. 402-408),

[2] Buchmeister, B., (2008) *Investigation of the bullwhip effect using spreadsheet simulation*, Int. j. simul. model., vol. 7, no. 1, (pp. 29-41), http://dx.doi.org/10.2507/IJSIMM07(1)3.093.

[3] Dorigo, M., Gambardella, L.M., (1997) *Ant Colonies for the Traveling Salesman Problem*, BioSystems, (pp. 73-819).

[4] TSPLIB:http://www.iwr.uni-heidelberg.de/groups/comopt/software/TSPLIB 95, [accessed 10/5/2008

[5] Dorigo, M., Maniezzo, V. and Colorni, A., (1996) *Ant System: Optimization by a colony of cooperating agents*, IEEE Transactions on Systems, Man, and Cybernetics - Part B, (pp. 29-41).

[6] DiCaro G., Dorigo M., (1998) AntNet: Distributed Stigmergetic Control for Communications Networks, J. Artif. Intell. Res. 9, (pp. 317-365).

[7] Dorigo M., Gambardella L. M., (1997) *Ant Colonies for the Traveling Salesman Problem*, BioSystems 43, (pp. 73-81).

[8] Gambardella L. M., Taillard, E. D. and Dorigo M., (1999) *Ant Colonies for the Quadratic Assignment Problem*, J. Op. Res. Soc. 50, (pp. 167-176).

[9] Fu, K.S., Gonzales, R.C. and Lee, C.S.G., (1987) *Robotics Control, Sensing, and Intelligence*, Mc'Graw and Hill International edition.

[10] Bonabeau, E., Dorigo, M. and Theraulaz G., (1999) Swarm Intelligence: From Natural to Artificial Systems, Oxford Univ. Press, New York.

[11] Foo, K.S., Gonzales , R.C. and Lee C.S.G., (1987) Robotics Control, Sensing, Vision and Intelligence. International edition, McGRAW HILL.

Authors: **Assoc. Prof. Dr. Miran Brezocnik, Simon Brezovnik B.Sc, Prof. Dr. Joze Balic**, University of Maribor, Faculty of Mechanical Engineering, Smetanova 17, 2000 Maribor, Slovenia, **Prof. Dr. Bogdan Sovilj,** University of Novi Sad, Faculty of Technical Sciences, Trg Dositeja Obradovica 6, 21000 Novi Sad, Serbia,

E-mail: mbrezocnik@uni-mb.si
simon.brezovnik@uni-mb.si
joze.balic@uni-mb.si
bsovilj@uns.ns.ac.yu

Journal of Production Engineering
Vol.12 No.1

Javorova , J. G. , Sovilj , B., Sovilj-Nikic, I.

INFLUENCE OF FLUID INERTIA ON THE STABILITY OF EHD JOURNAL BEARINGS

Abstract: *In the analysis of HD journal bearings the effect of fluid inertia is generally neglected in view of its negligible contribution compared with viscous forces. However, there is a necessity to evaluate its influence at moderate values of the modified Reynolds number. An attempt is made to study the effect of lubricants inertia forces on the stability of finite journal bearing for a flow in a laminar regime. Furthermore, the stability analysis is extended to bearing with elastic layer on the shaft. In this way a complex solution of the problem is achieved with consideration of the shaft motion, instigated from the unbalanced HD forces of lubricant. The generalized Reynolds equation is obtained by averaged acceleration method. To solve the elastic part of the problem without linear approximations, a new, more precise method of displacements determination is used. In present study modified stability criteria by Hurwitz and Ljapunov are introduced. An adaptive procedure for determination of critical stability of the considered dynamic system is used.*
Key words: *stability analysis, journal bearing, fluid inertia*

1. INTRODUCTION

In most cases the fluid film bearings provide stable support for the rotor, but not always. One of the basic reasons for unstable motion and appearance of self-induced oscillations is the fluid film motion - especially its unbalanced HD forces. This instability mechanism is one of the well-known problems in rotor dynamics that has received intensive study [1-5, etc.], but this problem is not solved completely yet.
In the contemporary investigations of the similar kind of problems as shown, that different effects must be taken into consideration - deformability of the bearing surfaces, surface roughness, lubricant's rheological behaviour, lubricants inertia forces, thermoelasticity, etc. Along with that, for a better understanding of the HD instability mechanism, a complex solution with simultaneous rendering an account of some of the above mentioned effects must be achieved, which is the main goal of this work. Focusing particular attention on the influence of the elastic deformations of the shaft liner on the bearing stability, the effect of local inertia forces of the lubricant is taken into consideration as well.

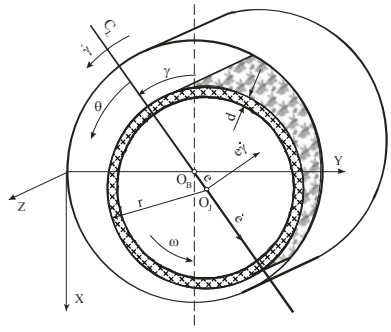

Fig.1 Journal bearing with a soft layer on the shaft

In this study the motion of Newtonian incompressible lubricant in finitely long journal bearing under isothermal conditions is considered. The shaft is covered with a thin resilient layer, whose radial displacements are of the same order of magnitude as the film thickness (Fig. 1). The generalized Reynolds equation is obtained by averaged acceleration method. The elasticity problem is solved in nonlinear treatment. The solution of pressure distribution equation is referring to prescribed loci of the shaft centre.
By the other hand, the estimate for stability of the system reduces to determination of a functional relation between non-dimensional load parameter (Sommerfeld number), shaft angular velocity and the fixed position of the shaft centre on the trajectory of her movable equilibrium [2, 3]. To this end the solution of the stability problem presupposes determination of the critical stability of the dynamic system in the plane of indicated parameters.

2. EHD MODEL AND STABILITY STUDY

Considering the fluid local inertia forces, the momentum equations and continuity equation for a journal bearing are

$$\frac{\partial u}{\partial t} = -\frac{1}{\rho}\frac{\partial p}{\partial x} + \upsilon\frac{\partial^2 u}{\partial y^2}\,;\; 0 = \frac{\partial p}{\partial y}\,;$$

$$\frac{\partial w}{\partial t} = -\frac{1}{\rho}\frac{\partial p}{\partial z} + \upsilon\frac{\partial^2 w}{\partial y^2}\,;\; \frac{\partial u}{\partial x} + \frac{\partial v}{\partial y} + \frac{\partial w}{\partial z} = 0 \qquad (1)$$

At the considered case, the partial differential equation that governs hydrodynamic lubrication for

two-dimensional incompressible thin fluid films can be written as

$$\frac{\partial}{\partial x}\left(\frac{h^3}{\eta}\frac{\partial p}{\partial x}\right)+\frac{\partial}{\partial z}\left(\frac{h^3}{\eta}\frac{\partial p}{\partial z}\right)=6\omega r\frac{\partial h}{\partial x}+$$
$$+12\frac{\partial h}{\partial t}-\frac{1}{\upsilon}\left[\frac{\partial\left(h^3 a_{x,av}\right)}{\partial x}+\frac{\partial\left(h^3 a_{z,av}\right)}{\partial z}\right] \quad (2)$$

where $a_{x,av}=\frac{1}{h}\int_0^h\frac{\partial u}{\partial t}dy$ and $a_{z,av}=\frac{1}{h}\int_0^h\frac{\partial w}{\partial t}dy$ represent averaged accelerations across the film on x and z directions.

The final form of this modified Reynolds can be presented in a form as in [6]

Because of the elastic deflection of the journal liner, the film profile between contact surfaces is represented by:

$$h(x,z,t)=c+e\cos\theta+\delta_y=$$
$$=c+e\cos\theta+\frac{(1+\mu)}{2\pi E}\int_0^{x_1}p(\xi)\ \Psi\left(\frac{x-\xi}{d}\right)d\xi\,, \quad (4)$$

where the last term expresses the elastic layer distortion. The liner surface point radial displacements are calculated in accordance with non-linear approach [7], which is based on the Papkovitch and Neuber stress functions.

Considering small plane oscillation about a position of equilibrium corresponding to the own weight of the rotor, the differential equations of motion of the shaft centre can be written in the form:

$$M\ddot{x}+R_x+S_x=0\,;\ M\ddot{y}+R_y+S_y=0\,, \quad (5)$$

where M - mass of the rotor; $R_x=C_1x-D_1y$, $R_y=C_2y+D_2x$ are the components of the HD forces and $S_x=\psi_{xx}\dot{x}+\psi_{yx}\dot{y}$, $S_y=\psi_{yy}\dot{y}+\psi_{xy}\dot{x}$ are damping forces components.

With application of standard approach to solve the last equation, the relevant characteristic equation is obtained. From its coefficients the modified stability criteria (which are based on the Hurwitz and Ljapunov theorems) are worked out:

$$\bar{\Delta}_1=\alpha_1>0\,;\ \bar{\Delta}_2=\alpha_1\alpha_2-\alpha_3>0\,;$$
$$\bar{\Delta}_3=\alpha_3\bar{\Delta}_2-\alpha_1^2\alpha_4>0\,;\ \bar{\Delta}_4=\alpha_4\bar{\Delta}_3>0\,. \quad (6)$$

Detailed determination of HD and damping forces, as well as determination of modified stability criteria are presented in [8].

3. SOLUTIN TECHNIQUE,RESULTS AND DISCUSSION

The critical stability of considered tribological system is accomplished by specially created adaptive calculating procedure. An adequate algorithm and program system, which is developed in MATHCAD 2000 PROFESSIONAL environment, are founded to verify the stability of dynamic system by introduced criteria.

Solution of the stability problem with consideration of the investigated effects must include a solution of the EHD part of the complex problem (Fig. 2). To this end the HD pressure and basic bearing characteristics are calculated by simultaneous solution of the modified Reynolds equation and elasticity equations. The partial differential equation is solved numerically by successive over-relaxation technique on a finite difference grid. The calculated values of Sommerfeld number S and corresponding load W represent initial data for the program system, which verifies the stability of the dynamic system "lubricant-shaft".

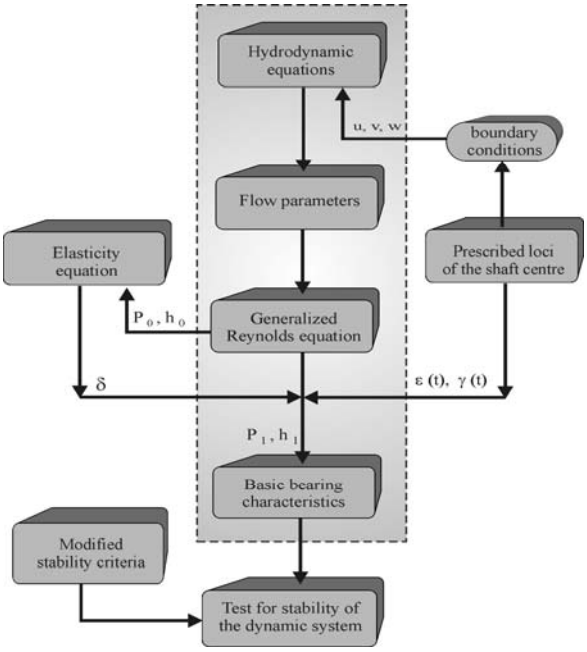

Fig. 2 Solution scheme

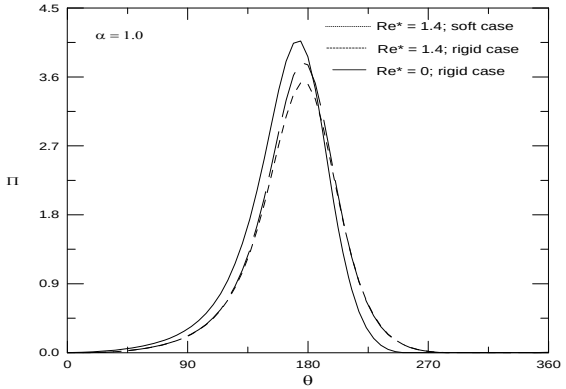

Fig. 3 Pressure distribution

Figure 3 illustrates the pressure distribution in the case in which the local inertia forces and elastic deformations of the shaft liner are taken into account. On the next Figure 4 is given the time variation of pressure for two basic cases - with and without inertia terms. The dependence of Sommerfeld number on the generalized Reynolds number is presented on a Fig. 5.

Along with that to see the effect of shaft's deformation and lubricants local inertia forces on the system stability the total load W values are plotted against the eccentricity ratio ε in last Fig. 6. The obtained results are concerned to three considered cases: (a) $\mathrm{Re}^*=0$, rigid case; (b) $\mathrm{Re}^*=1$, rigid case;

(c) $\mathrm{Re}^*=1$, soft case ($\delta_y \neq 0$, $E=1,63.10^8$ [Pa], $\mu=0,38$).

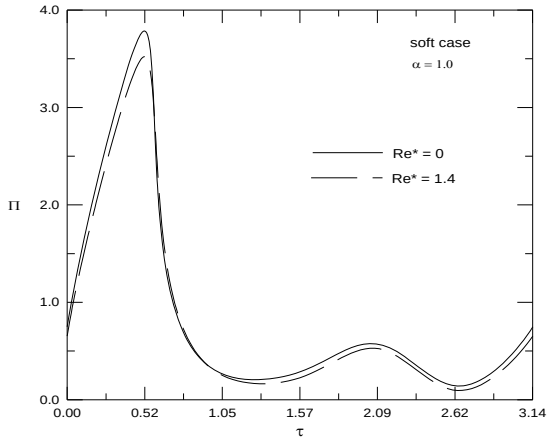

Fig. 4 Time variation of pressure

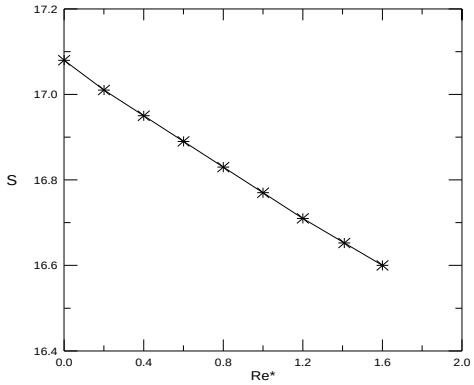

Fig. 5 Sommerfeld number vs Re*

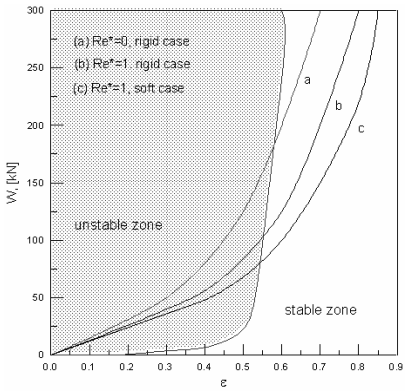

Fig. 6 Load versus eccentricity ratio

The results on this figure show that for the concrete value of load the system can be located in a stable zone if layer's deformations are considered (for example → $W=90$ [kN]) and/or the lubricants accelerations are taken into account (for example → $W=150$ [kN]), as the stable zone expanding at heavier loads.

4. CONCLUSION

It was found that consideration of the bearing surfaces deformation and lubricant's inertia forces are conducive to the stability state of the system. This phenomenon can be explained as result of the HD pressure (and respectively Sommerfeld number) change at rendering an account of the above mentioned effects.

5. REFERENCES

[1] Pincus, O. and Sternlicht, L.: *Theory of Hydrodynamic Lubrication*, Mc Grow-Hill Co, New York (1961)

[2] Voskresenskii, V.A., Djakov, V.I.: *Calculation and design of journal bearings*, Mashinostroenie, Moscow (1980)

[3] Hebda, M., Chichinadze A.B.: *Tribotechnics reference book*, Mashinostroenie, Moscow, (1990)

[4] Majumdar, B.C., Brewe, D.E., Khonsary, M.M.: *Stability of a rigid rotor supported on flexible oil journal bearings*, ASME, J. of Tribology, Vol. 110, (1988) 181-187.

[5] Kakoty, S.K., Majumdar, B.C.: *Effect of fluid inertia on the dynamic coefficients and stability of journal bearings*, Proc. Inst. Mech. Engrs., Vol. 214-J, (2000) 229-242

[6] Javorova J.G.: *One solution of the non-stationary problem of the EHD theory of lubrication*, PhD Thesis, University of Transport, Sofia (1998)

[7] Alexandrov, V.A., Javorova, J.G.: A more precise method of determination of the contact surfaces deformation in case of EHD friction, Proc. Jub. Sci. Conf. - UACEG, Sofia, (2002) 181-191

[8] Javorova, J.G., Alexandrov, V.A.: *Journal bearing instability and modified criteria for stability*, Proc. Intern. Conf. "Bultrib'03", Sofia, (2003) 81-89.

[9] Javorova J.G., Alexandrov V.A., Stanulov K.G., Zaharieva I., Chelu P.: *Effect of fluid inertia on the stability of journal bearings*, Proc of 5-th Int. Conf on Tribology "Balkantrib'05", Kragujevac, Serbia, (2005), 521-525.

Authors: PhD.Juliana G. Javorova University of Chemical Technology and Metallurgy,Kliment Ohridski Blvd. 8., 1756 Sofia, Bulgaria**, Prof. Dr. Bogdan Sovilj, Ivan Sovilj-Nikić PhD student**, University of Novi Sad, FTS, 6 Dositeja Obradovica Str., 21000 Novi Sad, Serbia, Phone: +381214852343
E-mail: : july@uctm.edu
bsovilj@uns.ac.rs
diomed17@gmail.com

Acknowledgments
The authors would like to thank for the financial support provided by Research and Development Sector at UCTM - Sofia for this project.

Journal of Production Engineering
Vol.12 No.1

Krizan, P., Soos, Ľ., Vukelic, Dj.

COUNTER PRESSURE EFFECTING ON COMPACTED BRIQUETTE IN PRESSING CHAMBER

Abstract: *The aim of this contribution is to present designed methodology of calculation of counter pressure effecting in pressing chamber at compacting process. Counter pressure is very important for compacting machines engineers because if they know counter pressure they are able to calculate radial pressure and length of pressing chamber. These parameters are needed for design of pressing chamber. Also lonely counter pressure helps at compacting process increase the briquette density – which is the main indicator of final briquette quality.*
Key words: *compacting process, briquetting process, counter pressure in pressing chamber, briquette quality*

1. INTRODUCTION

Counter pressure effecting on compacted briquette in pressing chamber is very important parameter at compacting process. Disallows material to leave the pressing chamber before compacting and helps with briquette compacting in pressing chamber. Counter pressure can be at horizontal way and also at vertical way of compacting generated: by counter pressure plug, by collet at the end of chamber with adjustable choking, by friction coefficient between briquette and chamber, by shape of pressing chamber (conicalness) and by length of compacted column consist from briquettes. For design of pressing chamber is very useful to know the value of effecting counter pressure.

2. KNOWN MATHEMATICAL MODELS OF COMPACTING

On our department we have done experiment for main influencing parameters evaluation. We know that at compacting process are more important pressing temperature (T), compacting pressure (p), fraction largeness (L) and input material humidity (w_r). We designed mathematical model which describes influence of all named parameters on final briquette density (ρ). This model is very useful at counter pressure calculation because we know definitely dependence ρ = f (p) [1].

The second mathematical model which we need at counter pressure calculation is model describing pressing conditions in closed pressing chamber by single-axis pressing on vertical press (Fig.1). By this compacting process is counter pressure generated by counter pressure plug. Maximal compacting pressure p_k which is rising by pressing depend on pressing chamber length and shape; depend on friction relations between pressed material and wall of the chamber. Drag friction is backward assigned by radial pressure p_r, applied to chamber wall, by friction coefficient μ and length of pressed briquette H. Equation (1) describes Fig.1.

$$\left[p_m - (p_m + dp_m)\right]\frac{\pi D_k^{\,2}}{4} - \mu p_r \pi D_k dx = 0 \qquad (1)$$

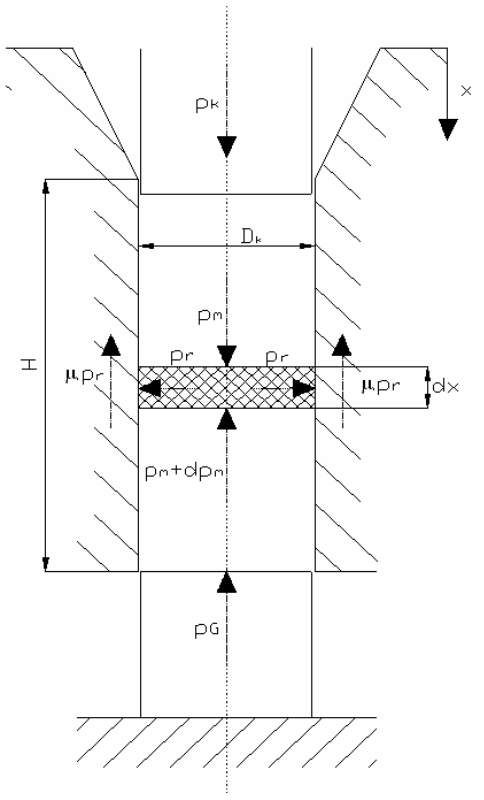

p_k – axial pressure of press (MPa)
p_G – counter pressure in chamber (MPa)
p_r – radial pressure (MPa)
p_m – axial pressure on the briquette (MPa)
D_k – diameter of pressing chamber (mm)
μ – friction coefficient (-)
H – length of pressed briquette (mm)

Fig. 1. Pressing conditions in pressing chamber by single-axis pressing on vertical press [1]

By equation (1) solving and by border conditions substituting they get equation (2) and (3).

$$p_k = p_G.e^{\frac{4.\lambda.\mu.H}{D_k}} \quad (MPa) \qquad (2)$$

Equation (2) specifies relation between axial pressure p_k and counter pressure effecting on compacted briquette p_G.

$$p_G = p_k.e^{\frac{4.\lambda.\lambda.\mu}{D_k}} \quad (MPa) \qquad (3)$$

3. COUNTER PRESSURE CALCULATION

Counter pressure value with value of radial pressure influencing length of pressing chamber. Next calculation will show you how important are founded dependence ρ = f (p) and equation (3) for calculation of counter pressure which effecting on compacted briquette. For calculation we use as an example dimensions of our experimental pressing stand. This stand supplies closed vertical way of compacting. If we want calculate the counter pressure from equation (3) we have to know other parameters in this equation. We chose axial pressure p_k according to Fig. 2 (p_k = 120 MPa). With this pressure we are able to compact briquettes by Standard given quality [2 ,3, 4].

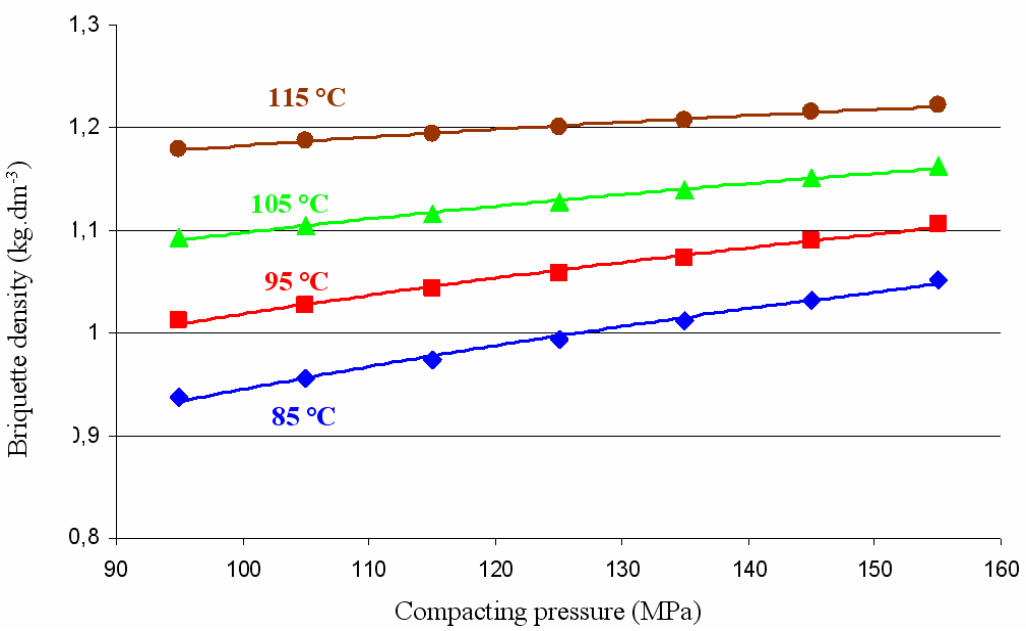

Fig. 2 Dependence of briquette density on compacting pressure at various pressing temperatures (w_r=10%; L=2 mm)

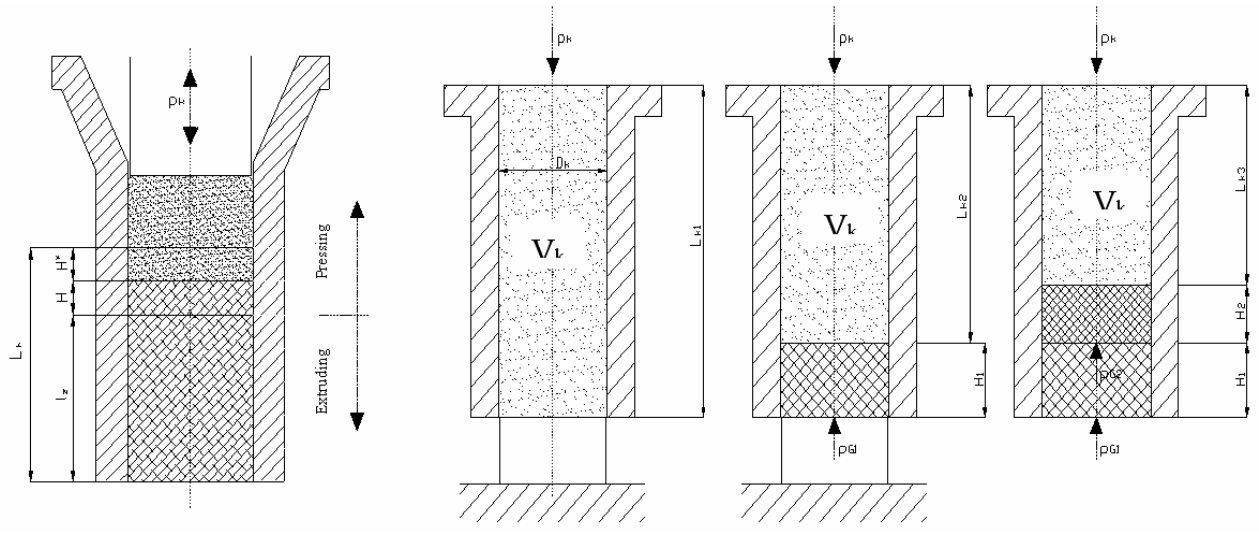

Fig.3 Single-axis pressing process on vertical press (a.) and individual phases of compacting – b.) filling of pressing chamber; c.) pressing of the 1st briquette + filling of pressing chamber; d.) pressing of the 2nd briquette + filling of pressing chamber

Friction coefficient between pressed material (wood) and wall of pressing chamber (steel) is μ = 0,35. λ is ratio of main strains σ_r/σ_m (Fig. 1). For dispersive materials is this ratio from interval $0<\lambda<1$. Diameter of pressing chamber is given by construction of pressing stand, therefore D_k = 20 mm. For calculation of length

of pressed briquette (H) we need also compacting ratio for wood. This ratio is ratio of volume before compacting and after compacting. This ratio was calculated from briquette density (by pressure 120 MPa and temperature 105 ºC) and from length of pressing chamber L_k. The compacting ratio is 1:8. Know we can calculate length of pressed briquette after each pressing on the pressing stand. Note, that in our case, in case of closed chamber, has each briquettes various length. On the figure 3 you can see what is situation in closed chamber at compacting. In the table 1 you can see calculated each length of pressed briquettes. After than we can calculate according to equation (3) and values in Tab.1 searched counter pressure (p_G). These calculated values you can find also in Tab.1. We can say that value of counter pressure increasing with reduction of the length of pressed briquettes. In closed system of pressing is pressed briquette after each pressing shorter because after each pressing is volume of pressing chamber reduced. According to these results we can say that value of counter pressure will decrease with increasing of length of pressed column. Now we can try to apply this theory to horizontal continuous way of pressing. On the figure 4 you can see what is situation at horizontal continuous pressing. Figure 4 describes the compacting process and effecting of counter pressure at horizontal continuous pressing. The main difference is that the length of pressed briquette is equal for each briquette. Briquettes which were pressed sooner will continuously move through the full pressing chamber until to the end of chamber. We use again dimensions of experimental pressing stand at calculation but with considering of continuous way of pressing.

i	**1**	**2**	**3**	**4**	**5**	**6**	**7**	**8**
L_{ki} (mm)	140	122,5	107,19	93,79	82,07	71,81	62,83	54,98
H_i (mm)	17,5	15,31	13,40	11,72	10,26	8,98	7,85	6,87
p_{Gi} (MPa)	39,84	45,74	51,59	57,35	62,87	68,15	73,18	77,84

Table. 1 Table of calculated parameters for counter pressure calculation [3]

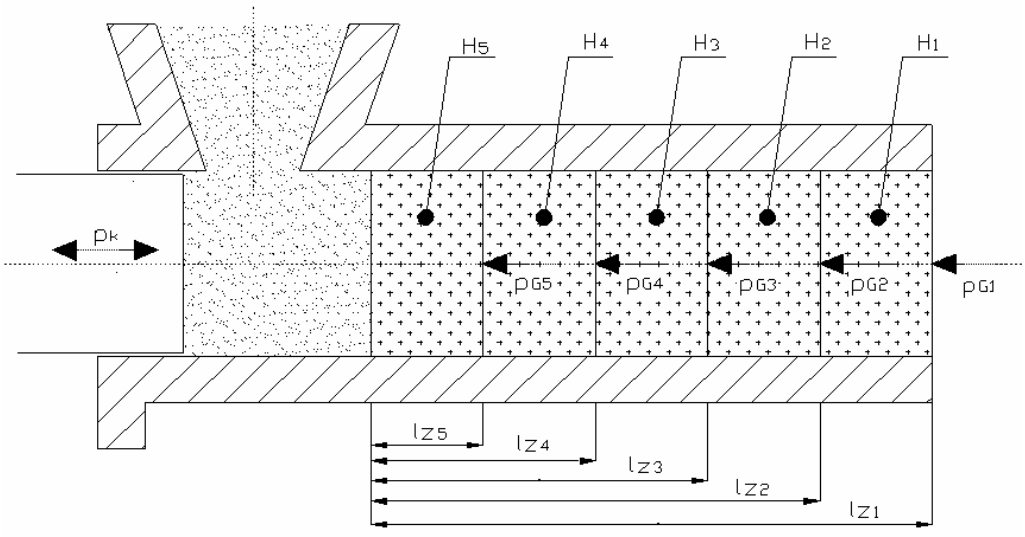

Fig.4 Counter pressure effecting at horizontal continuous pressing

In the table 2 you can see the calculated values of counter pressure at continuous way of pressing. We can say that counter pressure decreasing with increase of length of pressed column or with increase of length of pressing chamber. With other experiment in the future we have to verify this claim. Also is much needed to find the optimal length of pressing chamber in dependence on compacting pressure or counter pressure. Optimal length of pressing chamber is when the briquette reaches by Standard given density, when is able to overrun the counter pressure and when it is able to leave the pressing chamber without fall to pieces. Optimal length of pressing chamber will change in dependence on effecting compacting pressure or counter pressure. Optimal length of pressing chamber will depend also on radial strains. Radial strains we can calculate from the ratio of main strains λ (radial / axial). It will be very useful if we could execute experiment for radial strains find out.

i	**1**	**2**	**3**	**4**	**5**
l_{zi} (mm)	87,5	70	52,5	35	17,5
p_{Gi} (MPa)	0,48	1,45	4,39	13,23	39,84

Table.2 Table of calculated values of counter pressure at continuous way of pressing

On the figure 5 you can see the dependence of effecting counter pressure in pressing chamber on length of pressed column of briquettes. This figure comes from previously calculations. You can see that the counter pressure is higher when the length of pressed column is shorter and vice versa.

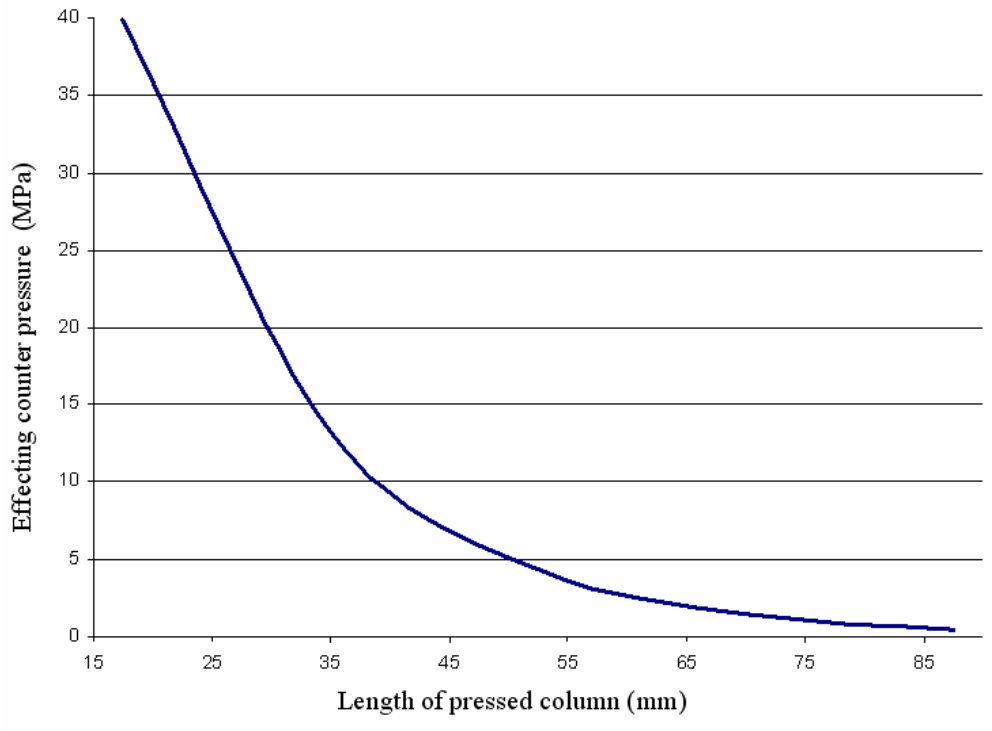

Fig.5 Dependence of counter pressure effecting on briquette in pressing chamber on length of pressed column

4. CONCLUSION

This presented methodology and calculations are very useful for design of pressing chambers. We are able to design the shape and dimensions of pressing chamber. When we will know the value of effecting radial strains we can calculate the place in pressing chamber when the briquette can leave the chamber without fall to pieces. Every design and calculation has to be according to briquettes density which is given by Standards.

5. REFERENCES

[1] Holm, J.; Henriksen, U.; Hustad, J.; Sorensen, L.: *Toward an understanding of controlling parameters in softwood and hardwood pellets production*, American Chemical Society, published on web 09/09/2006.

[2] Šooš, Ľ., Križan, P.: *Analyze of forces interaction in pressing chamber of briquetting machine (in Slovak)*, In.: Proceedings from 11. International conference TOP 2005, pp. 299-306, Častá - Papiernička, Slovakia, FME STU, ISBN 80-227-2249-9, 29.06.-01.07.2005.

[3] Križan, P.: *Wood waste compacting process and conception of presses construction (in Slovak)*, Dissertation thesis, FME STU in Bratislava, Slovakia, 2009

[4] Križan, P.; Vukelić, D.: *Shape of pressing chamber for wood biomass compacting,* In.: Quality Festival 2008: 2nd International quality conference, Kragujevac, Serbia, ISBN 978-86-86663-25-2, 13.-15. May 2008.

ACKNOWLEDGEMENT

The paper is a part of the research done within the project SK-SRB-0011-07. The authors would like to thank to the Slovak Research and Development Agency.

Authors: **M.Sc. Peter Križan, prof. Ľubomír Šooš**, Slovak Technical University in Bratislava, Faculty of Mechanical Engineering, Nám. Slobody 17, 81231 Bratislava, Slovakia, Phone.: +421 2 572 96 537, Fax: +421 2 524 97 809.

M.Sc. Djordje Vukelić, University of Novi Sad, Faculty of Technical Sciences, Trg Dositeja Obradovica 6, 21000 Novi Sad, Serbia, Phone.: +381 21 450-366, Fax: +381 21 454-495.

E-mail: peter.krizan@stuba.sk
lubomir.soos@stuba.sk
vukelic@uns.ac.rs

Journal of Production Engineering
Vol.12 No.1

Sovilj, B., Javorova, J. G. , Geric, K., Brezocnik, M.

INFLUENCE OF TEMPERATURE ON THE PHASE TRANSITION IN CoPt ALLOY

Abstract: *The variations of internal friction, magnetic susceptibility and loss angle with time and temperature of disoredered CoPt equi-atomic alloy, during annealing induced phase transition from cubic to tetragonal are shown.*

The paper presents results of investigation of magnetic and anelastic relaxation of "as-quenched" CoPt alloy measured from 300 K to 840 K versus annealing induced ordering starting from 460 K.

Internal friction and magnetic susceptibility/ time and temperature signatures can enable a better understanding of ordering processes and mechanisms.

Key words*:phase transition, CoPt alloy, magnetization*

1. INTRODUCTION

Atomic ordering can affect the anelastic and ferromagnetic properties of metals and alloys. The internal friction (IF) level, the initial magnetic susceptibility, its magnetic after-effect (MAE) and magnetic loss angle can be used as an indication of the degree of order.

CoPt has a cubic (Al) structure in the "as-quenched" (disordered) phase. It transforms during annealing into the tetragonal (Ll_0) phase. The transformation is of diffusion like type and can be attributed to the ordering processes and establishing of short - range order.

In the disordered phase CoPt exhibits a high level of IF (magneto- elastic damping) and soft ferromagnetic properties, while in the ordered phase it show a low magnetic susceptibility and IF level.

The aim of the present paper is to investigate the change of IF, magnetic susceptibility and loss angle during continuous or successive annealing of disordered samples from the room temperature up to 840K. Reason for this type of research is to study the magnetic and anelastic properties of pure, equi-atomic CoPt alloy by controlling the heat treatment and temperature during the ordering and phase transition processes.

2. EXPERIMENTAL PROCEDURE

The measure of IF in the case of a wire is the logarithmic decrement 5 of free torsional vibrations of a CoPt sample:

$$Q^{-1} = \frac{\delta}{\pi} \qquad (1)$$

The inverted torsion pendulum is working at low frequency, fo=60 Hz, and at strain amplitude of 2×10^{-3}.

Electronic timer with the accuracy of the order of 10 JIS has been used.

Magnetic measurements - performed by differential ac technique based - on a Wilde bridge [1] at a frequency of 3 kHz in a field directed parallel to the wire has been also done.

After demagnetization of the sample at t_1=30s in ac field of about $10^3 Am^{-1}$, MAE measurements started at t_2=32 s and are continued up to 1800 s. The measuring field amplitude of 0.24 Am^{-1} has been chosen.

Expressions for the loss angle

$$\tan\phi = \frac{\chi``}{\chi`} \qquad (2)$$

following from the complex initial magnetic susceptibility

$$\chi = \chi` - \chi`` \qquad (3)$$

and for the **MAE** :

$$\frac{\Delta r}{r_1} = \frac{r(t_2,T) - r(t_1,T)}{r(t_1,T)} \qquad (4)$$

are used, where the reluctivity $r = 1/\chi`$ and $\chi`$ is the real part of the complex initial susceptibility; t_1 = 30 s, and t_2 varied from 32 s to 1800 s; T is the temperature of the sample.

2.1. Sample preparation

A high purity, equi-atomic CoPt (50 at % Pt) sample in the form of a wire, the diameter of 1.0 mm has been sealed off under a vacuum of 10^{-5} Pa in a quartz tube,

annealed above the critical temperature of 1100 K (see Fig. 1) for five hours, and than ice - cold water quenched in order to obtain the disordered fee phase.
IF and magnetic measurements have been taken on the "as-quenched" (disordered) samples during heating up to the Curie point. The rate of temperature change during these measurements has been 0.3 K/min.

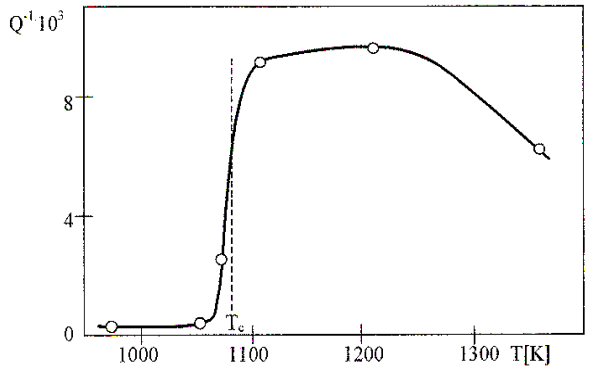

Fig.l. The change of IF level of CoPt alloy as function of the quenching temperature. Tc is the critical temperature [2].

In samples quenched from temperature $T > T_C$, a high IF level is observed in Fig. 1. The high internal friction level in "as-quenched" samples is due to the magneto-mechanical damping of the Bloch domain walls as observed in the micro-scale, or due to the losses caused by the magneto-elastic hysteresis as measured in the macro-scale[3].

3. RESULTS AND DISCUSSION

The **IF** measuring results for two different heating rates of CoPt during ordering are shown in Fig. 2. The high level of internal friction as seen in Fig.2 at T < 450K is observed after quenching the samples from 1430 K to 273 K.

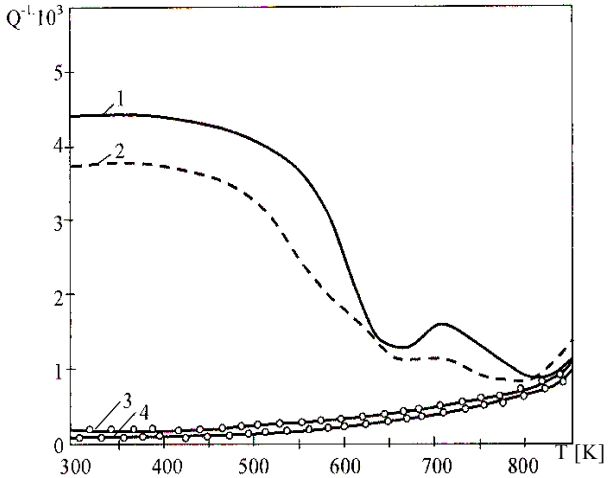

Fig.2. The temperature dependence of IF of disordered CoPt alloy for two different heating rates: 2 K/min. - curve 1, and 6 K/min. - curve 2. Curves 3 and 4 represent damping for saturated and ordered sample respectively [6].

Between 300 K and 450 K, IF changes only a little, but from 450K to 650 K, it decreases significantly - up to the level of partly ordered sample.

In the second temperature region, where the ordering process started, we see in Fig. 3, a maximum of $\Delta r / r_1$ and simultaneously a decrease of the real part of the initial susceptibility χ'.

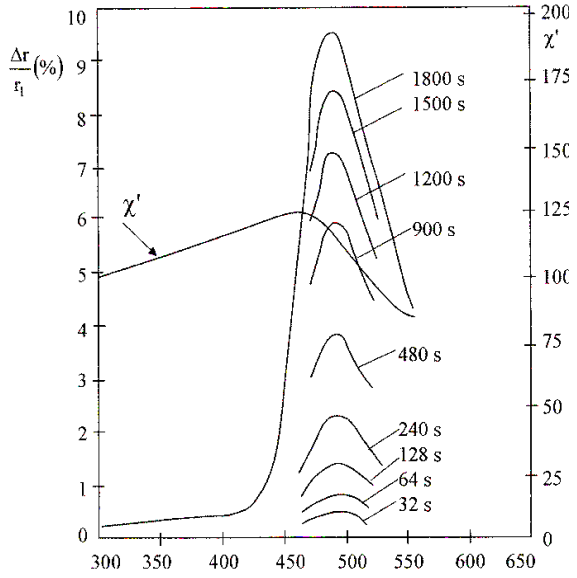

Fig.3. The magnetic after-effect and the initial magnetic susceptibility of disordered CoPt sample versus annealing temperature during a run from 300 K to 556 K, as determined at t_1 =30 s after demagnetization; t_2 varied from 32 s to 1800 s.

We suppose that during annealing of disordered sample in this step of ordering the frozen in vacancies, produced during quenching, are moving to the partially ordered regions, increasing the level of order, as observed by the initial susceptibility measurement during two successive annealing runs: A from 3000 K to 556 K and run B from 300 K to 650 K as seen in Fig.4, and as calculated in paper [4] and [5]. The maximum of the initial susceptibility observed at about 460 K anneal and has completely annealed out by measurements in the run B.

In [5] we have shown, that the MAE maximum at 500 K in Fig.3 is due to the rotation of the easy magnetization vector from [111] to the [001] axis, its position depends upon the heating rate and it disappears in the course of the two successive annealing runs A and B as seen in Fig.4.

The Richter type, reversible magnetic relaxation maximum at 500 K, seen in Fig.3 has an activation energy of E_R = 1.4 eV, and is ascribed to the reorientation of Co - Pt atomic pairs [6].

The high temperature IF peak at 700 K, whose amplitude increase with decreasing heating rate, as seen in Fig.2, and huge increase of magnetic losses,

seen in Fig.5, are due to a structural relaxation process that occur during annealing induced phase transition from cubic to tetragonal.

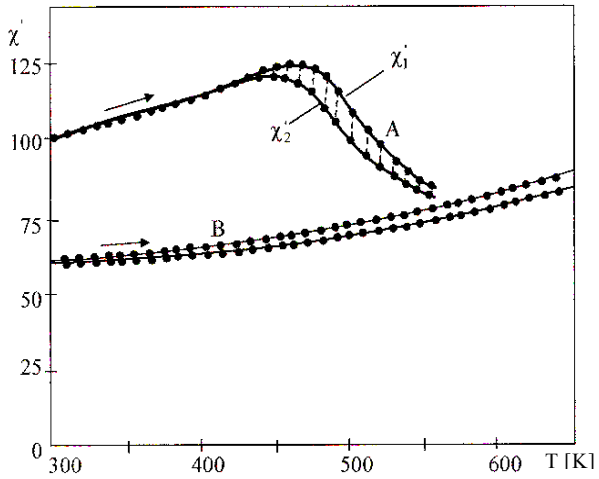

Fig.4. Variation of the real part of initial susceptibility of disordered CoPt sample, measured during two successive annealing runs A and B; χ_1'' - at t_1=ls and χ_2'' - at t_2=30min. after demagnetization [7].

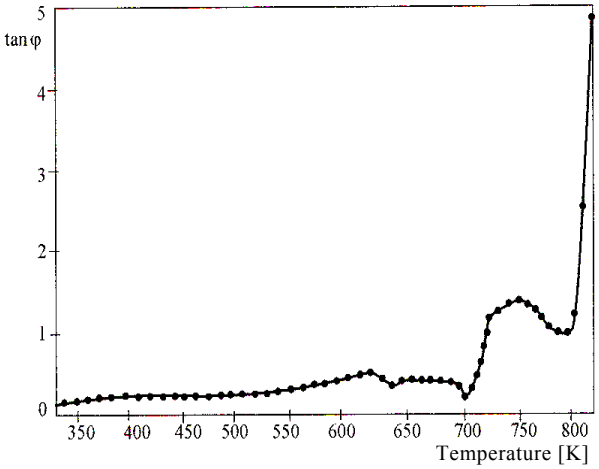

Fig.5. Loss angle versus annealing temperature of disordered CoPt alloy after quenching the sample from 1450 K to 273 K.

In Fig. 2 we observe at T> 800 K a high temperature background (HTBG) of IF. The HTBG is higher for higher heating rates. The characteristics of the background are basically dependent from interaction between dislocations, point defects and other defects like residual fcc-phase or stacking faults.

By applying a steady magnetic saturation field it is possible to reduce the IF to the level of saturated magneto-mechanical damping (curve 3 in Fig.2), which is very close to the IF level of ordered sample (curve 4 in Fig.2).

The background of IF follows the function:

$$Q_{BG}^{-1} = a \cdot \exp\left(\frac{-E}{kT}\right) \qquad (5)$$

with E=1.5 eV for $Q_{BG}^{-1} = 1.3 \cdot 10^{-4}$ at T=530 K, and $a = 1/\omega\tau_0$ [3] at $\tau_0 = 10^{-13} s$ and $\omega = 2\pi f_0 = 377\,Hz$

As seen in Fig.5, at T >530 K, the structural changes started influencing the increase of the magnetic losses.

4. CONCLUSION

Annealing from 300 K up to 840 K of disordered by quenching equi-atomic CoPt alloy results in:

- phase transition from cubic to tetragonal,
- decrease (about ten times) of the initial magnetic susceptibility,
- rapid, thermally-activated reorientationa! relaxation of Co-Pt atomic pairs, leading to short- range order,
- a slower, migrational, structural ordering process, which results in reduction of Co - Co atomic pairs with ferromagnetic bonding, leading to long - range order. Our approach could be extended up to the Curie point (T^{A1}= 830 K) [7], therefore we could observe a huge increase of magnetic losses (in Fig.5).

5. REFERENCES

[1] E. Klugmann, HJ. Blythe, F. Walz, *Investigation of Thermo magnetic Effects in Mono crystalline Cobalt near the Martensitic Phase Transition, phys.* stat. sol (a) 146 (1994), 803-813

[2] W. Chomka, *Internal Friction in Ordered Mg-Cu, Ag-Mg and Co-Pt Systems*, Sci. Papers of the Technical University of Gdansk (Poland), Fizyka, No 176 (1971), 3-66

[3] W. Chomka, *The Mechanism of Internal Friction in Metals,* Sci. Papers of the University of Katowice (Poland), No 165 (1977), 80-113

[4] E.V. Gomonaj, E. Klugmann, *Atomic and Magnetic Ordering in CoPt Alloy,* J. AppL Phys. 77 (5) (1995), 2160-2165

[5] E. Klugmann, *Relationship Between Structure and Internal Friction in CoPt and FePd Alloy*, Fundamentals of Tribology and Bridging the Gap Between the Macro- and Micro/Nanoscales, Ed. B. Bhushan, Kluwer Academic Publishers, NATO Sci. Series, Printed in Netherlands, 2001, pp. 299-304

[6] E. Klugmann, HJ. Blythe, B. Augustyniak, *Kinetic of Ordering in Equi-Atomic CoPt Alloys*, J. de Phys.

Colloq. C8, 48 (1987), 513-517

[7] E. Klugmann, HJ. Blythe, *Atomic and Magnetic Ordering in CoPt Alloys Studies by Magnetic and Internal Friction Measurements*, J. Magn. Magn. Mater. 101 (1991), 99-101

[8] SOVILJ, B., *Identifikacija triboloških procesa pri odvalnom glodanju*, Doktorska disertacija, Fakultet tehničkih nauka, Novi Sad, 1988.

Authors: **Prof. Dr. Bogdan Sovilj, Assoc. Prof. Katarina Gerić** University of Novi Sad, Faculty of Technical Sciences, Trg Dositeja Obradovica 6, 21000 Novi Sad, Serbia, **PhD.Juliana G. Javorova** University of Chemical Technology and Metallurgy,Kliment Ohridski Blvd. 8., 1756 Sofia, Bulgaria **Assoc. Prof. Dr. Miran Brezocnik,** University of Maribor, Faculty of Mechanical Engineering, Smetanova 17, 2000 Maribor, Slovenia,
E-mail: bsovilj@uns.ac.rs
july@uctm.edu
kgeric@uns.ac.rs
mbrezocnik@uni-mb.si

Journal of Production Engineering
Vol.12 No.1

Sovilj, B., Radonjic, S., Kovac, P., Sovilj-Nikic, I.

ANALYSIS OF GEAR CHARACTERISTICS AND SERATION PROCESSING IN "KOLUBARA - METAL" FACTORY

Abstract: *The introduction of modern technology in the production of profiled gear milling cutters requires a complete analysis of the application of the tools in the industry of our country. This paper presents the analysis of the application of the aforementioned tools in the company 'Kolubara-Metal '. With regard to the fact that a wide assortment of gears is produced in this company, the analysis included different types of serration machines as well as various profiled gearing tools utilised in the gear production.*
The paper includes some tool-related issues, i.e. producer, geometry, tool materials and tool sharpening as well as workpiece-related ones, i.e. material, dimensions, complexity, quality of manufacture and scale of production.
Key words*: serration machines, profiled gear milling cutters, serration, tool exploitation, tool sharpening.*

1. INTRODUCTION

Despite the bad economic situation some fields must work, because other economic and social fields depend on them. There are commercial organizations that still produce something for others, but they primarily work for their own needs. One such factory is "Kolubara-Metal" which has in own program wide variety of production gear. Given the wide range of different gear, size (dimensions up to 2 m), shape (cylindrical and conoid), with real teeth, screw ,..., has a number of special machines with intended usege.

It is pleasure to see all machines in the plant for serration work. After having different machines for making gears of different sizes and dimensions, this paper presents the machine with their characteristics

2.ANALYSIS OF THE PRODUCT ON WHICH SERRATION PROCESSING

Working piece or gear that are processed may be of soft material: bronze, brass, cast iron or steel, usually Č.4732 steel alloy steel for improvement (improved from 25 to 27 HRC) is used.

Working gear diameter: maximum without support pillar 2000 mm, maximum with extra column 1200mm minimum 300 mm. The maximum length of milling of straight-teeth and slant-teeth gears: with vertical milling is 560 mm and with radial milling 760 mm.
For sharpening of milling machine for this purpose is used. This machine is of Russian descent. On this machine are sharpened milling all the modules from the smallest to the largest one (from 5 to 24 mm). Milling cutter sharpened by face area until the sides to be clean of the damage. Sharpening depends on the quality of the work peace, and the quality of tools. If the work peace which already thermally enhanced is processed, tool will be more weared, and have to be often sharpen more often or more milling cutters are used. average sharpening milling cutter for 24 hours is three times.

Milling machine is placed on the spindle, the number of teeth put dividing plate that match the number of teeth of milling cutter. The grindstone is introduced into hollow between, teeth under certain angle and approach to sharpening. When sharpening is done by cooling to prevent heating of milling, which would lead to changes in the structure of material tools, and thus change the hardness. Wear depends on the type of material analyzed, the number of teeth and the shift in average after a sharp tool 16 to 32h of work .

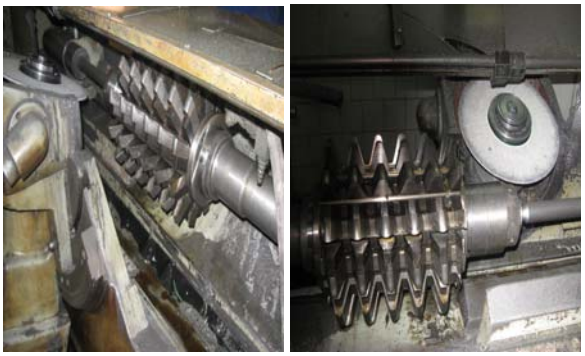
Fig. 1 Sharpening of milling cutter.

3.ANALYSIS OF MACHINES FOR PROCESSING OF SERRATION

Semiautomatic milling machine 5K32P mill is designed for rough and fine gear seration with straight and oblique teeth. The highest productivity of machines is given in terms of serial production, but on it can produce and gears in small batches and in very broad limits. The machine 5K32P can be make gear with straight and oblique teeth of the core module $0.5 \div 10^{th}$. Its structure is designed for larger modules. Working length of the machine is 250 mm and maximum diameter of the work piece is 800mm. This machine uses milling cutters. The choice depends on the mode of processing modules, the diameter and length of gears that are made.

For example, a gear module 8 is made with the three passages, where 1mm is left for the final passage to the final measures. Rotation per minute (Rpm) of milling cutter must not be below 56 rpm, and shift 0.8 mm.

Fig.2. Semiautomatic milling machine 5K32P

Fig.3. Machine 5K32P uses gear milling cutter.

Fig.4. Different types of gears, which are produced on the machine 5K32P

Universal milling machines for serration, model 5A342, is provided for processing of serration of cylindrical gears, applying the method of relative rolling milling cutter method and individual sharing and milling, with squamous or spindle gear milling cutters.

The machine can process serration the following types of gears: the gears with traight and oblique teeth for external coupling, gears with straight and oblique teeth for internal coupling, worm gears, gears with teeth arrow channel and no channel for output of milling, with the right gears teeth, with a small angle cone at the top.

Universal milling machines for serration uses various tools, thus modes of treatment are broad spectrum, which depends on the material that is processed if the processes softer materials-bronze, brass, cast iron, use the higher modes of processing, which in turn depends on the module gears. Processing of serration of steel are used less cutting conditions.

The main motion is circular and it is made by a tool that processes serration of gear; also mounting tools can have two extra movements that are linear; addition of further movement of the same circular that working piece is performed which depends on the type of milling cutters that are used for certain gear.

Fig.5. Development of different gears on the universal milling machines

Milling machines for serration model ZFWZ3150 / 3 is provided for processing of serration of cylindrical gears.

There are three types of processing: sharing unit, relative motion and tangential milling.

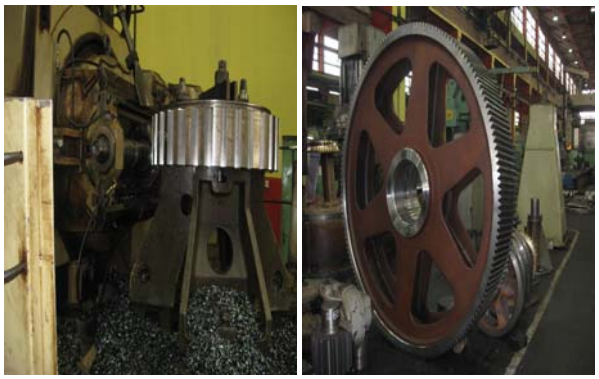

Fig.6. Production of cylindrical gears on the machine ZFWZ3150 / 3

3.1. Wear and sharpening of milling cutter

The wear process of milling cutters affects many factors (Figure 1). Increased wear of milling cutter first milling machine operator perceives first. It can observe the worn cutting edges of teeth of milling cutter, and is characterized by a blunt sound of the milling, which also attracted attention. In this case the cause of blunt edge of milling cutters, the occurrence of sand in the cast of worm wheel. Other common reasons for wearing of milling cutters are: hardness of gears and the phenomenon of great chip, chip on deposits milling cutter . Asynchronous speed of milling cutter and work piece, fraying blade due to periodic variable load certain stages of creating a chip, separation parts of tools with periodic separation deposits from tools (Figure 5). In Figure 6 gives a general form of wear and tear of the process of cutting elements of milling cutter are given.

Depending on the damage or blunt of cutting edge of milling cutters, it needs to be sharpen. Frequently damage and wear of milling cutter ranges from 0.1 to 0.7 mm in normal use, ie. normal regime. Focuses on the mill until the damage can not leave the wings and head milling. Side and head of milling get from factory sharpened by the module and profile, and be sharp while retaining module and profile, ie. until it remains only back part of milling. Each sharpening of milling cutter increases the space between the radical-relief angle and rake angle

Fig.7.The traces of wear on milling cutter

When sharpening specifical oil for cooling of milling cutter called "RIZOL" is used. On this machine 46 grain grinder granulation is used. Less modules is easier and faster sharpen than of the larger modules. Milling cutter can sharpen whet approximately 50 sharpening with normal modes of serration. The process of sharpening milling briefly looks like this: grinder goes straight to hollow between teeth of milling to sarpen rake angle, a machine with guitars that fixed for that milling machine adjusts coil (step) by taking every passing from 0.03 to 0.01 mm depending on the module. Smaller modules to m_n - 10 can sharpen for about 90 minutes of normal mode sharpening. Module 24 for 4 hours with normal wearness. This machine sharpens the largest module, m_n - 24

The machine is semi-automatic, by preparing and fixing for necessary milling cutter. The machine itself divides automaticly the number of teeth-by-step perform feed of sharp stone (grinder), and the number of passages in one cycle is about 20 passages.

Fig.8. Grindstone for sharpening of milling cutters

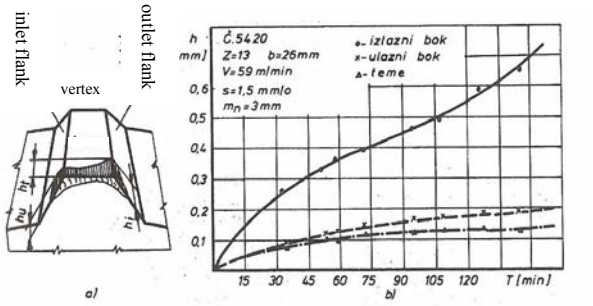

Fig.9.The general form of wear (a) and development of wear processes (b) cutting element milling cutter

4. CONCLUSION

In this paper analysis of application of gear milling cutters for making gears in the factory "Kolubara-Metal" is given. The machines that are used for serration are included. The characteristics of machines, tools, and gear that are produced on them are given. All machines in the factory work, mostly produced gears for its own purposes, for maintenance of excavators working in the mines. Sometimes they work on the order for other customers. Continuous production of gears includes tools for serration consumption. From the aspect of consumer of tools, the introduction of modern technology in the production of profiled gear milling cutters makes sense.

5. REFERENCES

[1] Kimer, J.: Tehnološki postupci i alati, I deo-Alati za obradu rezanjem, Novi Sad, 1973.

[2] Nikić, Z., Radonjić, S., Jugović, V. , Jovanović, B.: *Eksploatacione karakteristike PFAUTER glodala presvučenih slojem TiN*, Zbornik radova, 24. Savetovanje proizvodnog mašinstva Jugoslavije, Redni broj strane 127-133, Novi Sad, 1992,.

[3] Nikić, Z., Radonjić, S.:*Exploiting characteristics of Pfauter Milling cutte coated with TiN layers*, 12th ICPR – International Conference on Production Research Preliminary Programme, Finland, 1993.

[4] Radonjić, S., Nikić, Z., Jovanović, B.: *Tajlorovi izrazi pri ozubljenju Pfauter glodalom*, 25. Savetovanje proizvodnog cmašinstva Jugoslavije, Redni broj strane 45-50 Beograd, 1994.

[5] Radonjić, S., Sovilj, B., Sovilj-Nikić,I., Analiza leđnog struganja zuba odvalnih glodala klasičnim postupkom, 32. Savetovanje proizvodnog mašinstva Srbije sa međunarodnim učećem, Novi Sad, 18.-20. septembra 2008.

.

[6] Sovilj. B.: *Identifikacija triboloških procesa pri odvalnom glodanju*, Novi Sad, IPM, FTN, 1988.

[7] Sovilj, B.,Prapotnik, B., Mitrović, R., Todić, V.: *Influence of gearing process on the occurence of cutting edge break by hob milling tools*, Tribology in industry, Vol. 21, No. 2, Redni broj strane 53-58, 1999.

Authors: **Prof. Dr. Bogdan Sovilj, Prof. Dr. Pavel Kovač, Ivan Sovilj-Nikić Phd student,** University of Novi Sad, Faculty of Technical Sciences, Trg Dositeja Obradovica 6, 21000 Novi Sad, Serbia, Tel.: +381214852343

Prof. dr Snežana Radonjić, University of Kragujevac, Technical Faculty of Čačak, Svetog Save 65, 32000 Čačak, Tel.: +381 32 302-763 Fax.: +381 32342-101

E-mail: *bsovilj@uns..ac.rs*
pkovac@uns.ac.rs
snezar@tfc.kg.ac.yu
diomed17@gmail.com

Journal of Production Engineering
Vol.12 No.1

Sovilj, B., Radonjic, S., Sovilj-Nikic, I.

ANALYSIS OF APPLICATION OF PROFILED TOOLS FOR SERATION IN "KOLUBARA - METAL" FACTORY

Abstract: *The introduction of modern technology in the production of profiled gear milling cutters requires a complete analysis of applying these tools in the domestic industry: In the paper the analysis of application of profiled gear milling cutters for serration in the factory "KOLUBARA-METAL" Vreoci. Considering that in this factory a wide range of gears is produced, the analysis included the type and performance of profiled milling cutters used in the manufacture of gears.*
Keywords: *gear profiled milling cutters, milling cutters, disc-shaped milling cutters and palmate milling cutters.*

1. INTRODUCTION

Profiled milling cutters with the backstroke teeth are very widespread in the processing of profiled parts. These are: convex milling cutters, concave milling cutters, gear cutters, splines of splined shafts of straight-line profiles, tapping as well as milling cutters for special applications designed to process the most complex profiles. The biggest advantage of profiled milling cutters comes to the fore when processing parts with greater length by the width of the profiled surface. Other advantages of profiled milling cutters are:

- Ease of manufacture, processing by back surface profile is performed only with a knife without grinding and applying of special auxiliary tools;
- Ease of sharpening that is done by face surface, while retain the original profile is retained "KOLUBARA-METAL" in its program has a wide variety of gear production , both in form and size.

2. ROLE AND IMPORTANCE OF HOB MILLING CUTTER DURING GEAR SERRATION

Hob milling, as one of the most complex processing cutting, is the broadest application of processing cylindrical gear teeth due to high productivity process. Complicated kinematical and geometric relationship between hob milling workpiece and cutting tool creates a series of difficulties and problems that prevent optimal use of tools and machines, such as: determining the optimal cutting speed and displacement, determining the existence of rational hob milling, the maximum and evenly to use as multi tooth tools, which determines the geometry of productive hob milling etc.[1].

Improving the process of hob milling is significant and useful for manufacturers of gears as well as manufacturers of hob milling cutters. Because of the complicated process, high values of gears, especially the tools, research of backgrounds for hob milling process optimization and optimization of geometrical parameters require considerable financial resources and the significant efforts of researchers. There are many factors that influence the process of hob milling. Numerous factors and their interaction make the wear process difficult for the study

Figure 1 presents the factors which influence the wear during hob milling process

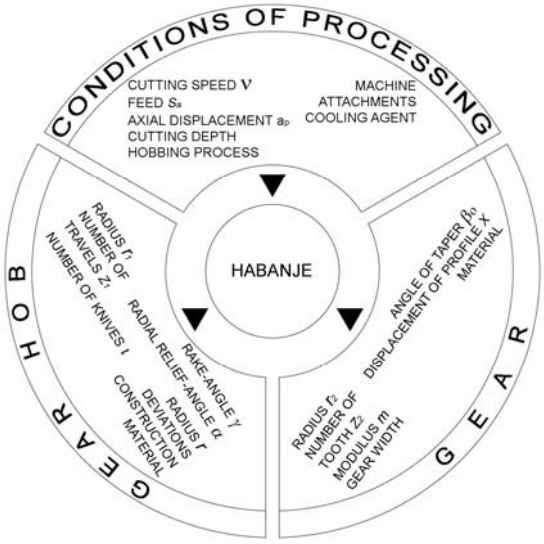

Fig. 1 Factors influencing wear during hob milling process

Hob milling process is one of the most important link in the chain of mechanical processing because of it has great impact on productivity, the final geometric accuracy and the quality of serration surface. By development of hob milling technology hob milling, hob milling is successfully applied for the rough machining as well as fine machining of serration. Therefore, the demand for the optimization process increased as from the standpoint of surface quality, and from the standpoint of productivity. A

prerequisite for the successful optimization and adaptive management of the process is its identification, and identification of phenomena arising in hob milling. Therefore, research activities in this field are directed to to development of new hob milling cutters and technological improvements in machinery as well as completely new methods for identifying a credible description of the processes and phenomena arising during hob milling [6].

Hob milling cutters are used for making gear serration with straight, oblique and helical teeth and making worm wheels for external conjugation with involute profile (Figure 2).

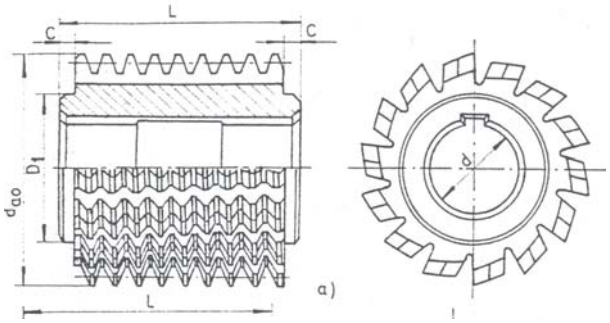

Fig. 2. Integral gear hob

Hob milling cutters is usually made as single-thread especially if they are used for fine machining. For the rough and previous machining are made with two or more threads due to faster and less processing. Construction of milling cutter with inserted teeth (Figure 3) allows savings in material costs over 50%, greater durability of tools for over 60%, cost reduction of serration for over 25%, and increased process productivity 1.5 times compared to the integral hob milling cutters.

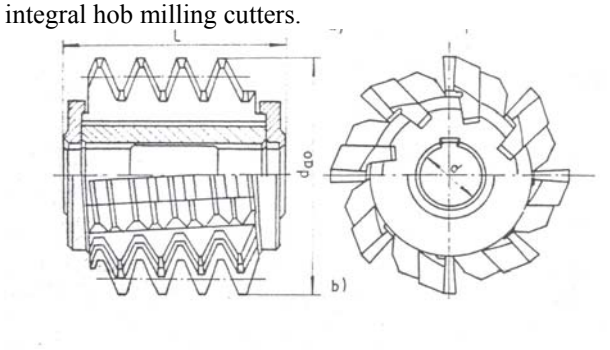

Fig.3. Milling cutter with inserted teeth

3. TYPES PROFILED GEAR MILLING CUTTERS USED AT 5A342 MACHINE

Hob milling cutter is an indispensable tool for processing gear serration by hob milling method. It is made out of high-speed steel as one piece or of hard metal with inserted teeth.

There is different classification of hob milling cutters. Direction of milling is essential for setting machines, there are schemes of setting in which the relationship (direction) miller – gear is presented.

In Figure 4 is a milling head with engraved signs: module, angle of milling cutter, steel, etc is shown.
Hob milling cutters are differed in module size. It is from 0.5 to 30 depending on the required gear that serrated. There are milling cutters with multiple starting points.

Fig. 4. Milling head with engraved signs

Fig. 5. Hob milling cutter

Fig. 6. Hob milling cutters for making fluts

Hob milling cutters are marked divided by the tooth profile. Three basic profiles can be differentiated that are marked with Roman numerals I, II, III . Profile I is outside standards, i.e. it has a short profile of the teeth and it gives shallower teeth, or it is made as the template - to be used for dedicated tasks. Profile II is a standard profile that is used mostly. Profile III is profile of milling cutter used for

making gears with predimension for grinding. This profile leaves deeper hollow between teeth because of passage of abrasive grinding wheel grinder at machine for grinding the gears. This type of milling cutters has a wider head because of end of the grinding wheel. There are also more milling cutters for serration processing that have different profiles (Figure 6.).

Milling machine for making chain wheel whose cogs have radius shape is shown in Figure 7. This milling cutters are defined by pitch and diameter of rolls or cylinder, also with profiles I, II and III.

Fig. 7. Milling cutters for making chain wheel

Most of the milling cutters has cutting angle of 20 degrees.

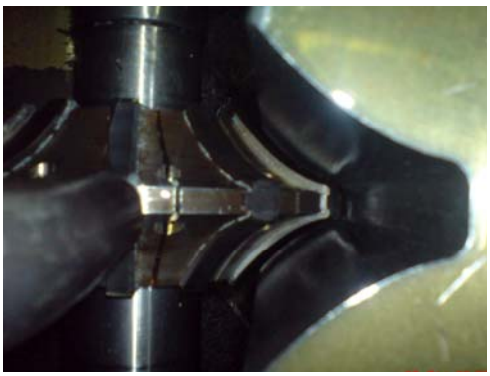

a)

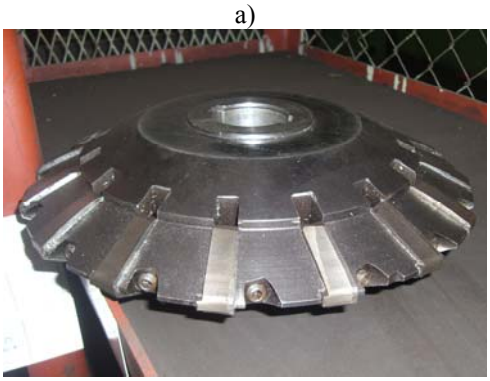

b)

Fig. 8. Disc-shaped milling cutters (a,b)

Disc-shaped milling cutters(Figure 8.) are mainly used for processing of gear serration with large module. These milling cutters are made of high-speed steel: Č9780, Č7880, Č7680. Hardness of cutting piece is $63^{\pm 1}$ HRc.

Disc-shaped milling cutters have all the modules. Some milling cutters are made by made or sharpen by patterns. Templates are mounted on the machine for sharpening.

Disc-shaped milling cutters with variable hard metal plates are used in processing of gear serration gear on predimension When the gear is mounted on the machine, previous processing is performed by disc-shaped milling cutter with removable plates, and then it is taken off and milling cutter of high-speed steel is put which is used for fine machining. Milling cutters with removable plates are generally used. With such type of milling cutters productivity is much higher, achieving a much higher cutting speed and without cooling. When milling cutter of high-speed steel are used cooling is necessary and cutting speed is less.

a)

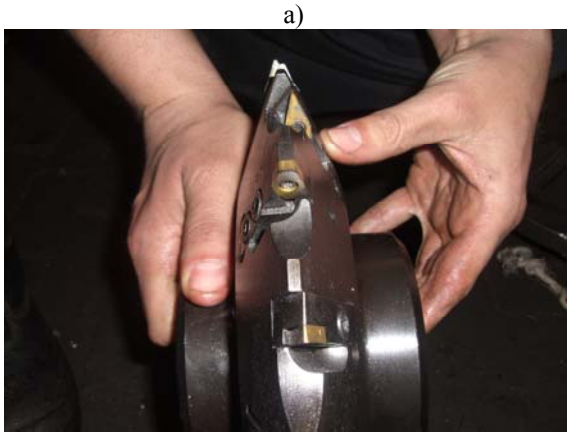

b)

Fig. 9. Disc-shaped milling cutters with changeable inserts (a,b)

There are all types, profiles and modules from -5 to larger modules 40 of palmate milling cutters. It is used in special cases when other milling cutters can not be applied. It is used by serration of arrow gears where arrow on the double gear is not separated by the or there is a small space where the arrows of double gears are broken. The palmate milling uses a

special head which has a cone of acceptance in which it fixed.

a)

b)

Fig.10. Palmate milling cutter (a,b)

4. CONCLUSION

One of the factories which in its production program making different gears, as in shape and size, on different machines is factory Kolubara-Metal ". It uses a different profiled gear milling cutters. Their production is focused on their own needs, related to the system for the production of coal, which is a continuous process in making gears.

The paper made a summary of tools for use in the factory "KOLUBARA-METAL. The characteristics of some tools for serration used in their production are given.

5. REFERENCES

[1] Kimer, J.: Tehnološki postupci i alati, I deo-Alati za obradu rezanjem, Novi Sad, 1973.

[2] Nikić, Z., Radonjić, S., Jugović, V. , Jovanović, B.: *Eksploatacione karakteristike PFAUTER glodala presvučenih slojem TiN*, Zbornik radova, 24. Savetovanje proizvodnog mašinstva Jugoslavije, Redni broj strane 127-133, Novi Sad, 1992,.

[3] Nikić, Z., Radonjić, S.:*Exploiting characteristics of Pfauter Milling cutte coated with TiN layers*, 12th ICPR – International Conference on Production Research Preliminary Programme, Finland, 1993.

[4] Radonjić, S., Nikić, Z., Jovanović, B.: *Tajlorovi izrazi pri ozubljenju Pfauter glodalom*, 25. Savetovanje proizvodnog cmašinstva Jugoslavije, Redni broj strane 45-50 Beograd, 1994.

[5] Radonjić, S., Sovilj, B., Sovilj-Nikić,I., Analiza leđnog struganja zuba odvalnih glodala klasičnim postupkom, 32. Savetovanje proizvodnog mašinstva Srbije sa međunarodnim učećem, Novi Sad, 18.-20. septembra 2008.

[6] Sovilj. B.: *Identifikacija triboloških procesa pri odvalnom glodanju*, Novi Sad, IPM, FTN, 1988.

[7] Sovilj, B.,Prapotnik, B., Mitrović, R., Todić, V.: *Influence of gearing process on the occurence of cutting edge break by hob milling tools*, Tribology in industry, Vol. 21, No. 2, Redni broj strane 53-58, 1999.

Authors: **Prof. Dr. Bogdan Sovilj, Ivan Sovilj-Nikić Phd student,** University of Novi Sad, Faculty of Technical Sciences, Trg Dositeja Obradovica 6, 21000 Novi Sad, Serbia, Tel.: +381214852343

Prof. dr Snežana Radonjić, University of Kragujevac, Technical Faculty of Čačak, Svetog Save 65, 32000 Čačak, Tel.: +381 32 302-763 Fax.: +381 32342-101

E-mail: *bsovilj@uns.ns.ac.yu*
snezar@tfc.kg.ac.yu
diomed17@gmail.com

Journal of Production Engineering
Vol.12 No.1

Vukelic, DJ., Tadic, B., Hodolic, J., Matin, I., Krizan, P.

DEVELOPMENT A DATABASE OF MODULAR FIXTURES

Abstract: *Importance of fixtures in the productional systems with automated production and automated product design imposes the need for modern approach to those designs. The aim is to create conditions which could provide the choice and construction of fixtures with the aid of computer hardware and modern applicative software which accelerate and facilitate the resolution of needed fixtures. This paper shows a model of database for designing and archiving of fixtures as well as segment of output data. The Application is developed on PC using Microsoft Access and ProENGINEER applicative software. The paper finally butlines relevant conclusions and expected future trends of the research.*
Key words: *Fixture, database*

1. INTRODUCTION

Computer application has reached an enviable level in the last decades, and hence, began to be used in almost every human working and living segment; in some areas, it has become almost irreplaceable. One of these areas is certainly manufacturing industry. Constant development in computer technology enables continual increase in its application possibilities in the engineering activities. The illustration can be numerous worldwide examples stating about developed CAx systems and software with various purposes for automated task solutions in product design area.

Increasing the automation level with the simultaneous increase in production system flexibility is possible to achieve only by applying CNC – Computer Numerical Controlled, and the increase in flexibility and productivity of the completely manufacturing system by applying CIM – Computer Integrated Manufacturing. Computer application in modern engineering practice is certainly multiple; however, one of applications that are more important is definitely manipulation and control of large sum of information and data of technical or some other nature, realized by new and increasing software class known as databases or DBMS – Database Management System. In every production system there is a need for manipulating a large sum of data, whether it is product design, technology preparation, control, and the like. Efficient database is only the one enabling fast access to the desired data and efficient data manipulation, and today it is impossible without a modern DBMS system.

2. PROBLEM DEFINITION

Modern production systems in manufacturing industry are characterized by product range extension, high frequency in changing the range, demands for constant product quality improvement, shortenings in production time, constant need for increasing technological level of products and decreasing their manufacturing costs. With such market demands, and intensive development of science, technique and new technologies, the level and the trend of further development of technological processes in manufacturing industry depend on all the composing factors. The factors with the highest influence on the quality of technological solutions are the following: preparation type of blank, machining processes, order of operations, operation structure, machine tools, tools, fixtures, measurements, etc. In order to raise technological solutions to a higher level, it is necessary to solve optimally all these elements.

To set the adequate measures for rational fixture usage, it is necessary to analyze the existing situation. Today, inadequate organizational conception in almost all companies obstructs the optimal usage of the already present fixtures. The unexploited capital is shown after the research of fixture constructions in a company (Fig. 1). The diversity in fixture constructions indicates the presence of a number of same or similar fixture drawings (fixture construction). Very often new constructions are being elaborated although minor change on the existing drawings would do the job. New fixtures are being made although the existing one could be redesigned with a small cost. In addition, there are cases when there is a suitable fixture, but a new one is designed and manufactured.

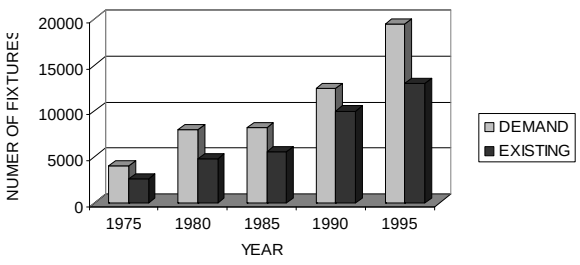

Fig. 1. Proportion between the existing fixtures and a demand for them

Second example, also presenting current situation in the field of fixtures, is given in Fig. 2. According to some researches elaborated in the USA, the average

cost of an individual Flexible manufacturing cell (FMC) is around $1,000,000. A significant financial segment from that amount goes to fixtures. The costs are increased proportionally in relation to the final costs. Fixture value share in the costs is 19% in average, which demonstrates that they are complex, precise, qualitative and efficient elements.

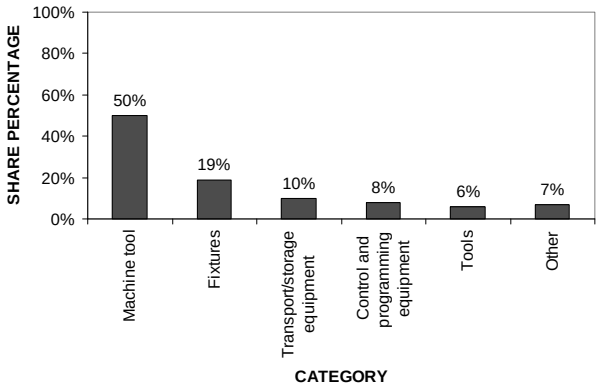

Fig. 2. Participation of individual components of FMC in total price

The problem of time analysis has a special importance when dealing with fixtures (Fig. 3). The reason lies in the fact that fixture design, as a rule, can begin only after technological process has been completely defined. As it can be observed in the picture, this time is six weeks in average, while two weeks are needed for fixture design.

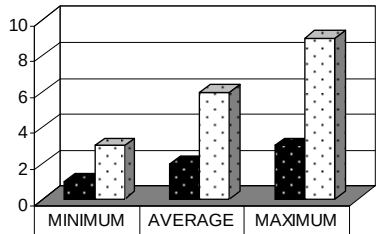

	MINIMUM	AVERAGE	MAXIMUM
FIXTURE	1	2	3
TECHNOLOGICAL PROCESS	3	6	9

Fig. 3. Time needed for designing fixtures within the total time needed for defining technological process

Most time in manual fixture design and adjoining costs is related to the following: elaborating general construction aspect, detailed construction elaborating and searching for necessary information on the existing fixture solutions, fixture elements, and the like.

All other activities require significantly shorter time and smaller costs. These are, primarily, introducing design task, performing necessary calculations, composing the bill of material (BOM), control, etc. Therefore, it is appropriate to automate at least those functions whose realization requires more time, and subsequently more adjoining costs. The researches impose a need for introducing new technologies into fixture design process, which are based on the so-called flexible automation, and whose main objective is to shorten time and decrease costs when designing new fixture constructions and re-use the existing solutions with or without modification. Fixture design with computer applications presents a newer design aspect (first attempts of fixture design automation go back to the 1980s), originating as the cause-effect answer to the negative aspects of classic design methods. This aspect of fixture design implies the computer application that, partially or completely, automates the sequences of fixture design. The goal is to generate adequate fixture within the acceptable time period and to reduce the designer's subjective influence and labour to the minimum. The most important assumptions for computer application in fixture design process are "translating" the designer's knowledge and experience onto the language that is understandable to the computer, developing selection and decision-making logics, etc.

3. MODULAR FIXTURE DATABASE STRUCTURE

The objective of this paper is to set a concept for a database for automated modular fixture design, which would ensure an integral approach while selecting the existing fixtures, their possible corrections and modifications, as well as new fixture design. The system should enable selecting the necessary fixture to realize a machining operation with different degrees of operational readiness if there is such fixture in the database, or to modify offered solutions or design new ones when there is no solution.

Database ensures system functioning in a sense of qualitative performance of its main functions, data searching and updating. Likewise, it presents main system support to select the existing fixtures, modify them or design new solutions, by setting all the necessary information. For a system to function successfully, database has to have certain datafiles (Fig. 4): fixture datafile, workpiece datafile, and fixture elements datafile.

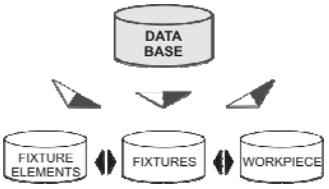

Fig. 4. Database general structure

Datafiles are easy to organize in tables, so that columns present the existing features, workpieces and fixture elements, and rows present their characteristics. Tables can be used in the automated system for selecting, modifying and designing fixtures as a means of formalizing the process of making an algorithm for selecting a variation from a group of possible ones, and as a means of automating the necessary tasks programming.

	Code		Name of operation	Machine		ID code workpiece	Note	Designer		Design date	Drawing	
	ID	CLASS		Name	Code			Name	Surname		2D	3D
Solution 1												
Solution 2												
...												
Solution n												

Table 1. Fixture datafile structure

	ID code	Name	Material	Batch size	Operation		Drawing		
					Code	Name	2D	3D	Operation
Workpiece 1									
Workpiece 2									
...									
Workpiece n									

Table 2. Workpiece datafile structure

	ID code	Name	Functional group	Group of elements	Mass	QTY	Drawing		Technological and geometric characteristics:			
							2D	3D	X_1	X_2	...	X_{tf}
Element 1												
Element 2												
...												
Element n												

Table 3. Fixture elements datafile structure

4. MODULAR FIXTURE DATABASE FUNCTIONING

The main principle used while modelling a database was the principle of hierarchic system decomposition. Modelling began from the demands significant to the future users. The following important processes have been identified:

- Database updating – the process involving data input, change and delete from the base,
- Database searching – the process ensuring the possibility to search through database by previously set criteria.

4.1. Database Updating

Database updating implies input, change or delete of data related to fixture elements, final constructive fixture solutions and their workpieces.

Deleting some data implies removing data from database, i.e. adequate datafile, primarily after usability of an element expires, and so it would not be used in the design process leading to confusion during the modular fixture assembly process.

Data change is done whenever there is a change (geometrical, technological, etc.) of an element, a fixture, or a workpiece, also with the aim to ensure reliable design process.

Data input into a database refers to the input of data linked to modular fixture constructions, modular fixture elements and workpieces, and it is performed in the following cases:

- Supply and/or manufacture of new additional elements of modular fixtures,
- Finished modular fixture design, when it is necessary to be stored into the database together with the adjoining workpiece so the latter could be used subsequently if the need appears.

Information update is performed using forms (Fig. 5). Data are input, changed or deleted in the fields reserved for it and they are automatically updated into appropriate tables in databases. Tables are organized so that rows present different fixture, fixture elements and workpiece variations, while columns show adequate geometric, technological, organizational and other characteristics of each of them individually.

From the form for data input, change and delete, it is possible to generate reports automatically like fixture report, workpiece report or fixture element report (Fig. 6).

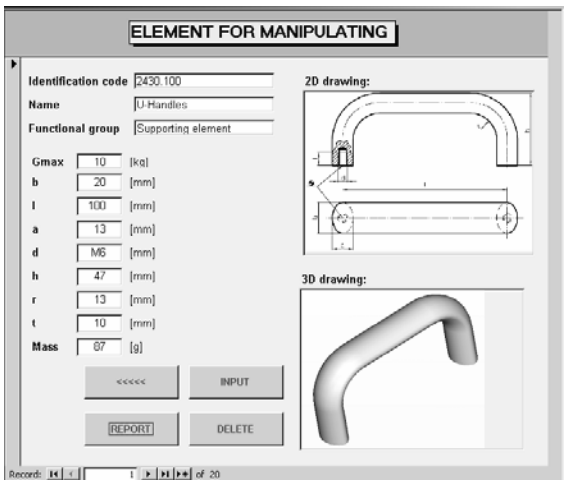

Fig. 5. Appearance of a form for updating fixture element data

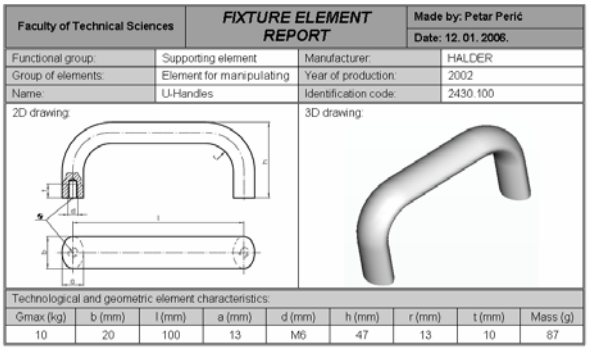

Fig. 6. Database general structure

4.2. Searching database by diverse criteria

The designer uses the option to search database to acquire information on elements and finished constructive fixture solutions. Depending on the demands, the designer defines search criteria. It is possible to name one or several criteria. On the basis of the chosen criteria, adequate forms are generated (Fig. 7), and within them, a selection and/or an input of the adequate parameters (one or more) are performed, since they are to be used for searching later.

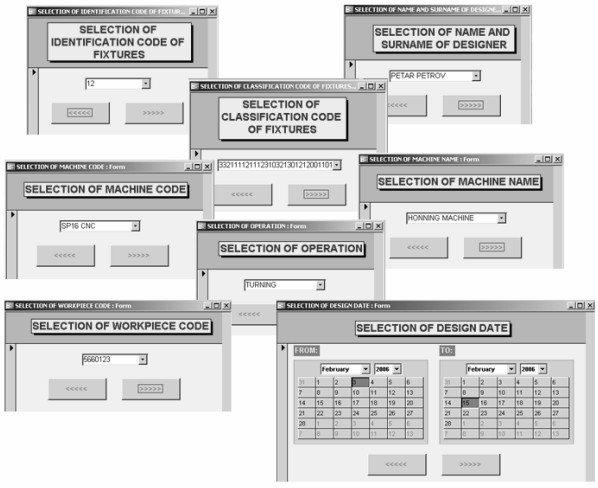

Fig. 7. Forms for searching databases by constructive fixture solutions

This is the way, by setting various inquiries and types of sorting necessary data, to generate different database search reports (Fig. 8). Generated reports are the basis to obtain system output results, i.e. adequate modular fixture necessary to realize a machining operation.

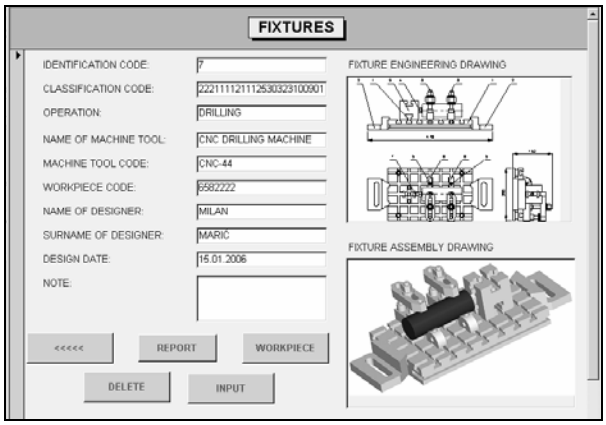

Fig. 8. Form for presenting fixtures

5. CONCLUSION

Modern production is doubtlessly directed towards the increase in productivity, economy, flexibility and working quality. To achieve it, it is necessary to have general databases that efficiently integrate all technical, technological, and organizational functions of an industrial system. The developed database for modular fixtures is one of foundations for developing an integral CAD/CAPP/CAM system that would significantly increase industrial system efficiency in total.

The developed database for automated modular fixture design enables, within technological production preparation, to efficiently reach adequate fixture solutions in the ongoing production, and for given conditions, to find or design the best fixture while conquering a new product or its parts, which is a way to influence the increase in techno-economic output presentations of the total production process.

For wider application of the developed system for automated fixture design and to ensure practical production and financial effects, it is necessary to continue the activities on improving databases, with the adequate number of reliable information bases, that is, proposed and checked contents of adequate data files. Efficiency degree could be further increased if the database was to be integrally linked to some of the automated product design systems. Further research should also be directed towards the integration of the developed systems with program systems for machining process simulation to prevent possible collisions and FEM analyses. It is a way to predict the behavior of fixture and workpiece connections during processing (deformations, oscillations, etc.). That would be a basis to perform optimization of positioning and clamping place on the workpiece.

Finally, it could be said that fixture design with computer application presents a complex problem demanding the knowledge on conventional design methods, declarative and procedural knowledge in the field of fixture design, and knowledge on the application of new methods and design techniques. Since the computers, regarding capacity, memory, speed and working quality, significantly surpass human abilities, fixture design automation enables considerable decrease in design process, decrease in total design costs, and obtaining qualitative solutions. Furthermore, designer's level of satisfaction is higher, while working labour in almost all design phases is lower.

6. REFERENCES

[1] Balasubramanian, S.: *Fixture-Based Design Similarity Measures for Variant Fixture Planning*, University of Maryland, Department of Mechanical Engineering and Institute for Systems Research, 1999.

[2] Campbell, P.: *Basic Fixture Design*, Industrial Press Inc., 1994.

[3] Cecil, J.: *Computer Aided Fixture Design - A Review and Future Trends*, The International Journal of Advanced Manufacturing Technology, Vol. 18, No. 11, 2001, pp 790 - 793.

[4] Henriksen, K. E.: *Jig and Fixture Design Manual*, Industrial Press Inc., 1973.

[5] Hoffman, G. E.: *Jig and Fixture Design*, Thomson Delmar Learning, 2003.

[6] Lin, Z. C. Huang. J. C.: *The fixture planning of modular fixtures for measurement*, IIE Transactions, Vol. 32, No. 4, pp. 345-359, 2000.

[7] Joshi, P. H.: *Jigs and Fixtures Design Manual*, McGraw-Hill Professional, 2002.

[8] Nee, A.Y.C., Tao, Z. J. and Senthil Kumar, A.: *Advanced Treatise on Fixture Design and Planning*, World Scientific, 2004.

[9] Pehlivan, S., Summers, J. D.: *A review of computer-aided fixture design with respect to information support requirements*, International Journal of Production Research, Vol. 46, No. 4, pp. 929-947, 2008.

[10] Rong, Y., Zhikun, H. and Huang, S. H.: *Advanced Computer-aided Fixture Design*, Academic Pr, 2005.

Authors: **Mgr. MSc Djordje Vukelic**, **Prof. dr Janko Hodolic**, **MSc. Ivan Matin**, University of Novi Sad, Faculty of Technical Sciences, Trg Dositeja Obradovica 6, 21000 Novi Sad, Serbia, Phone: ++381 21 458 2326.

Prof. dr Branko Tadic, University of Kragujevac, Faculty of Mechanical Engineering, Sestre Janjic 6, 34000 Kragujevac, Serbia, Phone: ++381 34 335 990.

MSc. Peter Krizan, Slovak University of Technology, Faculty of Mechanical Engineering, Námestie Slobody 17, 812 31 Bratislava, Slovakia, Phone: ++421 2 572 96 537.

E-mail: vukelic@uns.ac.rs
btadic@kg.ac.rs
hodolic@uns.ac.rs
matini@uns.ac.rs
peter.krizan@stuba.sk

Journal of Production Engineering
Vol.12 No.1

Zuperl, U., Cus, F.

AUTOMATION OF MILLING FIXTURE VERIFICATION PROCESS

Abstract: *The paper presents the automation of analysis and verification process of clamping devices, suitable for fixing of thin-wall workpieces. These workpieces will likely undergo deformations due to clamping and cutting forces during machining, which are the result of inconsiderate fixture design. An automation program has been made for the evaluation of fixtures intended for clamping of prismatic and rotational products, for determination of the optimum magnitude and positioning of clamping forces, required to enable the workpiece to be safely clamped during machining. The automation procedure ensures reduction of fixture planning process and prevention of defects and deformation during the machining process.*
Key words: *fixtures, milling, automation, clamping force.*

1. INTRODUCTION

The developed system is of great importance for designing fixtures since it can routinely determine within a short time the optimum sizes, direction and application points of clamping and locating forces for different cases of clamping. The purpose of the procedure is to improve the design of fixture and thus to increase the geometrical accuracy of the thin-wall product made. Designing of fixtures is a complex and intuitive process for which an experienced technologist is required. For each workpiece there are several possible solutions of the design of modular fixtures, therefore the scope of possible solutions is large.

The development of the artificial intelligence has contributed to limiting the scope of possible solutions and, consequently, to achieving better designs. Developed automation procedure (Figure 1) contains the fixture design, analysis, optimization and simulation module. The highly capable structure offers also the possibility of rationalization and visualization of the fixture solution obtained. It is important to consider the cutting forces, the clamping forces, the friction forces and the dimensions and availability of fixtures as well as the space on the machine limiting the possibility of clamping. The designing and manufacturing costs of the fixture amount even to 18 % of the total production costs [1]. In addition to searching for the mathematical solution for positioning and clamping of workpieces the development is oriented towards searching for the solutions by means of the computer routine. Researches [2] proposed the model "workpiece-fixture" based on the screw theory and used the linear programming method for determination of clamping forces. By the use of the non-linear programming method the quadratic model for verification of the fixture configuration is derived [3]. Mittal [4] proposes the dynamic model "fixture-workpiece" for the determination of the required clamping forces ensuring the equilibrium of the workpiece during machining. All the above mentioned methods use simplified models which do not take the friction into account in their calculations [5].

2. ASSUMPTION IN MAKING THE AUTOMATION PROCESS

When making the automation programme it was assumed that the workpiece would be fixed by a flexible modular fixture ensuring clamping of workpieces of different shapes. The worked out programme works on the (industrial computer) IPC and is programmed in the C++ programme language. The developed programme determines [6]:

- Minimum number and position of locating and clamping elements,
- Motion allowed by locating elements,
- Reactions at the places of the contact "workpiece-fixture" (locating forces),
- Minimal clamping forces required for balancing of cutting forces,
- Collision detection system,
- Fixture cost calculation system,
- The cost of fixture automation (pneumatic in combination with hydraulic) [7],
- Animation of fixture assembling, machining [8],
- Visualization of clamping control.

The clamping forces on the workpiece must not create internal stresses and must not damage or deform the workpiece surface. This argument affords great importance to the model made since it specifies the minimum required clamping forces, their application points and orientations with which the workpiece is still safely clamped. The purpose of the Force analysis is to find out whether the workpiece will lose the contact with the locating and positioning elements during machining due to cutting forces and moments.

3. CLAMPING SCHEME ANALYSIS AND OPTIMIZATION

The scene is more complex when friction between

the workpiece and fixture is taken into account (Fig. 2).

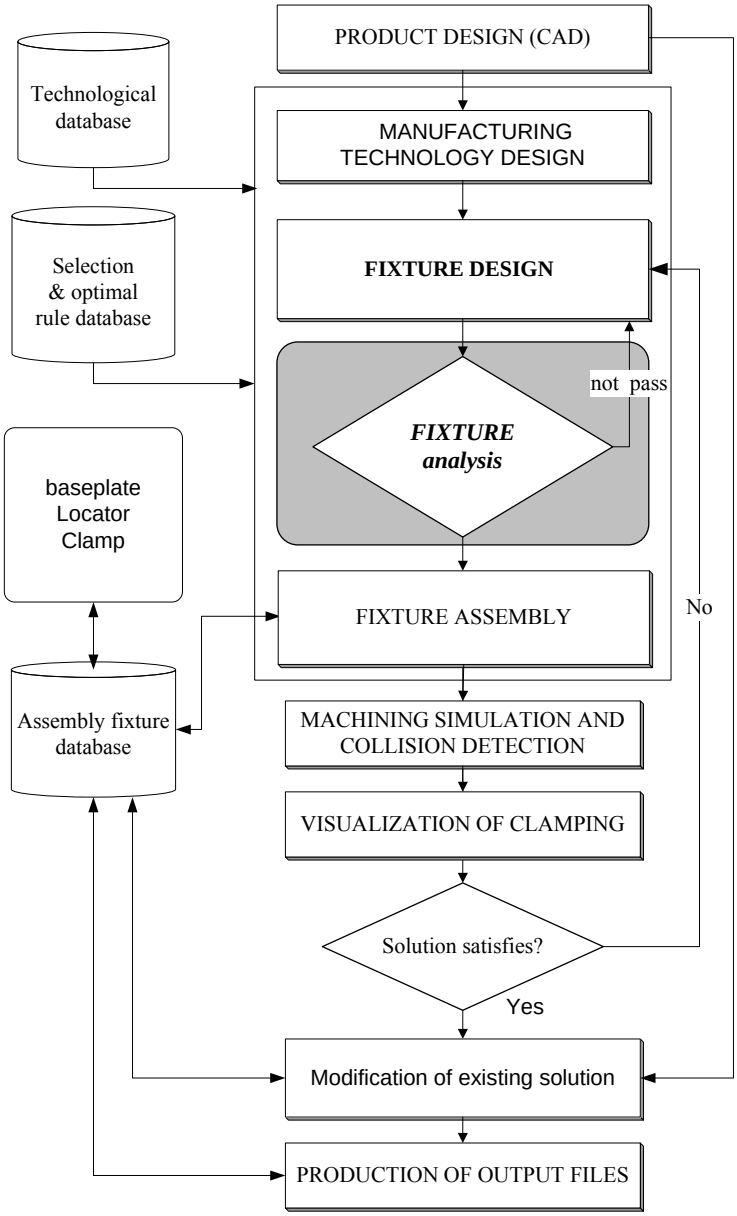

Fig. 1. Block diagram of the automated system for selection, analysis, optimization and visualisation of fixtures.

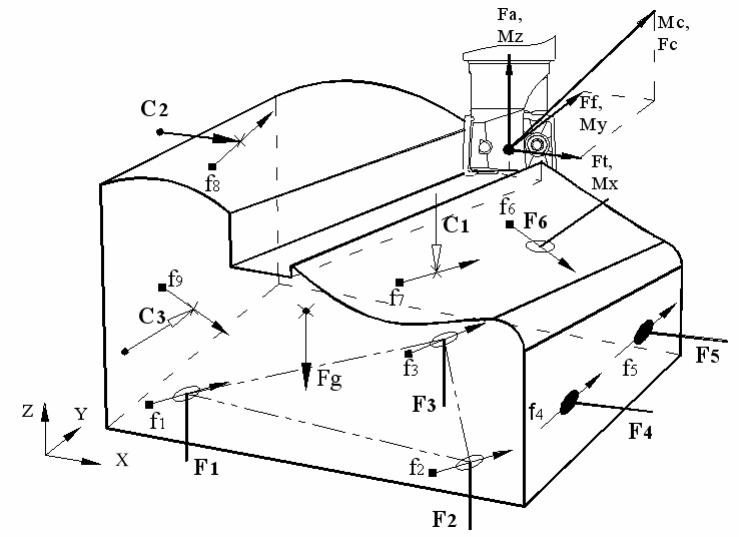

Fig. 2. Forces on workpiece during the milling process

.
Where:

- (F_1 - F_6)- reactions acting on locating elements (N)
- (C_1, C_2, C_3)- clamping forces acting in the direction of the normal onto positioning planes (N)
- (F_t, F_a, F_f - components of cutting force F_c (N)
- (M_x, M_y, M_z)- components of cutting moment M_c (Nm)
- f_i, (i=1...6)- resulting friction forces in contact points (N)
- F_g- force of workpiece weight (N)
- μ - friction coefficient

In general when the friction forces are taken into account, the number of unknowns is far more than that of the equilibrium equations. In order to solve for clamping forces the case must be simplified, and an iteration method is used in the force analysis routine. The workpiece is located on the six-point P_1-P_6, and is held by three clamping forces C_1, C_2, C_3 at points P_7, P_8, P_9, respectively. The resulting force of friction f_i between the locator and workpiece is $\mu \cdot F_i$ and between the fixing element and the workpiece it is $\mu \cdot C_j$, ($j=1...3$). The reactions on the locating elements must be positive because otherwise the contact between the workpiece and the fixture is lost.

4. MATHEMATICAL SYSTEM FOR CALCULATION OF CLAMPING AND LOCATING FORCES

To achieve static equilibrium and dimensional accuracy in machining the resultant force and moment on the workpiece must be zero. The equations of equilibrium are:

$$\begin{aligned}
&\sum \mathrm{F_i} = 0 \\
&\left(\sum_{i=1}^{6} \mathrm{F_i}\right)_x - \mathrm{R_x} = \left(\sum_{i=1}^{6} \mathrm{F_i}\right)_y - \mathrm{R_y} = \\
&= \left(\sum_{i=1}^{6} \mathrm{F_i}\right)_z - \mathrm{R_z} = 0
\end{aligned} \qquad (1)$$

$$\begin{aligned}
&\sum \mathrm{M_i} = 0 \\
&\left(\sum_{i=1}^{6} (\mathrm{F_i} \times \mathrm{r_i})\right)_x - \mathrm{M_x} = \left(\sum_{i=1}^{6} (\mathrm{F_i} \times \mathrm{r_i})\right)_y - \mathrm{M_y} = \\
&= \left(\sum_{i=1}^{6} (\mathrm{F_i} \times \mathrm{r_i})\right)_z - \mathrm{M_z} = 0
\end{aligned} \qquad (2)$$

Where: r_i- the vectors defining the locating points, (R_x, R_y, R_z) - components of the resultant cutting force F_c.

Because of the numerical solving of the problem the equilibrium equations are written in matrix form:

$$[A]_{lok} \cdot [F]_{lok} + [w_e] = 0 \qquad (3)$$

The normalised geometrical matrix $[A]_{lok}$ is as followed:

The vector of supporting forces $[F]_{lok}{}^T$:

$$[F]_{lok}{}^T = [F_1 \quad F_2 \quad F_3 \quad F_4 \quad F_5 \quad F_6] \qquad (5)$$

When the coefficient of the friction between the workpiece and the clamping elements is equal to zero, the above equation is simplified. After entering the geometrical matrix $[A]_{lok}$ and the vector of external forces $[w_e]$ into the Equation 3 the clamping and locating forces are calculated.

The normalized geometrical matrix $[A]_{lok}$ and the vector of external forces $[w_e]$ are as followed:

$$[A]_{lok} = \begin{bmatrix}
f_{1x} & f_{2x} & f_{3x} & -1 & -1 & f_{6x} \\
f_{1y} & f_{2y} & f_{3y} & f_{4y} & f_{5y} & -1 \\
1 & 1 & 1 & -f_{4z} & -f_{5z} & -f_{6z} \\
\hline
r_{1y} & r_{2y} & r_{3y} & \begin{matrix}-f_{4y} \cdot r_{4z} - \\ -f_{4y} \cdot r_{4y}\end{matrix} & \begin{matrix}-f_{5y} \cdot r_{5z} - \\ -f_{5z} \cdot r_{5y}\end{matrix} & \begin{matrix}-f_{6z} \cdot r_{6y} + \\ +r_{6z}\end{matrix} \\
-r_{1x} & -r_{2x} & -r_{3x} & \begin{matrix}-r_{4z} + \\ +f_{4z} \cdot r_{4x}\end{matrix} & \begin{matrix}-r_{5z} + \\ +f_{5z} \cdot r_{5x}\end{matrix} & \begin{matrix}f_{6x} \cdot r_{6z} + \\ +f_{6z} \cdot r_{6x}\end{matrix} \\
\begin{matrix}-f_{1x} \cdot r_{1y} + \\ +f_{1y} \cdot r_{1x}\end{matrix} & \begin{matrix}-f_{2x} \cdot r_{2y} + \\ +f_{2y} \cdot r_{2x}\end{matrix} & \begin{matrix}-f_{3x} \cdot r_{3y} + \\ +f_{3y} \cdot r_{3x}\end{matrix} & \begin{matrix}r_{4y} + \\ +f_{4y} \cdot r_{4x}\end{matrix} & \begin{matrix}r_{5y} + \\ +f_{5y} \cdot r_{5x}\end{matrix} & \begin{matrix}-r_{6x} - \\ -f_{6x} \cdot r_{6y}\end{matrix}
\end{bmatrix} \qquad (4)$$

$$[w_e] = \begin{bmatrix}
f_{7x} + f_{9x} + C_2 + R_x \\
f_{7y} + f_{8y} + C_3 + R_y \\
-f_{8z} - f_{9z} - F_g + R_z \\
-f_{7y} \cdot r_{7z} - f_{8y} \cdot r_{8z} - f_{8z} \cdot r_{8y} - f_{9z} \cdot r_{9y} - C_1 \cdot r_{7y} - C_3 \cdot r_{9z} - F_g \cdot r_{gy} + M_x \\
f_{7x} \cdot r_{7z} + f_{8z} \cdot r_{8x} + f_{9x} \cdot r_{9z} + f_{9z} \cdot r_{9x} + C_1 \cdot r_{7x} + C_2 \cdot r_{8z} + F_g \cdot r_{gx} + M_y \\
-f_{7x} \cdot r_{7y} + f_{7y} \cdot r_{7x} + f_{8y} \cdot r_{8x} - f_{9x} \cdot r_{9y} - C_2 \cdot r_{8y} + C_3 \cdot r_{9x} + M_z
\end{bmatrix} \qquad (6)$$

The Equation 3 is suitable for further numerical solving. The system has the non-trivial solution when the determinant of the system is: $\det|F_{lok}| \neq 0$.

By the iteration procedure the Equation 3 is solved; thus the minimum required clamping forces are calculated. The iteration starts with the initial value of clamping force $C_j=0,\ j=1,2,3$, afterwards this value gradually increases incrementally, until all forces F_i are positive. In this way we reach the basic-fundamental solution of the problem. The obtained values of C_1, C_2 and C_3 will be the first set of possible solutions. The basic solution can be optimised in this following way: The value of the basic solution is adapted to the first clamping force whereas the values of the others are gradually increased incrementally until all the calculated locating forces are positive. Then the procedure is repeated for each clamping force.

5. RESULTS AND MODEL EVALUATION

The tests confirmed correctness of the results of the propose automated system. The deviation of the predicted forces from the actual forces is slightly greater only in case of very little coefficient of friction ($0.01 \leq \mu \leq 0.2$) between the workpiece and the fixture. We tried to compensate the deviation of the predicted results in the mathematical model itself, but the corrections made did not improve significantly the values of the predicted forces. Therefore the required correction was made by introducing the artificial neural network into the model.

By using the artificial neural network (ANN) all the influencing factors, not taken into account in the equilibrium matrix equation, are included [9]. Five-layer feed-forward neural network was used. It contained 18 neurons in the input layer, and 9 in the output layer. The input vector consists of components of cutting forces, co-ordinates of point of machining, co-ordinates of position of the clamping and supporting parts, workpiece weight and friction coefficient. The output vector contains 9 corrections factors by which the values of the calculated forces are multiplied. Training was performed with the help of the error back-propagation. The training was supervised; the desired outputs (the nine clamping / locating forces) of the ANN are also being supplied during training.

Training of the ANN was made with experimental data of 1500 full training examples. Additional 800 examples were used to test the trained network.

The data for training and testing are obtained from the experimental measurements on the fixtures already made. Due to the introduction of the ANN the accuracy of the predicted forces was improved for 94% in case of $\mu \leq 0.3$ and for 4% in case of $\mu > 0.3$. The average estimation error was about 7.4% which is low compared to the 12,7% estimation error of the analytical model.

6. CONCLUSION

A automation system is presented that considered the effect of frictional forces for verification, rationalization and improvement of a fixture design.

A new iteration method is introduced for determining the clamping and locating forces at more reasonable level. By the system developed we have significantly reduced the time of conceiving the fixture (18%) and we have reached a greater manufacturing accuracy.

By the described model it is possible to anticipate and prevent the defects on the workpiece, fixture and cutting tool during the clamping and machining process.

In the research it has been found out that by taking the friction into account the value of the required clamping force as well as the number of the required clamping elements are strongly decreased.

Automated procedure enables even the inexperienced technologist to prepare high-quality (optimal) fixturing schemes.

7. REFERENCES

[1] Ma, W., Li, J., Rong, Y.: *Developement of automatzed fixture planning system*, Int. J. Adv. Manuf.Technol., Vol. 15, p.p. 171-181, 2006.

[2] Senthil, A., Subramaniam, V., Seow K.C.: *Conceptual design of fixtures using genetic algorithms*, Int. J. Adv. Manuf. Technol. Vol. 15, p.p. 79-84, 2004.

[3] Cus, F., Kopac, J.: *Inclusion of geometrical shape of cutter into optimization of milling process*, Metall, Vol. 10/11, p.p. 602-610, 1998.

[4] Mittal, R.O.: *Dynamic modeling of the fixture-workpiece system*, Robotics Computer-Integr Mfg Vol. 8, p.p. 201-217, 1998.

[5] Li, Y., Liang S.Y.: *Cutting force analysis in transient state milling processes*, Int. J. Adv. Manuf. Technol., Vol. 15, p.p. 785-790, 2001.

[6] Zuperl, U.: *Development of systems for computer-aided design of modular fixtures*. Proceedings of the 11th International DAAAM, Opatija, 19.-21. October 2000.

[7] Zuperl, U., Cus, F.: *A determination of the characteristic technological and economic parameters during metal cutting*, Stroj. vestn. 50(5), p.p. 252-266, 2004.

[8] Milfelner, M., Cus F.: *System for simulation of cutting process*, International Scientific Conference on the Occasion of the 50th Anniversary of Founding the Faculty of Mechanical Engineering, Ostrava, September 2000.

[9] Zuperl, U., Cus, F., Mursec, B., Ploj, A.: *A Hybrid analytical-neural network approach to the determination of optimal cutting conditions*, J. mater. process. technol. 157/158, pp. 82-90, 2004.

Authors: **Assistant prof. Uros Zuperl, prof. Dr. Franci Cus, dipl. oec,** University of Maribor, Faculty of Mechanical Engineering, Production Engineering Institute, Smetanova, 17, 200 Maribor, Slovenia, Phone.: +386 2 220-7621, Fax: +386 2 220-7996.
E-mail: uros.zuperl@uni-mb.si
franc.cus@uni-mb.si

Journal of Production Engineering
Vol.12 No.1

Borojevic, S., Jovisevic, V., Jokanovic, S.

MODELING, SIMULATION AND OPTIMIZATION OF PROCESS PLANNING

Abstract: *Designing of production systems from the standpoint of necessary resources for carrying out the production process for many years present an important set of engineering tasks. In the scope of design of production systems, in addition to design of process planning, it is necessary to make the determination of normative parameters, by which the effectiveness of the production process will achieve a high level. This is possible using application of the software system Tecnomatix Plant Simulation. This software system implementation is one step closer to the automation design of process planning, by modeling and simulation of technological processes. In this paper it process planning was a modeled and simulated in concrete conditions, applying this program system, in 2D and 3D environment and also determining optimal parameters of production.*
Key words: *Tecnomatix Plant Simulation, Design, Modeling, Simulation.*

1. INTRODUCTION

Designing of production systems from the standpoint of necessary resources for carrying out the production process for many years present an important set of engineering tasks. This process is determined by a number of influential factors of different degrees of intensity, direction and effect direction. In terms of growing competition the procedures of optimization of process planning are gaining in importance.

Process planning in metal manufacturing industry has variety of characteristic solutions in all its phases, i.e. operations. These characteristics were caused by the input data, which are encompassed with drawings and volume of production, the available technological equipment and raw materials, as also techno-economical conditions and subjective commitment of technologists.

In general, process planning variants of making a certain product are arising as a result of conventional design from technologist or application of automated systems design.
No matter which way of design is used, each adopted variant of the process planning is a logical set of appropriate technology development operations, whose solutions depend as from solutions of previous operations, as from solutions of the following operations.

Thus, the j-th variant of the process planning of production can be represented as a set of corresponding operations, i.e.:

$$(TP)_j = \{O_{j1}, O_{j2}, O_{jk}, \ldots\ldots, O_{jp}\} \qquad (1)$$

where letter p is the number of manufacturing operations, for the observed variations of the process planning.

Within the design of the manufacturing process planning, in addition to designing technologies of production, it is necessary to make the determination of norms (standards of time, materials, areas, etc.), by which the effectiveness of the production process will achieve a high level. During this, the most important role has work needs norms of production systems that are closely related to the time of production and quantity of products (parts).

To achieve high performance of the production systems, it is necessary to optimize process planning. Optimization in most cases is performed by applying some of the known methods and it taking into account the processing time , hold time, off time, preliminary-final time, set-up time, extra time and etc.
This paper contains presentation of computational system Tecnomatix Plant Simulation, which allows one step closer towards automation design processes of production, by modeling and simulation of process planning.

2. SIMULATION OF PROCESS PLANNING

The aim of the simulation is to achieve results that can be transferred into the real world. In addition, the simulation defines the preparation, execution and evaluation of carefully targeted experiments in a projected simulating model. Simulation of process planning is executed using the following steps:

- Assessment and collection of data from real production processes, which are necessary for designing simulation models,
- Determination of simulation studies goals and creation of simulation models in accordance with defined goals,
- Running experiments to perform the simulation, in context of simulating model. This gives a certain number of results, such as: how often the machines in the state of failure, how often are blocked, setting of machine, process times, utilization of the machines, etc.,
- Interpretation of simulation data.

In the process of defining tasks and goals of the

simulation studies, usually we need to ask the following questions:

- What kind of bandwidth and the output can be expected?
- What is the optimal number of resources (machines, workers, tools)?
- Where buffer zones are required?
- What is the optimal size of buffer zones?
- What optimal number of working pieces can be processed?
- What strategies are most appropriate for the task?
- How to combine and interact some or all of these factors to produce different results?

After all that, it is necessary to decide on the scope of simulation: only process plan or other areas of production (receiving, storage, delivery, etc.).
Developing a simulation model is cyclic and evaluation process. The simulation is executed on the first or initial model, and then with its improvement and enhancement, model becomes operational to provide optimum results after completion of the process simulation. Finally, after several cycles of improvement and enhancement, optimum simulation model is reached. Thus defined optimal simulation model represents a real process plan in the production system, for which is necessary to conduct needed research and analysis.

In general, the process simulation technology is applied in cases:

- where new production system is planning,
- for improving the existing production system and
- for introducing a plan that is defined in practice.

3. OVERVIEW OF PROGRAM SYSTEM TECNOMATIX PLANT SIMULATION

Tecnomatix Plant Simulation is a software system which is designed for modeling, simulation and optimization of manufacturing process planning. Optimization of manufacturing process planning using this software system is based on time-oriented simulation and event-oriented simulation.

Time-oriented simulation takes into account a wide range of different types of production time, while event-oriented simulation takes into account only these points in time which events have an impact, within the simulation model.

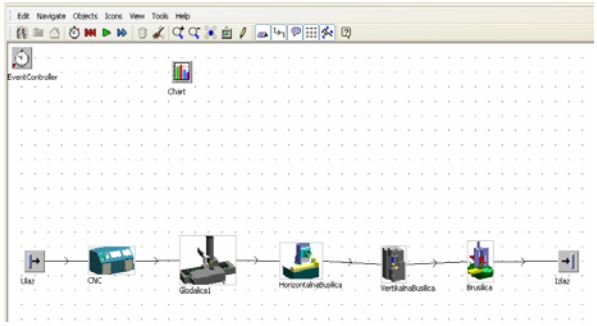

Fig 1. Modeling of process planning in 2D environment

Modeling of technological processes and the creation of simulation models of real production processes by applying the system Tecnomatix Plan Simulation can be performed in 2D and 3D environments.

Modeling in 2D environment, shown in Figure 1, is applied to complex optimization problems, related primarily to the time balancing the technological process, i.e. analysis of the production process from the point of time (production times, extra and additional times, a preliminary-final time, cycles production, etc.).

Modeling in 3D, shown in Figure 2, is primarily used for monitoring the distribution of technological systems and devices, which is necessary to spatially arrange in the appropriate production system.

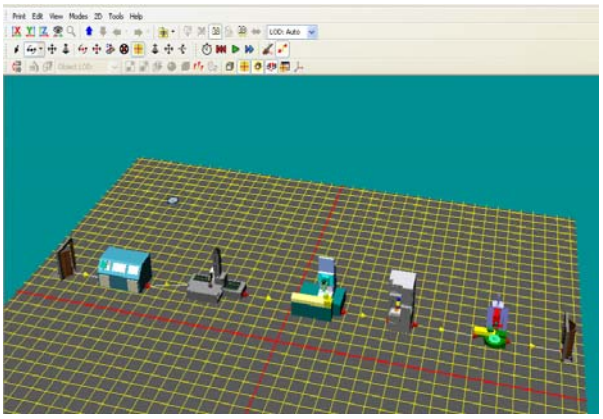
Fig 2. Modeling of process planning in 3D environment

Modeling in 2D and 3D environments is possible to connect, so when model in 3D environment is being created, model in the 2D environment was generated automatically.
The course of creating simulation models is carried out as follows:

- Generation of the 2D or 3D models of appropriate technological systems, devices, methods of transport material, inputs, outputs, etc. from the database of mentioned technological units,
- Development of spatial distribution of selected technological units and their adjustment to the conditions related to real production processes,
- Connecting the appropriate technological units in the production line. Thus defined product lines represent the actual product flows, which occur in the appropriate production system,
- Setting of parameters for each of the selected technology unit, which is a part of appropriate production flows. Data which are being entered in this step, should correspond as much as possible to the values of the real production process,
- Defining the appropriate objects, in the form of diagrams, tables, histogram, etc., which have the function of monitoring and presenting the results of simulations of the production process,
- Modeling of the production process and its setting in order to create conditions for the execution of

process simulation, i.e. testing of the simulation model,

- If the designer is not satisfied with the results of model simulations, he/she correct the input parameters until he/she get a model that gives satisfactory simulation results.

Capabilities of the system Tecnomatix Plan Simulation from the aspect of objects and methods of simulation are reflected through the simulation and modeling of:

- Process plan with a number of different strategies of production,
- Production process using the process planning,
- Condition: in malfunction, in work, in pause, etc.,
- Participants in the work and tasks they perform,
- Working shifts systems,
- Transportation systems etc.

4. APPLICATION OF PROGRAM SYSTEM TECNOMATIX PLANT SIMULATION

4.1 Process plan model

Application of the program system Tecnomatix Plan Simulation in this paper is shown on the model of process plan for production and assembly of crankshafts for production of motor saws. The production process in the specific situation involves making a three parts of crankshafts: one half of the magnet, one half clutch and piston rod.

Following data was used as input parameters for process of simulation and modeling using program system Tecnomatix Plan Simulation: the manufacturing process plan for parts of crankshafts (sequence of operations, production time, extra time, list of machines) and the number of pieces crankshafts annually.

4.2 Process plan simulation

Simulation of manufacturing process plan and assembly for crankshafts using the system Tecnomatix Plan Simulation in 2D environment consists of several steps:

- Defining the spatial model and generation of individual processes, which represent the operations in the production process from the process plan,
- Defining the distance between the individual technological systems in order to effectuate the simulation time which is lost during transportation of parts prior to the following operations,
- Linking individual processes in the flows of materials processing according to designed process plan,
- Defining the required time for individual processes,
- Defining the methods and rules of the transition work pieces during processing of materials,
- Defining objects for monitoring and recording the results of simulations
- Performing initial process simulation,
- Analysis of the results of simulation,
- Modification of simulation models and
- Performing the final process simulation.

Simulation of manufacturing and assembly process plan for crankshafts by the system Tecnomatix Plan Simulation in 2D environment is shown in Fig. 3

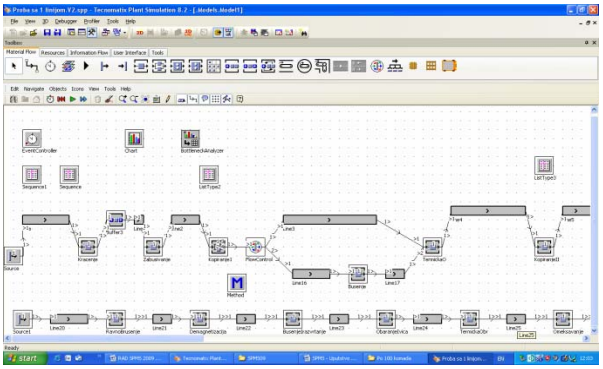

Fig. 3. Segment from simulation model shown in 2D

After designing satisfactory model of the manufacturing and assembly process plan for crankshafts in the 2D environment, it is being made a modeling of process plan in 3D environment. The purpose of modeling the 3D environment is primarily to determine the spatial layout of machinery and equipment in the production plant.

Fig. 4. Simulation model shown in 3D

By placing the machines and devices in precise defined locations in the production plant in 3D environment it is determined the precise distance between the machines that affect optimization for earlier designed models.

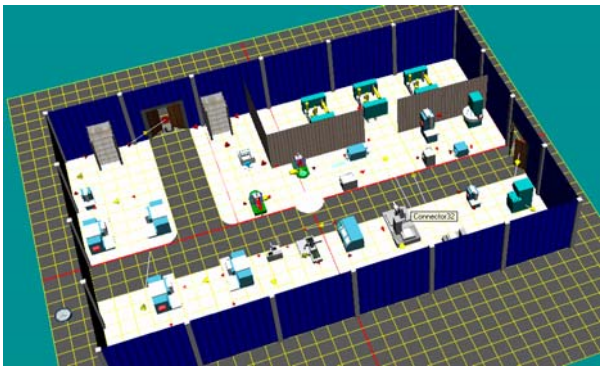

Fig. 5. Simulation model located in the corresponding production plant

Simulation model and production plant of the manufacturing and assembly process plan for crankshafts by the system Tecnomatix Plan Simulation in 3D is shown in Figure 4 and Figure 5. This model is founded on the basis of previous information on the number, layout and positions of the necessary technological systems and equipment.

4.3 Simulation results

Improving the simulation model is performed through initial process simulation and analysis of simulation results. In the model after the analysis of results, bottlenecks of production are being identified and accumulation of working pieces of precisely defined operations of the process plan. Efficiency of machines performing the initial process of simulation, i.e. before performing the optimization process, is unsatisfactory as shown in Figure 6.

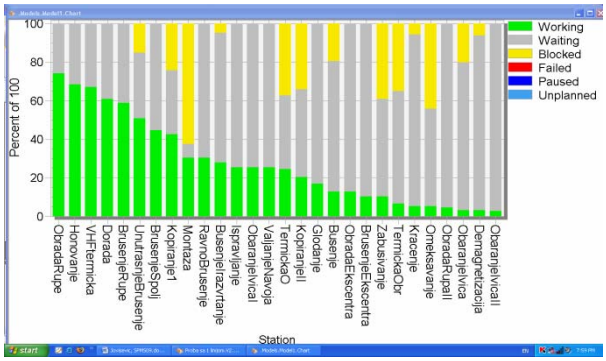

Fig. 6 Efficiency of machines before optimization

After analysis of influential factors, process optimization of process plan was performed, where goal is set as a function of high efficiency machines and minimum time duration of the cycle of production, while the limits were defined by the process plan. Resolving the above-mentioned shortcomings, introduction of buffer zones and increasing the number of machines, it was achieved a significantly shorter production cycle time. For example batch of 100 pieces of crankshafts, saving time in manufacturing process after the simulation was about 40%.After completion of design and simulation of process plan in the 3D environment, it was determined the exact location of machines and devices in the spatial layout of production facilities. Based on this information manufacturing cycle is reduced by 5% as a result of savings in time in transport parts between machines.

Based on the layout and location of machines and devices, it was designed a preliminary solution for production plant with the appropriate characteristics (departments, roads, entrances, exits, etc.).

Within results from execution of simulation of process plan, cycle times were generated for the appropriate size of batch parts and percentage utilization of machines in the manufacturing process. According to optimal designed simulation model, for the case of simulation of process plan and for the batch of 100 pieces crankshafts, the percentage utilization of machines is shown in Figure 7.

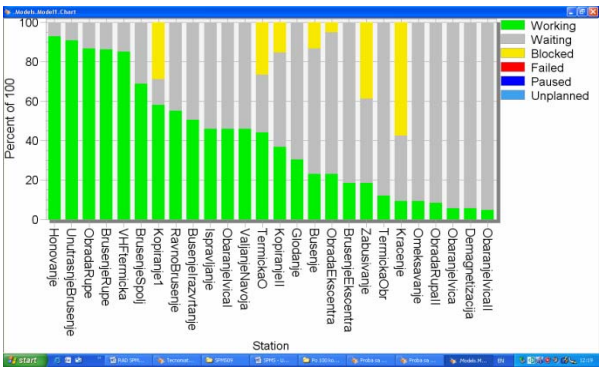

Fig. 7 Efficiency of machine after the optimization

5. CONCLUSION

Process plan modeling and simulation allows creating of models that represent adequate production processes, which generates the following benefits:

- Improving the productivity of existing production systems,
- Reduce investment in planning new production facility and capacity,
- Reduce inventory and flow time,
- Optimization of production systems dimensions, including backup size,
- Reducing investment risk through early proof of production concept,
- Maximizes utilization of productive resources,
- Improvement in design and layout of production line and machines.

In the example, final result of performing simulations showed data related to the duration of the manufacturing cycle, utilization of resources, as well as the required dimensions of the production plant that meet the set requirements from process plan.

6. LITERATURE

[1] Jokanović, S.: *Geometrijsko modeliranje*, Mašinski fakultet Banjaluka, Banjaluka, 2006.

[2] Jovišević, V.: *Projektovanje tehnoloških procesa,* Mašinski fakultet Banjaluka, Banjaluka, 2005.

[3] Programski sistem *Tecnomatix Plant Simulation* – UGS Corporation - Siemens Product Lifecycle Management Software Inc., 2009.

[4] Zelenović, D.: *Projektovanje proizvodnih sistema*, Fakultet tehničkih nauka, Novi Sad, 2003.

[5] Zelenović, D., Ćosic, I., i dr.: *Automatizovani postupak za oblikovanje proizvodnih sistema* – APOPS 08, Novi Sad 1990-92.

Authors: **PhD. Vid Jovišević, PhD. Simo Jokanović, Stevo Borojević,univ,eng** University in Banjaluka, Faculty of Mechanical Engineering, Department for Production Engineering, Stepe Stepanovica 75, 78000 Banjaluka, Bosnia and Herzegovina, Tel.: +387 51 465-473, Fax: 051 462-400

E-mail:vid.jovisevic@blic.net simoj@urc.bl.ac.yu stevoborojevic@hotmail.com

Journal of Production Engineering
Vol.12 No.1

Luzanin, O., Plancak, M., Barisic, B.

GESTURE RECOGNITION USING DATA GLOVE AND ANN-BASED PROCESSOR

Abstract: *Discussed in this paper is the problem of gesture recognition using a commercial data glove 5DT 5 Ultra, with the aim to improve its ergonomic features and usability for Mechanical CAD (MCAD). The authors improved the standard gesture dictionary by eliminating 11 original simple static gestures and substituting them with new complex static gestures. Since the restructuring of the original gesture dictionary imposed a problem of lower gesture recognition rate, this issue was approached using artificial neural networks. Obtained results indicate that the proposed restructuring of data dictionary can be efficiently supported by application of ANN-based processing.*
Key words: *virtual reality, data glove, static gesture, artificial neural network.*

1. INTRODUCTION

Virtual reality-based technologies are common in modern production manufacturing. As the result, a number of simulations exist which, besides the classical human-computer interface (HIC), also use multi-modal HIC. Multi-modal interaction puts a human in the center of the interface, focusing on extraction and interpretation of information gathered from hand gestures, speech, tactile feedback and other modalities of communication.

Since the second half of the 1970s when their use was pioneered by M. Krueger, hand gestures have been recognized as a natural and intuitive way of communicating not only with virtual environments, but with computers in general. However, despite of some three decades of development, the application of gestures in virtual environments is far from desired. As Poupyrev et al. noted, there exists no unified framework for virtual environment interaction, no desktop-style metaphor familiar to the majority of users, and no optimal interaction technique for all possible task and input devices in virtual environments [1].

Amongst various definitions of the gesture found in general dictionaries and scientific papers, a definition by Turk seems to be most comprehensive stating that a gesture is a meaningful body motion - i.e. physical movement of the fingers, hands, arms, head, face or body with the intent to convey information or interact with the environment [3]. A number of authors have contributed to the development of classification and taxonomy of gestures [2-8].

Discussion in this paper is confined to hand gestures. In addition, the distinction is made between hand gestures based on two fundamental properties: complexity and dynamics, which are required for proper gesture recognition. According to these criteria, hand gestures can be classified into:

- simple static gestures (postures) – in which finger configurations consist of either fully closed or fully open fingers,
- complex static gestures (postures) – in which fingers can be flexed at an arbitrary angle,
- simple dynamic gestures – in which either just a hand is moved or the fingers are moving with the hand in a fixed position,
- complex dynamic gestures – which involve the movement of fingers, as well as changes in location and orientation of a hand.

With this classification in view, the scope of this paper is limited to simple and complex static gestures.

2. PROBLEM DEFINITION

Owing to its all-round characteristics and low price, 5DT 5 Ultra data glove (Fifth Dimension Technologies) is very popular among industry professionals and researchers. The glove is equipped with five proprietary optical sensors, which allow it to measure finger flexure using one sensor per finger. Thus, signals from the sensors represent mean value of finger flexions at metacarpophanlangeal and proximal joints [10]. It also comes with a ready software support for the detection of the predefined set of 16 gestures. The authors have used this glove with an experimental VR desktop system, which is described in more detail in [11]. However, the glove is not suitable for use with MCAD without some important modifications:

- only a third of the predefined gesture set are ergonomically suitable for prolonged use, since they cause muscle fatigue,
- although thumb flexure is measured, none of the standard-dictionary gestures include the use of thumb, which not only prevents the simulation of grasping but also makes it impossible to simulate useful gestures which require the use of thumb,

- owing to the ergonomic issues and the principles of operation of the optical sensors, the gestures are sometimes misinterpreted or undefined,
- most of the gestures lack symbolical meaningfulness which is necessary for efficient use with MCAD applications.

Gestures supported by 5DT 5 Ultra are coded as the combination of binary states (open = 1 / closed = 0) of the four fingers, excluding the thumb. Thus, it is possible to create 24=16 gestures as combinations of open/closed fingers. The gestures are assigned numbers from 0 to 15, 0 representing the fist (all fingers closed) and 15 representing the open hand (all fingers open). Gesture recognition is based on boundary values. If the sensor reading for a particular finger is above the predefined boundary value, the finger is considered closed (flexed).

Conversely, if the reading falls below the boundary value, the finger is open (no flexion). All readings which fall between the boundary values are considered as errors, and the gesture is undefined.

This simple method of gesture recognition works well in some situations but is not always reliable. This can be attributed to anatomical variations in various users, as well as to the disposition of optical sensors and their cross-coupling, which can often result in incorrect recognition of a gesture [12].

3. MODIFICATION OF STANDARD GESTURE DICTIONARY

Ergonomic and cognitive issues of the existing gesture dictionary were addressed by restructuring the predefined gesture dictionary, eliminating some simple gestures and substituting them with the complex ones.

Considering the ergonomic features and iconic and metaphoric meaningfulness, the existing gesture dictionary was restructured in order to allow the elimination of:

- finger configurations which involve full extension of the middle finger with the index and ring finger fully flexed,
- finger configurations which involve full extension of the ring finger with the middle finger or middle and index finger fully flexed,
- finger configurations which involve full flexion of the index, middle and ring finger with the small finger and thumb fully extended.

Following the above stated guidelines, a total of eleven gestures were eliminated from the standard 5DT gesture. Of the remaining five gestures, three were left in their original form while the two remaining gestures were modified. Thus, gesture designated 1, was modified into gesture G03, while gesture 3 became gesture G05. Also added were five novel gestures, G04, G06, G08, G09 and G10 (Fig. 1).

The modified gesture dictionary comprises twelve static gestures and, according to conditional classification proposed by LaViola [7], belongs to small gesture dictionaries. This is an advantage regarding the efficiency of gesture recognition. Should the dictionary require an extension at any point, this can be solved with a context-dependent gesture recognition where a single gesture can be attributed with several meanings, depending on the suggested context of the application.

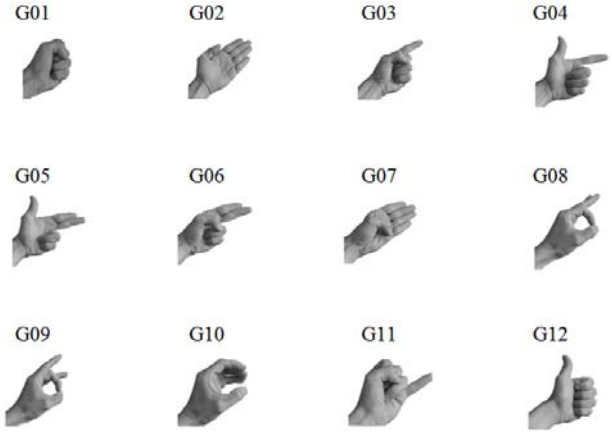

Fig. 1 Modified dictionary comprising 12 gestures

4. DEVELOPMENT OF ANN-BASED GESTURE RECOGNITION PROCESSOR

4.1 Architecture of experimental desktop VR platform

The experimental platform for which the processor was designed and built is based on a PC graphics workstation, with a stereo graphics card (Fig. *2*) which operates at double refresh rate. Having in mind that the user which wears LCD shutter glasses has a field of view which is limited to the size of the monitor screen, this platform is equipped with a 22" CRT monitor. Stereoscopic LCD shutter glasses function in a wireless mode, while the synchronization between the stereo graphics adapter and the glasses is performed by an infrared emitter.

As can be seen in Fig.2, the platform has two 6 DoF input devices - a data glove 5DT 5 Ultra and a trackball - Spaceball 5000. Software platform consists of OS *Windows XP*, CAD/CAE/CAM system *NX* and a VR CASE tool *Vizard (WorldViz)*. Integration of the data glove into the VR system is performed by a custom-developed recognition system for static gestures which is based on a probabilistic neural network (PNN) [10]. The PNN-based gesture recognition system allows two basic advantages over conventional approach: (i) better gesture recognition rate and (ii) enhancement of standard gesture library with new static gestures. Acquisition of a magnetic tracking system is in progress, which will allow the data glove to be used for dynamic gestures within the simulation space.

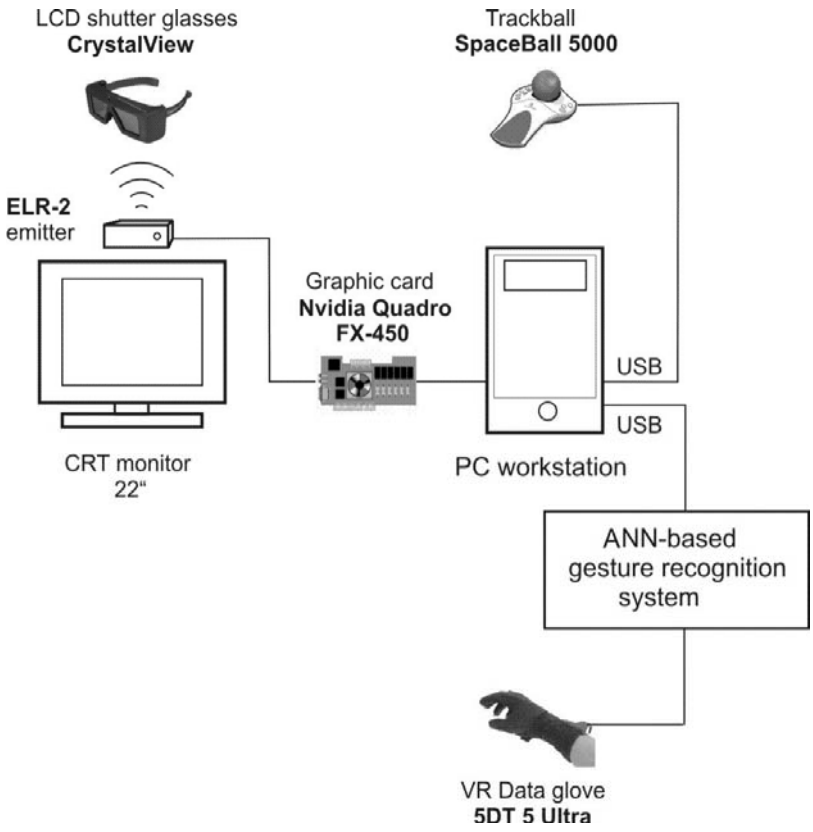

Fig. 2 Architecture of experimental desktop VR platform at the Laboratory for plastic forming technologies, DPM, Novi Sad

4.2 Realization and testing of ANN processor

The gesture recognition task was fulfilled using an ensemble of neural networks, i.e. multilayer perceptrons (MLPs) with one hidden layer and back propagation learning. Simulations were performed in the neural networks module of Statistica 7. Instead of using just one neural network for the task, a set of ten

MLPs was formed, trained, validated and tested in order to select the best five MLPs which formed an ensemble. Ensembles improve performance since averaging across different MLPs lowers the expected variance, i.e. the sensitivity of MLPs to the choice of the data set which would otherwise cause variations in classification error. Logistic and linear transfer functions were used for the neurons in the hidden and output layer, respectively.

The summary statistics for classification results obtained by the ensemble are given in Table 1. The data represent average values scored by the five member networks (MLPs).

	G01	G02	G03	G04	G05	G06	G07	G08	G09	G10	G11	G12
Total	200	200	200	200	200	200	200	200	200	200	200	200
Correct	193	199	196	199	196	191	200	190	175	200	200	185
Wrong	7	1	4	1	4	9	0	10	25	0	0	15
Unknown	0	0	0	0	0	0	0	0	0	0	0	1
Correct (%)	96.5	99.5	98.0	99.5	98.0	95.5	100	95.0	87.5	100	100	92.5
Wrong (%)	3.5	0.5	2.0	0.5	2.0	4.5	0.0	5.0	12.5	0.0	0.0	7.0
Unknown	0.0	0.0	0.0	0.0	0.0	0.0	0.0	0.0	0.0	0.0	0.0	0.5

Table 1 The results of gesture classification by ANN-based processor

5. DISCUSSION OF RESULTS

The five member networks used in final experiment differed in the number of neurons in the hidden layer. The number of neurons ranged from 18 to 30. The mean value of test errors for the five member networks equaled 0.35443.

The classification results for individual gestures (Table 1) reveal that gestures G7, G10 and G11 were classified with 100% accuracy. As expected, the ensemble performed worst in the case of two very similar gestures, G8 and G9, and gesture G12, which is very similar to G01. In addition, a single case of gesture G12 was unclassified and thus labeled as unknown gesture. Its class could not be decided by voting due to a disagreement between the five member networks.

In all, gesture recognition using the five-membered ensemble yielded satisfactory results showing that the modified gesture dictionary can be successfully used without significant deterioration of recognition accuracy.

6. CONCLUSION

The restructuring of the standard static gesture dictionary of 5DT 5 Ultra data glove successfully tackled the issue of ergonomy and symbolic meaning. Improvements were made by introducing complex static gestures which not only improved the ergonomic features of the gesture dictionary, but also imposed a distinct symbolic framework which helps users to pinpoint the function of particular gestures without extensive training. The problem of gesture recognition was efficiently solved using an ensemble of five MLPs.

The authors are currently designing and testing a novel system for static gestures recognition which would be flexible enough to allow efficient introduction of novel static gestures, as well as new users of data glove. Multilayer perceptrons with backpropagation are not suitable for this task primarily due to the fact that they require lengthy retraining with old and new data sets in case of any modifications. For that reason, the system shall be based on a probabilistic neural network (PNN) which shall be trained on a clustered data set to allow the necessary reduction of network complexity and higher processing speed.

7. REFERENCES

[1] Poupyrev, I., Billinghurst, M., Weghorst, S., Ichikawa T. (1997) A Framework for testbed for studying manipulation techniques for immersive virtual reality. Proc. of the ACM Symposium on Virtual Reality Software and Tech., p.21-28.

[2] Cerney, M., Vance, J. (2005) Gesture Recognition in Virtual Environments: A Review and Framework for Future Development. Iowa State University Human Computer Interaction Technical Report, ISU-HCI-2005-01

[3] Turk, M. (2002) Gesture recognition, Handbook of Virtual Environments, Design, Implementation and Applications, K.Stanney (Ed.), Lawrence Erlbaum Associates, 2002, ISBN: 080583270X, p.223-239.

[4] Bowman, D., Kruijff, E., LaViola, J., Poupyrev, I. (2005) 3D User Interfaces–Theory and Practice, , ISBN: 0-201-75867-9.

[5] Förster, J., Lang, H., Rinker, B., Santos, F. (2005) Gestenerkennung/Gesture-Recognition, Referat im Rahmen der Vorlesung Benutzerschnitstellen

[6] Funck, S., Fuchs, S. (2005) Entwicklung eines gestisch-intuitiven Mensch-Maschine-Interface auf basis der videogestütztest Erkennung von Handzeichen, Technischer Berricht, TUD-FI02-05, Technische Universität Dresden, ISSN 1430-211x,

[7] LaViola, J. (1999) A Survey of Hand Posture Recognition Techniques and Technology, Technical Report CS-99-11, Department of Computer Science, Brown University, Providence

[8] Nielsen, M., Störring, M., Moeslund, T., Nielsen, E.,G. (2003) A Procedure For Developing Intuitive and Ergonomic Gesture Interfaces for Man-Machine Interaction, Technical Report CVMT 03-01, ISSN 1601-3646, CVMT, Aalborg University

[10] Fifth Dimension Technologies (2004), 5DT Data Glove Ultra Series, User's Manual

[11] Lužanin, O., Plančak, M. (2008) Virtual Reality Technologies in Virtual manufacturing - Current Trends and Applications, Journal of Technology of Plasticity, Vol.33, Number 1-2, ISSN:0354-3870, p.103-111

[12] Kahlesz, F., Zachmann, G., Klein, R. (2004) Visual-fidelity dataglove calibration. Computer Graphics International (CGI), June 16-19, Crete, Greece, IEEE Computer Society Press Workshop on Human Motion (HUMO'00), p.121-126.

Authors: **Ognjan Lužanin, Miroslav Plančak,** University of Novi Sad, Faculty of Technical Sciences**,** Institute of Production Engineering, V. Perica Valtera 2, Novi Sad, Serbia, **Branimir Barišić,** University of Rijeka, Technical Faculty, Vukovarska cesta, Rijeka Croatia,
E-mail:luzanin@ns.ac.rs plancak@ns.ac.rs
barisic@riteh.hr

This paper is the result of the work on the following CEEPUS project: Concurent product and technology development- teaching, research and implementation of Joint programs oriented in production and Industrial Engineering, Ceepus CII-HR-0108-03-0809-M.

Journal of Production Engineering
Vol.12 No.1

Milosevic, M., Todic, V., Lukic, D.

MODEL DEVELOPMENT OF COLLABORATIVE SYSTEM FOR PROCESS PLANNING

Abstract: *With competition in global markets, more and more enterprises seek to make up virtual enterprise or cooperate with each other in the manufacturing process in order to reduce cost of product and increase competitive abihty. For this reason, some of the key technologies are developing in the field of collaborative work between enterprise, besides collaborative design, the collaborative process planning also very important among them. With process planning collaborative platform engineers whom belong to the different enterprise may be work more efficiently than before, and the manufacturing resource of virtual enterprise will be utilized more optimized. In this paper the model of system for process planning in collaborative environment are shown.*
Key words: *Collaborative systems, PLM, Process planning, CAPP*

1. INTRODUCTION

Manufacturers are facing increasing challenges of better product quality with tighter delivery requirements for customers. Global competition is increasing with pressure on prices, smaller orders, shorter life cycles, more suppliers and increasing material and energy costs. These new business drivers make manufacturers follow more competitive manufacture model, such as collaborative manufacturing, to closely collaborate with their customers, suppliers, manufacturers and partners for the most advanced competitiveness by leveraging core competencies throughout the entire product lifecycle.

PLM systems support the management of data for products, processes and services from initial concept, through design, engineering, launch, production and use to final disposal. They coordinate and collaborate products, project and process information throughout the entire product value chain among various levels, internal and external to enterprise. They also support a product-centric and process-centric solution that unifies product lifecycle by enabling online sharing of product and process knowledge and applications [1].

In the age of heterogeneous markets, rapid expansion of technologies and excessive reductions in product life cycle, collaborative engineering has been recognized as a strategy for the total life cycle. This collaborative engineering is getting more and more important as manufacturing activities require more expertise and more involvement from a lot of people on networks, including design engineers, production managers, process planners, production engineers, delivery managers, customers and expert advisors.

2. COLLABORATIVE ENGINEERING

The traditional approach to product development and production is *Sequential Engineering , SE*. In this method, works are divided into many sub-tasks, and the optimization is defined by these task sequences (Fig. 1).

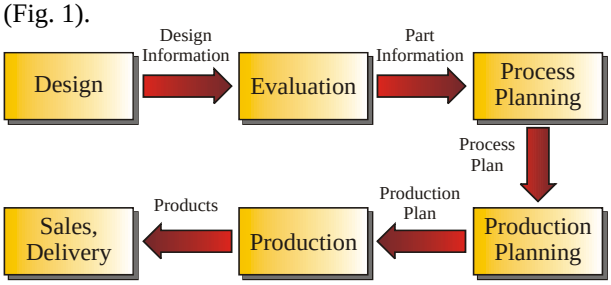

Fig. 1. Product development and production activities in Sequential Engineering approach

The opposite method is *Concurrent Engineering, CE*. It is a systematic approach to the integrated and concurrent design of products and their related processes. In the concurrent engineering approach, a complex, dependent and diverse model is used, and optimization is determined by task dependency, organization behavior and uncertainty.

One of the key words in current researches in concurrent engineering is *Co-operation*. This co-operation means *Collaboration* and it is becoming more and more important. Consequently, *Collaborative Engineering* means co-operating, sharing information and knowledge of global and multi-company engineering (Fig. 2) [2].

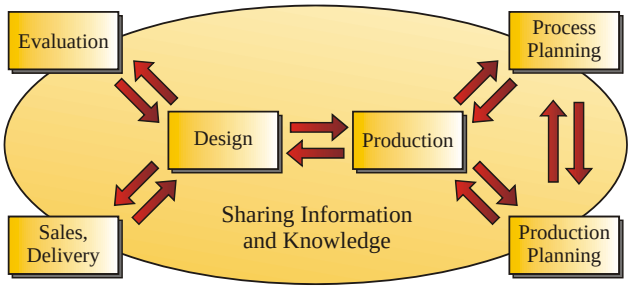

Fig. 2. Product development and production activities in Collaborative Engineering approach

According to the functions and roles of users participating in a collaborative design activity, a collaboration product development system can be organised in either a 'horizontal' or a 'vertical' mode.

The *horizontal collaboration* puts the emphasis on gathering a design team from the same or different disciplines to carry out a task systematically.

The *vertical collaboration* can establish an effective communication channel between the upstream design and the downstream manufacturing simulation and optimisation tools, and it can enrich the principles and methodologies of concurrent engineering to link diversified engineering tools dynamically. Due to these different levels of collaboration and interaction between users, the collaboration can be generally categorised into three types (Fig. 3):

- Visualisation-based collaboration,
- Co-design collaboration and
- CE-based collaboration.

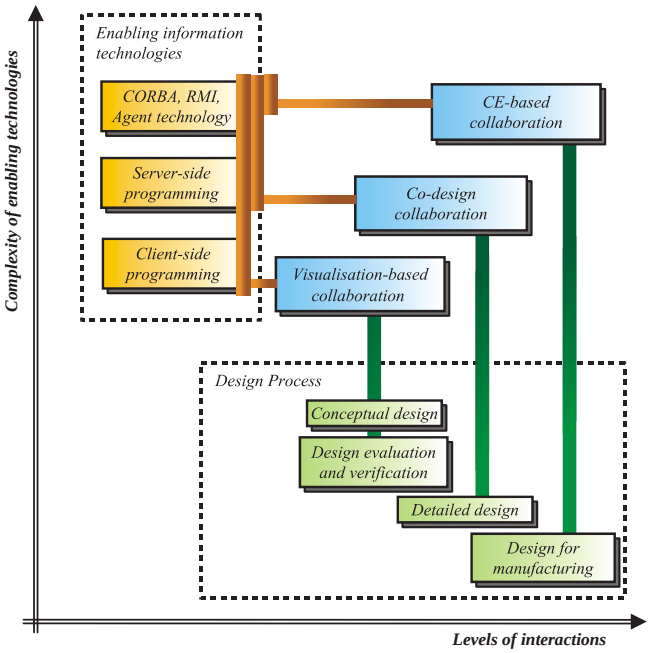

Fig. 3. Different design processes with different collaborations [3]

2.1 Visualisation-based collaboration

Visualisation-based collaboration has the advantage of facilitating collaborative and distributed product or process preview/review. In such an environment, a multi-disciplinary team involving a manager, designer, process planner, customer, etc., can be formed to look at or review the same visualised design model, which is often steered by a chief designer or chief planner. To alleviate the sluggish transfer of large-volume design models over the Internet, concise 3D formats for Web applications, such as virtual reality modelling language (VRML) or Extensible 3D standard (X3D), have been launched to simplify the models as triangular meshes for visualisation purposes. Under this collaboration, the communication can be maintained through either an asynchronous manner or a synchronous manner.

2.2 Co-design collaboration

Co-design collaboration targets a more interactive collaboration activity for a conceptual or detailed design with more complex requirements of co-ordination and organisation among users. Co-design can be conducted either asynchronously or synchronously. An asynchronously collaborative Technologies and methodologies for collaborative product development systems activity can be organised in a hierarchical assembly structure, through which a chief designer outlines the assembly configuration and the detailed component design tasks are assigned to individual designers to carry on separately. Managements, co-ordination and project review of tasks, which can be assisted by some advanced project management or PDM systems, are vital to the whole process. A synchronous collaborative activity is conducted in a way such that a group of designers are dedicated to the same task actively. Teamwork techniques, such as user commitment, roles and responsibilities, are crucial to guarantee this simultaneous co-design activity.

2.3 CE-based collaboration

CE-based collaboration extends the CE principle, which is based on the integration of design and the related manufacturing processes for a life-cycle consideration, to support distributed applications, and geographically dispersed users, systems and resources can be integrated in an Internet/Intranet environment beyond the traditional boundaries of physical and time zones. In a CE-based collaborative system, product design systems and some evaluation or simulation service tools diversified in terms of functionalities, communication protocols, programming languages and data structure representations are integrated as a multi-disciplinary environment for optimising design. In such a system, application services in product design, process planning, engineering analysis and simulation, can be conveniently embedded as *Application Service Providers* (ASPs) for remote invoking and manipulation.

2.4 Product lifecycle collaboration

As such, a new technology solution, called, ''product lifecycle collaboration'', is required. Functions of to enable product lifecycle collaboration include, but not limited to (Fig. 4) [1]:

- Product portfolio management,
- Collaborative product customization,
- Collaborative product development,
- Collaborative product manufacturing,
- Collaborative component supply and
- Extended product service.

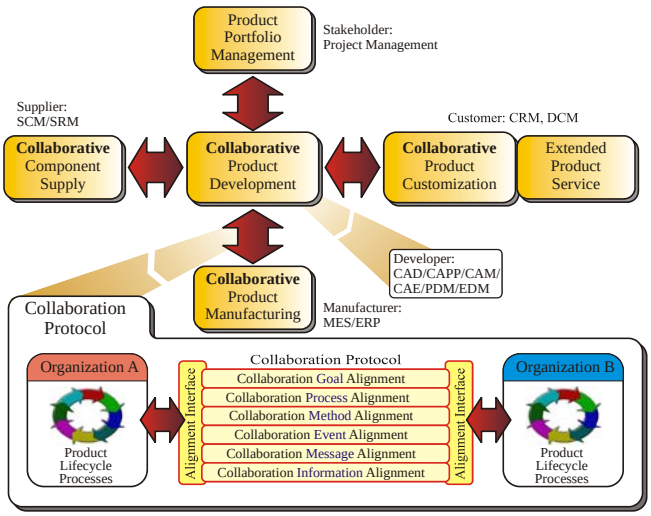

Fig. 4. Product lifecycle collaboration

In particular, the collaboration protocol, which provides different companies with general regulation to facilitate real time collaboration throughout the entire lifecycle, is imperatively required. This collaboration protocol includes different layers of collaboration alignment, such as goal, process, method, event, message and information.

3. FRAMEWORK OF COLLABORATIVE PROCESS PLANNING SYSTEM

An integrated manufacturing process planning framework includes process planning activities and integration with other application systems (Fig. 5).

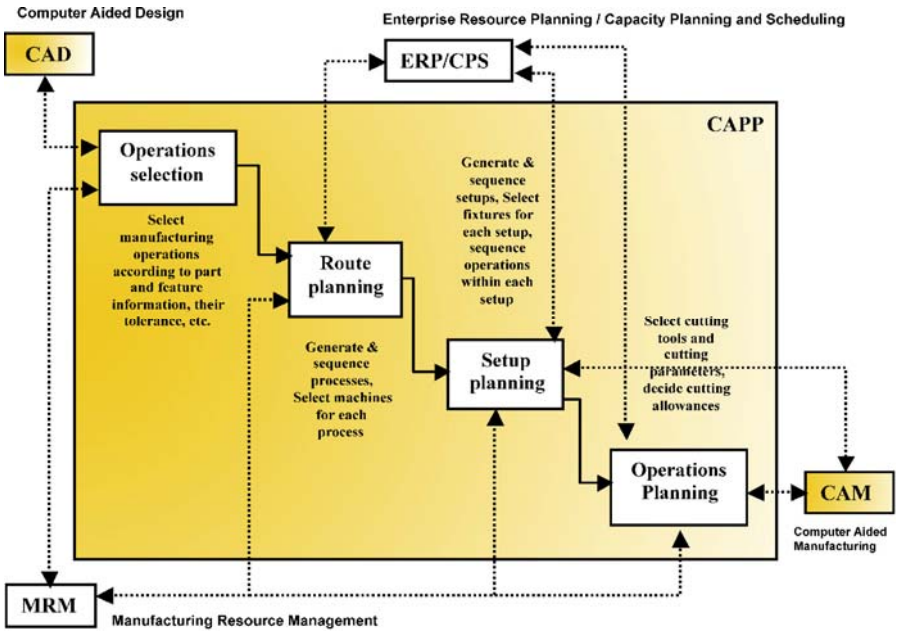

Fig. 5. Framework of an integrated CAPP system [1]

Operations selection function selects manufacturing operations according to part and feature information, material, tolerance, etc. Routing planning function generates and sequences processes, selects machines for each process. Setup planning generates and sequences setups, selects fixtures for each setup, sequences operations within each setup. Operations planning function selects cutting tools and cutting parameters, etc. Manufacturing resource management module provides the necessary capabilities to define the required resources and the capabilities to enable the implementation of the operations selection, route planning, setup planning and operations planning functions. Operations selection function normally integrates with the CAD system to retrieve the defined manufacturing features and select the corresponding manufacturing operations. Route planning, setup planning, and operations planning functions usually interact with the ERP/CPS systems by providing the necessary manufacturing process routings, setups, and operations for project, production and shop-floor scheduling. Setup planning and operation planning functions communicate with the CAM system by providing setups, and operation information, which includes cutting tools and cutting parameters to generate the NC codes.

The conceptual framework of process planning collaborative system are shown in the Fig. 6. On the server side, a collaborative server program is running for the entire request from the client side. It composed of process planning module, collaborative simulation module and collaborative discussion and optimization module.

At the beginning, the process plan for the part is created within the CAPP system that uses an internal Knowledge Base and Manufacturing resource Database. After that, the process planner engineers are operating on the client side to do process planning work, they can collaborative discuss the process plan of the part, and finally select suited equipment, machine tools, cutting tools, fixtures, cutting parameters from the manufacturing resource database.

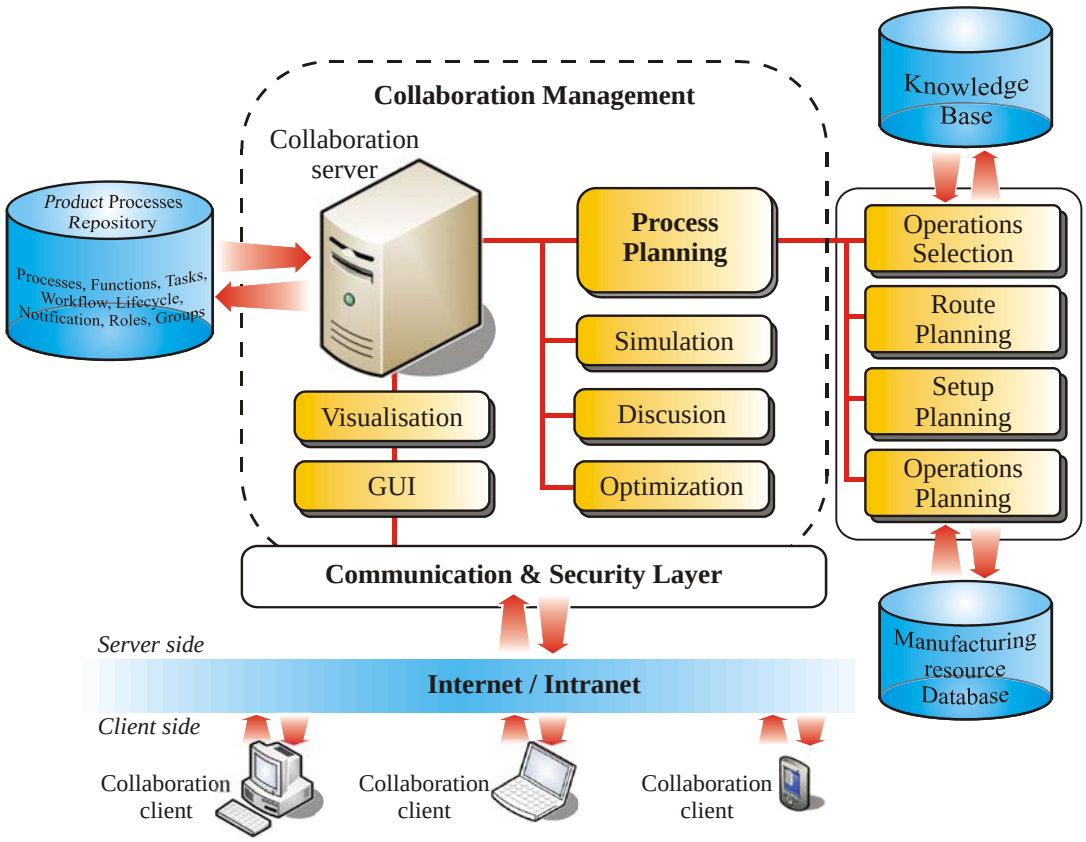

Fig. 6. Conceptual view of Collaborative process planning system

On this way, process engineers collaboratively make optimized manufacturing process of the part. When the proccess plan is finished and optimized then it is stored on the Product Process Repository in order to future use.

4. CONCLUSION

To satisfy new collaborative business requirements in modern e-manufacturing era, particularly, the increasing needs in collaborative product lifecycle management, a model of collaborative process planning system has been proposed. This model provides a platform for engineers to view, evaluate and optimize a process plan through dynamically invoking remote collaboration system.

With this system the young engineer will be advantaged from the system and other professional engineer, on the other hand, the partners of the enterprise will be benefited from the view and sharing manufacturing resource.

5. REFERENCES

[1] Ming, X.G., Yan, J.Q., X.H. Wang, et.al.: Collaborative process planning and manufacturing in product lifecycle management, Computers in Industry No.59, pp.154-166, Elsevier, 2008.

[2] Sangado, N.: Networked Virtual Manufacturing System for Collaborative Engineering, A Dissertation Submitted to the Department of Mechanical Design and Production Engineering of Seoul National University, 1999.

[3] Li, W.D., Ong, S.K., Nee, A.Y.C., Integrated and Collaborative Product development Environment: Technologies and Implementations, World Scientific Publishing Co.Pte.Ltd, 2006.

[4] Zhou, Z., Li, M., Shen, L.: Manufacturing Resource Management For Collaborative Process Planning, Intemational Federation for Information Processing (IFIP), Vol. 207, Knowledge Enterprise: Intelligent Strategies In Product Design, Manufacturing, and Management, Boston: Springer, pp. 926-931., 2006.

[5] Todic, V., Lukic, D., Stevic, M., Milosevic, M.: Integrated CAPP System for Plastic Injection Mold Manufacturing, The Journal Revista de Materiale Plastice, Vol. 45, No. 4, pp. 381-389, Romania, 2008.

Authors: **Prof. dr Velimir Todic, M.Sc. Mijodrag Milosevic, M.Sc. Dejan Lukic**, University of Novi Sad, Faculty of Technical Sciences, Department for Production Engineering, Trg Dositeja Obradovica 6, 21000 Novi Sad, Serbia,
Phone.: +381 21 485-2346, Fax: +381 21 454-495.
E-mail: todvel@uns.ac.rs
mido@uns.ac.rs
lukicd@uns.ac.rs

Note: This paper present a part of researching at the project *"Development of the Typical Process Plans for Rolling Bearings Manufacturing"* Project number TR 14053, financed by Ministry of Science and Technological Development of Serbia.

Journal of Production Engineering
Vol.12 No.1

Reibenschuh, M., Cus, F.

STRESS ANALYSIS OF A BRAKE DISC CONSIDERING CENTRIFUGAL LOAD

Abstract: *Disc brakes appear in all transportation systems. They are also used in railway transport. Because of the influence of different loads on a brake disc, an analysis is carried out with a finite elements method (FEM). The goal is to find out the influence of the centrifugal force on a brake disc. The analysis is carried out for a brand new disc and a worn out disc because of its operation. After the analysis the results are interpreted and suggestions for improvements are made.*
Key words: *railway transport, brake disc, centrifugal load, FEM.*

1. INTRODUCTION

Brake discs are exposed to a variety of loads during their use. While driving without braking the disc is affected only with the centrifugal force. When the brake cycle starts, two additional forces affect the disc. These forces represent the force from the brake calliper and the force from the heat impute (as a result of friction). In this analysis only the influence of the centrifugal force is being determined.

The first goal of this research is to find out the maximum stress in the disc and the second goal is to find out the maximum extension of the disc, caused by the high centrifugal force. During the analysis two models of the brake disc are considered:

- a brand new disc,
- a worn out disc because of its daily operation (this disc has a permitted wearing of 7 mm on both sides).

Fig. 1. The brake mounted on the hub

2. NUMERICAL ANALYSIS OF A BRAKE DISC

In the beginning of the analysis the brake disc is simplified. Only one section of the whole disc is used. Considering the systems boundary conditions and the symmetry of the disc, only 1/12 of the disc is chosen. The analysis is carried out with help of FEM in the program Abaqus 6.7.1, which gives the results in numerical and picture form. With this program it is also possible to determine the spot where the stresses and extensions reach their maximum.

The material of the disc brake is spherical graphite, defined according to SIST EN 1563:1988 and with the characteristics according to EN-GJS-500-7 (EN-JS 1050) with surface roughness of Ra = 3.2 mm. Disc brakes were machined on CNC machine tool with cutting conditions which were previously optimized by an intelligent optimization software [5]. Surface roughness and cutting forces acting on the disc during machining were kept constant by continuous adaptation of cutting parameters [6] to current machining conditions.

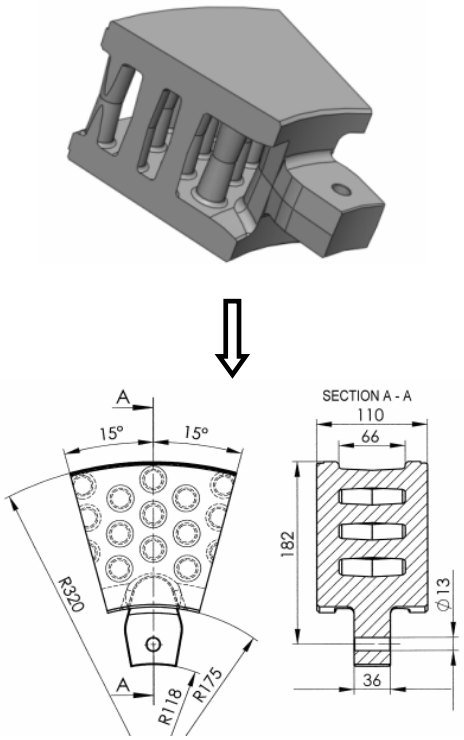

Fig. 2. The chosen section of the brake disc

2.1 The analysis

In this analysis the stresses, that are a direct result of the centrifugal load, are determined. This load comes

as a result from high travelling speeds of the train. Beside that the weight distribution of the vehicle is also considered. The vehicle has one front and one back bogie. Each bogie consists of two axles with 3 brake discs. The weight arrangement is 50:50 – all discs are treated equal. In our case only 8.33 % of the whole brake force is applied to one disc of the carriage. All the data, used in the calculation and needed to run the analysis, are shown in Table 1.

Number of axles	4
Number of discs per axle	3
Diameter of the wheel d_{wheel}	0,92 m
Effective radius of the wheel r_{disc}	0,247 m
Deceleration at braking	1,4 m/s^2
Maximum velocity	250 km/h=69 m/s
Density of the material	7100 kg/m^3
Elastic module	169000 N/mm^2
Poisson number	0,275
Heat conductivity	35,2 W/m^{2}K
Specifically heat of the material	515 J/ kgK
$R_{p0,2}$	320 MPa
R_m	500 MPa
Minimal extension	7%
Total mass of the vehicle	70000 kg
Time to standstill	50 s
Initial temperature of the disc	150°C
Temperature of the environment	50°C

Table 1. The data used for calculation

The consequences of centrifugal loads (caused by the high travelling speed of the vehicle) applied to the disc were determined and calculated in the analysis. The results were stresses. To begin the calculation, the angular velocity was needed:

$$\omega = \frac{v}{r} = 151\left[s^{-1}\right] \qquad (1)$$

where the v [km/h] represents the maximum velocity of the vehicle and r [m] the radius of the wheel. It is also necessary to determine the holding force of the brake clamps on the disc. The surface pressure between the disc brake and the brake pads was determined on the basis of the calculated braking force and because the brakes work on the brake disc by means of pneumatic system, the pressure was:

$$p = \frac{F_{disc}}{A_c \cdot \mu}\left[MPa\right] \qquad (2)$$

The surface pressure was 1.14 MPa. This boundary condition was also considered in the calculation although because of its low value, it could be disregarded.

The braking force on the disc is equal:

$$F_{disc} = \frac{0.0833 \cdot \frac{1}{2} \cdot M \cdot v_0^2}{2 \cdot \frac{r_{disc}}{r_{wheel}} \cdot \left(v_0 \cdot t_s - \frac{1}{2} \cdot a \cdot t_s^2 \right)}\left[N\right] \qquad (3)$$

The force permitted on one side of the disc is 17500 N; the calculated value is lower. This means that the calculated force does not exceed the maximum value. Other parameters and material properties are from international standards for materials and from the internal standards defined by the maker of the disc. The section of the disc and its geometry is transferred from the program SolidWorks 2008 to the program Abaqus 6.7.1. Immediately after the transfer the geometry is scaled. Because of that, the results are in N/mm2. After that, the models boundary conditions are determined and the material properties are put into the program.

Additional boundary conditions were determined on the surfaces where the brake disc was cut up. The symmetrical boundary condition on the edge of the selected section was modelled with slide supports in radial direction. After that, the main load is determined. The main load is the centrifugal load caused by the maximum travel velocity of the vehicle.

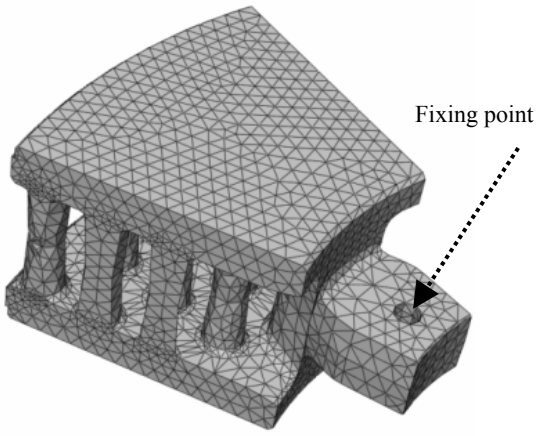

Fig. 3. Meshed section of the disc

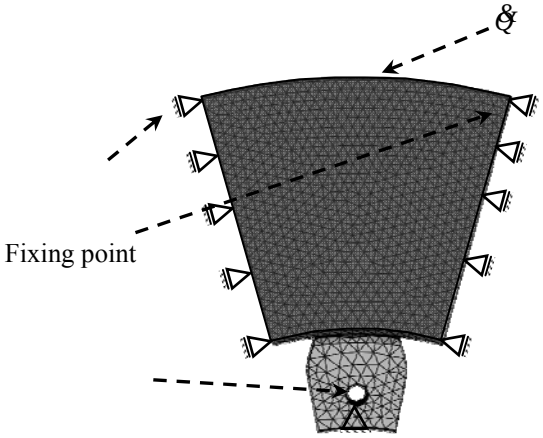

Fig. 4. Load, fixing and mesh of the selected section

In the next step the model is meshed. Because of the complex geometry of the model it is not possible to use hexagonal mesh element. Instead tetrahedral mesh elements were used. The creation of a mesh volume was conducted automatically by the software package Abaqus CAE 6.7.1. The mesh consists of 86713 tetrahedral elements (element code C3D4AT – allows linear thermo – deformational analysis). The average

size of the elements is 6mm and the number of nodes is 18135. Figure 3 shows the meshed model.

3. THE RESULTS

3.1. The calculation of centrifugal load for the new disk 195H6

In the first phase of the analysis, the new disc was analysed. This disc is without wear. The figure 4a and 4b show the calculated results. On behave of the analysis a comparison of stresses on von Mises and maximum extension was made.

The analysis was carried out at the maximum velocity of the vehicle - 250 km/h. The maximum value for stress is in the hole where the disc is attached to the hub, which is later on press fitted onto the axle, and on the passage from the fixing point to the disc rim, on the figure 5a marked with the line. The maximum value for stress amounted to 77.06 MPa.

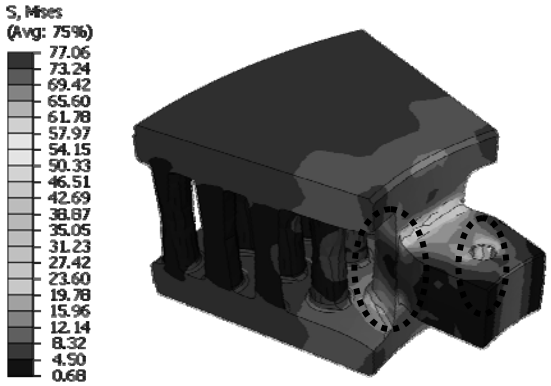

a)

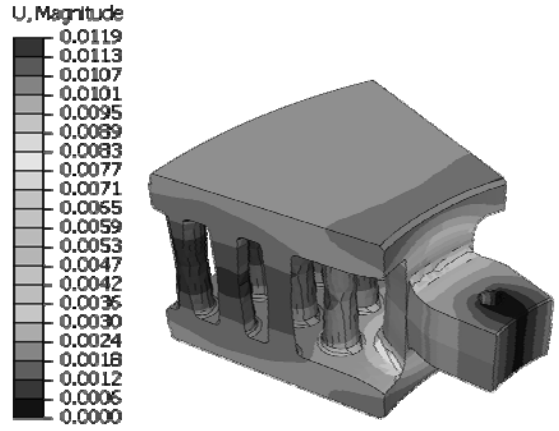

b)

Fig. 5. Stress on von Mises and extension

The figure 5b shows the movement respectively the extension because of the influence of the centrifugal load. From the figure 5b we can see that the maximum extension lies in the boundary of 0.012 mm.

3.2 The calculation of centrifugal load for the worn out disk 195H6

The figure 6a shows values for the amounted stress for the chosen section of the disc. The maximum value for stress is in the hole, where the disc is attached to the axle and on the passage, on the figure 6a marked with the line. The maximum value for stress amounted to 75.58 MPa.

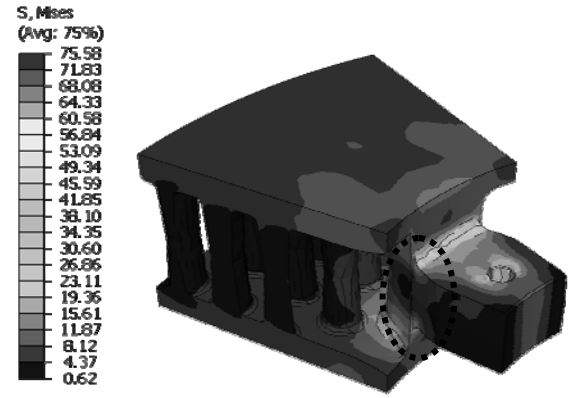

a)

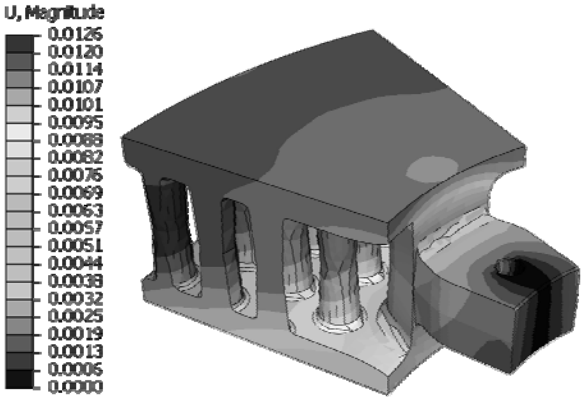

b)

Fig. 6. Stress on von Mises and extension

Figure 6b shows the maximum extension of the disc–the value amounted to 0.0126 mm.

4. DISCUSION OF THE RESULTS

Table 2 shows the results, which are a consequence of the influence of the centrifugal load on the material of the brake disc. This analysis is made for the worst case scenario. In our case, this occurs at the maximum velocity of 250 km/h. The stresses are high but in comparison with the allowed stress for this material, which includes a safety factor of 1.5, the brake disc is adequately dimensioned. The difference in stress between the brand new disc and the worn out disc is a consequence of the material properties. All materials have the tendency to elongate or shrink under certain circumstances. In this case the more material we have, the harder it is to deform it. Consequently the less material we have, the easier the high centrifugal forces can deform it. The material deforms and the stresses are lower. Although too little of the material on one spot can cause a catastrophic failure of the brake disc. That is why the brake discs should regularly undergo an inspection.

Brake disc	σ_{max} [MPa]	extension [mm]
Brand new	77.06	0.012
Warn	75.58	0.0126

Table 2. The results

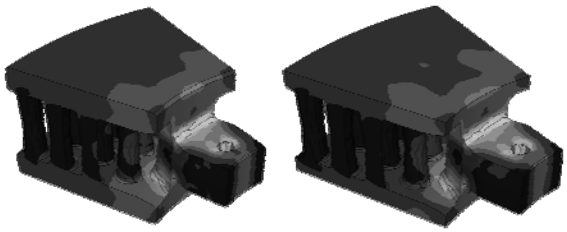

Fig. 7. Direct comparison of stress fields, left the new disc and right the worn out

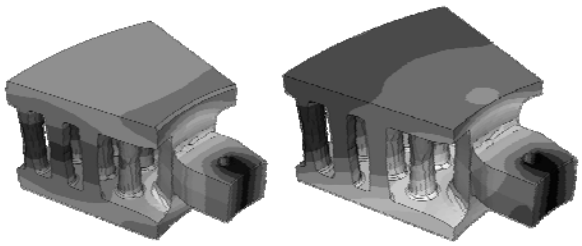

Fig. 8. Direct comparison of extension, left the new disc and right the worn out

On figure 7 and 8 we can directly see how the stress fields are distibuted in both sections and also how the extenson is affecting the disc.

5. CONCLUSION

The results of the analysis show what a centrifugal load can do to a solid object, in our case a brake disc. In conclusion the brake disc needs to be primarily analyzed for centrifugal load. Also a whole array of other forces is affecting the brake disc. For further analyses we would recommend to add additional boundary conditions to the centrifugal force and run through more test. Also a field test would be recommended to compare the results. An analysis could also be run through, to determine the affect of milling process on the structural integrity of the disc.

To lower the stress and extension we recommend two constructional improvements:

- choosing another material with better mechanical properties,
- changing the passages respectively the radiuses where the stresses are the highest.

6. REFERENCES

[1] Mackin, T. J.: *Thermal cracking in disc brakes*. *Engineering Failure Analysis* (2002), no. 9

[2] Ren, Z.; Ulbin M.: *FEM practical course for Abaqus:* Faculty of mechanical engineering Maribor, 2002. Acquired 13.04.2009 at http://lace.uni-mb.si/Num _meth _konst / *ABAQUS 6.7.1*

[3] Reibenschuh, M.: *Napetostna analiza zavornega diska s sredobezno in termicno obremenitvijo*: diplomsko delo. Maribor: Fakulteta za strojnistvo, 2008

[4] Oder, G.: *Dolocitev nestacionarnih termicnih in napetostnih polj zavornih diskov*: diplomsko delo. Maribor: Fakulteta za strojnistvo, 2008

[5] Zuperl, U.; Cus, F.: (2008) *Machining process optimization by colony based cooperative search technique*. Strojniski vestnik - Journal of Mechanical Engeneering, vol. 54, no. 11, p. 751-758.

[6] Cus, F.; Zuperl, U.; Kiker, E.: (2007) *A model - based system for the dynamic adjustment of cutting parameters during a milling process*, Strojniski vestnik - Journal of Mechanical Engeneering, vol. 53, no. 9, p. 524-540.

[7] Potrc, I.; Lerher, T.; Sraml, M.; Samec, B.; Oder, G.: *Expert advice on the levels of tensions in A, B, C, D and M versions of brake discs*, Maribor 2008.

[8] Reibenschuh, M.; Oder, G.; Cus, F.; Potrc, I.: *Modelling and Analysis of Thermal and Stress Loads in Train Disc Brakes – Braking from 250 km/h to Standstill*. Strojniski vestnik - Journal of Mechanical Engeneering, vol. 55, no. 7-8, p. 494-502.

[9] Weitz&Luxenberg P.C.: *Recent Train Accidents*. Acquired 14.05.2009, at http:// www.weitzlux.com/ trainaccident_4533.html

[10] Yevtushenko, A.A.; Kuciej, M.: *Frictional heating during braking in a three - element tribosystem*, International Journal of Heat and Mass Transfer, vol. 52, no. 13-14, p. 2942-2948, *2009.*

[11] *ECONOMIC expert, List of rail accidents. Acquired 14.05.2009 at http://www.economi cexpert.com/2a/ List:of:railway: disasters.htm*

[12] Panier, S.; Dufrénoy P.; Weichert D.: *An experimental investigation of hot spots in railway disc brakes,* Wear, vol. 256, no. 7-8, p. 764-773, 2004.

[13] Zhen-cai Z.; Yu-xing P.; Zhi-yuan S.; Guo-an C.: (2009) *Three-dimensional transient temperature field of brake shoe during hoist's emergency braking*, Applied Thermal Engineering, vol. 29, no. 5-6, p. 932-937.

[14] Bagnoli, F.; Dolce, F.; Bernabei, M.: (2009) *Thermal fatigue cracks of fire fighting vehicles gray iron brake discs*, Engineering Failure Analysis, vol. 16, Iss. 1, p. 152-163.

Authors: **Prof. Dr. Franci Cus, Marko Reibenschuh, uni. dipl. ing.,** University of Maribor, Faculty for Mechanical Engineering, Smetanova 17, 2000 Maribor, Slovenija, Phone.: +386 220 7606,
E-mail: franci.cus@uni-mb.si,
marko.reibenschuh@uni-mb.si

Journal of Production Engineering
Vol.12 No.1

Geric, K., Sovilj, B.

PROPERTIES OF SPRAY FORMED TOOL STEELS

Abstract: *The spray forming for microstructural refining can be very beneficial for the production of tool steels. Spray forming process shortens the production time. Properties of spray forming steels are between conventional and powder metallurgy steels. The spray formed high speed steel has a finer and more uniform microstructure than the conventionally cast steel. Spray formed tool steel shows smaller abrasion wear, better impact energy and static banding stress.*
Key words*: spray forming, tool steels, carbides*

1. INTRODUCTION

All industrial branches are faced with the necessity to reduce the cost of their production. One suitable method is to extend the performance of the tools. The chances to develop new tool steels by simply adjusting their chemical composition to the increased demands are restricted. The application of the innovative spray forming technology promises a high potential in the development of new tool steels as well as in the improvement of existing tool steels. During the past decades spray forming has been developed to a technology, which today is suitable to produce high alloyed tool steels on an industrial scale.

The most frequently used method to produce tool steels is conventional ingot casting or alternatively continuous casting of the melt followed by forging or rolling processes. Tool steels produced in that way cover a wide range of applications. If higher demands on properties such as ductility, homogeneity or cleanliness have to be fulfilled usually remelted tool steels are applied. The used metallurgical technologies are the electro-slag remelting (ESR) or the vacuum-arc-remelting (VAR) process. In all these technologies the range of producible steel compositions is limited. Segregations, which are unavoidable during the solidification, limit the steels hot formability and thus the industrial applicability of such steel. The development of powder metallurgy (PM) allowed to intensively widen up the limits of steel compositions. Due to the rapid solidification of the powder particles the development of segregations is suppressed to a high extend. Therefore the development of PM tool steels concentrated on high alloyed steel compositions with very high carbide contents.

Similar to the PM technology spray forming is based on the atomization of a melt, which allows using the benefits of a rapid solidification. The main difference to PM is that spray forming directly produces a solid billet whereas in PM the powders have to pass a complex and expensive process of classification, mixing, and compaction in order to achieve a solid block of steel. As a new technique spray forming is able to provide materials with well-balanced compositions allowing to meet customers demands with a spectrum of properties between conventional and PM tool steels.

Such a spray formed material is free of macro-segregations and cavities. It has a refined structure and achieves density values above 99% of its theoretical density. Spray forming is a production technology especially suitable for many highly alloyed tool steels such as high-speed tool steel or extremely wear resistant cold-work tool steels. Similar to powder metallurgy spray forming offers the chance to widen up the range of producible alloy compositions but as the comparison or different production routes in Fig. 1 shows, with definitely less steps in the process [1].

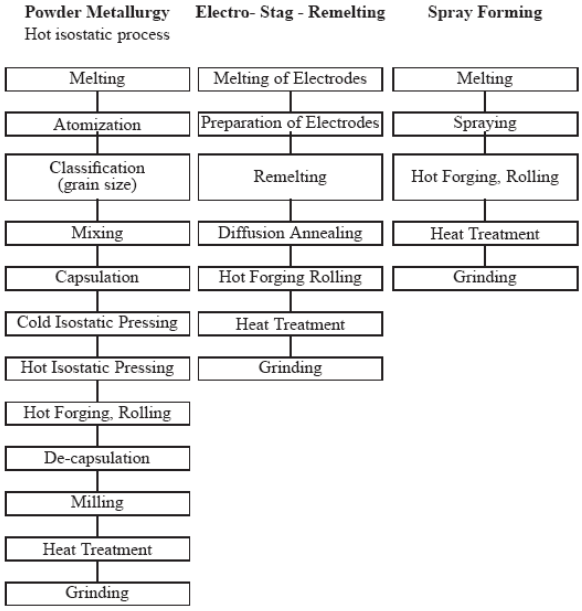

Fig. 1. Comparison of different processing routes.

2. SPRAY FORMING

Melting occurs in the induction furnace under an inert gas atmosphere (nitrogen) using classified scrap, pre-alloys and further additions. After the chemical composition and casting temperature have exactly been

balanced the melt is poured into the casting furnace. Via the furnace's bottom- tapping the melt is transferred into the atomizing unit with oscillating atomizing nozzles ("Twin Atomizer"). Here the gas stream atomizes the melt into droplets of approx. 5–500 µm. Nitrogen is used as atomising gas in the spray chamber.

The stream of droplets is accelerated from the two oscillating nozzles to a rotating target. The adjustable oscillation of the nozzles and the rotation of the target allow a uniform compaction of the atomized particles and thus homogeneous growth of a round billet. The presently most discussed model of deposition and solidification of the atomized melt droplets is described in Fig. 2. The globular droplets with diameters varying between 50 and 500 µm solidify at different rates.As small particles might solidify completely during the flight medium sized particles might be partly solidified and larger still completely liquid. A properly adjusted downward movement of the growing billet allows for a permanently constant distance between the atomizing unit and the billet during spray forming. The billet dimension is a maximum of 500 mm in diameter and 2,5 meter in length, with a weight of approximately 4 tons.

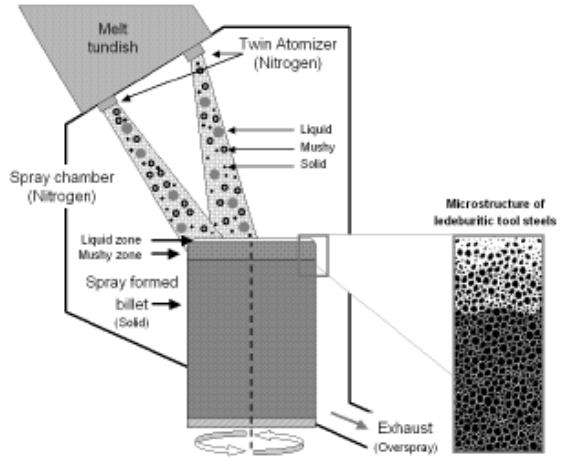

Fig. 2. Solidification process during spray forming [21]

The productivity of the spray forming technology is very high. A four tone spray formed billet can be produced in significantly less time than with the PM or ESR routes, see Fig. 3 [1].

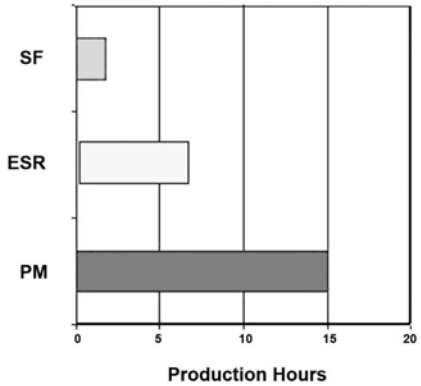

Fig. 3. Productivity compared between the different technologies.

3. MICROSTRUCTURE

The high cooling rates in combination with an extremely fast solidification of the atomized molten particles lead to the formation of a fine-grained microstructure with a homogeneous distribution of the alloying elements.

As an example the microstructure is compared between a high alloyed 8%Cr-1.5%Mo-10%V steel produced via PM and spray formed, Fig.4 , clearly illustrate the difference in the microstructure when traditionally cast steel, spray-formed steel and PM materials. The carbides in the traditionally cast steel are clustered in large strings and the sizes can be up to 100 µm in length. This can be a main reason for brittleness and this steel is often hardened to lower hardness in order not to lose too much ductility.

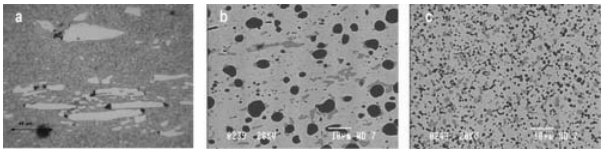

(a) (b) (c)

Fig. 4. High alloyed Cr-Mo-10%V steel traditionally cast steel (a), spray-formed steel (b) and powder metallurgy (PM) steel (c) [1].

Figure 5 shows the typical solidified structure of the ledeburitic coldwork tool steel X155CrVMo12-1 (Mat.-No. 1.2379, AISI D2). It reveals a fine and homogeneous globulitic structure with an extremely fine ledeburitic carbide network with a mesh size of approx. 5 – 40 µm.

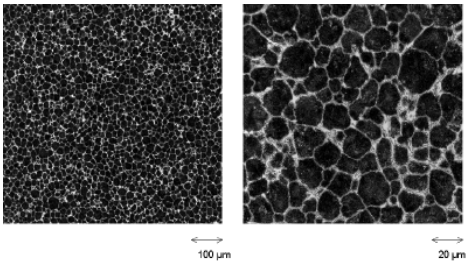

Fig. 5. Microstructure of a ledeburitic cold-work tool steel in the as sprayed condition [2]

The as-cast microstructures of conventionally cast and SF M3:2 steel are compared in Fig. 6. The SF steel microstructure is considerably finer than that of conventionally cast steel due to increased capacity of heat extraction during SF solidification.

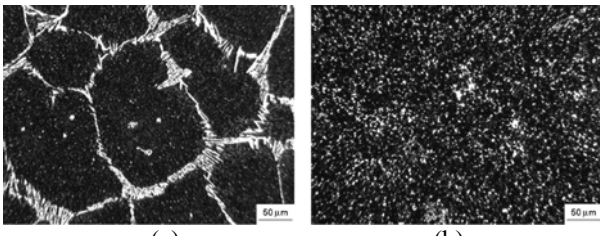

(a) (b)

Fig. 6. As-cast microstructure of (a) conventional and (b) spray formed high speed steels [3].

All microstructures are light microscopy etched with nital 4%.

4. WEAR RESISTANCE

The wear resistance of a tool steel is closely related to the carbide type, carbide amount, size, and distribution of the carbides embedded in the steels matrix. An increasing amount of carbides improves the wear resistance of a steel, an increasing size of the carbides reduces it. The influence of the carbide size also explains the different behavior of conventional and PM tool steels. The very fine distribution of fine carbides lowers the wear resistance of the PM tool steels

The carbides which appear in high alloyed tool steels are M_6C and MC carbide, and the morphology differs for conventional and sprey formed high speed steel.

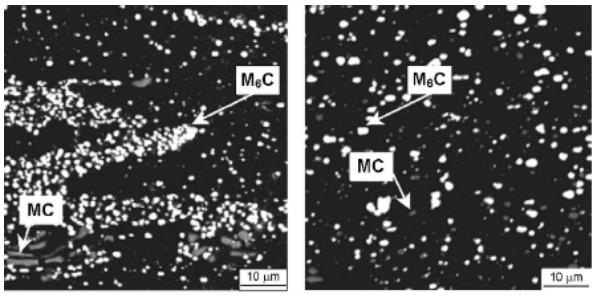

Fig. 7. Scanning electron microscopy images of carbides in (a) conventional and (b) spray formed M3:2 high speed steel. Back scattered images of samples [3]

High alloyed 8%Cr-1.5%Mo-10%V steel produced conventionally, via PM and spray formed results in a fine and homogeneous distribution of small, hard and wear resistant vanadium rich carbides (MC with hardness 2800HV). Abrasion wear was done with pin-on-disc test with SiO_2 paper. Results are shown in Fig. 8, where a comparison of various steels manufactured via different processes is visualized. The larger MC carbide in the spray formed version results in very good abrasive wear resistance [1].

Very uniform distribution of fine carbides offers almost no resistance against abrasive wear. Larger carbides in a networks tructure do not improve the wear resistance as the network does not protect the matrix against wear. Best wear resistance can be achieved if the carbides have reached a certain size and are evenly distributed in the steel.

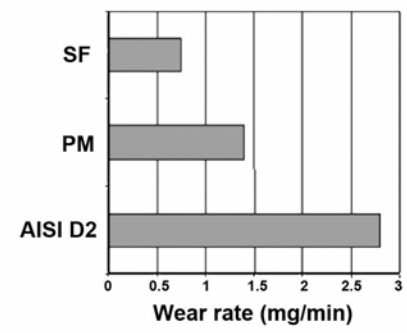

Fig 8. Weight rate for some cold work tool steels[1].

5. MECHANICAL PROPERTIES

Impact energy with unnotched specimens for some cold work tool steels, was shown in Fig. 9. The steels are manufactured by different metallurgical processes and heat treated to 60–61 HRC. Results of the PM and spray forming method, a much higher safety against chipping/cracking of the tool part is achieved compared to conventional manufactured high alloyed steels

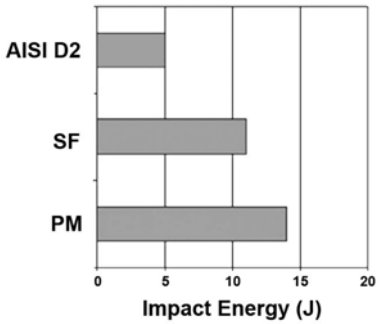

Fig. 9. Impact energy for some cold work tool steels[1]

Carbides and precipitates are small and evenly distributed within spray formed alloys, but an increased nitrogen concentration in the standard alloys must be considered during heat treatment and negatively affects the toughness [4].

The differences in carbide size and distribution are most evident and most likely to influence the mechanical properties of the steels. Bend strength was testing on specimens with section of 5 mm x 7 mm, from mid-from of longitudinal and transverse direction of 116mm squared bar, heat treated to hardness between 63.8 and 64.3 HRC.

The results shown in Fig.10 are directly related to microstructure and carbide distribution. In conventional M3:2,the reduced isotropy is related to the coarse carbide network. In longitudinal stressing, cracks propagate throughout the material crossing the carbide cells. Carbide size may have a larger influence on longitudinal toughness rather than carbide distribution. The similar carbide size in SF and conventional M3:2 may thus explain the similar longitudinal values.

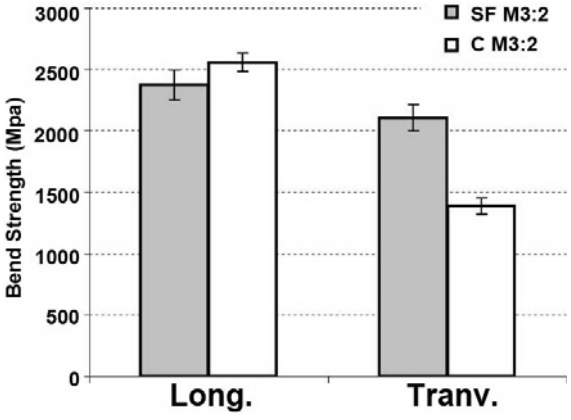

Fig. 10. Bend strength results, longitudinal and transverse direction Error bars represent standard deviation of results[3].

For transverse stressing, however, fracture occurs when cracks propagate parallel to carbide cells or stringers. In this situation, the coarse carbide networks of conventional material are preferential locations for crack propagation, thus decreasing toughness. In SF M3:2, carbide arranges are uniformly distributed and therefore longitudinal and transverse direction bend strength is similar. The SF M3:2 microstructure offers important benefits over conventional steels, considering real tooling conditions.

During complex states of stresses, better isotropy of SF high speed steel may lead to improvements in tool performance.

Coarse carbide distributions also have consequences during heat treatment. Such regions have different thermal expansion and, as a consequence, may cause distortion. The uniformly distributed carbide micro structures of SF high speed steel may also reduces heat treating distortions.

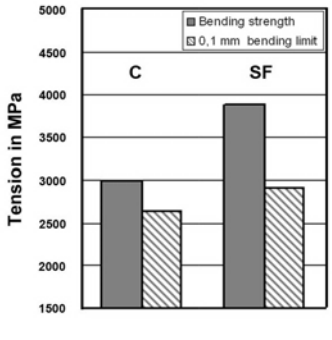

(a)

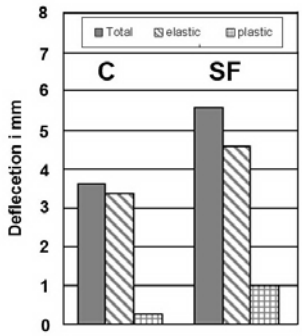

(b)

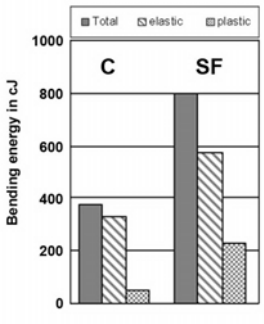

(c)

Fig 11. Ductility of cold-work tool steel 1.2379, measured in static bending tests – spray formed vs. conventional production (hardness: 58 HRC) [2].

The fine and homogeneous microstructure of a spray formed cold-work tool steel is of advantage for many properties. Fig. 11 clearly points out that the spray formed cold-work tool steel reveals a better ductility even if it was less deformed. This improvement is related to both the elastic as well as plastic deformation of the steel.

6. CONCLUSION

Spray forming has been developed to a new and interesting technology for the production of high grade and high alloyed tool steels, with highest productivity

Fast solidification of the atomized molten particles lead to the formation of a fine-grained microstructure with a homogeneous distribution of the alloying elements.

Related to carbide distribution, the spray formed high speed steel has a finer and more uniform micro structure than the conventionally cast steel. In small diameter bars, SF material has no carbide stringers.

High speed steel produced through spray forming has higher transverse direction properties, that lead to higher isotropy in mechanical properties.

During complex states of stresses, better isotropy of SF high speed steel may lead to improvements in tool performance.

Spray formed tool steel reveals a better abrasive wear, impact energy, and static banding stress

Compared to conventionally cast materials the improved mechanical, technological and processing properties of spray formed materials open chances to many new alloying and application concepts.

7. REFERENCES

[1] Spiegelhauer, C.: Industrial production of tool steels using the spray forming technology, 6th Int.Tooling Conference, pp 1101-1109, Karlstad, Sweden,2002

[2] Schruff I., Schüler V., Spiegelhauer C.: Advanced tool steels produced via spray forming , 6th Int.Tooling Conference, pp 1159-1174, Karlstad, Sweden, 2002.

[3] Mesquita R.A, Barbosa C.A. : Spray forming high speed steel—properties and processing, Materials Science and Engineering A 383 (2004) 87–95

[4] Schulz A.: Nitrogen pick-up during spray forming of high-alloyed steels and its influence on microstructure and properties of the final products, Materials Science and Engineering A 383 (2004) 58–68

Authors: **Prof. Dr Katarina Geric, prof.Dr Bogdan Sovilj** University of Novi Sad, Faculty of Technical Sciences, Department for Production Engineering, Trg Dositeja Obradovica 6, 21000 Novi Sad, Serbia, Phone.: +381 21 4852320, Fax: +381 21 454-495.
E-mail: gerick@uns.ns.rs
soviljb@uns.ns.rs

INSTRUCTIONS FOR CONTRIBUTORS

No. of pages:	4 DIN A4 pages
Margins:	left: 2,5 cm
	right: 2 cm
	top: 2 cm
	bottom: 2 cm
Font:	Times New Roman
Title:	Bold 12, capitals
Abstract:	Italic 10
Headings:	Bold 10, capitals
Subheadings:	Bold 10, small letters
Text:	Regular 10
Columns:	Equal column width with 0,7 cm spacing
Spacing:	Single line spacing
Formulae:	Centered and numerated from 1 in ascending order. Equations must be typed in Equation Editor, with following settings: Style>Math – Times New Roman Size>Full 12pt, Subscript/Superscript 7pt, Symbol 18 pt
Figures:	High quality, numerated from 1 in ascending order (e.g.: Fig.1, Fig. 2 etc.); Figures and tables can spread over both two columns, please avoid photographs and colour prints
Tables:	Numerated from 1 in ascending order (e.g..: Tab. 1, Tab. 2, etc.)
References:	Numerated from [1] in ascending order; cited papers should be marked by the number from the reference list (e.g. [1], [2, 3] ...)
Submission:	**Papers prepared in MS Word format should be e-mailed to: mma2009@uns.ac.rs, savkovic@uns.ac.rs, pkovac@uns.ac.rs**
Notice:	**Papers are to be printed in Journal of Production Engineering** Sample paper with detailed instructions can be found at: **www.ftn.uns.ac.rs/mma2009**

FOR MORE INFORMATION, PLEASE CONTACT:

Prof. Pavel Kovač, PhD, MEng.
Borislav Savković, *MSc. Assistant*
FACULTY OF TECHNICAL SCIENCES
Department for Production Engineering
Trg Dositeja Obradovica 6
21000 Novi Sad
Serbia
Tel.: (+381 21) 485 23 24; 485 23 20 ; 450 366;
Fax: (+381 21) 454 495
E-mail: mma2009@uns.ac.rs
http://www.ftn.uns.ac.rs/mma2009